In-Line Monitoring of Red Wine Fermentation

by

Kiera Nareece Lambrecht

Thesis presented in partial fulfilment of the requirements for the degree of

Master of Science in Wine Biotechnology

at

Stellenbosch University

Department of Viticulture and Oenology, Faculty of AgriSciences

Supervisor: Dr José Luis Aleixandre Tudo

Co-supervisor: Prof. Wessel Johannes du Toit

Co-supervisor: Dr Hélène Nieuwoudt

March 2021

Declaration

By submitting this thesis electronically, I declare that the entirety of the work contained therein is my own, original work, that I am the sole author thereof (save to the extent explicitly otherwise stated), that reproduction and publication thereof by Stellenbosch University will not infringe any third party rights and that I have not previously in its entirety or in part submitted it for obtaining any qualification.

Date: 17/12/2020

Summary

Phenolic compounds may only account for a small percentage of the final composition of a finished red wine but are vital to its sensory attributes. During red wine making, extraction of these phenolic compounds takes place, whereby there is mass transfer from the solids of the grape into the liquid phase. The rate and the extent to which this extraction occurs is dependent on many factors. There are many different methods employed in the wine industry which can influence the composition of the wine. These techniques are varied and can involve manipulating process conditions such as temperature or the addition of certain oenological products. As the final composition of the wine is a major contributing factor to the quality of the wine, it is vital to be able to monitor and control this process. It has been demonstrated through a variety of studies that the use of infrared spectroscopy along with chemometrics provides an avenue for implementation of monitoring and control systems in wineries. However, the limiting factors in these studies are the extensive sample pre-treatment to remove solids before scanning as well as their discrete and off-sight sampling.

In the contents of the first research chapter (Chapter 3), a system was designed for the purpose of automatic sampling directly from vessels containing fermenting wines. This was an extensive design process which required separate sampling pumps and sampling lines which delivered samples to a single instrument. Another requirement was automation of different components and synchronisation of these in an individual system. The resulting design was put through a series of stress tests to ensure functionality and reliability. The results showed that the automated system was capable of full-time operation without experiencing component failures and, therefore, it was applied to actual fermentations. For this, 24 hours of real time monitoring was achieved.

The turbidity remained a challenge as a perfectly clarified sample was not achievable. This led to the development of partial least squares (PLS) calibrations for three different spectroscopy techniques where the samples used incorporated differing degrees of sample pre-treatment to reduce turbidity. The results of this endeavour compiled in Chapters 4 and 5 showed favourable results for samples with different levels of turbidity as well as for contactless methods of conducting analysis. With further optimisation of the models using spectral pre-processing and wavenumber selection, it was possible to develop models suitable for application in an industrial setting.

Finally, in Chapter 6, these models were deployed for use with a series of fermentations, where the ability to monitor phenolic extraction of fermentations receiving different treatments was explored. The results show that the system can be used to monitor trends in phenolic extraction in an industrial set-up. In addition to this, the system has the capacity for updated models and different methods of process control, thereby allowing it to be tailored to each unique scenario.

Opsomming

Fenolverbindings is slegs 'n klein persentasie van die finale samestelling van 'n voltooide rooiwyn, maar is van uiterste belang vir die sensoriese eienskappe daarvan. Tydens die vervaardiging van rooiwyn vind ekstraksie van hierdie fenoliese verbindings plaas, en daar word massa-oordrag vanaf die vaste stowwe in die druif in die vloeistoffase plaasgevind. Die tempo en die mate waarin hierdie ekstraksie plaasvind, hang van baie faktore af. Daar is baie verskillende metodes in die wynbedryf wat die samestelling van die wyn kan beïnvloed. Hierdie tegnieke is uiteenlopend en kan die prosestoestande soos temperatuur of die toevoeging van sekere wynkundige produkte insluit. Aangesien die finale samestelling van die wyn 'n belangrike bydraende faktor tot die kwaliteit van die wyn is, is dit noodsaaklik om hierdie proses te kan monitor en beheer. In verskillende studies is aangetoon dat die gebruik van infrarooi spektroskopie en chemometrie 'n baan bied vir die implementering van monitering- en beheerstelsels in wynkelders. Die beperkende faktore in hierdie studies is egter die uitgebreide voorbehandeling van monsters om vaste stowwe te verwyder voor skandering, sowel as die diskrete en buite sig-monsterneming daarvan.

In die inhoud van die eerste hoofstuk vir navorsing (Hoofstuk 3) is 'n stelsel ontwerp vir die outomatiese monsterneming direk vanaf vate wat fermenterende wyne bevat. Dit was 'n uitgebreide ontwerpproses wat afsonderlike monsternemingspompe en monsternemingslyne vereis wat monsters aan 'n enkele instrument gelewer het. 'N Ander vereiste was die outomatisering van verskillende komponente en sinkronisering hiervan in 'n individuele stelsel. Die gevolglike ontwerp is deur 'n reeks spanningstoetse deurgesit om funksionaliteit en betroubaarheid te verseker. Die resultate het getoon dat die outomatiese stelsel in staat was om voltyds te werk sonder om komponente te mislukking, en daarom is dit op werklike fermentasies toegepas. Hiervoor is 24 uur real-time monitering bereik.

Die troebelheid was 'n uitdaging omdat 'n volkome opgeklaar monster nie haalbaar was nie. Dit het gelei tot die ontwikkeling van kalibrasies vir gedeeltelike minste vierkante (PLS) vir drie verskillende spektroskopietegnieke, waar die monsters wat gebruik is, verskillende grade van voorbehandeling bevat om troebelheid te verminder. Die resultate van hierdie poging wat in hoofstuk 4 en 5 saamgestel is, het gunstige resultate getoon vir monsters met verskillende vlakke van troebelheid, sowel as vir kontaklose metodes om analise uit te voer. Met verdere optimalisering van die modelle met behulp van spektrale voorverwerking en seleksie van golwe, was dit moontlik om modelle te ontwikkel wat geskik is vir toepassing in 'n industriële omgewing. Laastens, in hoofstuk 6, is hierdie modelle gebruik vir 'n reeks fermentasies, waar die vermoë ondersoek is om fenoliese ekstraksie van fermentasies wat verskillende behandelings ontvang, te monitor. Die resultate toon dat die stelsel gebruik kan word om tendense in fenoliese ekstraksie in 'n industriële opset te monitor. Daarbenewens het die stelsel die vermoë om opgedateerde modelle en verskillende metodes van prosesbeheer te bewerkstellig, waardeur dit op elke unieke scenario aangepas kan word.

This thesis is dedicated to my family and friends, my partner, and the countless people who have shown faith in me. This thesis is also dedicated to marginalized people and those with disabilities who have pursued their passion for knowledge regardless of the unique challenges they face.

Biographical Sketch

Kiera Nareece Lambrecht was born on the 19th March 1996 and was homeschooled in Kempton Park. She completed her Cambridge AS Levels before enrolling in the BEng (Chemical) programme at Stellenbosch University. She completed this undergraduate degree in 2018 and enrolled in MSc (Wine Biotechnology) at the Department of Viticulture and Oenology.

Acknowledgements

I wish to express my sincere gratitude and appreciation to the following persons and institutions:

DR J.L. ALEIXANDRE TUDO, PROF. W.J. DU TOIT and DR. H.H. NIEUWOUDT, my supervisors for their support and guidance throughout the project.

WINETECH, for their financial support.

PROF M. KIDD for his assistance with statistical analysis.

THE STAFF of the Department of Viticulture and Oenology and SAGWRI, for their ongoing assistance.

MY FRIENDS, Aldert Cilliers, Elizma van Wyngaard, Brannigan du Preez, Isabel dos Santos, and Natasha Luyt for their support and understanding.

MY FAMILY, Davon and Aurora Lambrecht, for their encouragement and support.

MY PARTNER, Teunis Schlebusch for his love and support.

THE STAFF AT VLOTTENBURG STABLES, for their friendship, kind words and advice, and for going above and beyond their duties, allowing me to work long hours without having to worry about the well-being of my horse

Preface

This thesis is presented as a compilation of 8 chapters.

Chapter 1 **Project Introduction and Objectives**

Chapter 2 **Literature review**
In-line Monitoring of Red Wine Fermentations

Chapter 3 **Research results**
Prototype Development and Instrumentation

Chapter 4 **Research results**
Moving Towards Automated, In-Line Monitoring of Phenolic Extraction During Red Wine Fermentations. Part 1: Influence of Sample Preparation and Instrumentation

Chapter 5 **Research Results**
Moving Towards Automated, In-Line Monitoring of Phenolic Extraction During Red Wine Fermentations. Part 2: Optimisation of PLS Calibrations for Samples with Varying Levels of Turbidity

Chapter 6 **Research results**
Monitoring Phenolic Extraction During Fermentation with Infrared Technology and PLS Calibrations

Chapter 7 **General Discussion and Conclusions**

Chapter 8 **Supplementary Material**

Table of Contents

List of Figures

List of Tables

Chapter 1

Project Introduction and Objectives

Chapter 1 - Project Introduction and Objectives

1.1 Introduction

From as early as 6000 BC in Mesopotamia and Caucasus, winemaking has been a part of human civilisation (Robinson, 2014). Records show that the grape vine was spread and cultivated throughout the Mediterranean regions and eventually spread into Africa via Egypt (Robinson, 2014). These records also show that it was held in high regard by pharaohs and other nobles in the upper echelons of Egyptian society and that recording information about the wine's maker, origin and vintage took place (Robinson, 2014).

From a less historical perspective, the process of wine making is a complex bioprocess. After grapes are processed through destemming, crushing and, in some cases, pressing, the juice undergoes alcoholic fermentation (de Villiers, Alberts, Tredoux, *et al.*, 2012). Whilst alcoholic fermentation occurs, many compounds are utilised, formed or extracted from the solid constituents of red grapes (Bely, Sablarolles & Barre, 1990; Buratti, Ballabio, Giovanelli, *et al.*, 2011; Ma, Guo, Zhang, *et al.*, 2014; Setford, Jeffery, Grbin, *et al.*, 2017). Sugars, such as D-Glucose and D-Fructose, are found in aqueous form in grape juice and as such can take part in a wide variety of chemical reactions and yeast metabolic activities (Gil-Muñoz, Moreno-Pérez, Vila-López, *et al.*, 2009). Ethanol, carbon dioxide, glycerol and other compounds are produced from the yeast's consumption of these sugars (Boulton, 1980). At the end of alcoholic fermentation, a finished wine is roughly composed of 95% alcohol and water. The remaining 5% consists of carbohydrates, acids, glycerol, phenolics and other components (Aleixandre-Tudo, Buica, Nieuwoudt, *et al.*, 2017). The phenolics, therefore, constitutes less than 5% of the total chemical make-up of a finished wine. Their contribution to the perception of a red wine is important however, as the mouthfeel and colour are attributed to phenolic compounds found in wine (Cozzolino, Kwiatkowski, Parker, *et al.*, 2004). It is important to note that the final composition can be influenced by many different factors from vineyard practices to fermentation and aging in the cellar (Aleixandre-Tudo, Nieuwoudt, Aleixandre, *et al.*, 2018; Aleixandre-Tudo & du Toit, 2018; Apolinar-Valiente, Williams, Mazerolles, *et al.*, 2014; Bosso, Guaita, Panero, *et al.*, 2009; Gambuti, Strollo, Erbaggio, *et al.*, 2007; Ivanova, Vojnoski & Stefova, 2012).

In modern markets, wine consumers require wines of good quality and consistency (Aleixandre-Tudo, Nieuwoudt, Aleixandre, *et al.*, 2018; Lochner, 2006). Process monitoring and, possibly, process control utilised at different stages during winemaking could assist to achieve this. For this to be possible it becomes necessary to define quantitative parameters, such as sugar depletion or phenolic extraction, and to employ methods to measure these parameters during winemaking.

As wine is a highly complex matrix (Jackson, 2008), the methods of measurement needed should be robust, rapid and multiparametric (Karoui, Downey & Blecker, 2010).

One such way that rapid, multivariate, in-line and non-destructive analysis can be achieved is through the use of infrared instrumentation and chemometrics (Bauer, Nieuwoudt, Bauer, *et al.*, 2008; Bureau, Ruiz, Reich, *et al.*, 2009; Huang, Yu, Xu, *et al.*, 2008; Urtubia, Ricardo Pérez-Correa, Meurens, *et al.*, 2004). These instruments rely on the way in which electromagnetic radiation in the infrared band of the electromagnetic spectrum interacts with matter. In the wine industry, implementation of both near-infrared technology and mid-infrared technology has been used to detect and quantify wine constituents (Cavaglia, Schorn-García, Giussani, *et al.*, 2020; Cozzolino, Cynkar, Shah, *et al.*, 2011a,b; Lorenzo, Garde-Cerdán, Pedroza, *et al.*, 2009; Patz, Blieke, Ristow, *et al.*, 2004; Soriano, Pérez-Juan, Vicario, *et al.*, 2007). Whilst the measurement and quantification of wine compounds, such as the phenolic compounds, has been reported in literature, these measurements have been conducted manually and off-line (Aleixandre-Tudo, Nieuwoudt, Aleixandre, *et al.*, 2018; Aleixandre-Tudo, Nieuwoudt, Olivieri, *et al.*, 2018; Canal & Ozen, 2017; Cavaglia *et al.*, 2020)

As such, the study presented in this thesis aims to address the need for automated and in-line measurement systems. In order to achieve this, there are a few elements which must be considered. The first element is the design, development and installation of an automatic sampling system which can be used to sample directly from the fermentation vessel without the need for personnel to perform this task manually. Secondly, it becomes necessary to explore the use of a variety of instrumentation as well as to consider the effect of no or minimal sample preparation. Finally, the ability of the system to monitor the progression and phenolic extraction of an alcoholic fermentation will be examined. The completion of the above-mentioned elements can hopefully contribute to the application of current research to industry.

1.2 Project Aims and Outputs

Aim 1: Development and Implementation of the Hardware Necessary for In-Line Sampling System

Objective 1: Evaluate literature to assess what in-line systems may currently be in use in food, beverage and pharmaceutical industries and the common components that form part of these. Once current systems have been identified, it is necessary to identify the key requirements and limitations of the specific project and adapt the current methods to better suit this.

Objective 2: Design the in-line system in such a way that it can be successfully implemented to existing technology in the research environment. The rationale behind the decision to retrofit

existing systems rather than employ a new system is that the decision is beneficial in two ways. The first advantage is that it is cost efficient and time efficient. Secondly, it is applicable to industry in that wineries will not have to renovate entire sections of cellars if in-line monitoring is desired for their products.

Objective 3: The installation of the automated sampling system to existing infrastructure. After installation, testing the system on a single tank fermentation to ensure that it performs as expected and meets the key requirements identified in Objective 1, such as accurate sample delivery and food grade materials. Finally, expanding the testing regime to multiple tanks to ensure that the system can be applied to multiple fermentations taking place simultaneously.

For this Aim, it is expected that a protype sampling and analysis system which can be retrofitted will be achievable, however, it is also expected that some form of turbidity will remain present in the samples. A system such as this will have impact in that it can be implemented to allow full-time monitoring of a fermentation.

Aim 2: Optimisation of PLS Calibrations Utilising Mid Infrared and Near Infrared Instruments and Samples of Varying Turbidity

Objective 1: Collection of a sample set containing samples of juice, must and wine of different cultivars. For this sample set, different sample treatments, such as filtration or centrifugation, were to be applied.

Objective 2: Perform spectral measurements on this sample set in addition to analytical methods to quantify wine phenolic parameters such as tannin concentration, anthocyanins concentration, polymeric pigment concentration, total phenol index, and colour density.

Objective 3: Utilise chemometric techniques such as Partial Least Squares Regression to build infrared calibrations for this sample set.

Objectve 4: Evaluate the performance of the calibrations with the use of statistical methods.

Due to the spectroscopic methods available and the wide range of pre-processing methods which can be applied to the system, it is expected that the resulting PLS calibrations will be able to incorporate the effects of turbidity and will, therefore, be able to yield accurate and reliable predictions.

Aim 3: Monitoring Phenolic Extraction During Fermentation

Objective 1: To select different winemaking techniques, such as enzyme addition or temperature variation, which can influence the phenolic extraction during fermentation. Once these treatments have been selected, fermentations would be conducted employing these methods.

Objective 2: To utilise calibrations built in Objective 2 on samples collected directly from an outlet installed into the tank during the fermentations performed in Aim 1 to predict values for tannin concentration, anthocyanin concentration, polymeric pigment concentration and colour density in order to determine the ability of these calibrations to monitor phenolic extraction.

It is expected that the automated sampling system will be able to distinguish between different levels of phenolic compounds across multiple fermentations.

1.3 Literature Cited

Aleixandre-Tudo, J.L. & du Toit, W. 2018. Cold maceration application in red wine production and its effects on phenolic compounds: A review. *LWT - Food Science and Technology*. 95(April):200–208.

Aleixandre-Tudo, J.L., Buica, A., Nieuwoudt, H., Aleixandre, J.L. & Du Toit, W. 2017. Spectrophotometric Analysis of Phenolic Compounds in Grapes and Wines. *Journal of Agricultural and Food Chemistry*. 65(20):4009–4026.

Aleixandre-Tudo, J.L., Nieuwoudt, H., Aleixandre, J.L. & du Toit, W. 2018. Chemometric compositional analysis of phenolic compounds in fermenting samples and wines using different infrared spectroscopy techniques. *Talanta*. 176(August 2017):526–536.

Aleixandre-Tudo, J.L., Nieuwoudt, H., Olivieri, A., Aleixandre, J.L. & du Toit, W. 2018. Phenolic profiling of grapes, fermenting samples and wines using UV-Visible spectroscopy with chemometrics. *Food Control*. 85:11–22.

Apolinar-Valiente, R., Williams, P., Mazerolles, G., Romero-Cascales, I., Gómez-Plaza, E., López-Roca, J.M., Ros-García, J.M. & Doco, T. 2014. Effect of enzyme additions on the oligosaccharide composition of Monastrell red wines from four different wine-growing origins in Spain. *Food Chemistry*. 156:151–159.

Bauer, R., Nieuwoudt, H., Bauer, F.F., Kossmann, J., Koch, K.R. & Esbensen, K.H. 2008. FTIR Spectroscopy for Grape and Wine Analysis. *Analytical Chemistry*. 80(5):1371–1379.

Bely, M., Sablarolles, J.M. & Barre, P. 1990. Description of Alcholic Fermentation Kinetics: Its Variability and Signficance. *American journal of enology and viticulture*. 41(4):319–324.

Bosso, A., Guaita, M., Panero, L., Borsa, D. & Follis, R. 2009. Influence of Two Winemaking Techniques on Polyphenolic Composition and Color of Wines. *American Journal of Enology and Viticulture*. 60(3):379–385.

Boulton, R. 1980. The Prediction of Fermentation Behaviour by a Kinetic Model. 31(1).

Buratti, S., Ballabio, D., Giovanelli, G., Dominguez, C.M.Z., Moles, A., Benedetti, S. & Sinelli, N. 2011. Monitoring of alcoholic fermentation using near infrared and mid infrared spectroscopies combined with electronic nose and electronic tongue. *Analytica Chimica Acta*. 697(1–2):67–74.

Bureau, S., Ruiz, D., Reich, M., Gouble, B., Bertrand, D., Audergon, J.M. & Renard, C.M.G.C. 2009. Rapid and non-destructive analysis of apricot fruit quality using FT-near-infrared spectroscopy. *Food Chemistry*. 113(4):1323–1328.

Canal, C. & Ozen, B. 2017. Monitoring of Wine Process and Prediction of Its Parameters with Mid-Infrared Spectroscopy. *Journal of Food Process Engineering*. 40(1).

Cavaglia, J., Schorn-García, D., Giussani, B., Ferré, J., Busto, O., Aceña, L., Mestres, M. & Boqué, R. 2020. ATR-MIR spectroscopy and multivariate analysis in alcoholic fermentation monitoring and lactic acid bacteria spoilage detection. *Food Control*. 109:1–7.

Cozzolino, D., Kwiatkowski, M.J., Parker, M., Cynkar, W.U., Dambergs, R.G., Gishen, M. & Herderich, M.J. 2004. Prediction of phenolic compounds in red wine fermentations by visible and near infrared spectroscopy. *Analytica Chimica Acta*. 513(1):73–80.

Cozzolino, D., Cynkar, W., Shah, N. & Smith, P. 2011a. Feasibility study on the use of attenuated total reflectance mid-infrared for analysis of compositional parameters in wine. *Food Research International*. 44(1):181–186.

Cozzolino, D., Cynkar, W., Shah, N. & Smith, P. 2011b. Technical solutions for analysis of grape juice, must, and wine: The role of infrared spectroscopy and chemometrics. *Analytical and Bioanalytical Chemistry*. 401(5):1479–1488.

Gambuti, A., Strollo, D., Erbaggio, A., Lecce, L. & Moio, L. 2007. Effect of Winemaking Practices on Color Indexes and Selected Bioactive Phenolics of Aglianico Wine. *Journal of Food Science*. 72(9):623–628.

Gil-Muñoz, R., Moreno-Pérez, A., Vila-López, R., Fernández-Fernández, J.I., Martínez-Cutillas, A. & Gómez-Plaza, E. 2009. Influence of low temperature prefermentative techniques on chromatic and phenolic characteristics of Syrah and Cabernet Sauvignon wines. *European Food Research and Technology*. 228(5):777–788.

Huang, H., Yu, H., Xu, H. & Ying, Y. 2008. Near infrared spectroscopy for on/in-line monitoring of quality in foods and beverages: A review. *Journal of Food Engineering*. 87(3):303–313.

Ivanova, V., Vojnoski, B. & Stefova, M. 2012. Effect of winemaking treatment and wine aging on

phenolic content in Vranec wines. *Journal of Food Science and Technology*. 49(2):161–172.

Jackson, R. 2008. *Wine Science*. Third Edit ed. San Diego.

Karoui, R., Downey, G. & Blecker, C. 2010. Mid-Infrared Spectroscopy Coupled with Chemometrics: A Tool for the Analysis of Intact Food Systems and the Exploration of Their Molecular Structure - Quality Relationships - A Aeview. *Chemical Reviews*. 110(10):6144–6168.

Lochner, E. 2006. The evaluation of Fourier transform infrared spectroscopy (FT-IR) for the determination of total phenolics and total anthocyanins concentrations of grapes by.

Lorenzo, C., Garde-Cerdán, T., Pedroza, M.A., Alonso, G.L. & Salinas, M.R. 2009. Determination of fermentative volatile compounds in aged red wines by near infrared spectroscopy. *Food Research International*. 42(9):1281–1286.

Ma, W., Guo, A., Zhang, Y., Wang, H., Liu, Y. & Li, H. 2014. A review on astringency and bitterness perception of tannins in wine. *Trends in Food Science and Technology*. 40(1):6–19.

Patz, C.D., Blieke, A., Ristow, R. & Dietrich, H. 2004. Application of FT-MIR spectrometry in wine analysis. *Analytica Chimica Acta*. 513(1):81–89.

Robinson, J. 2014. *The Oxford Companion to Wine*.

Setford, P.C., Jeffery, D.W., Grbin, P.R. & Muhlack, R.A. 2017. Factors affecting extraction and evolution of phenolic compounds during red wine maceration and the role of process modelling. *Trends in Food Science and Technology*. 69:106–117.

Soriano, A., Pérez-Juan, P.M., Vicario, A., González, J.M. & Pérez-Coello, M.S. 2007. Determination of anthocyanins in red wine using a newly developed method based on Fourier transform infrared spectroscopy. *Food Chemistry*. 104(3):1295–1303.

Urtubia, A., Ricardo Pérez-Correa, J., Meurens, M. & Agosin, E. 2004. Monitoring large scale wine fermentations with infrared spectroscopy. *Talanta*. 64(3):778–784.

de Villiers, A., Alberts, P., Tredoux, A.G.J. & Nieuwoudt, H.H. 2012. Analytical techniques for wine analysis: An African perspective; a review. *Analytica Chimica Acta*. 730:2–23.

Chapter 2

Literature Review: In-line Monitoring of Red Wine Fermentation

Chapter 2 – Literature Review: In-line Monitoring of Red Wine Fermentations

2.1 Introduction

The bioprocess whereby grape juice undergoes alcoholic fermentation is complex and involves the interaction, formation and utilisation of many different compounds (Bely, Sablarolles & Barre, 1990; Buratti, Ballabio, Giovanelli, *et al.*, 2011). The complexity of this process is due to the many different factors which must be considered during winemaking. These factors include, but are not limited to, cultivar, and the region from which the grapes were obtained, health status of the grapes, the strain of yeast used in inoculated fermentations, and the fermentation conditions. Each of these factors can ultimately affect both the progression of the alcoholic fermentation as well as the final chemical composition of the wine once the fermentation is completed (Setford, Jeffery, Grbin, *et al.*, 2017).

As previously mentioned, grape juice and wine are composed of many different compounds. For grape juice, there is a high concentration of sugars before the fermentation begins in addition to water. Once alcoholic fermentation begins, the yeast utilises the sugars present in the juice to increase their biomass (Blanco, Peinado & Mas, 2004) and in doing so, by-products of this bioprocess such as alcohol, glycerol and carbon dioxide are produced (Boulton, 1980). For a finished wine, the most abundant of the compounds is water, followed by alcohol. However, even though present in much smaller quantities than water and alcohol, other compounds such as phenolic compounds and acids are also present in the must during alcoholic fermentation. Whilst these only account for a small percentage of the overall composition, their role in the overall perception of the wine is not negligible (Cozzolino, Kwiatkowski, Parker, *et al.*, 2004). The phenolic compounds, in particular, are of great interest due to their role in mouthfeel and colour, of especially red wine (Cozzolino, D; Dambergs, 2009; Setford, Jeffery, Grbin, *et al.*, 2019). Over the course of alcoholic fermentation, the concentrations of all these listed compounds will change and have an impact on the finished wine.

With this in mind, it is necessary to consider the competitive nature of the wine industry. It is becoming increasingly important to use technology to monitor the quality and consistency of products and the wine industry is no different (Aleixandre-Tudo, Nieuwoudt, Olivieri, *et al.*, 2018) As such, measuring the concentration of the compounds present is an important factor when monitoring the progress of the fermentation as well as ensuring the composition of the finished product. In order to quantitatively determine progression and quality, however, it is necessary to establish certain parameters. Another benefit of establishing these parameters is to ensure that

measures can be taken to mitigate the effects of a deviation which can lead to either a lower quality product or impact on the progression. Such deviations can include stuck and sluggish fermentations or poor extraction of phenolic compounds from the berry solids (Bisson, 1999). Examples of the parameters could potentially be sugar depletion, extent of phenolic extraction, and conversion of malic acid to lactic acid.

In industries which manufacture products intended for human consumption, technologies to monitor their production are common. In particular, spectroscopy is of use to the food and beverage industry due to the simplicity and non-invasive nature of the analysis (Bauer, Nieuwoudt, Bauer, *et al.*, 2008; Bureau, Ruiz, Reich, *et al.*, 2009; Huang, Yu, Xu, *et al.*, 2008). The instrumentation used in these processes utilises the way in which electromagnetic radiation interacts with the matter. The resulting spectra are then interpreted with the use of mathematical and statistical tools (Bu, 2007; Gishen, Dambergs & Cozzolino, 2008).

Initially, this will highlight the compounds of interest in wine. The history of spectroscopy and the principles upon which these instruments are based will be explored to demonstrate how these compounds can be monitored. Finally, the principles of in-line monitoring will be highlighted in order to demonstrate how the principles of spectroscopy can be combined with certain process equipment and certain engineering principles to allow for real-time and robust monitoring of oenological properties during alcoholic fermentation of wine. At this point it should be noted that, although many technologies and methods exist which can be used for the purposes of quantification of compounds in wine, only those used over the duration of the project are reported in the Literature Review.

2.2 Compounds and Variables of Interest Associated with Red Wine During and After Fermentation

2.2.1 Sugars

Sugars form part of a larger family of molecules known as carbohydrates (Ribéreau-Gayon, Glories, Maujean, *et al.*, 2006). In grape juice, the two main sugars, which form a mixed substrate for the yeast during fermentation, are the hexose sugars D- Glucose and D – Fructose (Boulton, 1980). Typically, the total concentration of sugar in ripened grapes should be between 150 g/L and 250 g/L, and the ratio of glucose to fructose can vary, however, it normally sits below 1 in mature grapes. This ratio is of great importance as the yeast will utilise the glucose preferentially (Ribéreau-Gayon *et al.*, 2006).

The structure of the hexose sugars can be seen in Figure 2.1 below(Ibrahim, Alaam, El-Haes, *et al.*, 2006).

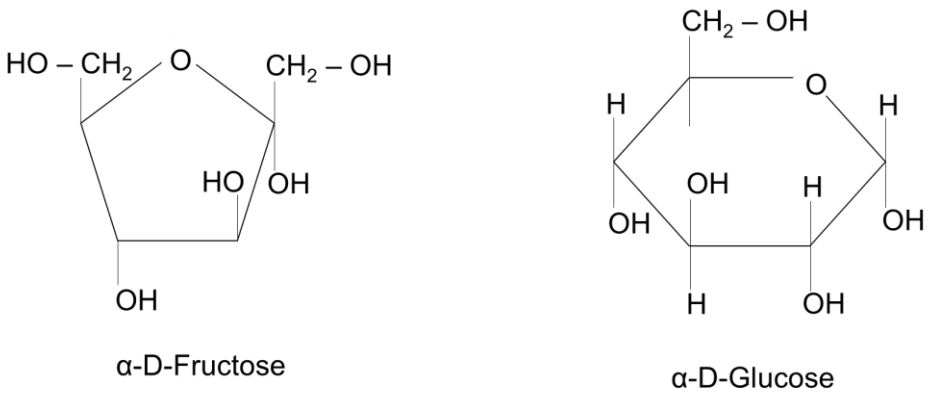

Figure 2.1: Structure of D-Fructose and D-Glucose, redrawn from Ibrahim et al., 2006

Whilst in solid state, these sugars are stable. However, when forming part of an aqueous solutions, such as grape juice, they are incorporated in a wide array of different biochemical and metabolic reactions (Moreno-Arribas & Polo, 2009). For alcoholic fermentation of grape juice, this refers to the sugars forming the nutrient base for yeast for both the growth and the maintenance of biomass (Yoon, Klinzing & Blanch, 1977).

For a typical fermentation, it is assumed that the yeast utilises this mixed substrate according to a generalised Monod Model (Monod, 1949) which accounts for the preferential metabolism of glucose, with the result being alcohol and carbon dioxide. This is shown in the Equation below:

$$C_6H_{12}O_6 \rightarrow 2CH_3CH_2OH + 2CO_2 \quad (2.1)$$

It should be noted that this is an ideal case where no other by-products are produced.

2.2.2 Ethanol

The primary form of alcohol that is found in wine is a primary alcohol known as ethyl alcohol or ethanol. The structure of this molecule can be seen in Figure 2.2 below (Ribéreau-Gayon *et al.*, 2006)

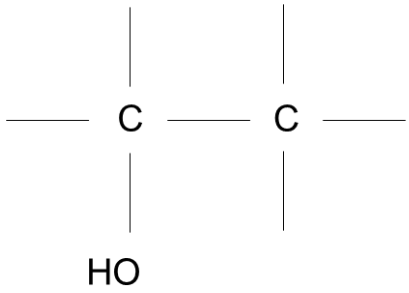

Figure 2.2: Structure of ethyl alcohol, redrawn from Ribéreau-Gayon et al., 2006

From a qualitative perspective, this compound is important in wine as it contributes towards the sensory qualities of the wine and its stability, and as such it becomes important to measure the ethanol content (Jackson, 2008). It also serves as a solvent during the course of fermentation and aids in the extraction of different compounds from the grapes (Jackson, 2008; Ribéreau-Gayon *et al.*, 2006). From a legal standpoint, it is important to know the percentage of alcohol which makes up the finished wine. When a standard fermentation is considered, namely where the fermentation reaches completion, the ethanol can compose approximately 14-15% v/v of the finished red wine (Jackson, 2008).

2.2.3 Main Phenolic Compounds in Red Wines

Polyphenolic compounds in wine contribute towards colour and mouth feel properties and have been reported to have antioxidant properties (Aleixandre-Tudo, Buica, Nieuwoudt, *et al.*, 2017). These compounds contain at least one aromatic ring and one hydroxyl group. Two separate groups of polyphenolic compounds can be distinguished based on the orientation and number of phenolic sub-units that form the structure of the molecule. These groups are flavonoid and non-flavonoid phenols (Lochner, 2006). The flavonoid group consists of anthocyanins, tannins, polymeric pigments, flavonols, and flavanols, while the non-flavonoid group consists of hydroxycinnamic acids and their esters, hydroxybenzoic acids and stilbenes (Aleixandre-Tudo *et al.*, 2017; Casassa, 2017; Lochner, 2006). For the purposes of this project and literature review, only anthocyanins, tannins and polymeric pigments are considered due to their relevance in the project.

Several methods have been reported to quantify the concentrations of phenolic compounds in wine samples, of which one is the total phenolic index. This index is a value determined from a correlation between total phenolic content and the sample's absorbance value at 280nm (Glories, 1984; Iland, Ewart, Sitters *et al*, 2000). This measurement, however, cannot discriminate between the different types of phenolic compounds and so methods for the quantification of the individual compounds will be discussed in each relevant section.

2.2.3.1 Tannins

Tannins are regarded as reactive phenolic compounds (McRae, Day, Bindon, *et al.*, 2015). Tannins, as a whole, can be considered as a group of phenolic molecules which are water-soluble, have molecular weights between 600 to 3500 and possess properties which allow precipitation of proteins (Jackson, 2008; Khanbabaee & van Ree, 2001; Moreno-Arribas & Polo, 2009; Ribéreau-Gayon *et al.*, 2006; Waterhouse, 2002). The main group of tannins found in red wine are the condensed tannins which consist of coupled flavonoid units (Waterhouse, 2002). These are also primarily found in the skin, seeds, and stem of the grape bunch.

The importance of tannins in wine comes from the way in which these molecules interact with proteins. Tannins can form bonds to more than one protein simultaneously and therefore influence mouthfeel properties of wine (Ma, Guo, Zhang, *et al.*, 2014). As such, condensed tannins are the main source of both astringency and bitterness in wine (Jackson, 2008).

For the quantification of tannins in a wine sample, a common method used is the methylcellulose precipitation assay as it is simplistic and robust (Mercurio, Dambergs, Herderich, *et al.*, 2007). This method is based on the precipitation of the condensed tannins with methylcellulose (Mercurio *et al.*, 2007). It is a subtractive method requiring the preparation of both a control sample, which contains the total phenolic content of the sample, and a treatment, where the tannins have precipitated out of solution. Both the control and the treatment are measured at 280nm and the difference between the absorbances determined. This difference represents the absorbance of the tannins at 280nm and it can be reported as either the aforementioned difference or converted into epicatechin equivalent concentration (Mercurio *et al.*, 2007).

2.2.3.2 Anthocyanins and Polymeric Pigments

Located primarily in the skin of the berry, anthocyanins are responsible for colour in red wine (Setford *et al.*, 2019). Five main anthocyanins have been discovered to be present in wine and these are malvidin, peonidin, cyanidin, delphinidin and petunidin. (Jackson, 2008; Moreno-Arribas & Polo, 2009; Ribéreau-Gayon *et al.*, 2006). Of these, malvidin is the most abundant and will normally account for more than 40% of the total anthocyanin concentration in a wine sample

(Setford *et al.*, 2017). The basic structure of this molecule can be seen in Figure 2.3 where the branches labelled ‘R’ refer to different substituents.

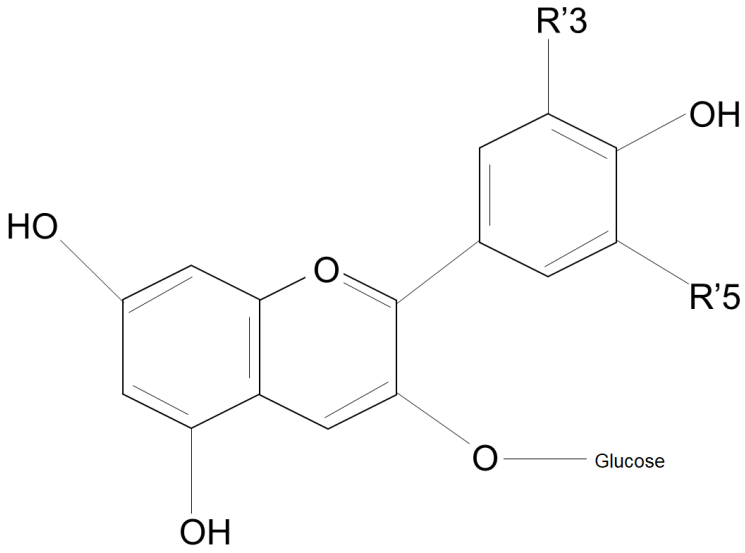

Figure 2.3: Basic Anthocyanin Molecule, redrawn from Ribéreau-Gayon et al., 2006

However, free anthocyanins themselves are not stable. For colour stability to be achieved in red wine, polymerisation must occur between anthocyanins and other compounds present in wine, such as tannins or other anthocyanins (Jackson, 2008). The compounds of interest which form when anthocyanins bond to other flavonoids (such as tannins) are known as polymeric pigments and these pigments help maintain the colour of the wine after bottling (Harbertson, Picciotto & Adams, 2003; Morata, 2019; Setford *et al.*, 2017). The colour change involving the purple tint turning to a brick-red tint during ageing is attributed to the formation of polymeric pigments (Setford *et al.*, 2017).

The total anthocyanins and the polymeric pigments can be quantified with the use of the modified Somers Assay. For the total anthocyanin content of a sample, the pH is lowered with the use of hydrochloric acid to convert all anthocyanins to their coloured forms before recording the absorbance at 520nm. However, for the polymeric pigments, an excess of SO_2 is added and a measurement taken at 520nm to assess the contribution of the SO_2 resistant pigments towards the colour (Somers & Evans, 1997).

As the colour is an important factor with regards to the organoleptic property of wine, it is also necessary to classify wine colour objectively. The colour density or colour intensity refers to the total amount of colour in a sample of wine or juice and can be calculated as the sum of the absorbance values at wavelengths 420, 520 and 620 nm (Li, Zhu, Li, *et al.*, 2017). These wavelengths account for the blue, red and yellow components in wines (Aleixandre-Tudo,

Nieuwoudt & du Toit, 2019; Aleixandre-Tudo, Nieuwoudt, Olivieri, *et al.*, 2018; Fragoso, Aceña, Guasch, Mestres, *et al.*, 2011).

2.2.4 Acids

In wines, compounds such as organic acids contribute to qualities of wine such as the stability and sensory properties, while the pH of the wine is directly influenced by the organic acid composition. Regarding the organoleptic properties of wine, the pH plays a role in the development of certain flavour compounds during fermentation and a lower pH is reported to accentuate the astringency in wine (Volschenk, van Vuuren & Viljoen-Bloom, 2017). A low pH can delay the onset of oxidation in wine, thus preserving the aroma and flavour (Volschenk *et al.*, 2017). In addition to this, some acids play an important role in metabolism of the microorganisms associated with wine (Ribéreau-Gayon *et al.*, 2006).

The total acidity refers to the combined concentration of the different types of acids which are found in the juice or wine. In either of these matrices, the most common acids which can be found are tartaric, malic, citric, lactic and phenol acids(Jackson, 2008; Ribéreau-Gayon *et al.*, 2006). Of these acids, tartaric acid and malic acid can be considered the most prevalent.

2.3 Red Wine Making Variables and Techniques and Their Effect on Wine Parameters

Red winemaking begins with the mechanical crushing and destemming of grapes, followed by an addition of SO_2 to prevent the growth of unwanted microorganisms and the prevention of browning due to oxidation. The alcoholic fermentation can either begin spontaneously due to the presence of indigenous yeast or commercial yeast cultures can be added to the juice. The alcoholic fermentation during red wine production takes place at approximately 25^{o}C in the presence of the skins. As these skins will form a cap due to the formation of carbon dioxide, it should be frequently immersed using pump overs or punch downs (Apolinar-Valiente, Williams, Mazerolles, *et al.*, 2014; Gambuti, Strollo, Erbaggio, *et al.*, 2007; Jackson, 2008; Weber, Nelson & Gay, 2002).

Whilst there are generally certain common steps that occur in the winemaking process, winemakers can make use of different procedures and parameters to influence phenolic composition and to achieve certain wine styles. Certain wine making techniques have been identified for the purposes of this literature review to show how certain compounds and variables can be influenced by the techniques applied during the wine making process.

2.3.1 Temperature Related Techniques

One technique involves altering the temperature at which the fermentation takes place. In these cases it has been reported that a higher fermentation temperature will result in increased extraction of phenolic compounds and polymeric pigments (Beaver, Medina-Plaza, Miller, *et al.*, 2020; Sacchi, Bisson & Adams, 2005; Setford *et al.*, 2017). An increased temperature can also lead to a faster fermentation (Beaver, Miller, Medina-Plaza, *et al.*, 2019; Boulton, 1980).

Another technique which involves temperature manipulation is known as thermovinification. Whilst some variation in the technique is always present, the general procedure which takes place during thermovinification involves heating the must to 60^{o}C to 70^{o}C for a limited period of time before extraction, cooling and then fermentation (Sacchi *et al.*, 2005) This technique has been reported to improve the colour of the wine due to increased extractions of anthocyanins.

In contrast to thermovinification, cold soaking is also a technique that can applied. Rather than exposing the skins to heat, this technique involves lowering the temperature prior to fermentation to approximately 10^{o}C to 15^{o}C for a period of time before the fermentation begins (Apolinar-Valiente *et al.*, 2014; Sacchi *et al.*, 2005). The cold soaking before fermentation is done to allow the phenolic extraction to occur, whilst the cold temperature prevents the onset of fermentation (Aleixandre-Tudo & du Toit, 2019). It has been reported in literature that an increase in

anthocyanin and other flavanol levels occurred when cold soaking was applied to wine (Favre, Peña-Neira, Baldi, *et al.*, 2014; Federico Casassa, Bolcato, Sari, *et al.*, 2016; Ortega-Heras, Pérez-Magariño & González-Sanjosé, 2012; Wang, Huo, Zhang, *et al.*, 2016). However, it is also important to note that contradictory findings to this have also been reported that showed no increase in levels of these phenolic compounds with cold maceration (González-Neves, Gil, Barreiro, *et al.*, 2010). This technique was reported to have an effect on specific polysaccharide sugars such as rhamnose, xylose and galactose in that there was a decreased concentration in comparison to controls (Apolinar-Valiente *et al.*, 2014). Another effect that was reported by Gardner et al, 2011, was that a 1.5% increase in the alcohol content occurred when must underwent this treatment.

Finally, freezing the must or the grapes is also a technique which can be applied. This involves the use of dry ice addition to freeze the must (Apolinar-Valiente *et al.*, 2014; Girard, Yuksel, Cliff, *et al.*, 2001; Sacchi *et al.*, 2005). This technique has been found to increase the concentration of tannins and anthocyanins in the finished wine, whilst leading to slight decreases in polysaccharide concentration in certain wines such as Syrah (Apolinar-Valiente *et al.*, 2014; Sacchi *et al.*, 2005).

2.3.2 Enzyme Addition

In order to allow for better extraction from the fruit skin, enzymes can be added which decrease the integrity of the cell wall by degrading its pectin (Smith, Mcrae & Bindon, 2015). In the case of tannins, an increase in concentration is expected due to the enzymes both facilitating the movement of tannins from the solids, and due to the enzymes limited tannin loss to sediment and adsorption (Cozzolino, Cynkar, Shah, *et al.*, 2011a). Enzymatic addition has also been reported to have a positive effect on colour intensity (Kelebek, Canbas & Selli, 2008; Ortega-Heras *et al.*, 2012).

However, in the case of anthocyanins, there are varying reports as to the effect of enzymatic addition (Ortega-Heras *et al.*, 2012). Whilst there are reports of enzymatic additions increasing the levels of anthocyanins in wines (Gil-Muñoz, Moreno-Pérez, Vila-López, *et al.*, 2009; Kelebek *et al.*, 2008), other authors indicated that the enzymatic addition did not have an effect (Ortega-Heras *et al.*, 2012).

2.3.3 Skin Contact

One technique which involves the actual skin contact is maceration time. This involves varying the time span during which the wine or must is in contact with the solid constituents of the grapes. Longer contact with the solid parts of the fruit showed that tannins, anthocyanins and polymeric pigments increased (Gómez-Plaza, Gil-Muñoz, López-Roca, *et al.*, 2001; Ivanova, Vojnoski &

Stefova, 2012; Sacchi *et al.*, 2005). In addition to this, it was shown that increased skin contact will also result in an increase in gallic acid and colour intensity in wines (Auw, Blanco, O'Keefe, *et al.*, 1996; Gambuti *et al.*, 2007). It should be noted that the phenolics that are extracted from the skins can be reabsorbed by the same mass transfer (Medina-Plaza, Beaver, Miller, *et al.*, 2020). In contrast, less time spent in contact with the skins, will have the opposite effect regarding phenolic compounds (Schmidt & Noble, 1983).

Another technique to influence the phenolic composition of red wine involves changing the ratio of juice to skins before fermentation, known as bleeding. In such cases it has been reported that removing some of the juice prior to fermentation resulted in increased colour intensity as well as higher concentrations of anthocyanins, polymeric pigments and total phenolics (Bautista-Ortín, Fernández-Fernández, López-Roca, *et al.*, 2007).

2.3.4 Oxygen Addition

The management of oxygen in wine is extremely important as oxygen influences the phenolic composition of wine and, by extension, the sensory attributes (Geldenhuys, 2009; Moenne, Saa, Laurie, *et al.*, 2014). Oxygen in wine contributes towards the formation of polymers and in turn can also affect the colour of the wine (Geldenhuys, 2009). Whilst most wine making techniques limit the exposure of wine to oxygen, controlled addition of oxygen to the fermenting must can be beneficial to the wine in that it can lead to colour stabilisation and reduced astringency (Garrido-Bañuelos, 2018).

It has been reported that wines exposed to oxygen during fermentation showed a lower concentration of anthocyanins whilst also showing a higher level of polymeric pigments. This could have been as a result of polymerisation reactions being favoured or decolourisation of the anthocyanins through oxidation reactions with other compounds (McRae *et al.*, 2015). Oxygen addition during fermentation can also lead to reduced tannin concentration in a finished wine due to the oxidised tannins being more easily bound to grape solids and less water-soluble (McRae *et al.*, 2015).

2.4 Infrared Radiation and Infrared Spectroscopy

2.4.1 History of Infrared Spectroscopy

The early developmental stages of Infrared (IR) Spectroscopy saw mechanical models employed as a means of demonstrating the vibrations in molecules. In these cases, the planar vibrations were studied with the use of steel balls and helical springs which represented the nuclei and the bonds respectively (Colthup, 1961).

The late 1930's saw organic chemists utilizing infrared spectroscopy as the initial technique for structural spectroscopy (Larkin, 2011). However, there were few researchers using this technique due to the challenging nature of it. However, 1946 was the first year in which instruments became commercially available (Larkin, 2011). Gradually, it became a more widely accepted technique because of improvements in the technology, concepts and applied experimental methods.

2.4.2 Infrared Radiation

Infrared (IR) light forms part of the greater electromagnetic (EM) spectrum. It consists of both electric and magnetic fields (Sun, 2010), however, when dealing with spectroscopy, only the electric field will be considered further. As a form of radiation, it takes the form of a continuous and sinusoidal wave (Larkin, 2011). The IR region of light can be found in the region next to red light in the visible light spectrum as shown in Figure 2.4. The IR region can be broken down further into three sections which are (Larkin, 2011):

- Near Infrared (NIR) which has a wavenumber range of 14000 – 4000 cm^{-1}
- Mid Infrared (MIR) which has a wavenumber range of 4000 – 400 cm^{-1}
- Far Infrared (FIR) which has a wavenumber range of 400 – 10 cm^{-1}

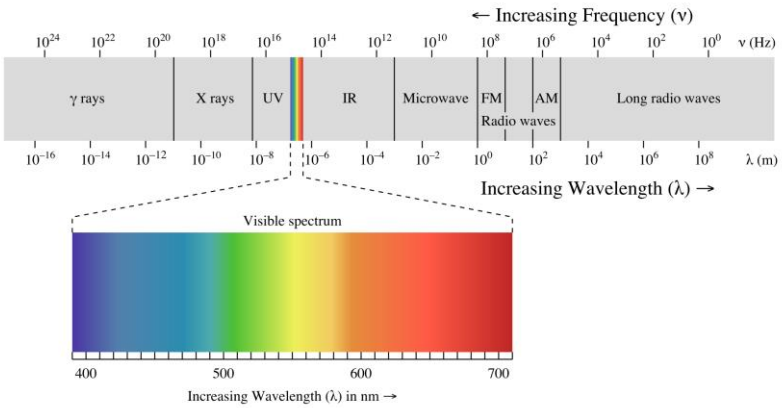

Figure 2.4: The Electromagnetic Spectrum, by Philip Ronan, Wikimedia Commons, is licensed under CC BY-SA 3.0

The way in which this form of electromagnetic radiation can be used to determine the composition of a sample is by understanding the way in which this radiation interacts with matter, which forms the basis of Infrared Spectroscopy.

2.4.3 Basics of Infrared Spectroscopy

Molecules in a material will raise and lower energy levels continuously through the emitting and absorbing of energy. This energy can be absorbed from photons at specific frequencies, including those in the IR spectrum (Abbott, 1999; Larkin, 2011; Sun, 2010). When a surface is struck by an electromagnetic wave, the wave will interact with the material and a measurement of the intensity of transmission, reflectance or absorbance can be taken.

Utilising the MIR region results in spectral “fingerprints” that arise from the fundamental bending, rotation and stretching of the molecules contained in the sample material. In contrast to this, when using the NIR region, these “signatures” are as a result of overtones and combinations of bands (Aleixandre-Tudo, Nieuwoudt, Aleixandre, *et al.*, 2018; Cozzolino, Cynkar, Shah, *et al.*, 2011b; Garlick, 2013).

2.4.4 Chemometrics

MIR and NIR spectra are extremely complex data sets. One of the reasons for this complexity is the interactions between the many variables which constitute a sample, which may have an influence on the spectra. For the information contained in the spectra to be useful and to be able to quantitatively determine the concentration of specific compounds, it is necessary for multivariate data analysis techniques or chemometrics to be applied (Garlick, 2013). Chemometrics involves the use of mathematics and statistics to understand information generated by instrumentation and to correlate this with quality parameters or other physical parameters (Lourenço, Lopes, Almeida, *et al.*, 2012; Medina, Perestrelo, Silva, *et al.*, 2019).

One such chemometric technique, which is of great use with spectroscopy, is partial least square regression (Bu, 2007; Garlick, 2013). This is the most used approach in chemistry related fields (Medina *et al.*, 2019). This technique is used to find a relationship between two data sets through a linear multivariate model (Pasquini, 2018). One data set is projected onto a smaller number of components known as “latent variables” to reduce dimensionality. These are a linear combination of the variables in the original dataset which have been rotated to ensure that there is maximum correlation with the other data set (Genisheva, Quintelas, Mesquita, *et al.*, 2018; Lavine &

Workman, 2010). The maximum covariance is then found between the two data sets (Garlick, 2013). However, the models must undergo validation to determine their predictive performance.

Many different metrics exist to validate these models and ensure that their performance is adequate for a specific purpose. These include values such as the coefficient of correlation (R^2), the root mean square error of prediction (RMSE), the residual predictive deviation (RPD), inter-class correlation coefficient (ICC) and standard error of measurements (SEM) (Aleixandre-Tudo, Nieuwoudt, Aleixandre, *et al.*, 2015; Ayvaz, Plans, Towers, *et al.*, 2015; Fragoso, Aceña, Guasch, Mestres, *et al.*, 2011; Olivieri, 2015; Santos & Colnago, 2018; Shen, Ying, Li, *et al.*, 2011; Westad & Marini, 2015; Williams, Dardenne & Flinn, 2017). Additionally, regression tests, such as the Deming test or Passing-Bablock, can be performed to investigate whether systematic error exists and to compare the accuracy of the predictions and determine their similarity.

Using the aforementioned values, the criteria for models to be considered suitable for analysis are as follows:

- The R^2 indicates the percentage of variation explained by a model. R^2 values closer to 1 indicate strong correlation, but R^2 values above 0.8 is considered a high coefficient of correlation (Aleixandre-Tudo, Nieuwoudt, Aleixandre, *et al.*, 2018).
- As this is a measure of consistency in predicted values, an ICC value as close to 1 as possible indicates high levels of agreement and reliability (Aleixandre-Tudo, Nieuwoudt, Aleixandre, *et al.*, 2018)..
- The RPD is the ratio of a data set's standard deviation and RMSE (SD/RMSE) and therefore a high standard deviation coupled with small errors in prediction is desirable. Certain authors consider models with RPD values above 2.5 suitable (Aleixandre-Tudo *et al.*, 2015; Petrovic, Aleixandre-Tudo & Buica, 2020; Santos & Colnago, 2018) while other authors consider models with an RPD above 3 as suitable (Fragoso, Aceña, Guasch, Busto, *et al.*, 2011; Wu, Xu, Long, *et al.*, 2015). However, this parameter is application dependent and needs to be placed in context.
- SEM values indicate error that can be attributed to measurement error. These values should ideally be lower and in the same order of magnitude as the (RMSE) as this indicates increased accuracy of the model (Aleixandre-Tudo, Nieuwoudt, Aleixandre, *et al.*, 2018)..
- Accepted null hypothesis in both the Deming and Passing-Bablock analysis as this indicates that no significant differences exist between the IR models and the reference methods (Aleixandre-Tudo, Nieuwoudt, Aleixandre, *et al.*, 2018; Linnet, 1993; Petrovic *et al.*, 2020).

2.5 Infrared Spectral Techniques for In-Line Analysis

2.5.1 Necessity of Batch Process Monitoring

A batch process is one where the process variables continually change with time, with wine fermentation being such a process. The primary challenge of batch processes is to ensure consistency between batches (Geörg, Schalk, Methner, *et al.*, 2015; Seborg, Edgar, Mellicamp, *et al.*, 2010). For this consistency to be possible, the process needs to be monitored with the use of instrumentation and batch production management. In this case, batch production management refers to the practice of advising a plant manager, or wine maker in this case, on how to interact with the equipment, controls and recipes. The term recipe has many different meanings, however, in terms of process monitoring and control it refers to the procedure that must take place.

Monitoring of a batch process can lead to a more efficient use of the resources available to staff controlling the production process. As such, more emphasis is being placed on instrumentation and technology which allows for rapid monitoring of compounds and reactions. In addition to this, use of automation in the monitoring processes is also increasing to further aid in reducing time between measurements and therefore between actions to ensure the process continues along a desired course (Daghbouche, Garrigues, Teresa Vidal, *et al.*, 1997). There are different monitoring systems which can be implemented into a process and these are namely in-line or off-line systems. An in-line system will be situated directly in a process line or process vessel, which an off-line system will rely on measurements taken from discrete samples (Geörg, Schalk, Methner, *et al.*, 2015; Seborg, Edgar, Mellicamp, *et al.*, 2010). These can be displayed on multiple platforms with internet connectivity, resulting in on-line systems, however this is not required.

In most industries which make use of batch processes, monitoring of the products and automation of the control is becoming more common place due to the increase in availability of cutting-edge instrumentation and software. It is becoming more common to monitor batch processes in these industries with rapid in-line measurements rather than to manually draw and analyse samples.

2.5.2 Infrared Technology in Process Monitoring

For many industries, there is a need to monitor certain parameters to determine the quality, as well as authenticity or origin of their products. In addition to this, it is always beneficial to be able to do this as rapidly and non-destructively as possible. For this to be possible, spectroscopic methods can be applied. With the use of spectroscopy specific to the food and beverage

industries, information can be obtained regarding the structure, chemical composition, geographical origin, botanical origin and freshness (Medina *et al.*, 2019).

Many different industries utilize infrared technology in order to monitor variables and concentrations of certain compounds. The appeal of the technology is due to its non-invasive, rapid and multiparametric nature whereby one specialised measurement, such as an IR spectrum, can yield multiple predictions with minimal sample preparation often required (Ayvaz *et al.*, 2015; Ayvaz, Sierra-Cadavid, Aykas, *et al.*, 2016). The versatility of the technology also allows it to be used on samples in both liquid and solid phases.

IR spectroscopy has shown promise with fruits, vegetables, meat, dairy products, pharmaceutical and chemical products. Examples of industries which currenlty use IR spectroscopy, both in-line and off-line, can be seen in Table 2.1 along with the parameters measured in these applications. This table does not contain all industries which use IR, but rather serves to demonstrate the wide ranges of uses of this technology.

Table 2.1: Summary of Parameters Measured Using Infrared Spectroscopy

Parameters	**Industry Type**	**References**
Crystallisation in paracetamol production	Pharmaceutical	(Helmdach, Feth, Minnich, *et al.*, 2013)
Solution polymerisation of methyl methacrylate	Polymer Industry	(Šašić, Ozaki, Olinga, *et al.*, 2002)

Properties of apricot fruits such as firmness, soluble solids, sugar and acid content	Food	(Bureau *et al.*, 2009)
Fatty acids and triacylglycerols in virgin olive oil		(Dupuy, Galtier, Ollivier, *et al.*, 2010)
Moisture, acidity, ascorbic, soluble solids, and total sugar in guava and passion fruit pulp		(Alamar, Caramês, Poppi, *et al.*, 2016; Oliveira-Folador, Bicudo, de Andrade, *et al.*, 2018)
Colour, pH and water holding capacity of lamb meat		
Individual sugars, carotenoids, malic and citric acids in passion fruit		(Isaksson, Nilsen, Tøgersen, *et al.*, 1996; Kamruzzaman, ElMasry, Sun, *et al.*, 2012)
Moisture content, ash content, particle size and pasting property of corn meal grit		(de Oliveira, de Castilhos, Renard, *et al.*, 2014)
		(Ayvaz *et al.*, 2015)
Fat, dry matter, nitrogen content, pH and sodium chloride in cheeses	Dairy	(Karoui, Mouazen, Dufour, Pillonel, *et al.*, 2006; Karoui, Mouazen, Dufour, Schoonheydt, *et al.*, 2006)

Caffeine content in soft drinks	Beverage	(Daghbouche *et al.*, 1997)
Fructose, glucose, soluble solids, serum viscosity, Bostwick consistency, pH, Bostwick and total reducing sugars of tomato juice		(Ayvaz *et al.*, 2016)
Tartaric and citric acid in orange juice		(Cen, Bao, He, *et al.*, 2007)
Glucose, maltose, pH, lactic acid, total sugar, isomaltotriose, panose, nitrogen, isomaltose, non-sugar solids and total acids in Chinese Rice wine		(Shen *et al.*, 2011) (Zeaiter, Roger & Bellon-Maurel, 2006)

While the above information demonstrates the versatility of IR spectroscopy, it is still necessary to explore the potential for processes utilising this technology for in/on-line application and real-time monitoring of the processes.

Many different industries have studied the use of IR spectroscopy and have concluded that it is appropriate for use in on-line monitoring. Examples of these studies include one conducted by Isaksson et al., (1996) which concluded that IR spectroscopy can be used in meat production processes with success as well as by Zeaiter et al., (2006) which looked at a new method to ensure that on-line measurements for beverages remain robust when unknown influences are present.

2.6 Spectroscopy and In-Line Monitoring for Red Wine Making

2.6.1 IR Principles and Red Wine Compounds

As mentioned before, spectroscopy relies on how matter interacts with EM radiation. Covalent bonds present in many compounds are known to absorb certain frequencies in the IR range of the EM spectrum (Bauer *et al.*, 2008), that applies to compounds present in wine and grape must.

The different compounds in wine can be seen to interact in specific ways with the IR radiation. It is possible to utilize and observe bands which form in the IR region as a result of the different vibrations of C-H, O-H, N-H and S-H bonds (Budic-Leto, Gajdoš Kljusuric, Zdunic, *et al.*, 2011; Cozzolino *et al.*, 2011a). For example, in the case of hydrolysable tannins distinct absorption patterns can be seen in the region 1820 – 950 cm^{-1} when exploring the MIR range (Basalekou, Kallithraka, Tarantilis, *et al.*, 2019). The different absorption bands in this region are caused by the stretching vibration peaks of the carbonyl molecules and the benzene rings as well as the stretching of the C-O, C=O and C-C bonds (Basalekou *et al.*, 2019; Fernández, Labarca, Bordeu, *et al.*, 2007; Tondi & Petutschnigg, 2015). Similarly, this is true for other compounds in wine. For alcohol and water, the OH bond present produces bands, however, it is possible to distinguish between the band produced by water and that produced by ethanol (Bauer *et al.*, 2008).

2.6.2 IR Monitoring of Red Wine

IR spectroscopy and chemometrics have been reported to be valuables tools in the quantification of many different compounds and variables in fermenting wine and grape juice. Studies demonstrated that a combination of NIR and chemometrics showed promise as a method to monitor the progress of alcohol formation and phenolic extraction of a red wine fermentation from the start of alcoholic fermentation to the end (Aleixandre-Tudo *et al.*, 2017; Aleixandre-Tudo, Nieuwoudt, Aleixandre, *et al.*, 2018; Cozzolino, 2015; Cozzolino & Curtin, 2012; Cozzolino *et al.*, 2004; Patz, Blieke, Ristow, *et al.*, 2004; Urtubia, Pérez-correa, Pizarro, *et al.*, 2008; Wang, Li, Ma, *et al.*, 2014) Studies conducted by Blanco, Peinado and Mas, (2004) and Mazarevica et al., (2004) utilised IR spectroscopy to monitor the progression of alcoholic fermentation and found the models developed to have high correlations with reference data obtained. Earlier studies conducted by Cozzolino et al, (2004); Patz et al., (2004) and Urtubia et al., (2006) concluded that the use of NIR and IR technology would be a viable alternative to traditional analytical methods. Cozzolino et al., (2006) also predicted that more advanced systems, which incorporated aspects of automation could be used to monitor the progress of wine making. Many more studies which focus on phenolic compounds and acids have been conducted since these studies were published (Basalekou *et al.*, 2019; Basalekou, Pappas, Kotseridis, *et al.*, 2017; Cavaglia, Schorn-

García, Giussani, *et al.*, 2020; Parpinello, Ricci, Arapitsas, *et al.*, 2019; Petrovic *et al.*, 2020; dos Santos Costa, Oliveros Mesa, Santos Freire, *et al.*, 2019; Sen, Ozturk, Tokatli, *et al.*, 2016; Véstia, Barroso, Ferreira, *et al.*, 2019).

However, the vast majority of studies reviewed have performed analysis in a discontinuous manner with the IR spectroscopic analysis being conducted off-line and separate to the fermentation vessel (Cavaglia *et al.*, 2020; Cozzolino & Curtin, 2012; Cozzolino, Parker, Dambergs, *et al.*, 2006). Of the studies reviewed, only one utilised an automated, in-line pumping system for the monitoring of alcoholic fermentation (Mazarevica, Diewok, Baena, *et al.*, 2004).

Even though spectroscopy minimises sample preparation, it is necessary to determine the effect of this sample preparation as well as the turbidity caused by solids in suspensions of the sample. In the studies previously mentioned in this section, the vast majority involved complete removal of solids causing turbidity using centrifugation. In an article presented by Ferreiro-González et al., (2019), this was not the case. Instead, the samples were filtered through 0.45µm filters to remove impurities and reduce, but not completely remove, the components causing turbidity (Ferreiro-González, Ruiz-Rodríguez, Barbero, *et al.*, 2019). This appeared to be appropriate sample preparation as the models reported were suitable for the intended application in the optimisation of the ageing process.

2.7 Conclusion

Red wine is a complicated matrix with many different key compounds present. Certain of these compounds influence the important sensorial properties of the wine such as mouth feel and colour. As the wine industry is a highly competitive one, it is important to monitor the concentrations of the compounds at various stages of the winemaking process to ensure consistency between batches and to meet client expectations.

This becomes challenging as there are many different factors which can influence the concentrations of these compounds during the process of alcoholic fermentation. However, even though the concentrations of certain compounds can vary significantly depending on process conditions, many different wine making techniques have been shown to have certain predictable effects on these compounds. Knowing this, it is possible to manipulate these conditions to ensure certain trends occur during alcoholic fermentation. It would also be possible to form a database where this information is readily available for winemakers to use as part of a larger decision-making process.

As these compounds in wine have specific molecular structures and bonds, they will interact with electromagnetic radiation in unique ways. Due to this interaction with the infrared region of the electromagnetic spectrum, it becomes possible to determine what compounds are present in a

sample and to quantify their concentration with the use of IR technology and chemometrics. Currently methods exist to predict certain of these compounds in red wine.

To our knowledge, there has been little to no implementation of a suitable in-line and real-time monitoring system for monitoring the compounds of interest to winemakers in red wine fermentations. The implementation of a rapid, robust, and non-destructive system such as this would allow red wine fermentations to be more closely monitored. It could also potentially lead to new methods of process control to ensure that wines meet certain quantifiable specifications. As such, this project can provide new insight into utilising pre-existing IR technology and chemometric methods in a way that is more applicable to industrial wine making.

2.8 Literature Cited

Abbott, J.A. 1999. Quality measurement of fruits and vegetables. *Postharvest Biology and Technology*. 15(3):207–225.

Alamar, P.D., Caramês, E.T.S., Poppi, R.J. & Pallone, J.A.L. 2016. Quality evaluation of frozen guava and yellow passion fruit pulps by NIR spectroscopy and chemometrics. *Food Research International*. 85:209–214.

Aleixandre-Tudo, J.L. & du Toit, W. 2019. Understanding cold maceration in red winemaking: A batch processing and multi-block data analysis approach. *LWT - Food Science and Technology*. 111(May):147–157.

Aleixandre-Tudo, J.., Nieuwoudt, H., Aleixandre, J.. & Du Toit, W.. 2015. Robust Ultraviolet-Visible (UV-Vis) Partial Least-Squares (PLS) Models for Tannin Quantification in Red Wine. *Journal of Agricultural and Food Chemistry*. 63(4):1088–1098.

Aleixandre-Tudo, J.., Nieuwoudt, H. & du Toit, W. 2019. Towards on-line monitoring of phenolic content in red wine grapes: A feasibility study. *Food Chemistry*. 270(March 2018):322–331.

Aleixandre-Tudo, J.L., Buica, A., Nieuwoudt, H., Aleixandre, J.L. & Du Toit, W. 2017. Spectrophotometric Analysis of Phenolic Compounds in Grapes and Wines. *Journal of Agricultural and Food Chemistry*. 65(20):4009–4026.

Aleixandre-Tudo, J.L., Nieuwoudt, H., Aleixandre, J.L. & du Toit, W. 2018. Chemometric compositional analysis of phenolic compounds in fermenting samples and wines using different infrared spectroscopy techniques. *Talanta*. 176(August 2017):526–536.

Aleixandre-Tudo, J.L., Nieuwoudt, H., Olivieri, A., Aleixandre, J.L. & du Toit, W. 2018. Phenolic profiling of grapes, fermenting samples and wines using UV-Visible spectroscopy with chemometrics. *Food Control*. 85:11–22.

Apolinar-Valiente, R., Williams, P., Mazerolles, G., Romero-Cascales, I., Gómez-Plaza, E., López-Roca, J.M., Ros-García, J.M. & Doco, T. 2014. Effect of enzyme additions on the oligosaccharide composition of Monastrell red wines from four different wine-growing origins in Spain. *Food Chemistry*. 156:151–159.

Auw, J.M., Blanco, V., O'Keefe, S.F. & Sims, C.A. 1996. Effect of Processing on the Phenolics and Color of Cabernet Sauvignon, Chambourcin, and Noble Wines and Juices. *American Journal of Enology and Viticulture*. 47(3):279–286.

Ayvaz, H., Plans, M., Towers, B.N., Auer, A. & Rodriguez-Saona, L.E. 2015. The use of infrared spectrometers to predict quality parameters of cornmeal (corn grits) and differentiate between organic and conventional practices. *Journal of Cereal Science*. 62:22–30.

Ayvaz, H., Sierra-Cadavid, A., Aykas, D.P., Mulqueeney, B., Sullivan, S. & Rodriguez-Saona, L.E. 2016. Monitoring multicomponent quality traits in tomato juice using portable mid-infrared (MIR) spectroscopy and multivariate analysis. *Food Control*. 66:79–86.

Basalekou, M., Pappas, C., Kotseridis, Y., Tarantilis, P.A., Kontaxakis, E. & Kallithraka, S. 2017. Red wine age estimation by the alteration of its color parameters: Fourier transform infrared spectroscopy as a tool to monitor wine maturation time. *Journal of Analytical Methods in Chemistry*. 2017.

Basalekou, M., Kallithraka, S., Tarantilis, P.A., Kotseridis, Y. & Pappas, C. 2019. Ellagitannins in wines: Future prospects in methods of analysis using FT-IR spectroscopy. *Lwt*. 101(June 2018):48–53.

Bauer, R., Nieuwoudt, H., Bauer, F.F., Kossmann, J., Koch, K.R. & Esbensen, K.H. 2008. FTIR Spectroscopy for Grape and Wine Analysis. *Analytical Chemistry*. 80(5):1371–1379.

Bautista-Ortín, A.B., Fernández-Fernández, J.I., López-Roca, J.M. & Gómez-Plaza, E. 2007. The effects of enological practices in anthocyanins, phenolic compounds and wine colour and their dependence on grape characteristics. *Journal of Food Composition and Analysis*. 20(7):546–552.

Beaver, J.W., Miller, K. V., Medina-Plaza, C., Dokoozlian, N., Ponangi, R., Blair, T., Block, D. & Oberholster, A. 2019. Heat-dependent desorption of proanthocyanidins from grape-derived cellwall material under variable ethanol concentrations in model wine systems. *Molecules*. 24(19):1–13.

Beaver, J.W., Medina-Plaza, C., Miller, K., Dokoozlian, N., Ponangi, R., Blair, T., Block, D. & Oberholster, A. 2020. Effects of the Temperature and Ethanol on the Kinetics of Proanthocyanidin Adsorption in Model Wine Systems. *Journal of Agricultural and Food*

Chemistry. 68(10):2891–2899.
Bely, M., Sablarolles, J.M. & Barre, P. 1990. Description of Alcholic Fermentation Kinetics: Its Variability and Signficance. *American journal of enology and viticulture*. 41(4):319–324.
Bisson, L.F. 1999. Stuck and Sluggish Fermentations. *American Journal of Enology and Viticulture*. 50(1):107–119.
Blanco, M., Peinado, A.C. & Mas, J. 2004. Analytical Monitoring of Alcoholic Fermentation Using NIR Spectroscopy. *Biotechnology and Bioengineering*. 88(4):536–542.
Boulton, R. 1980. The Prediction of Fermentation Behaviour by a Kinetic Model. 31(1).
Bu, D. 2007. Chemometric Analysis for Spectroscopy. *Tech Flash*.
Budic-Leto, I., Gajdoš Kljusuric, J., Zdunic, G., Tomic-Potrebujes, I., Banovic, M., Kurtanjek, Ž. & Lovric, T. 2011. Usefulness of near infrared spectroscopy and chemometrics in screening of the quality of dessert wine Prošek. *Croat. J. Food Sci. Technol.* 3(2):9–15.
Buratti, S., Ballabio, D., Giovanelli, G., Dominguez, C.M.Z., Moles, A., Benedetti, S. & Sinelli, N. 2011. Monitoring of alcoholic fermentation using near infrared and mid infrared spectroscopies combined with electronic nose and electronic tongue. *Analytica Chimica Acta*. 697(1–2):67–74.
Bureau, S., Ruiz, D., Reich, M., Gouble, B., Bertrand, D., Audergon, J.M. & Renard, C.M.G.C. 2009. Rapid and non-destructive analysis of apricot fruit quality using FT-near-infrared spectroscopy. *Food Chemistry*. 113(4):1323–1328.
Casassa, L.F. 2017. Flavonoid Phenolics in Red Winemaking. in *Phenolic Compounds - Natural Sources, Importance and Applications*.
Cavaglia, J., Schorn-García, D., Giussani, B., Ferré, J., Busto, O., Aceña, L., Mestres, M. & Boqué, R. 2020. ATR-MIR spectroscopy and multivariate analysis in alcoholic fermentation monitoring and lactic acid bacteria spoilage detection. *Food Control*. 109:1–7.
Cen, H., Bao, Y., He, Y. & Sun, D.W. 2007. Visible and near infrared spectroscopy for rapid detection of citric and tartaric acids in orange juice. *Journal of Food Engineering*. 82(2):253–260.
Cetó, X., Gutiérrez, J.M., Gutiérrez, M., Céspedes, F., Capdevila, J., Mínguez, S., Jiménez-Jorquera, C. & Del Valle, M. 2012. Determination of total polyphenol index in wines employing a voltammetric electronic tongue. *Analytica Chimica Acta*. 732:172–179.
Chris Somers, T. & Evans, M.E. 1977. Spectral evaluation of young red wines: Anthocyanin equilibria, total phenolics, free and molecular SO2, “chemical age”. *Journal of the science of food and agriculture*. 28(3):279–287.
Colthup, N.B. 1961. Vibrating molecular models: Frequency shifts in strained ring double bonds. *Journal of Chemical Education*. 38(8):394–396.
Cozzolino, D; Dambergs, R.G. 2009. Wine and Beer. in *Infrared Spectroscopy for Food Quality Analysis and Control*. 127–168.
Cozzolino, D. 2015.
Cozzolino, D. & Curtin, C. 2012. The use of attenuated total reflectance as tool to monitor the time course of fermentation in wild ferments. *Food Control*. 26(2):241–246.
Cozzolino, D., Kwiatkowski, M.J., Parker, M., Cynkar, W.U., Dambergs, R.G., Gishen, M. & Herderich, M.J. 2004. Prediction of phenolic compounds in red wine fermentations by visible and near infrared spectroscopy. *Analytica Chimica Acta*. 513(1):73–80.
Cozzolino, D., Parker, M., Dambergs, R.G., Herderich, M. & Gishen, M. 2006. Chemometrics and Visisble-Near Infrared Spectroscopic Monitoring of Red Wine Fermentation in a Pilot Scale. *Biotechnology and Bioengineering*. 95(6):1101–1107.
Cozzolino, D., Cynkar, W., Shah, N. & Smith, P. 2011a. Technical solutions for analysis of grape juice, must, and wine: The role of infrared spectroscopy and chemometrics. *Analytical and Bioanalytical Chemistry*. 401(5):1479–1488.
Cozzolino, D., Cynkar, W., Shah, N. & Smith, P. 2011b. Feasibility study on the use of attenuated total reflectance mid-infrared for analysis of compositional parameters in wine. *Food Research International*. 44(1):181–186.
Daghbouche, Y., Garrigues, S., Teresa Vidal, M. & De la Guardia, M. 1997. Flow Injection Fourier Transform Infrared Determination of Caffeine in Soft Drinks. *Analytical Chemistry*. 69(6):1086–1091.
Dupuy, N., Galtier, O., Ollivier, D., Vanloot, P. & Artaud, J. 2010. Comparison between NIR, MIR, concatenated NIR and MIR analysis and hierarchical PLS model. Application to virgin olive

oil analysis. *Analytica Chimica Acta*. 666(1–2):23–31.
Favre, G., Peña-Neira, Á., Baldi, C., Hernández, N., Traverso, S., Gil, G. & González-Neves, G. 2014. Low molecular-weight phenols in Tannat wines made by alternative winemaking procedures. *Food Chemistry*. 158:504–512.
Federico Casassa, L., Bolcato, E.A., Sari, S.E., Fanzone, M.L. & Jofré, V.P. 2016. Combined effect of prefermentative cold soak and SO2 additions in Barbera D'Asti and Malbec wines: Anthocyanin composition, chromatic and sensory properties. *LWT - Food Science and Technology*. 66:134–142.
Fernández, K., Labarca, X., Bordeu, E., Guesalaga, A. & Agosin, E. 2007. Comparative Study of Wine Tannin Classification Using Fourier Transform Mid-Infrared Spectrometry and Sensory Analysis. *Applied Spectroscopy*. 61(11):1163–1167.
Ferreiro-González, M., Ruiz-Rodríguez, A., Barbero, G.F., Ayuso, J., Álvarez, J.A., Palma, M. & Barroso, C.G. 2019. FT-IR, Vis spectroscopy, color and multivariate analysis for the control of ageing processes in distinctive Spanish wines. *Food Chemistry*. 277(July 2018):6–11.
Fragoso, S., Aceña, L., Guasch, J., Mestres, M. & Busto, O. 2011. Quantification of phenolic compounds during red winemaking using FT-MIR spectroscopy and PLS-regression. *Journal of Agricultural and Food Chemistry*. 59(20):10795–10802.
Fragoso, S., Aceña, L., Guasch, J., Busto, O. & Mestres, M. 2011. Application of FT-MIR spectroscopy for fast control of red grape phenolic ripening. *Journal of Agricultural and Food Chemistry*. 59(6):2175–2183.
Gambuti, A., Strollo, D., Erbaggio, A., Lecce, L. & Moio, L. 2007. Effect of Winemaking Practices on Color Indexes and Selected Bioactive Phenolics of Aglianico Wine. *Journal of Food Science*. 72(9):623–628.
Garlick, J.L. 2013. Bioprocess monitoring and chemometric modelling of wine fermentations. [Online], Available: https://scholar.sun.ac.za/handle/10019.1/80033.
Garrido-Bañuelos, G. 2018. Factors influencing the colour and phenolic composition of Shiraz wine during winemaking by.
Geldenhuys, L. 2009. Influence of oxygen addition on the phenolic composition of red wine.
Genisheva, Z., Quintelas, C., Mesquita, D.P., Ferreira, E.C., Oliveira, J.M. & Amaral, A.L. 2018. New PLS analysis approach to wine volatile compounds characterization by near infrared spectroscopy (NIR). *Food Chemistry*. 246(November 2017):172–178.
Geörg, D., Schalk, R., Methner, F.J. & Beuermann, T. 2015. MIR-ATR sensor for process monitoring. *Measurement Science and Technology*. 26(6).
Gil-Muñoz, R., Moreno-Pérez, A., Vila-López, R., Fernández-Fernández, J.I., Martínez-Cutillas, A. & Gómez-Plaza, E. 2009. Influence of low temperature prefermentative techniques on chromatic and phenolic characteristics of Syrah and Cabernet Sauvignon wines. *European Food Research and Technology*. 228(5):777–788.
Girard, B., Yuksel, D., Cliff, M.A., Delaquis, P. & Reynolds, A.G. 2001. Vinification effects on the sensory, colour and GC profiles of Pinot noir wines from British Columbia. *Food Research International*. 34(6):483–499.
Gishen, M., Dambergs, R.. & Cozzolino, D. 2008. Grape and wine analysis - enhancing the power of spectroscopy with chemometrics.. *Australian Journal of Grape and Wine Research*. 11(3):296–305.
Glories, Y. (1984). La couleur des vins rouges, 2eme partie. Connaissance de La Vigne et Du Vin, 18, 253e271.
Gómez-Plaza, E., Gil-Muñoz, R., López-Roca, J.M., Martínez-Cutillas, A. & Fernández-Fernández, J.I. 2001. Phenolic Compounds and Color Stability of Red Wines: Effect of Skin Maceration Time. *American Journal of Enology and Viticulture*. 52(3):266–270.
González-Neves, G., Gil, G., Barreiro, L. & Favre, G. 2010. Pigment profile of red wines cv. Tannat made with alternative winemaking techniques. *Journal of Food Composition and Analysis*. 23(5):447–454.
Harbertson, J.F., Picciotto, E.A. & Adams, D.O. 2003. Measurement of Polymeric Pigments in Grape Berry Extracts and Wines Using a Protein Precipitation Assay Combined with Bisulfite Bleaching. *American Journal of Enology and Viticulture*. 54(4):301–306.
Helmdach, L., Feth, M.P., Minnich, C. & Ulrich, J. 2013. Application of ATR-MIR spectroscopy in the pilot plant—Scope and limitations using the example of Paracetamol crystallizations. *Chemical Engineering & Processing: Process Intensification*. 70:184–197.

Huang, H., Yu, H., Xu, H. & Ying, Y. 2008. Near infrared spectroscopy for on/in-line monitoring of quality in foods and beverages: A review. *Journal of Food Engineering*. 87(3):303–313.

Ibrahim, M., Alaam, M., El-Haes, H., Jalbout, A.F. & De Leon, A. 2006. Analysis of the structure and vibrational spectra of glucose and fructose. *Ecletica Quimica*. 31(3):15–21.

Iland, P., Ewart, A., Sitters, J., Markides, A., & Bruer, N. (2000). Techniques for chemical analysis and quality monitoring during winemaking (1st ed., pp. 1e111). Camp- belltown, South Australia: Patrick Iland Wine Promotions.

Isaksson, T., Nilsen, B.N., Tøgersen, G., Hammond, R.P. & Hildrum, K.I. 1996. On-Line, Proximate Analysis of Ground Beef Directly at a Meat Grinder Outlet. *Meat Science*. 43(3–4):245–253.

Ivanova, V., Vojnoski, B. & Stefova, M. 2012. Effect of winemaking treatment and wine aging on phenolic content in Vranec wines. *Journal of Food Science and Technology*. 49(2):161–172.

Jackson, R. 2008. *Wine Science*. Third Edit ed. San Diego.

Kamruzzaman, M., ElMasry, G., Sun, D.W. & Allen, P. 2012. Prediction of some quality attributes of lamb meat using near-infrared hyperspectral imaging and multivariate analysis. *Analytica Chimica Acta*. 714:57–67.

Karoui, R., Mouazen, A.M., Dufour, É., Pillonel, L., Schaller, E., Picque, D., De Baerdemaeker, J. & Bosset, J.O. 2006. A comparison and joint use of NIR and MIR spectroscopic methods for the determination of some parameters in European Emmental cheese. *European Food Research and Technology*. 223(1):44–50.

Karoui, R., Mouazen, A.M., Dufour, É., Schoonheydt, R. & De Baerdemaeker, J. 2006. A comparison and joint use of VIS-NIR and MIR spectroscopic methods for the determination of some chemical parameters in soft cheeses at external and central zones: A preliminary study. *European Food Research and Technology*. 223(3):363–371.

Kelebek, H., Canbas, A. & Selli, S. 2008. Pectolytic Enzyme Addition on the Anthocyanin. *Journal of Food Processing and Preservation*. 33(2009):296–311.

Khanbabaee, K. & van Ree, T. 2001. Tannins: Classification and Definition. *Natural Product Reports*. 18(6):641–649.

Larkin, P. 2011. *Infrared and Raman Spectroscopy; Principles and Spectral Interpretation*.

Lavine, B. & Workman, J. 2010. Chemometrics. 82(12):4699–4711.

Li, S.Y., Zhu, B.Q., Li, L.J. & Duan, C.Q. 2017. Extensive and objective wine color classification with chromatic database and mathematical models. *International Journal of Food Properties*. 20(53):S2647–S2659.

Linnet, K. 1993. Evaluation of Regression Procedures for Methods Comparison Studies. 39(3):424–432.

Lochner, E. 2006. The evaluation of Fourier transform infrared spectroscopy (FT-IR) for the determination of total phenolics and total anthocyanins concentrations of grapes by.

Lourenço, N.D., Lopes, J.A., Almeida, C.F., Sarraguça, M.C. & Pinheiro, H.M. 2012. Bioreactor monitoring with spectroscopy and chemometrics: A review. *Analytical and Bioanalytical Chemistry*. 404(4):1211–1237.

Ma, W., Guo, A., Zhang, Y., Wang, H., Liu, Y. & Li, H. 2014. A review on astringency and bitterness perception of tannins in wine. *Trends in Food Science and Technology*. 40(1):6–19.

Mazarevica, G., Diewok, J., Baena, J.R., Rosenberg, E. & Lendl, B. 2004. On-line fermentation monitoring by mid-infrared spectroscopy. *Applied Spectroscopy*. 58(7):804–810.

McRae, J.M., Day, M.P., Bindon, K.A., Kassara, S., Schmidt, S.A., Schulkin, A., Kolouchova, R. & Smith, P.A. 2015. Effect of early oxygen exposure on red wine colour and tannins. *Tetrahedron*. 71(20):3131–3137.

Medina-Plaza, C., Beaver, J.W., Miller, K. V., Lerno, L., Dokoozlian, N., Ponangi, R., Blair, T., Block, D.E., et al. 2020. Cell Wall–Anthocyanin Interactions during Red Wine Fermentation-Like Conditions. *American Journal of Enology and Viticulture*. 71(2):149–156.

Medina, S., Perestrelo, R., Silva, P., Pereira, J.A.M. & Câmara, J.S. 2019. Current trends and recent advances on food authenticity technologies and chemometric approaches. *Trends in Food Science and Technology*. 85(December 2018):163–176.

Mercurio, M.D., Dambergs, R.G., Herderich, M.J. & Smith, P.A. 2007. High throughput analysis of red wine and grape phenolics - Adaptation and validation of methyl cellulose precipitable tannin assay and modified somers color assay to a rapid 96 well plate format. *Journal of*

Agricultural and Food Chemistry. 55(12):4651–4657.

Moenne, M.I., Saa, P., Laurie, V.F., Pérez-Correa, J.R. & Agosin, E. 2014. Oxygen Incorporation and Dissolution During Industrial-Scale Red Wine Fermentations. *Food and Bioprocess Technology*. 7(9):2627–2636.

Monod, J. (1949).The Growth of Bacterial Cultures. Annual Reviews in M, 3(XI), 371 -394

Morata, A. 2019. *Red wine technology*. A. Morata (ed.).

Moreno-Arribas, M.V. & Polo, M.C. 2009. *Wine chemistry and biochemistry*. M.C.P.M.V. Moreno-Arribas (ed.). New York.

Oliveira-Folador, G., Bicudo, M. de O., de Andrade, E.F., Renard, C.M.G.C., Bureau, S. & de Castilhos, F. 2018. Quality traits prediction of the passion fruit pulp using NIR and MIR spectroscopy. *Lwt*. 95(October 2017):172–178.

de Oliveira, G.A., de Castilhos, F., Renard, C.M.G.C. & Bureau, S. 2014. Comparison of NIR and MIR spectroscopic methods for determination of individual sugars, organic acids and carotenoids in passion fruit. *Food Research International*. 60:154–162.

Olivieri, A.C. 2015. Practical guidelines for reporting results in single- and multi-component analytical calibration: A tutorial. *Analytica Chimica Acta*. 868:10–22.

Ortega-Heras, M., Pérez-Magariño, S. & González-Sanjosé, M.L. 2012. Comparative study of the use of maceration enzymes and cold pre-fermentative maceration on phenolic and anthocyanic composition and colour of a Mencía red wine. *LWT - Food Science and Technology*. 48(1):1–8.

Parpinello, G.P., Ricci, A., Arapitsas, P., Curioni, A., Moio, L., Segade, S.R., Ugliano, M. & Versari, A. 2019. Multivariate characterisation of Italian monovarietal red wines using MIR spectroscopy. *Oeno One*. 53(4):741–751.

Pasquini, C. 2018. Near infrared spectroscopy: A mature analytical technique with new perspectives – A review. *Analytica Chimica Acta*. 1026:8–36.

Patz, C.D., Blieke, A., Ristow, R. & Dietrich, H. 2004. Application of FT-MIR spectrometry in wine analysis. *Analytica Chimica Acta*. 513(1):81–89.

Petrovic, G., Aleixandre-Tudo, J.L. & Buica, A. 2020. Viability of IR spectroscopy for the accurate measurement of yeast assimilable nitrogen content of grape juice. *Talanta*. 206(April 2019):120241.

Ribéreau-Gayon, P., Glories, Y., Maujean, A. & Dubourdieu, D. 2006. *Handbook of Enology*. Second Edi ed. Sussex: John Wiley & Sons.

Sacchi, K.L., Bisson, L.F. & Adams, D.O. 2005. Effect of Winemaking Techniques on Phenolic Extraction. *American Journal of Enology and Viticulture*. 56(3):197–206. [Online], Available: https://www.ajevonline.org/content/ajev/56/3/197.full.pdf%0Ahttps://pdfs.semanticscholar.org/e40f/0c5a805a79380ae5645f0f78dca4893e02ee.pdf.

Santos, P.M. & Colnago, L.A. 2018. Comparison Among MIR, NIR, and LF-NMR Techniques for Quality Control of Jam Using Chemometrics. *Food Analytical Methods*. 11(7):2029–2034.

dos Santos Costa, D., Oliveros Mesa, N.F., Santos Freire, M., Pereira Ramos, R. & Teruel Mederos, B.J. 2019. Development of predictive models for quality and maturation stage attributes of wine grapes using vis-nir reflectance spectroscopy. *Postharvest Biology and Technology*. 150(May 2018):166–178.

Šašić, S., Ozaki, Y., Olinga, A. & Siesler, H.W. 2002. Comparison of various chemometric evaluation approaches for on-line FT-NIR transmission and FT-MIR/ATR spectroscopic data of methyl methacrylate solution polymerization. *Analytica Chimica Acta*. 452(2):265–276.

Schmidt, J.O. & Noble, A.C. 1983. Investigation of the Effect of Skin Contact Time on Wine Flavour. *American Journal of Enology and Viticulture*. 34(3):135–138.

Seborg, D., Edgar, T., Mellicamp, D. & Doyle III, F. 2010. *Process Dynamics and Control*.

Sen, I., Ozturk, B., Tokatli, F. & Ozen, B. 2016. Combination of visible and mid-infrared spectra for the prediction of chemical parameters of wines. *Talanta*. 161:130–137.

Setford, P.C., Jeffery, D.W., Grbin, P.R. & Muhlack, R.A. 2017. Factors affecting extraction and evolution of phenolic compounds during red wine maceration and the role of process modelling. *Trends in Food Science and Technology*. 69:106–117.

Setford, P.C., Jeffery, D.W., Grbin, P.R. & Muhlack, R.A. 2019. Mathematical modelling of anthocyanin mass transfer to predict extraction in simulated red wine fermentation scenarios. *Food Research International*. 121(October 2018):705–713.

Shen, F., Ying, Y., Li, B., Zheng, Y. & Hu, J. 2011. Prediction of sugars and acids in Chinese rice

wine by mid-infrared spectroscopy. *Food Research International*. 44(5):1521–1527.
Smith, P.A., Mcrae, J.M. & Bindon, K.A. 2015. Impact of winemaking practices on the concentration and composition of tannins in red wine. *Australian Journal of Grape and Wine Research*. 21:601–614.
Sun, D.W. 2010. *Hyperspectral Imaging for Food Quality Analysis and Control*.
Tondi, G. & Petutschnigg, A. 2015. Middle infrared (ATR FT-MIR) characterization of industrial tannin extracts. *Industrial Crops and Products*. 65:422–428.
Urtubia, A., Pérez-correa, J.R., Pizarro, F. & Agosin, E. 2008. Exploring the applicability of MIR spectroscopy to detect early indications of wine fermentation problems. *Food Control*. 19(4):382–388.
Véstia, J., Barroso, J.M., Ferreira, H., Gaspar, L. & Rato, A.E. 2019. Predicting calcium in grape must and base wine by FT-NIR spectroscopy. *Food Chemistry*. 276(February 2018):71–76.
Volschenk, H., van Vuuren, H.J.J. & Viljoen-Bloom, M. 2017. Malic Acid in Wine: Origin, Function and Metabolism during Vinification. *South African Journal of Enology & Viticulture*. 27(2):123–136.
Wang, J., Huo, S., Zhang, Y., Liu, Y. & Fan, W. 2016. Effect of different pre-fermentation treatments on polyphenols, color, and volatile compounds of three wine varieties. *Food Science and Biotechnology*. 25(3):735–743.
Wang, Q., Li, Z., Ma, Z. & Liang, L. 2014. Real time monitoring of multiple components in wine fermentation using an on-line auto-calibration Raman spectroscopy. *Sensors and Actuators, B: Chemical*. 202:426–432.
Waterhouse, A.. 2002. Wine Phenolics. *Annals New York Academy of Sciences*. 6(2):21–36.
Weber, R.O., Nelson, M.I. & Gay, S. 2002. Modelling wine production. *Emac*. (December 2013):237–240.
Westad, F. & Marini, F. 2015. Validation of chemometric models - A tutorial. *Analytica Chimica Acta*. 893:14–24.
Williams, P., Dardenne, P. & Flinn, P. 2017. Tutorial: Items to be included in a report on a near infrared spectroscopy project. *Journal of Near Infrared Spectroscopy*. 25(2):85–90.
Wu, Z., Xu, E., Long, J., Zhang, Y., Wang, F., Xu, X., Jin, Z. & Jiao, A. 2015. Monitoring of fermentation process parameters of Chinese rice wine using attenuated total reflectance mid-infrared spectroscopy. *Food Control*.
Yoon, H., Klinzing, G. & Blanch, H.W. 1977. Competition for Mixed Substrates by Microbial Populations. *Biotechnology and Bioengineering*. 19(8):1193–1210.
Zanoni, B., Siliani, S., Canuti, V., Rosi, I. & Bertuccioli, M. 2010. A kinetic study on extraction and transformation phenomena of phenolic compounds during red wine fermentation. *International Journal of Food Science and Technology*. 45(10):2080–2088.
Zeaiter, M., Roger, J.M. & Bellon-Maurel, V. 2006. Dynamic orthogonal projection. A new method to maintain the on-line robustness of multivariate calibrations. Application to NIR-based monitoring of wine fermentations. *Chemometrics and Intelligent Laboratory Systems*. 80(2):227–235.

Chapter 3

Automated System Prototype Development and Instrumentation

Chapter 3 – Automated System Prototype Development and Instrumentation

3.1 Introduction

As the technology for fermentation monitoring improves, there are many opportunities for it to be incorporated into wineries. In some cases, new wineries will be built, and existing wineries may expand. In both cases, the implementation of the instrumentation and necessary hardware can be incorporated into the design phase of these projects. However, if an existing winery should choose to implement this technology to pre-existing equipment, modifications should, ideally, be minimal. As such, new developments should aim for simplicity and ease of installation. It may seem as though the easiest solution would be to design bespoke systems for each individual case. However, systems with custom made components will come at a high cost with long waiting periods (Dalgleish, Williams, Golden, *et al.*, 2008). Additionally, maintenance will be challenging, and spare parts will be expensive and will not be readily available. As such, it is more beneficial to use standard and commercially available components. Therefore, selection of equipment becomes an important factor to consider.

These are just a few considerations when designing a prototype system and there are many more to be considered for the system to meet design specifications. Therefore, the design process is an iterative one which involves many steps where selections are made, and rigorous testing is conducted (Sinnot, 2005). Due to this iterative nature, the design process can yield numerous prototypes, each of which are refined until it meets the system specifications. When a design involves multiple subsystems that must work in conjunction with each other and with pre-existing systems, many steps can involve a “trial and error” approach. In these cases, fine adjustments need to be made until each subsystem is functioning properly. Whilst the physical design is very important, part of the design of a system includes careful selection of materials. When dealing with beverages, food safe material should be used (Siebert & Stoeker, 1997). These are materials which are non-reactive, hygienic and corrosion resistant. In addition to this, it is important to minimise the cost. This is the starting point when choosing equipment for a process such as this.

The aim of this chapter was to develop an automated sampling system which incorporated infrared instrumentation for the purpose of monitoring red wine fermentations. This chapter details this design process for a prototype system, where, in this case, the sample would be discarded after scanning. The design began with a material analysis to ensure that food safe material was used which showed good corrosion resistance to alcoholic beverages. Next, the specifications for each physical component of the system were considered and a selection process with rigorous

testing took place. Once the equipment had been selected and these parts connected, it was necessary to consider the software aspect. This process did not require the iterative and comprehensive testing process that the physical components required. Instead, the process of scanning and analysis was broken down into basic steps that could be coded efficiently. Finally, this chapter also details the basic proof of concept testing and the recommendations that this testing yielded for continued improvement.

The final system consisted of a series of dosing pumps leading into a junction, which in turn, led directly into the instrument. This did require the sample to be discarded afterwards as return to the tank was not possible without further implementation of valves.

3.2 Requirements and Selection of Equipment

3.2.1 Materials of Construction

When selecting a material to use in the design of a process, there are many things to first be considered. The most important aspects to keep in mind are (Sinnot, 2005):

- Physical and mechanical properties and how these may change based on fluctuations in temperature and pH
- Ease of manufacture and ease of obtaining the material in standard sizes
- Corrosion resistance
- Cost

Corrosion is a concern in many different processes as it can lead to equipment failure or contamination of the product. It can be caused by reactions taking place between the process fluid and the materials used in construction of the equipment (Siebert & Stoeker, 1997). Materials chosen for use in the food and beverage industry should be non-reactive and they should promote hygienic process conditions. Usually this means that the chosen material is either UNS S31600 or UNS S30400 stainless steel due to the passive oxide films providing corrosion resistance (Sinnot, 2005).

This is no different in the wine industry as many different chemical compounds form part of wine, and most of these have corrosive properties. The compounds present in wine which are most likely to corrode process equipment are water, ethanol, citric acid, tartaric acid, acetic acid, malic acid and bisulphites used in the wine making process (Salas, Wiener, Stoytcheva, *et al.*, 2012). This composition needs to be kept in mind during the selection of materials.

Of course, cost effectiveness and ease of use is also of utmost importance during the selection process. As stainless steel lends itself better to permanent and semi-permanent fixtures and requires specialised equipment to manufacture and install, it may not be the appropriate choice given that, in this case, corrosion resistance would be the only benefit. In addition, it can also become costly to manufacture process equipment entirely out of stainless steel. There are many other materials which possess good corrosion resistance and meet the requirements for cost and ease of use. For wine specifically, these include nylon, natural rubber, certain performance plastics and silicone (Cole-Parmer, 2020).

3.2.2 Modification of Original Fermentation Vessel

In certain cases, such as the expansion of an existing winery or a new winery being built, the incorporation of a sampling system and instrumentation would form part of the design phase.

However, a more likely scenario, would be the addition of such a system to the existing set-up in an established winery.

Figure 3.1 shows a basic diagram of the original fermentation vessel and pump-over system first considered for this system. The original fermentation vessels have a capacity of 60 L with a 20 mm inner diameter (ID) outlet leading to a pump. The piping of the pump-over system provided a convenient outlet for the addition of a junction which would allow sampling. The junction was designed to, firstly, provide an additional outlet from the vessel and its integrated pump over system and, secondly, to reduce the piping diameter from the original 20 mm ID to a 4 mm ID used in commercially available sampling pumps available.

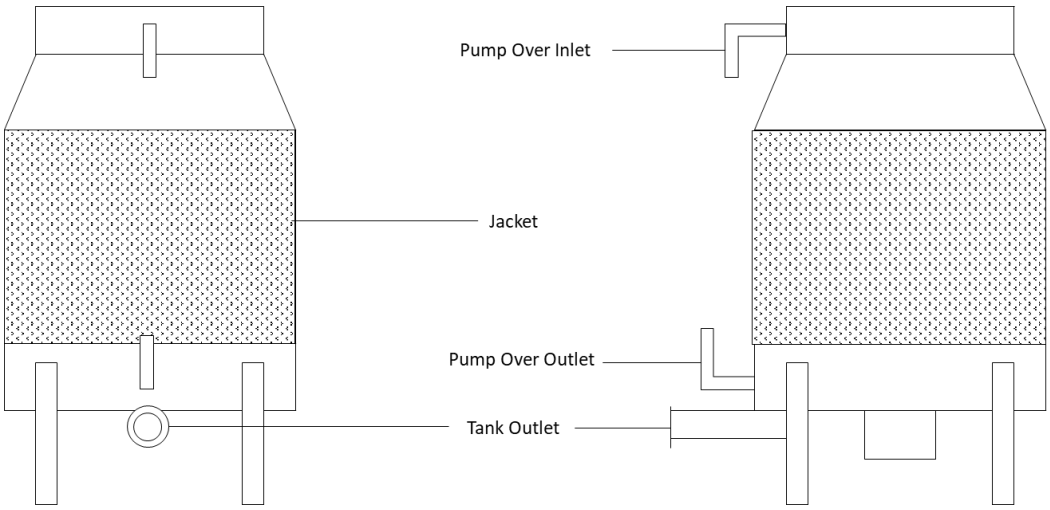

Figure 3.1: Diagram of Fermentation Vessel

Figure 3.2 shows a diagram of the junction designed for the system as well as how it can be connected to the outlet of the fermentation vessel. From Figure 3.2 the junction has a 20mm ID and fits in between the vessel outlet and the pump-over pipe. The outlet narrows from a 20mm ID to a 4mm ID nozzle where the plumbing for the sampling pumps can be connected. The nozzle can also be blocked off should the pump need to be disconnected for any reason.

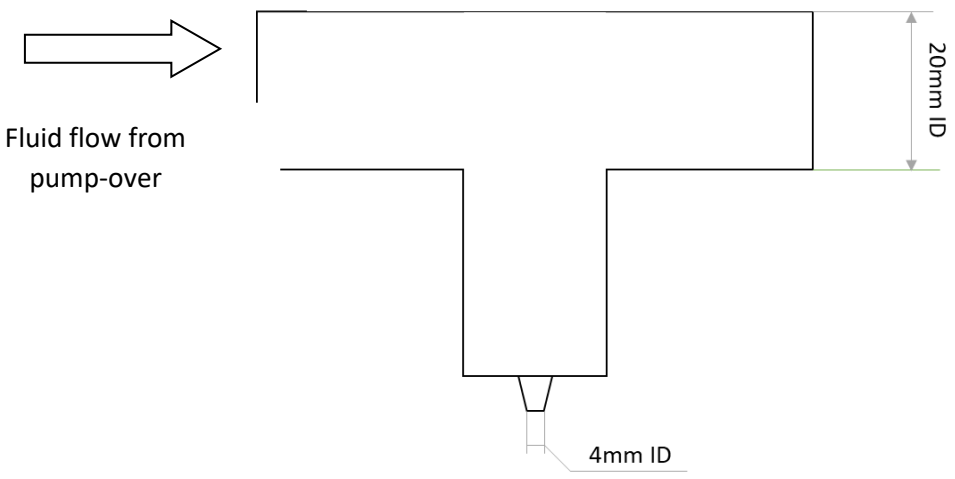

Figure 3.2: Diagram of Junction Designed for Sampling Outlet

3.2.3 Sampling Pump Requirements

To properly select a pump to sample from the tank, a few aspects must first be considered. The most important of these are the flow capacity, operating pressure, presence of solids, and physical and chemical properties of the liquid. Two different types of pumps will be discussed to provide context.

Centrifugal pumps consist of a shaft-mounted, rotating impeller encased in a cowl. Briefly, power is applied to the pump's shaft, cause the impeller to rotate. As this occurs, the pressure at the entrance of the pump is lowered and fluid flows into the impeller blades as a result of this. The fluid is forced towards the outer edges of the blades, where it then exits the pump via a volute chamber (Boyce, 1997). Positive displacement pumps have many different rotary or reciprocating mechanisms to achieve fluid displacement, however, all positive displacement pumps will achieve fluid flow via the alternate filling and emptying of a cavity with mechanical action (Boyce, 1997). Rotary pumps achieve this via the rotation of parts within a housing as shown in Figure 3.3 below.

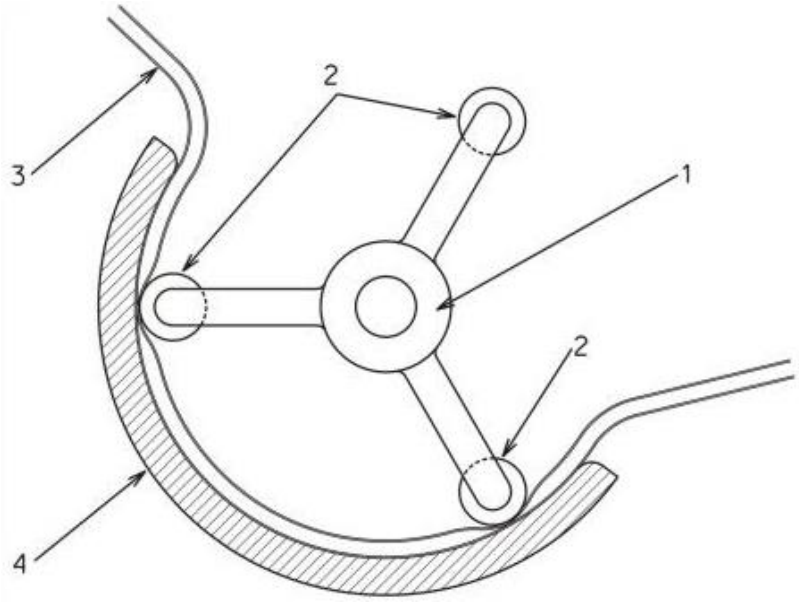

Figure 3.3: Diagram of a Peristaltic Pump, by Jonasz, Wikimedia Commons, is licensed under CC BY-SA 3.0

To not introduce unnecessary heating and shear to the sample and to ensure that no damage to a pump occurs due to solids content, the pump used should be a form of positive displacement pump rather than a centrifugal pump. As this system is automated, the pumps must be fully programmable. To ensure efficient and accurate operation, they must be able to automatically dispense a volume of fluid at a precise time. However, this sample must be dispensed at a low flow rate and a low pressure to avoid damage to the instrumentation and to maintain integrity of the sample. A further consideration was potential contamination if only one pump was used for the twelve-tank system as this would not allow complete isolation. To resolve this problem, a

sampling pump would be needed for each tank or a pump with multiple heads would have to be used. Finally, to ensure a cost-efficient system that can be assembled in a short time frame, only commercially available peristaltic pumps were considered.

Auto-dosing pumps were found to meet all the requirements listed above and are manufactured using inert, hygienic, and non-reactive materials due to their widespread use in marine tanks. There are many different dosing pumps available commercially such as the Jebao Programmable Auto Dosing DP-4 pumps, Bubble Magus T11, and the Kamoer X4 and F4 Wifi dosing pumps. Table 3.1a, which can be found in Supplementary Material (S5), details differences in these pumps. Of these the Jebao pumps were the cheapest and had the option of sampling up to 24 times per day. In contrast, the Bubble Magus only allowed for 11 samples per day. Whilst also allowing a maximum of 24 samples per day, the Kamoer pumps were double the cost of the others. In addition to this, it also required a device which could run the necessary app to program it as well as a stable Wi-Fi connection. Therefore, due to cost considerations and programmability, the pumps which we used were the Jebao Programmable Auto Dosing DP-4 pumps. Figure3.4 shows the pump selected for the system during its testing phase.

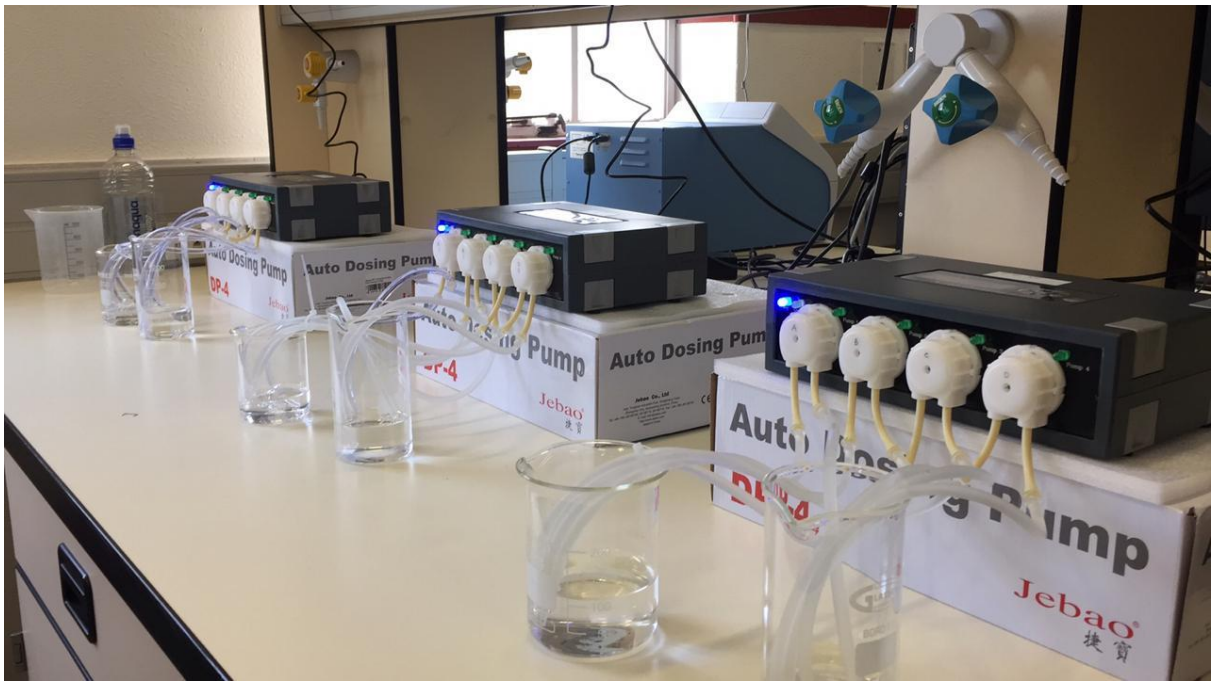

Figure 3.4: Photograph of Selected Sampling Pump

3.2.4 Filtration

Filtration involves the separation of solids from a liquid stream with the use of a physical barrier. Once filtered, the solids remaining are referred to as the filter cake and the remaining fluids are referred to as the filtrate (Dahlstrom, Bennett, Emmett, *et al.*, 1997). There are many different purposes for filtration, however, for this project, the goals are to remove solids to facilitate the

efficient operation of the system and to decrease and standardise the turbidity of the sample before scanning.

The requirements for the filtration are as follows:

- To ensure that seeds and large pieces of grape flesh and skin do not make their way into the sampling system where blockage can easily occur
- A filter which is easy to clean and does not require daily replacement of the barrier
- A filter made of non-reactive and food grade material
- A filter which can be installed in-line
- A filter which does not require high pressure operation
- A filter which is commercially available to reduce cost and lead-time

As there are many commercial filters available, the suitability had to be determined via small scale testing. There are many factors to consider when performing a small-scale filtration test such as cake thickness control, vacuum, pressure, and ensuring representative samples.

Twelve small scale wine fermentations of 20 kg were made using two different cultivars and different enzymatic treatments. The two cultivars used were Cabernet Franc and Shiraz both from the Cape Winelands region of the Western Cape. All grapes were crushed on the same day and all fermentations took place at 25 ^{o}C with punch downs occurring three times daily. Of the twelve fermentations, three consisted of Shiraz without enzymatic treatment, three were made with Shiraz with an enzymatic treatment (Lafase® HE Grand CRU Vin Rouge enzymes), three were Cabernet Franc without enzyme treatment, and finally Cabernet Franc with enzymatic treatment. Sampling took place once a day in the morning and each 100mL sample was filtered manually through the chosen filters.

The filters chosen for the small-scale testing were the following:

- Ecotao Enterprise 25 µm Nylon mesh
- Ecotao Enterprise 38 µm Nylon mesh
- Parker A-Lok 125 µm stainless steel inline water filters
- Xylem Flojet ¾” push-fit stainless steel 400 µm process pump filters

The first test was to determine whether the 100 mL samples could be filtered at low pressure without blockage occurring. If blockage occurred, the filters were excluded from further testing as they would not perform once in-line with the prototype as they also would not be able to filter larger volumes of liquid. The Ecotao filters both blocked after receiving only 2mL of fluid, which the Parker filter received three 100mL samples before blockage occurred. The only filter where

blockage did not occur for all twelve samples for the 10 days of fermentation was the Xylem Flojet. The filters were not cleaned in between consecutive days to better represent an in-line system.

The second test to determine the suitability was to connect the filter to a fermentation vessel and perform three pump overs a day for a 60 kg fermentation to determine whether the filter could be used in a real-world situation without blockage occurring. The filter developed a filter cake on the third day of fermentation, but pump overs were still possible by the end of the 10-day fermentation without complete blockages occurring. As such the filter selected for the prototype was the Xylem Flojet, which can be seen bellow in Figure 3.5

Figure 3.5: Filter Selected for System

3.2.5 Piping and Connections

High performance plastics were deemed to be a suitable and a cost-effective option for the piping in the sample system. After further consulting with suppliers of food-grade plastic tubing, the tubing selected was Tygon S3 B-44-3 4 mm ID food grade, high-performance plastic tubing. Nylon was shown to be suitable for fermentations, and as such all push-fit connectors and nozzles were manufactured from Nylon.

In Figure 3.6, the placement of the existing experimental cellar can be seen outlined in black. This set-up was adapted so that the instrumentation, pumping systems, and plumbing could be implemented to allow for automatic sample and in-line analysis. The placement of the plumbing and the external sampling pumps can be seen in Figure 3.6 in red while the placement of the instrumentation can be seen outline in green. The placement of the instrument was to minimise the amount of piping required and to reduce trip hazards to those working in the experimental cellar.

Key

PP – Pump-over Pump
SP – Sampling Pump
IR – Infrared Instrument

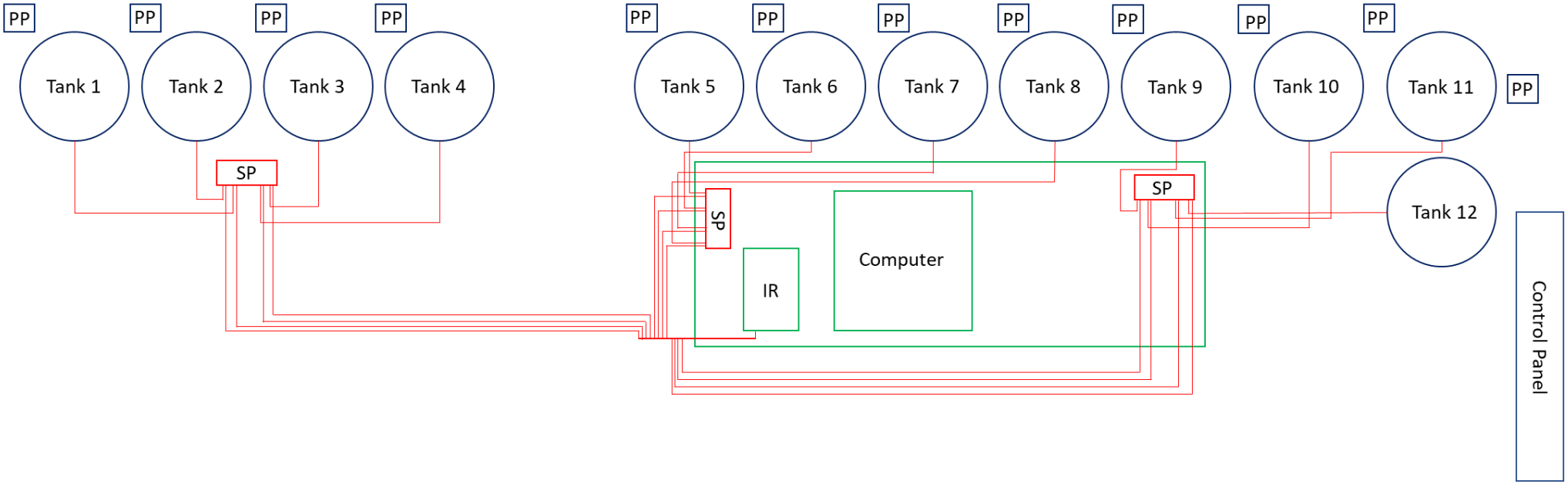

Figure 3.6: Piping and Instrument Layout of Experimental Cellar

3.2.6 Automation

As with the hardware components, the software was required to be an addition to an existing system. OPUS version 7.2.139.1294 (Bruker Optics) Wine Wizard running on Windows XP and Windows 7 operating systems was in use and as such this would determine some of the requirements for the automation code put into place.

The requirements for the automation software can be summarised as follows:

- Compatible with Windows operating systems dating as far back as Windows XP
- Cost effective and preferably open source
- Simplistic and stable
- Easily executed
- Able to work in conjunction with existing software that was designed for a user rather than automation
- A simple and effective integrated development environment (IDE)

The first point proved to be the most challenging as Windows XP is many years out of date and support has since ended. This meant that both the programming language and the IDE had to have previous versions available. As such, IDEs such as Eclipse with PyDev, Code Blocks and PyCharm could all be used as the source code for versions compatible with Windows XP is still available. Using these IDEs meant that the programming languages which could be used were Python, C, C++, and Fortran.

Of the programming languages, the most desirable language for this project was Python, due to its simplicity and the many additional software packages that can be installed for automation and graphing. As such, this excluded Code Blocks as an IDE as it does not support Python.

A comparison released in 2013 by Python Central was used to decide between Eclipse with PyDev and PyCharm. This comparison revealed that PyCharm was the better IDE due to its error detection, debugging and project navigation tools (Fruit, 2013) and as such this was chosen in conjunction with Python 3.7.3 (for use with the Windows 7 operating system) and Python 2.5.1.

3.3 Pump Testing Before Installation

It is necessary to ensure the correct functioning of system components before installation to ensure that they meet the requirements and to ensure that they are reliable. For the sampling pumps, specifically, it was necessary to first ensure that the pumps could deliver accurate volumes at specified times and activate/deactivate, as necessary. In addition to this, the reliability of the pump had to be tested to ensure that longer periods of operation would not result in a material or electronic failure. Power failures were also a concern, as there was uncertainty around what a sudden loss of power would do to the timing and programming of the pump.

Three different tests were conducted to ensure suitability of the pumps. The first was a 3-hour test to determine the volumetric accuracy of the pump head as well as the internal timer. Each pump was calibrated as per instructions in the user manual and subsequently programmed to deliver 20 mL of water every hour. The photograph in Figure 3.4 shows the pumps being tested in this manner.

To determine whether the sample volume was accurate, glass beakers were used. They were weighed before and after the pumps delivered a sample and this mass was used to calculate the volume of water. A stopwatch was used in between samples to determine whether the program was waiting a full hour before switching the pump on. All 12 pump heads passed the 3-hour test and the results from this test can be seen in Table 3.1 and Table 3.2.

Table 3.1: Table Showing Results from 3-hour Calibration Test: Volume

3 Hour Test - Supervised			
Criteria	**Pump head**	**Met Performance Criteria?**	**Notes**
Correct volume delivered	P-101 A	14:15 - Yes 15:15 - Yes 16:15 - Yes	Pumps will be started at 14:15 and will be expected to pump 20 ml each time. Power outage at 14:35. Good test to ensure that programming remains in the memory if a power outage occurs with the actual system
	P-101 B	14:15 - Yes 15:15 - Yes 16:15 - Yes	Pumps will be started at 14:15 and will be expected to pump 20 ml each time.
	P-101 C	14:15 - Yes 15:15 - Yes 16:15 - Yes	Pumps will be started at 14:15 and will be expected to pump 20 ml each time.
	P-101 D	14:15 - Yes 15:15 - Yes 16:15 - Yes	Pumps will be started at 14:15 and will be expected to pump 20 ml each time.
	P-102 A	14:15 - Yes 15:15 - Yes 16:15 - Yes	Pumps will be started at 14:15 and will be expected to pump 20 ml each time.
	P-102 B	14:15 - Yes 15:15 - Yes 16:15 - Yes	Pumps will be started at 14:15 and will be expected to pump 20 ml each time.
	P-102 C	14:15 - Yes 15:15 - Yes 16:15 - Yes	Pumps will be started at 14:15 and will be expected to pump 20 ml each time.
	P-102 D	14:15 - Yes 15:15 - Yes 16:15 - Yes	Pumps will be started at 14:15 and will be expected to pump 20 ml each time.
	P-103 A	14:15 - Yes 15:15 - Yes 16:15 - Yes	Pumps will be started at 14:15 and will be expected to pump 20 ml each time.
	P-103 B	14:15 - Yes 15:15 - Yes 16:15 - Yes	Pumps will be started at 14:15 and will be expected to pump 20 ml each time.
	P-103 C	14:15 - Yes 15:15 - Yes 16:15 - Yes	Pumps will be started at 14:15 and will be expected to pump 20 ml each time.
	P-103 D	14:15 - Yes 15:15 - Yes 16:15 - Yes	Pumps will be started at 14:15 and will be expected to pump 20 ml each time.
Overall Result: PASSED			

Table 3.2: Table Showing Results from 3-hour Calibration Test: Timing

3 Hour Test - Supervised			
Criteria	**Pump head**	**Met Performance Criteria?**	**Notes**
Correct timing	P-101 A	14:15 - Yes 15:15 - Yes 16:15 - Yes	All pump heads will be expected to operate at the same time and at the programmed time
	P-101 B	14:15 - Yes 15:15 - Yes 16:15 - Yes	All pump heads will be expected to operate at the same time and at the programmed time
	P-101 C	14:15 - Yes 15:15 - Yes 16:15 - Yes	All pump heads will be expected to operate at the same time and at the programmed time
	P-101 D	14:15 - Yes 15:15 - Yes 16:15 - Yes	All pump heads will be expected to operate at the same time and at the programmed time
	P-102 A	14:15 - Yes 15:15 - Yes 16:15 - Yes	All pump heads will be expected to operate at the same time and at the programmed time
	P-102 B	14:15 - Yes 15:15 - Yes 16:15 - Yes	All pump heads will be expected to operate at the same time and at the programmed time
	P-102 C	14:15 - Yes 15:15 - Yes 16:15 - Yes	All pump heads will be expected to operate at the same time and at the programmed time
	P-102 D	14:15 - Yes 15:15 - Yes 16:15 - Yes	All pump heads will be expected to operate at the same time and at the programmed time
	P-103 A	14:15 - Yes 15:15 - Yes 16:15 - Yes	All pump heads will be expected to operate at the same time and at the programmed time
	P-103 B	14:15 - Yes 15:15 - Yes 16:15 - Yes	All pump heads will be expected to operate at the same time and at the programmed time
	P-103 C	14:15 - Yes 15:15 - Yes 16:15 - Yes	All pump heads will be expected to operate at the same time and at the programmed time
	P-103 D	14:15 - Yes 15:15 - Yes 16:15 - Yes	All pump heads will be expected to operate at the same time and at the programmed time
Overall Result: PASSED			

The second test performed was more strenuous and required that the pumps deliver the maximum number of samples over a 24-hour period. This was not only to ensure that the accuracy and timing remained consistent over a longer period, but also to determine how robust the pumps were in terms of their physical components.

The pumps were programmed to deliver 5 mL (a total of 120 mL per pump head for the test) samples hourly for a period of 24 hours. Empty glass beakers were once again weighed before and after the test to determine sample volume delivered. As a stopwatch could not be used for the entire test, the timing was monitored throughout business hours.

At the end of the test, the pumps were inspected to ensure that there were no leaks anywhere in the piping system nor in the actual pump head. In addition to this, the pumps were also inspected to determine whether any electrical failure had occurred. Once again, all of the pumps passed the test, and the summary of this test can be found in Table 3.3 and Table 3.4.

The final test for suitability was to simulate power failures to gauge whether the programming would continue to work timeously. This was done by using the previous 24-hour programming and interrupting the power supply to the pumps for two hours. The pumps were restarted a few minutes prior to a scheduled sampling, and they were monitored to see if the sampling took place on time. The simulated load shedding appeared to have no effect on the programming and the sampling took place on time for all pump heads.

The tests determined that the pumps were indeed suitable for the prototype system and as such they could move onto the next phase of testing which would take place with all the system components installed.

Table 3.3: Table Showing Results from 24-hour Stress Test: Volume and Integrity

24 Hour Test - Unsupervised			
Criteria	**Pump head**	**Met Performance Criteria?**	**Notes**
Correct volume delivered and no leakage from pump heads	P-101 A	Yes	Pumps will be started at 09:00 and will be expected to pump 5mL on the hour. After 24 hours, if the pump is accurate, the volume of fluid in the beaker will be 120mL
	P-101 B	Yes	After 24 hours, if the pump is accurate, the volume of fluid in the beaker will be 120mL
	P-101 C	Yes	After 24 hours, if the pump is accurate, the volume of fluid in the beaker will be 120mL
	P-101 D	Yes	After 24 hours, if the pump is accurate, the volume of fluid in the beaker will be 120mL
	P-102 A	Yes	After 24 hours, if the pump is accurate, the volume of fluid in the beaker will be 120mL
	P-102 B	Yes	After 24 hours, if the pump is accurate, the volume of fluid in the beaker will be 120mL
	P-102 C	Yes	After 24 hours, if the pump is accurate, the volume of fluid in the beaker will be 120mL
	P-102 D	Yes	After 24 hours, if the pump is accurate, the volume of fluid in the beaker will be 120mL
	P-103 A	Yes	After 24 hours, if the pump is accurate, the volume of fluid in the beaker will be 120mL
	P-103 B	Yes	After 24 hours, if the pump is accurate, the volume of fluid in the beaker will be 120mL
	P-103 C	Yes	After 24 hours, if the pump is accurate, the volume of fluid in the beaker will be 120mL
	P-103 D	Yes	After 24 hours, if the pump is accurate, the volume of fluid in the beaker will be 120mL
Overall Result: PASSED			

Table 3.4: Table Showing Results from 24-hour Stress Test: Timing and Reliability

24 Hour Test - Unsupervised			
Criteria	**Pump head**	**Met Performance Criteria?**	**Notes**
Timing still correct after 24-hour period and pump still operational	P-101 A	Yes	The pumps will be expected to still be running with no burnouts over a 24-hour period. The pumps will be monitored during business hours over the two days to ensure that they run on time.
	P-101 B	Yes	The pumps will be expected to still be running with no burnouts over a 24-hour period.
	P-101 C	Yes	The pumps will be expected to still be running with no burnouts over a 24-hour period.
	P-101 D	Yes	The pumps will be expected to still be running with no burnouts over a 24-hour period.
	P-102 A	Yes	The pumps will be expected to still be running with no burnouts over a 24-hour period.
	P-102 B	Yes	The pumps will be expected to still be running with no burnouts over a 24-hour period.
	P-102 C	Yes	The pumps will be expected to still be running with no burnouts over a 24-hour period.
	P-102 D	Yes	The pumps will be expected to still be running with no burnouts over a 24-hour period.
	P-103 A	Yes	The pumps will be expected to still be running with no burnouts over a 24-hour period.
	P-103 B	Yes	The pumps will be expected to still be running with no burnouts over a 24-hour period.
	P-103 C	Yes	The pumps will be expected to still be running with no burnouts over a 24-hour period.
	P-103 D	Yes	The pumps will be expected to still be running with no burnouts over a 24-hour period.
Overall Result: PASSED			

3.4 Automation Code to Work with Pre-Existing Software

3.4.1 Brief Overview of Python and Related Programming Packages

The interface of the existing software, namely OPUS 7.2, is designed for a user to interact with and therefore poses a challenge with automation. However, software packages exist that can control the keyboard and mouse of a computer according to a list of pre-set commands. One such package is PyAutoGUI. This package has commands to move the mouse pointer to specific coordinates on a screen, click and type. In short, if programmed correctly, this can mimic the actions of a user and interact with the instruments user interface to effectively automate the system. A summary of the commands can be seen in Table 3.5 (Sweigart, 2020).

Table 3.5: Summary of PyAutoGUI Commands and Their Key Functions

Command	Function
pyautogui.size()	This function determines the size of the computer screen (in pixels) and returns the size of the screen to the user as coordinates.
pyautogui.position()	This function determines the current position of the mouse cursor and returns the coordinates to the user
pyautogui.moveTo(x, y)	This function, moves the mouse cursor to the position specified by the user
pyautogui.click()	This function commands the mouse to click at its current position
pyautogui.doubleClick()	This performs the same function as pyautogui.click with the exception that it performs a double click
pyautogui.typewrite(‘string’)	This function will type a string of text

To provide a visual representation of the progress of the fermentation or phenolic extraction, graphs would need to be used. As such, a graphing package was used to properly plot and display graphs for the different oenological factors. Matplotlib 3.1.1 was used as this is the most widely used graphing package with easily executable commands. It is capable of producing high quality 2D plots that can be exported and printed. A summary of the key commands used can be found in Table 3.6 (Hunter, Dale, Firing, *et al.*, 2020).

Table 3.6: Summary of Commands for matplotlib and Their Key Functions

Command	Function
matplotlib.subplot(n_1, n_2, … , n_k)	This allows more than one graph to be displayed in the same window
matplotlib.plot(x, y, n) [n refers to subplot number and is optional]	This function plots the x and y data on a set of axes
matplotlob.title('string')	This function generates a title for the plot
matplotlob.ylabel('string')	This function generates a label for the y axis
matplotlob.xlabel('string')	This function generates a label for the x axis

3.4.2. Methodology and Implementation

For this project, PyAutoGUI 0.9.48 was used. The flowcharts for the code can be found in Figure 3.7 to aid with following the logic used in coding the automated interface.

The code comprised of a series of nested loops. The outermost loop contains the information for the variables, and it contains all the arrays where information is stored throughout the fermentation. Inside this is a loop which controls the system daily, and which determines when the code will end. The next nested loop controls the entire measurement cycle, analysis of the spectra and displaying the graphical information. Finally, the innermost loop controls the user interface and initiates the IR scan for a sample.

Once the code is initiated, the variables, such as the number of measurements per day and number of tanks, are declared and stored and the code enters the daily loop where it repeats until the fermentation ends. When a measurement cycle starts, a list containing the sample names is created and the software opens OPUS. The sample name is a string containing the tank number and the number of hours into the fermentation. At this point, the code for each tank is entered. This code selects the option for a single sample scan, clicks on the field for the sample name and enters the new name for the sample. After this, the scanning is initiated, and the code pauses for 5 minutes for the scan to be completed and for the new sample to enter the instrument. This is repeated until a sample from each tank has been analysed.

After a measurement cycle has been completed, the spectra generated must be analysed by existing models and the information plotted. The code selects the QUANT method, loads a list of models as well as all the spectra generated for the whole fermentation and begins the analysis. The results of the analysis are displayed in a text format which can be imported into PyCharm.

Once imported, the values for each component can be read from the text file and plotted for each tank and displayed graphically with the use of Matplotlib.

The graphs remain open where they can be viewed until the next measurement cycle executes. At this point, the windows displaying the graphs close so that the new data can be plotted. Once the fermentation is complete, the spectra and the text files are stored and can be viewed at a later stage.

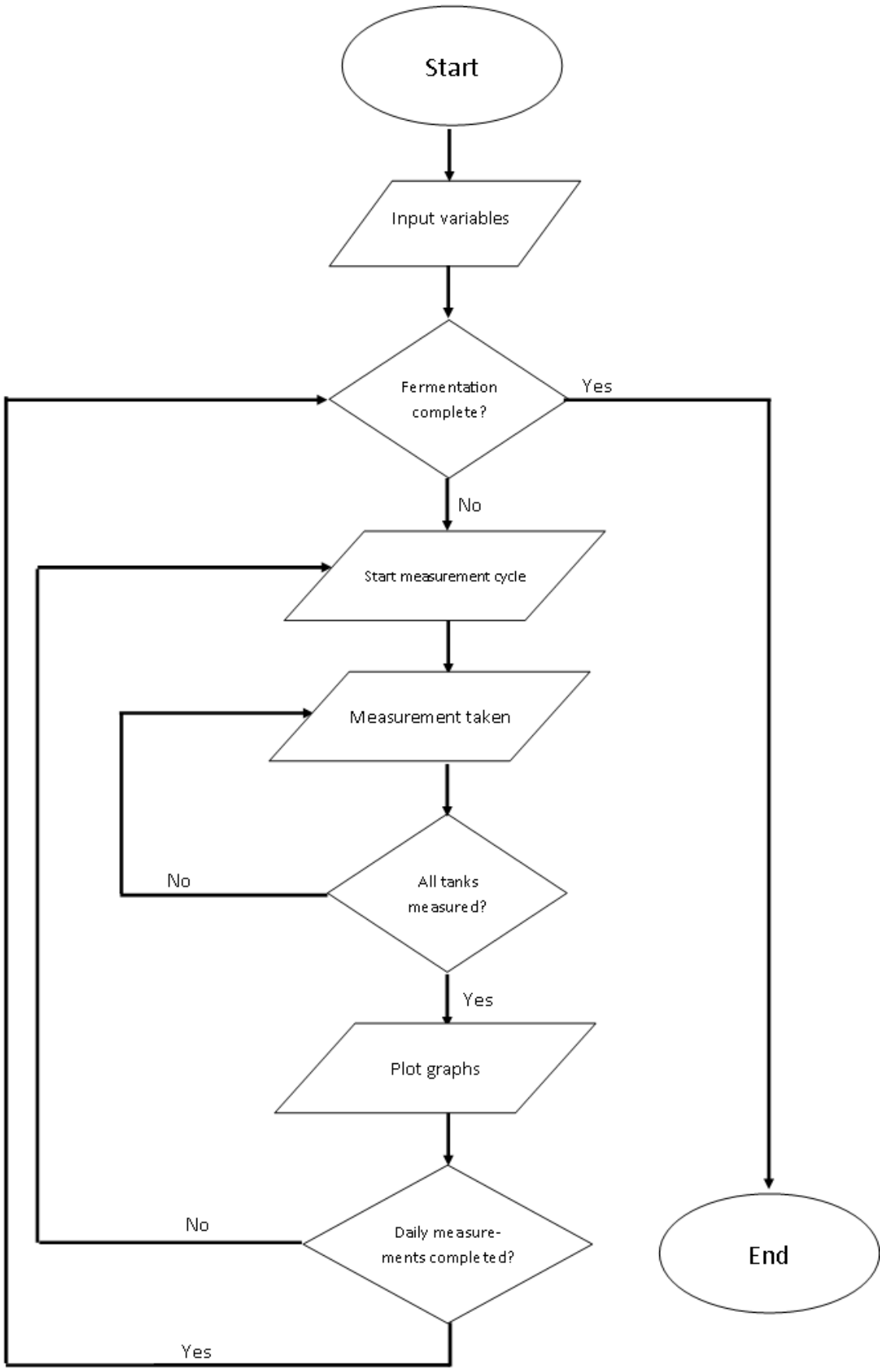

Figure 3.7: Flowchart of Code

3.5 Single Tank Installation

3.5.1 Operating Philosophies

The following operating philosophies/sequences are applicable to single and multiple tank systems.

3.5.1.1 Start up

1. Connect instrumentation and computer to plumbing and power source – the instrument and computer need to be positioned properly to ensure that the system piping and layout is maintained
2. Connect pumps to power – the pumps rely on an external power source and require this to run
3. Connect pipelines – the system must be connected in order to start up and calibrate
4. Set number of tanks – this is done so that the automation software can name the samples correctly
5. Set number of measurements – this is also done so that the software can name the samples correctly and so that it can start the analysis of the samples at the correct times
6. Calibrate and set pumps – The pumps must be calibrated to ensure that the volume of the samples is correct and also due to the fact that equipment standing for a while can lose calibration. The timing and volume of the sample also has to be set as this will determine when the sample is taken and the volume of the sample
7. Set pump overs – the pump overs must be timed so that they occur before the sampling if pumping over is necessary
8. Set stirrers and oxygen addition – The other tank parameters must be set up correctly during start-up so that they are running correctly
9. Charge tanks – the grape juice and yeast must be placed in the vessels for fermentation to begin
10. Manually fill pump lines – the pump lines must be filled so that the pumps don’t become damaged when they run for the first time. Calibration should also take place with fluid in the lines, so this is necessary for the sample volume of the first sample to be correct
11. Initiate software – The automation software is written in Python, which does require a user to manually start the software

3.5.1.2 Normal Operation

1. Pump over occurs – this is done to homogenise the contents of the fermentation vessel. It should be noted that a pump over does not occur before every sample as the head in the tank ensures an adequate volume of fluid in the pipelines for sampling to occur
2. A brief waiting period occurs – this is done in order for the pump controlling the pump over to completely switch off before the sampling pump switches on. This is necessary to prevent the sampling pump from attempting to draw a sample while the fluid is being pumped over and the sample is not yet homogenised
3. The sampling pump switches on – this is done in order to move a sample of wine from the tank to the instrument
4. The sampling pump switches off after a set sample volume is delivered to the instrument – this is to ensure flushing of the lines and adequate sample volume
5. A waiting period must be given – this is to ensure that the pumps have time to switch off and that there is a “hand-over” period between the drawing of the sample and the analysis of the sample
6. The automation program activates analysis sequence
7. The samples are analysed

3.5.1.3. Shutdown

1. Stop automation program – the program is designed to run with continuous loops, the program will terminate when the loop controlling the overall fermentation ends
2. Stop instrumentation and uncouple from system plumbing – the instrument must be disconnected from the system in order to clean the fluid lines and store the instrumentation
3. Remove pumps from power source – the pumps run on a separate power system to the fermentation vessels and the instrumentation. The pumps do not have a stop function and will have to be disconnected from power
4. Drain pump lines – the pump lines will be filled with wine. This wine must be drained from the pipelines after they have been uncoupled
5. Reattach pump lines to water – the pipelines as well as the pumps must be flushed with water in order to remove the wine residue
6. Manually flush pump lines and pumps with water – this will be manual as a small amount of fluid needs to be used in order to remove the residue from the silicon pipe inside the peristaltic pump head
7. Decouple pump lines and drain – in order to remove the water used to flush the lines, simply decoupling them and allowing the water to drain will empty them. The pipelines must be stored without fluid in then to prevent material fatigue

8. Drain pumps and store – the pumps can be manually drained without the piping to remove any fluid from the line and allow them to be stored without fluid in order to prevent fatigue
9. Drain tanks and either store or discard – the fermentation vessels must be drained of wine and the solids must be discarded. This wine can then be stored or discarded. The tanks must be empty in order to properly clean these
10. Flush tank with water manually – the tanks must first be flushed with water to remove any residue before proper cleaning in place (CIP) procedures can be performed
11. CIP on tanks

3.5.2 Implementation and Testing

The system set-up for a single tank fermentation can be seen in Figure 3.8 and Figure 3.9.
For safety and convenience, an isolation valve was added to the pump over line before the filter and the junction. This was done so that the fluid flowing out of the tank could be regulated or shut off completely in the event of a pipeline detaching from the system, a leak, or a component failure. The filter was added in-line before the junction and the 4mm outlet of the junction was initially blocked off. This was done to test the integrity of components along the 20mm line and to ensure that the line would remain filled in between pump overs.

The tank was filled with water at 25 ^{o}C and three 5-minute-long pump overs were conducted over the course of the day to check for water escaping from the system. No leaks were detected, and no components failed or uncoupled from the system.

The pump over pumps were reversed to return the water to the tank and the isolation valve was closed. The 4 mm pipeline was added and connected to one head of the sampling pump. Both pipelines were filled with water and the sampling pump could draw a sample of water from the tank and deliver it to the IR instrument connected to the system. Once again, no leaks or component failures occurred, and the system operated as expected.

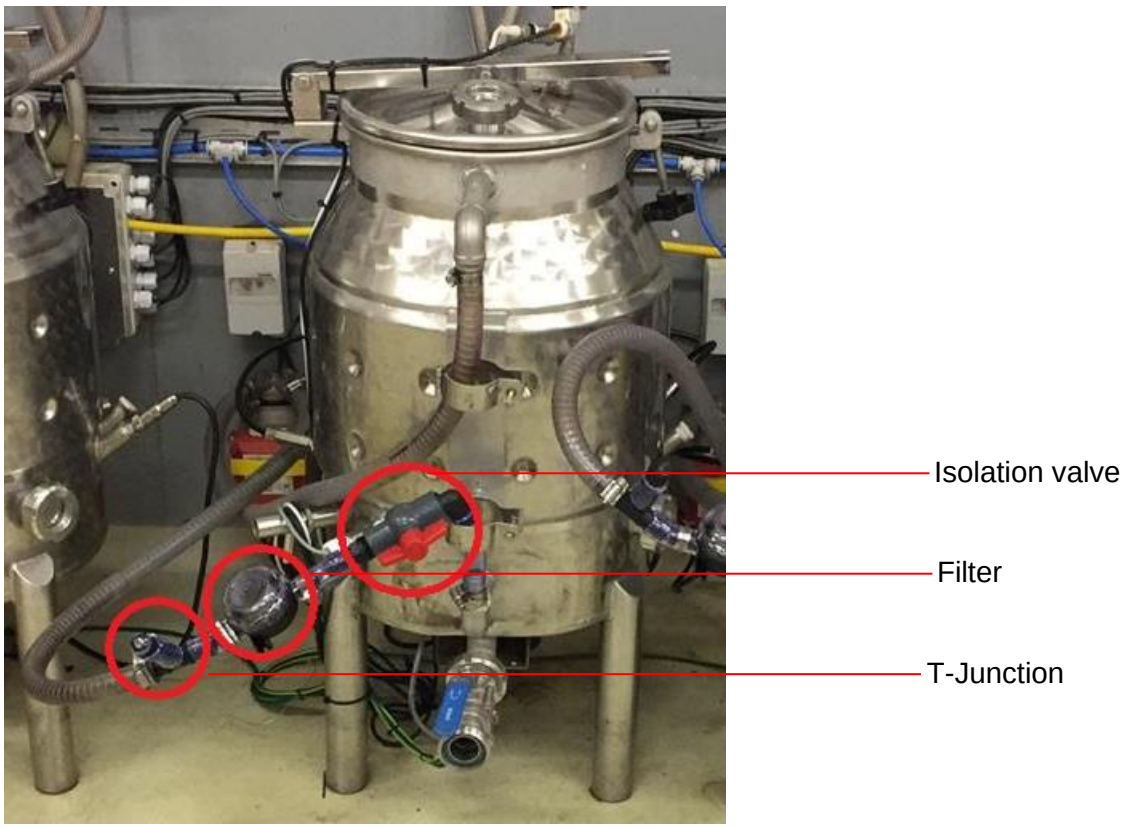

Figure 3.8: Components Installed Along 20 mm Pump Over Line

Figure 3.9: Position of Instrumentation and Sampling Pump

3.5.3 Single Tank Fermentation Monitoring Methodology

The hardware components were installed prior to charging the tank as per the Operating Philosophies. Seventy-five kg of Shiraz grapes sourced from Stellenbosch in the Cape Winelands region was used. The grape juice was previously frozen and was thawed for two days at 4^{o}C before being introduced to the tank. Once it reached 16^{o}C, the grape juice was inoculated with *Saccharomyces cerevisiae* (Lalvin ICV D21®). The fermentation took place at a constant temperature of 20 ^{o}C with pump overs occurring 3 times daily.

Once the cap had formed and the first pump over was conducted, the sampling pumps were switched on and the code was executed and allowed to run for 8 hours to determine whether spectra could be automatically obtained while the system was supervised. The instrumentation used was an Alpha P attenuated total reflectance Fourier transform mid infrared spectrometer (Bruker Optics, Ettlingen, Germany). This was fitted with a sample plate containing a 2 mm^{2} diamond crystal, which can be seen in Figure 3.9a in Supplementary Material (S5). The system was set to scan samples 128 times at a temperature of 30^{o}C over a wavenumber range of 4000 – 400 cm^{-1} at a resolution of 4 cm^{-1}. A reference measurement was done using distilled water.

3.5.4 Results and Discussion

The automated system was operational for a total of five days. During the first two days, debugging took place to ensure that the code was running optimally for the timing of the instrument and sampling pumps and to determine a naming convention which would easily work for this situation. The naming convention is extremely important as it can determine the ease with which samples are renamed and how they are stored in the directory. The naming convention used was:

Tank1_DATE_TIME

This convention was selected as it allowed for easier indexing in the directory where the spectra were stored, and the user could easily determine time and date. In addition to this, it allowed for the automation software to easily rename the samples. However, when the spectra were loaded into the QUANT2 method developed by Bruker Optics, the order was not correct. This indicates that a different naming convention should be used in future prototypes.

The final three days were used to test the sampling and scanning capabilities. The system was programmed to sample and scan approximately every four hours. As the system was always to be monitored to ensure no component failures occurred, the automated system only ran between 08:00 and 16:30 before the code ended. As such, it was restarted each morning after the first pump over. The following spectra were collected automatically:

Table 3.7: List of Spectra Collected with Automated Sampling System

File Name	Date and Time
Tank1_2019_09_04_08_06_20	04 September 2019 at 08:06:20
Tank1_2019_09_04_12_10_16	04 September 2019 at 12:10:16
Tank1_2019_09_05_08_44_22	05 September 2019 at 08:44:22
Tank1_2019_09_05_12_23_09	05 September 2019 at 12:23:20
Tank1_2019_09_05_16_29_14	05 September 2019 at 16:29:14
Tank1_2019_09_06_08_33_20	06 September 2019 at 08:33:20
Tank1_2019_09_06_12_34_01	06 September 2019 at 12:34:01

Table 3.7 shows that the samples were named correctly according to the chosen convention and that the timing is correct for all samples. For the first day and the last day, the final sample for the day was not sampled. This was not a failure on the part of the automation as both times it was due to the code being manually stopped. For the first and last day this was due to the uncoupling of a pipe in the system and to change a connector which had begun to leak. In this aspect, it was noted that the glue used in the development of the connectors was unsuitable. Whilst it was suitable for use with wine, it was discovered that it was unsuitable for use with the nylon. For future prototype tests a different product was used to ensure that this did not occur again.

An example of the spectra obtained using the ATR-MIR infrared instrumentation can be seen in Figure 3.10.

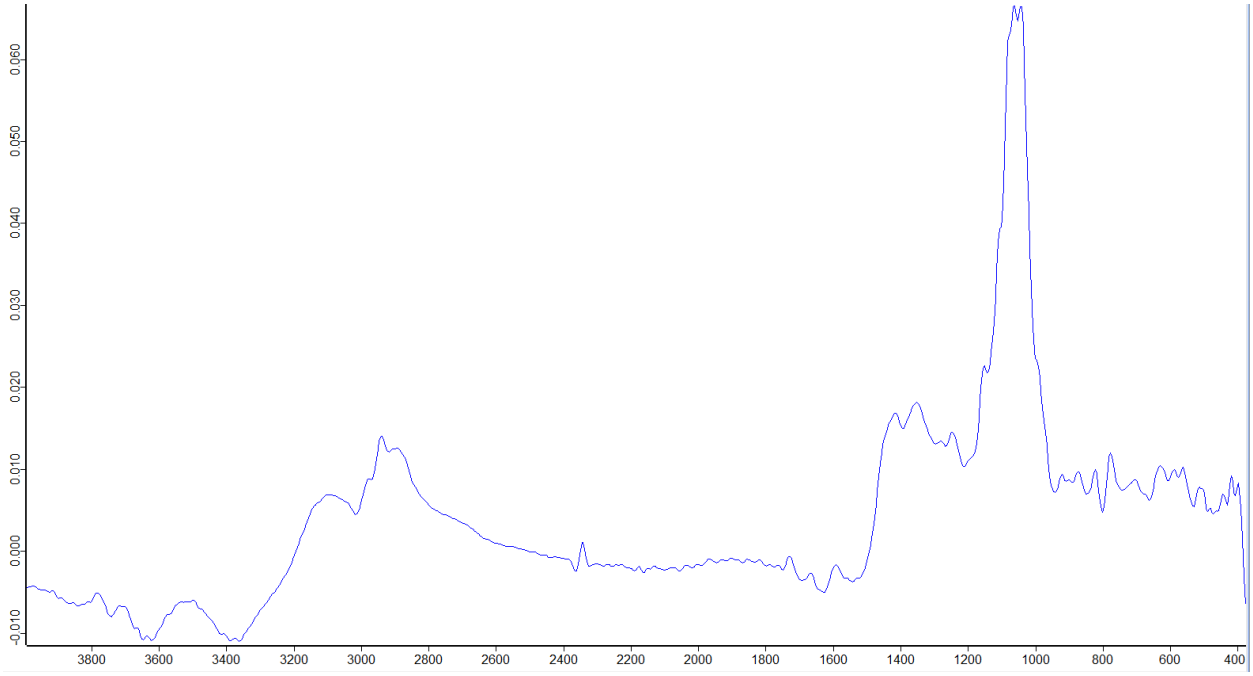

Figure 3.10: Spectrum from 5 September 2019 at 16:29:14

This spectrum generated is typical for red wine and as such it can be assumed that the system can be used for monitoring red wine. However, as the wine entering the system was not completely free of turbidity, it would still be necessary to either further clarify the wine or to explore models which account for the turbidity.

3.6 Multiple Tank Installation

3.6.1 Implementation and Testing of Multiple Tank Components

The plumbing on the tanks remained the same with the piping each leading to a separate pump head as shown in Figure 3.6. The pipes led to a junction where a single outlet led to the instrument and this can be seen in Figure 3.11.

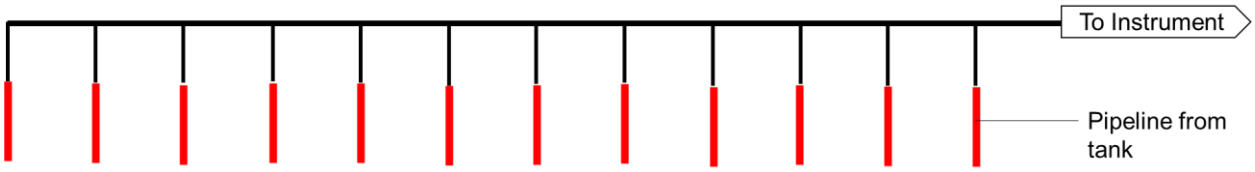

Figure 3.11: Diagram of Junction

In this scenario, the most prominent concern was contamination due to residue left over from previous samples. The simplest solution to this was to ensure that a sufficient volume was pumped through to completely flush the line and ensure that any remaining residue was removed. The volume of the pipeline was calculated, and the pumps were programmed to pump 110% of this volume before the measuring took place. This would ensure that the sample entering the instrument was both directly from the tank and it would ensure that residue on the pipeline was flushed out of the shared pipeline.

As the junction did not have solenoid valves to close off the other inlets, another concern was fluid from these pipelines leaking into the sample of interest during the pumping stage due to the pressure differentials. To determine whether this was a concern, lab testing was conducted. A beaker containing clear water was connected to the inlet furthest from the instrument while beakers containing water that had been strongly pigmented with blue food dye (500ml/L) were connected to the other inlets. The clear water was pumped through the junction and a visual observation was made to ascertain if the dye had entered the junction. The visual inspected showed that the dye had not entered the junction. However, to fully determine whether the dye had not entered the pipeline, a sample of the clear water and a sample after flowing through the junction was analysed using a UV-Visible spectrophotometer at 620 nm (Li, Zhu, Li, *et al.*, 2017). In addition to this, a calibration curve was obtained for different concentrations of the blue food dye to determine the concentration of the dye in the final sample should there be any. The calibration curve for the dye can be seen in Figure 3.12 and the absorbances of the two water samples can be seen in Table 3.8.

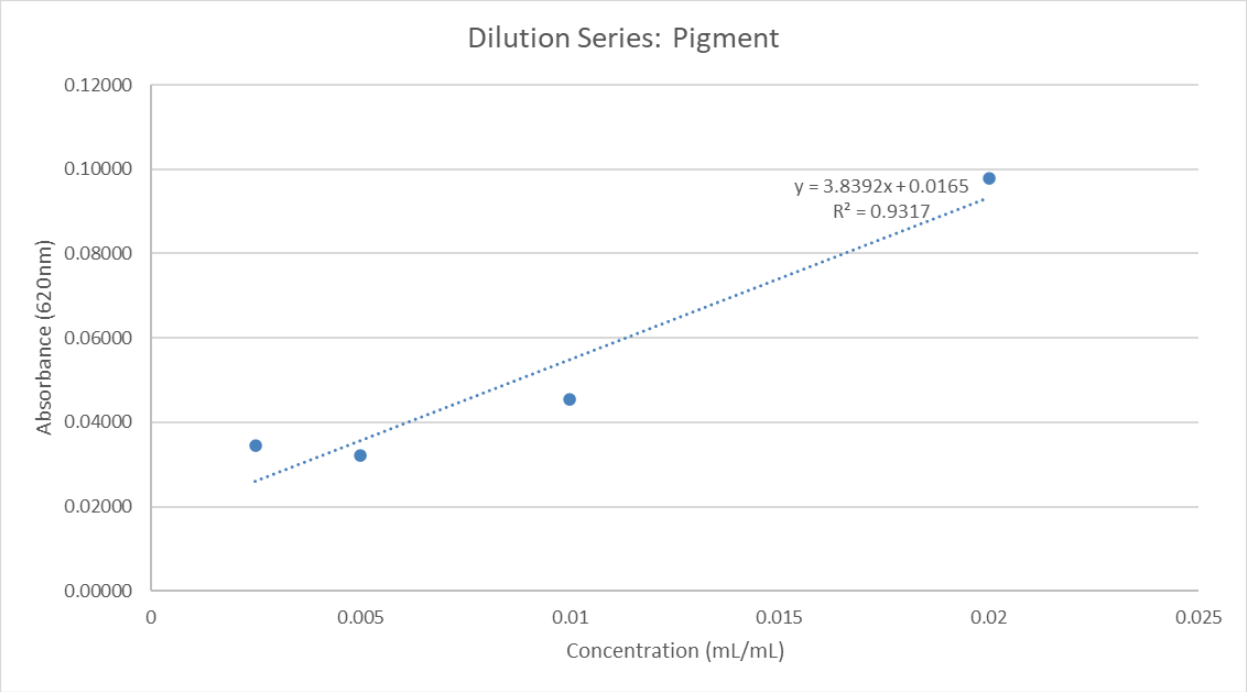

Figure 3.12: Calibration Curve for Pigment

Table 3.8: Absorbances of a Sample Before and After Junction

Sample	Absorbance (Abs at 620nm)	Concentration of Dye from Trendline (mL/mL)
Before Junction	0.00	0
After Junction	0.002683	-0.0032

As this value indicates that the concentration of dye in the final sample is too low for the trend line to accurately predict, it can be considered negligible. As such, this junction was considered appropriate for use in multiple tank scenarios.

3.6.2 Multiple Tank Fermentation Monitoring Methodology

Three different instruments were used with each instrument connected to two tanks. The first instrument was an Alpha-P ATR FT-MIR spectrometer (Bruker Optics, Ettlingen, Germany) using a 2 mm^2 diamond sample plate. The spectra were collected at a constant temperature of 30 ^oC using 128 sample scans with wavenumbers between 4000-400 cm^{-1} and a 4 cm^{-1} resolution. The scanner velocity was set at 75 kHz. The second instrument was a Multi-Purpose Analyser (MPA) FT-NIR instrument (Bruker Optics, Ettlingen, Germany) set to transmission mode. Spectra for this instrument were collected at a constant temperature of 20 ^oC with 64 sample scans between 12500-4000 cm^{-1} using a 2 cm^{-1} resolution. The scanner velocity was set to 10kHz. Finally, a Matrix-F FT-NIR (Bruker Optics, Ettlingen, Germany) was used for a no-contact method. In this case, 64 sample scans at a constant 20 ^oC were taken between 12500 – 4000 cm^{-1} at a resolution of 16 cm^{-1}.

300 kg of Shiraz from Stellenbosch in the Cape Winelands region was used. These were thawed for two days at room temperature before destemming and crushing. However, due to the time of the year, there were insufficient grapes for six tanks and, as such, the grape juice was mixed with water to ensure that there would be sufficient volume for the tanks. As models had also not been developed for highly turbid samples, this would not impede the proof of concept, as the purpose of this was to determine if continuous over-night scanning could be achieved. The grape juice was inoculated with *Saccharomyces cerevisiae* (Lalvin ICV D21®). Once a cap had formed, pump overs were conducted three times a day and the automation code for the three instruments was executed.

As discussed previously, a different naming convention was needed to ensure that the spectra could be analysed using the QUANT2 method. As such the naming convention chosen was:

h#_1tank#_2

Where *h* refers to hours, #_1 refers to the number of hours passed from start of fermentation and #_2 refers to the tank number. It will enable the file to be stored in the correct order both with regard to tank and with regards to sampling time.

3.6.3 Results and Discussion

As with the previous proof of concept, debugging occurred for the first two days to ensure proper timing and naming convention appropriate for the new code and graphing algorithms. The code was then executed to monitor the final days of fermentation. This proof of concept was to be unsupervised and continuous. It was therefore allowed to run overnight with only basic safety measures and interlocks in place to prevent component failure. The total testing time for this proof of concept was 33 hours.

It should be noted at this point that the Matrix F did not successfully complete the tests as the samples were unable to exit the sample vessel completely and extreme contamination occurred. This was primarily due to the shape of the sample vessel as it did not allow for the residue to be flushed out in the same manner as with the other instruments. As such, the recommendation for this instrument is to have a specialised sample vessel which can ensure proper drainage between samples.

Whilst the automation code did work as expected for the MPA, the age of the operating system did not allow for graphic display of the data. However, due to the correct collection and naming of samples, this was not a failure of the prototype. Rather, this can be considered a limitation and

can be overcome with more modern operating systems that are compatible with graphing software available.

With the Alpha-P ATR MIR, the files were saved successfully and were loaded into the QUANT2 method in the correct order along with the relevant models. Graphing algorithms were in place for this proof of concept and the graphs for certain compounds can be seen in Figure 3.13 through Figure 3.16. However, the models used to determine the concentrations of certain compounds, developed as part of the initial testing, were developed using samples with no turbidity and were used only as an indication of the system's automated sampling ability. The figures below, show a similar trend to those expected with alcoholic fermentation and phenolic extraction. The values can differ from normal red wine values as water was added to ensure a sufficient volume in the tanks. The occasional outliers can indicate an abnormal spectrum, and this can be as a result of an outdated background spectrum or settling of a solid particle on the crystal.

The overall result of the testing protocol for the Alpha-P instrument is positive. The system demonstrated that a sample could be taken automatically, named correctly, analysed and the results graphically displayed. A similar positive result was obtained from the MPA, limited only by software incompatibility.

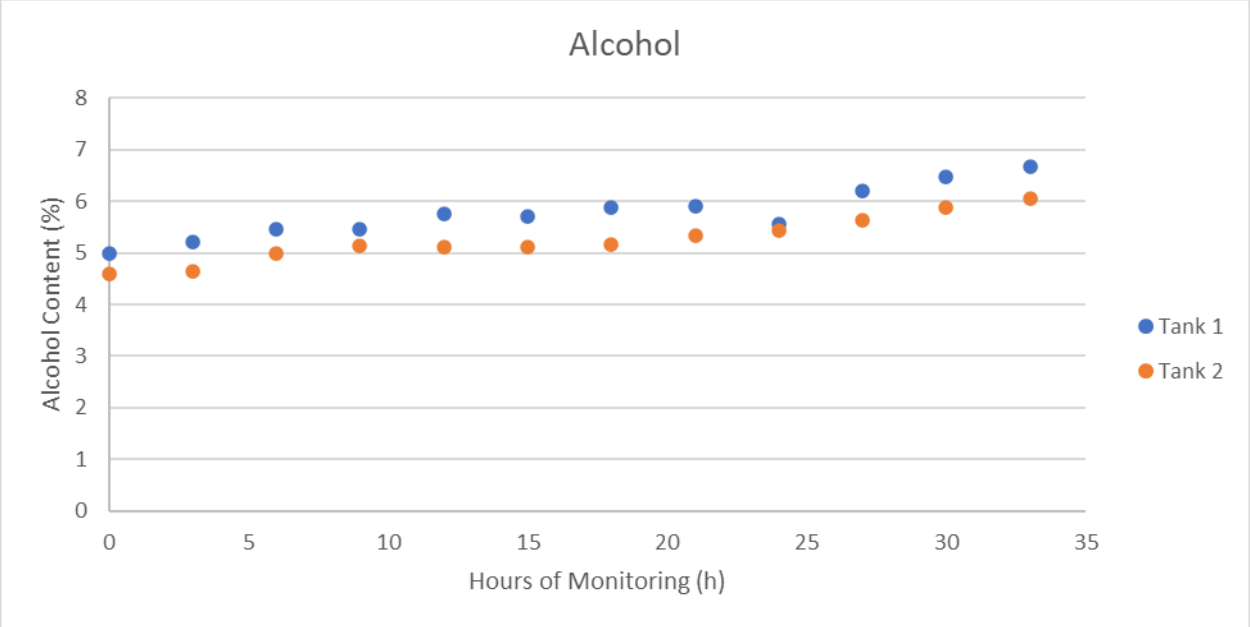

Figure 3.13: Monitoring of Alcohol Formation Using Automated Monitoring System

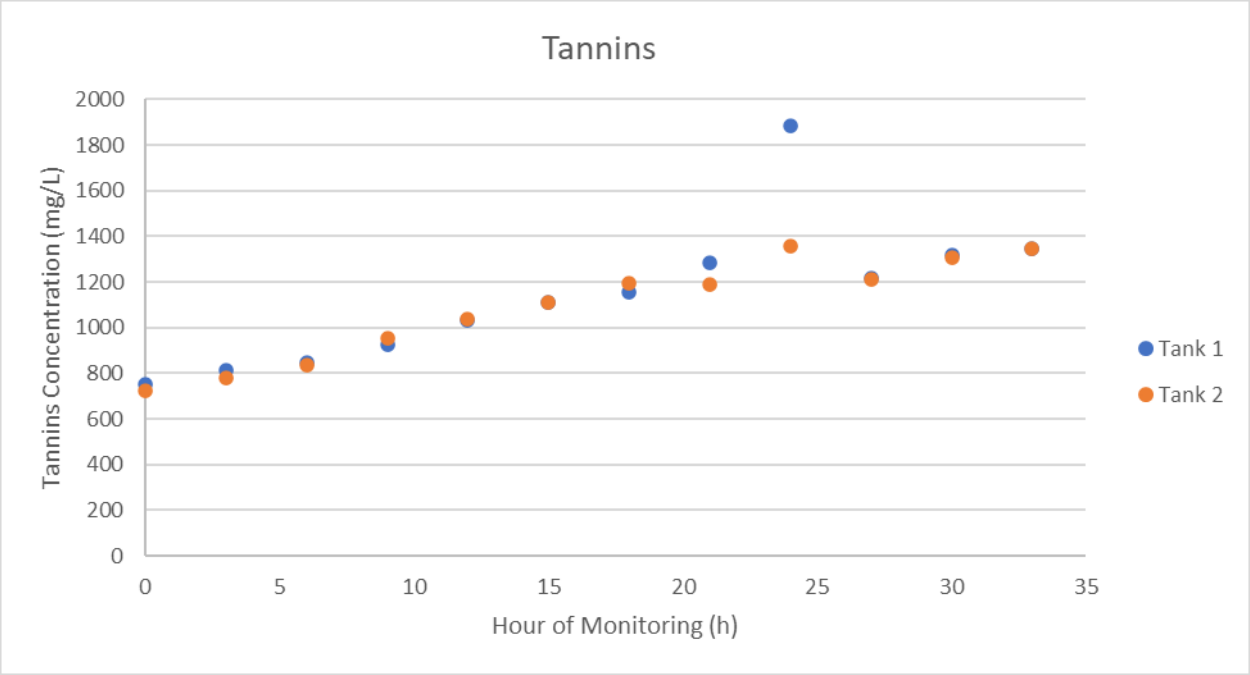

Figure 3.14: Monitoring of Tannin Concentration Using Automated Monitoring System

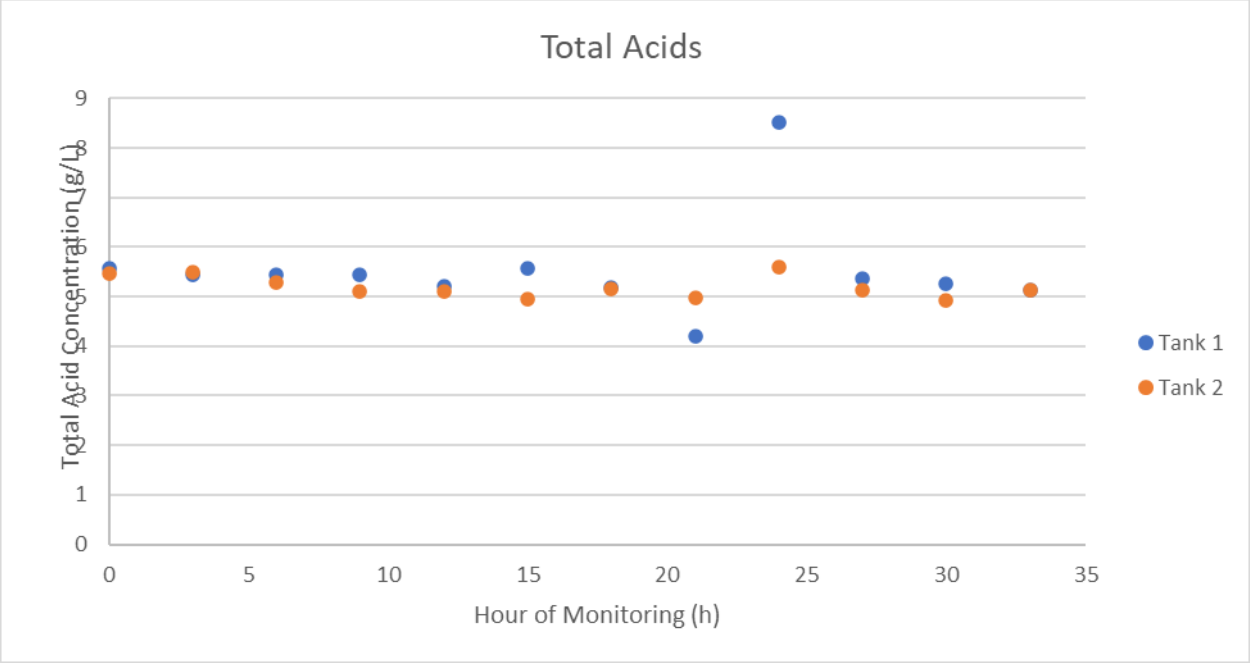

Figure 3.15: Monitoring of Total Acid Concentration Using Automated Monitoring System

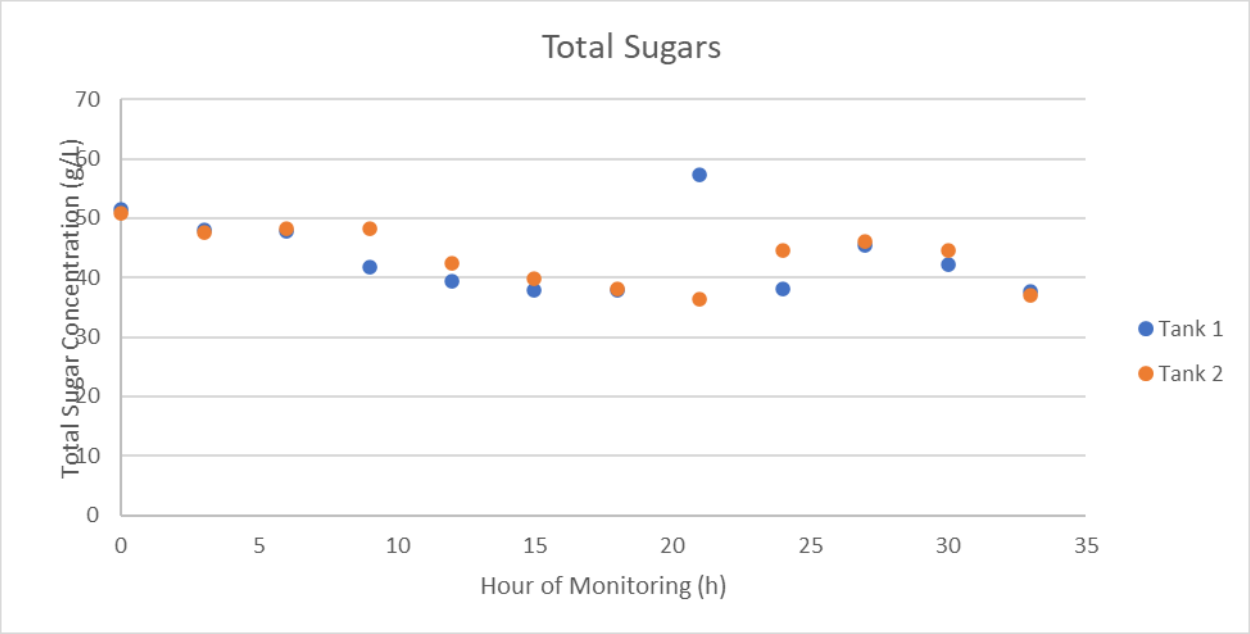

Figure 3.16: Monitoring of Total Sugar Concentration Using Automated Monitoring System

3.7 Conclusion

Design and development of an automated process monitoring system requires an iterative design process with multiple considerations. In general, systems such as these will have multiple subsystems that are required to work in conjunction with each other and this adds complexity to the design process.

The design process and equipment selection for the first prototype of an automated sampling and analysis system for red wine fermentation was explored in this chapter. Material of construction was the first consideration before any equipment was considered and a few appropriate and food safe materials were selected for further consideration. Functionality was balanced with cost effectiveness in all further equipment selections. The overall design for the system was based on the need for suitability to multiple different situations. Detachable subsystems with their own programming allowed for fast installation and for adjustments to made without removing large components. The result was a simple and cost-effective system which could enter a testing phase.

Positive results were obtained for two different proof of concept tests indicating that the system can perform the desired functions. However, as with all prototypes, refinement and improvement upon a core concept is always necessary. The initial proof of concept testing resulted in an improvement in the connectors between unit operations whilst, the second proof of concept showed that models accounting for turbidity in a sample are needed.

In both cases, there were limitations, however, the nature of the system allows for modification and results in a system capable of adapting to a unique situation. The next chapters explore the movement towards a fully functioning prototype system which addresses the current challenges posed with in-line sampling and monitoring. Thus far, however, the system shows promise towards being incorporated in industry and scientific applications.

3.8 Literature Cited

Boyce, M.P. 1997. Transport and Storage of Fluids. in *Perry's Chemical Engineers' Handbook* 7th ed. R.H. Perry, D.W. Green, & J.O. Maloney (eds.). New York: McGraw-Hill R.H. Perry, D.W. Green, & J.O. Maloney (eds.). 10-1-10–152.

Cole-Parmer. 2020. *Chemical Compatibility - Chemical Selected: Whiskey & Wine*. [Online], Available: https://www.coleparmer.com/chemical-resistance.

Dahlstrom, D.A., Bennett, R.C., Emmett, R.C., Harriott, P., Laros, T., Leung, W., McCleary, C., Miller, S.A., et al. 1997. Liquid-Solid Operations and Equipment. in *Perry's Chemical Engineers Handbook* 7th ed. New York. 18-1-18–151.

Dalgleish, T., Williams, J.M.G.., Golden, A.-M.J., Perkins, N., Barrett, L.F., Barnard, P.J., Au Yeung, C., Murphy, V., et al. 2008. *Perrys Chemical Engineering Handbook - 8Ed (2008)*. Vol. 136.

Fruit, J. 2013. *Comparison of Python IDEs for Development*. [Online], Available: https://www.pythoncentral.io/comparison-of-python-ides-development/ [2020, July 23].

Hunter, J., Dale, D., Firing, E. & Droettboom, M. 2020. *Matplotlib Release 3.3.0*.

Li, S.Y., Zhu, B.Q., Li, L.J. & Duan, C.Q. 2017. Extensive and objective wine color classification with chromatic database and mathematical models. *International Journal of Food Properties*. 20(53):S2647–S2659.

Salas, B.V., Wiener, M.S., Stoytcheva, M., Zlatev, R. & Beltran, M.C. 2012. Corrosion in the Food Industry and Its Control. *Food Industrial Processes - Methods and Equipment*. 29168.

Siebert, O.W. & Stoeker, J.G. 1997. Materials of Construction. in *Perry's Chemical Engineers' Handbook* 7th ed. D.W. Green, R.H. Perry, & J.O. Maloney (eds.). New York: McGraw-Hill D.W. Green, R.H. Perry, & J.O. Maloney (eds.). 28-1-28–64.

Sinnot, R.K. 2005. *Chemical Engineering Design*. Vol. 6.

Sweigart, A. 2020. *PyAutoGUI Documentation*. [Online], Available: https://pyautogui.readthedocs.io/en/latest/.

Chapter 4

Moving Towards Automated, In-Line Monitoring of Phenolic Extraction During Red Wine Fermentations. Part 1: Influence of Sample Preparation and Instrumentation

Chapter 4 - Moving Towards Automated, In-Line Monitoring of Phenolic Extraction During Red Wine Fermentations. Part 1: Influence of Sample Preparation and Instrumentation

Kiera Lambrecht, Wessel du Toit, Hélène Nieuwoudt, José Luis Aleixandre-Tudo
Department Viticulture and Oenology, SAGWRI, University of Stellenbosch, Private Bag X1, Matieland (Stellenbosch), 7602, South Africa

*Corresponding E-mail: joaltu@sun.ac.za

Abstract

Improvements to technology which allows quantification of phenolic compounds in red wine, such as tannins, anthocyanins, and polymeric pigments, are continually being made. Currently infrared (IR) technology is promising due to the rapidity and multivariate nature of the measurements and its non-destructive nature. However, most developments have been made on a laboratory scale with off-line or off-site analysis and these applications must now be adapted to become more suitable to large scale applications. As removal of turbidity poses a challenge with in-line systems during red-wine fermentations, an investigation was conducted to assess the effect of turbidity on the accuracy and reliability of predictive calibrations. Three different commercially available instruments with different spectroscopic acquisition methods were also utilised to evaluate its suitability for such an application. These instruments were chosen as they are widely available and, if suitable, would provide a variety of options for winemakers, including one which is non-invasive. Spectra obtained using both contactless DF-FT-NIR and ATR-MIR were the least affected by suspended solids in a turbid system as the calibrations obtained did not show poorer performance than those developed with clean samples. The PLS calibrations built for these instruments showed suitability for in-line measurement of phenolic compounds. The comparisons of the sample preparation and instruments are also discussed.

Key words: IR spectroscopy, phenolic parameters, turbidity, chemometrics, in-line sampling.

4.1 Introduction

Winemaking is a complex bioprocess consisting of many different stages and variables (Boulton, 1980). Due to the complexity of the process, there are many factors which can influence the progression including the conditions under which it proceeds and the cellar practices used (Cavaglia, Schorn-García, Giussani, *et al.*, 2020). These factors, amongst others, can influence phenolic extraction during maceration, alcoholic fermentation and, ultimately, the final phenolic composition of the end product (Setford, Jeffery, Grbin, *et al.*, 2017).

With this potential for large variation in the chemical composition, it is necessary to keep the nature of the global wine industry in mind. It is a highly competitive industry where high-quality products and consistency is in demand (Cusmano, Morrison & Rabellotti, 2010). A need is arising for the implementation of analytical technology to aid in the quantification of compounds during the different stages of winemaking (Shah, Cynkar, Smith, *et al.*, 2010). The ability to monitor the process can provide useful information which can aid in decision making on the part of the winemaker (Gishen, Dambergs & Cozzolino, 2008) to improve wine quality and consistency.

Many studies have explored the use of infrared technology (IR) and chemometrics as a means to monitor fermentation and phenolic extraction, and have determined that it can be appropriate for this application (Aleixandre-Tudo, Nieuwoudt & du Toit, 2019; Aleixandre-Tudo, Nieuwoudt, Olivieri, *et al.*, 2018; Basalekou, Kallithraka, Tarantilis, *et al.*, 2019; Basalekou, Pappas, Kotseridis, *et al.*, 2017; Cozzolino & Curtin, 2012; Cozzolino, Kwiatkowski, Parker, *et al.*, 2004; Patz, Blieke, Ristow, *et al.*, 2004; dos Santos Costa, Oliveros Mesa, Santos Freire, *et al.*, 2019; Sen, Ozturk, Tokatli, *et al.*, 2016; Urtubia, Pérez-correa, Pizarro, *et al.*, 2008; Wang, Li, Ma, *et al.*, 2014) . However, these studies have made use of a discontinuous approach where spectral analysis was conducted on samples manually taken from the fermentation vessels. These samples also received a degree of pre-treatment in the form of either centrifugation or freezing, both of which are not ideal unit operations for real-time and in-line systems. As such, the off-line analysis poses a limitation. One aspect which can influence the accuracy and reliability of the models is the presence of turbidity. Without centrifugation or high-pressure ultra-filtration, some suspended solids, caused by yeast and grape particulates, are an inevitability.

The extent of the influence of solids on partial least squares (PLS) calibration models built for phenolic analysis of red wine has not been studied in depth. As such the aim of this study was to better understand the impact, if any, of turbidity and dissolved gasses on the accuracy and reliability of predictive models for five phenolic parameters across a range of different infrared instruments. Predictive models were built for three different instruments using four different sample treatments. Different cultivars were used along with enzymatic treatments to broaden the range of the phenolic parameters. For collection of spectra, the spectrometric techniques used

were transmission Fourier transform near infrared (T-FT-NIR), diffuse reflectance Fourier transform near infrared (DR-FT-NIR) and finally attenuated total reflectance mid infrared (ATR-MIR).

The performance of the models was considered with a number of different methods and statistics. In addition to metrics such as regression coefficient (R^2), residual predictive deviation (RPD), interclass correlation (ICC), and root mean square error (RSME), slope and intercept (SI) tests were performed. This was done to determine the cause of differences between true and predicted values as well as differences between predicted values of different instruments, thus allowing a comparison to be made between different spectroscopies. Wave number selection and spectral pre-processing were in this case avoided to evaluate the real effect of sample pre-treatment on the accuracy of the PLS calibrations. Based on the statistics, the ability of the instrumentation and modelling techniques to overcome sample format was determined.

4.2 Materials and Methods

4.2.1 Small Scale Vinifications

For the small-scale fermentations, 120 kg batches of Shiraz and of Cabernet Franc were collected from a collaborating cellar in the Cape Winelands region of South Africa. Both cultivars were stored at 4 ^{o}C for two days before crushing and destemming took place. On the day of crushing and destemming, the cultivars were processed separately with the crusher/destemmer being thoroughly cleaned in between to ensure that there was no mixing of cultivars.

The skins and juice of each cultivar were mixed after crushing to ensure homogeneity and were then subdivided into six 20 kg containers. Once the must had been separated, the fermentation vessels were then moved into a 25 ^{o}C fermentation room and the SO_2 concentration of the must was adjusted to 30 mg/L using a 2% SO_2 solution. For the alcoholic fermentation (AF), the strain of *Saccharomyces cerevisiae* used was ICV D21® (Lalvin) and this was rehydrated, and the must inoculated according to manufacturer's instructions.

For each cultivar, three of the fermentations received enzyme (Lafase® HE Grand CRU Vin Rouge) additions at the same time as inoculation. As with the yeast, these enzymes were rehydrated and dosed according to manufacturer's instructions. During the alcoholic fermentation, three punch downs were done daily at 08:00, 12:00 and 16:00.

Figure 4.1 shows a flow diagram of the grape processing and subdivision for different treatments.

4.2.2 Sampling and Sample Preparation for Infrared Spectroscopy

Immediately after the 08:00 punch down was completed; a single 200 mL sample was taken from each fermentation. This single sample was homogenised with the use of a Vortex and immediately divided into four 2 mL samples (for the purposes of ATR-MIR spectroscopy) and eight 20 mL samples (for the purposes of FT-NIR spectroscopy) to prevent resettling of any solids. These 2 mL and 20 mL samples received the sample treatments described below. Figure 4.2 shows a flow diagram of the sample subdivision and preparation for IR scanning.

Four different sample treatments were applied to samples taken during a fermentation. The first type of sample treatment involved freezing the sample overnight, thawing the following day at room temperature and centrifuging for 5 minutes at 10000 rpm or 11180g (Eppendorf 5415 D, Hamburg, Germany) centrifuge (Aleixandre-Tudo, Nieuwoudt, Aleixandre, *et al.*, 2018). After centrifugation, the supernatant was removed from the solid constituents. One sample per instrument per day was to remain completely turbid and, therefore, the only treatment these

samples received was to vortex them before IR scanning. A third sample treatment involved degassing the samples with a vacuum apparatus after the same centrifugation as the frozen samples. Finally, one sample treatment involved filtering the samples through 400 µm 316L stainless steel mesh filters (Xylem Flojet Process Pump Filter, RS Components). The three sample treatments which were not frozen were analysed the same day as sampling, whilst the frozen treatment was analysed the following day.

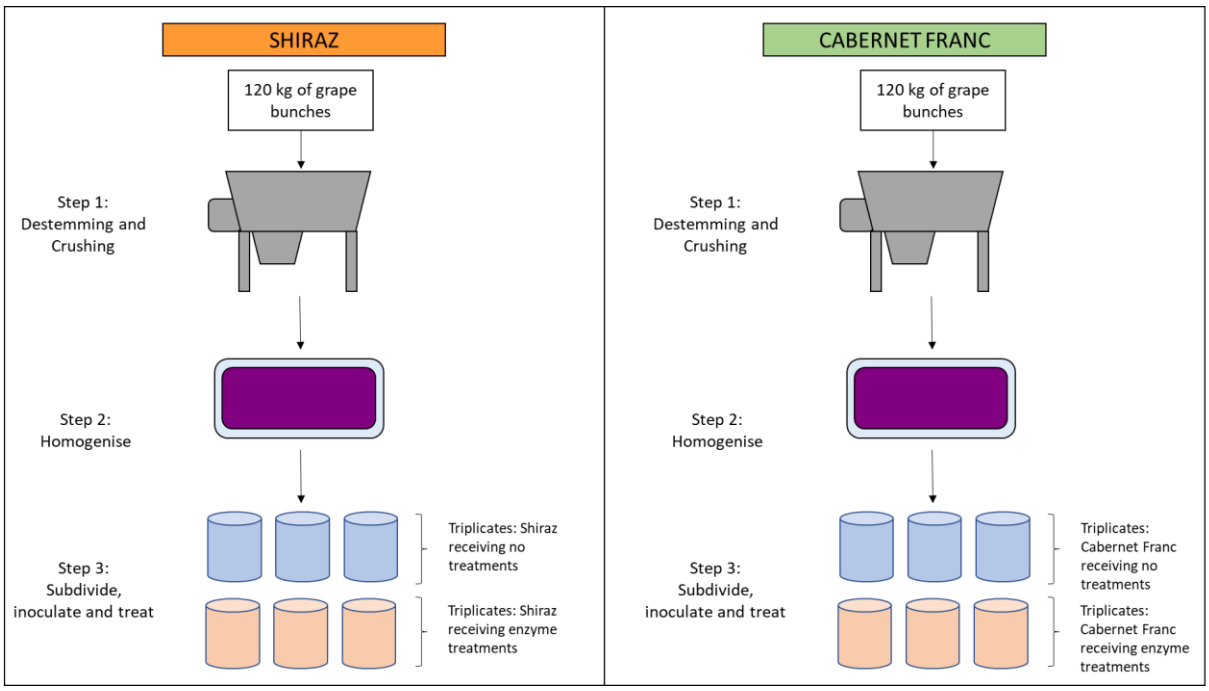

Figure 4.1: Flow diagram showing the crushing, destemming and division of the must

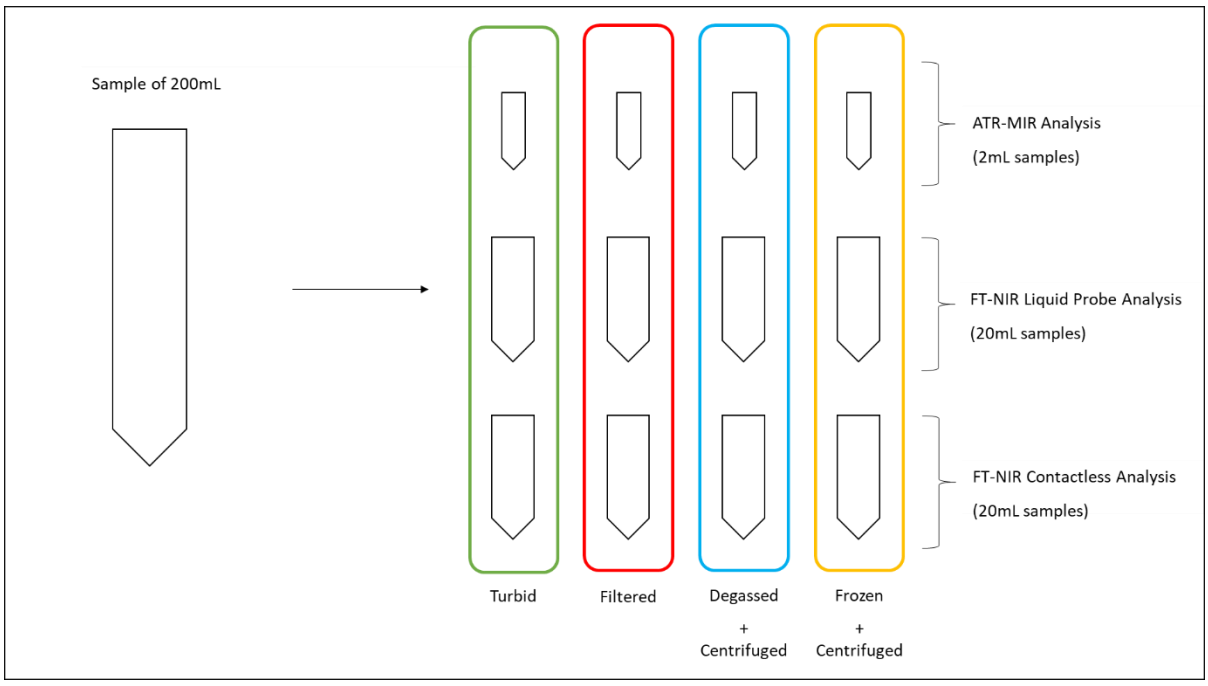

Figure 4.2: Diagram showing the subdivision of samples taken from the must

4.2.3 Reference Data Collection

4.2.3.1 Total Anthocyanin and Total Phenolic Content

For quantification of total anthocyanin concentration and total phenolic content, a method reported by Iland et al. (2000) was utilized (Aleixandre-Tudo, Nieuwoudt, Olivieri, *et al.*, 2018; Iland, 2000). In short, a 100 µL sample of fermenting must was diluted with 5 mL of 1M HCl and allowed to stand for 1 hour in the dark (Bindon, Kassara, Cynkar, *et al.*, 2014). The absorbances at 280 nm and 520 nm were then recorded using a UV-vis spectrophotometer (Multiskan GO Microplate Spectrophotometer, Thermo Fisher Scientific, Inc., Waltham, MA, USA). The total phenolics index (TPI) was calculated by multiplying the absorbance at 280nm by the dilution factor. The anthocyanin content was calculated, as malvidin-3-glucoside equivalents, using the following equation (Iland, 2000):

$$Anthocyanins\ \left(\frac{mg}{L}\right) = \frac{A_{520nm} \cdot MW \cdot DF}{\varepsilon\ x\ L} \tag{4.1}$$

Where A_{520nm} refers to the absorbance at 520 nm, MW and ε refer to the molecular weight (529 $\frac{g}{mol}$) and the extinction coefficient (28.000 $\frac{L}{cm \cdot mol}$) of malvidin-3-glucoside respectively, DF refers to the dilution factor of 51 and L refers to the standard 1 cm pathlength.

4.2.3.2 Methylcellulose Tannin Assay

The method for tannin quantification adapted by Mercurio, Dambergs, Herderich, and Smith (2007) to a high throughput format was used. The reagents required for this method are 0.04% w/v methylcellulose solution (Sigma Aldrich) and a saturated ammonium sulphate solution (Sigma Aldrich) (Mercurio, Dambergs, Herderich, *et al.*, 2007). For the preparation of the control sample, 50 µL of fermenting must was pipetted into a 2 mL microfuge tube, followed by 400 µL of saturated ammonium sulphate solution and 1550 µL of distilled water. The treatment sample was prepared by adding 600 µL of methyl cellulose solution to a 50 µL sample of fermenting must in a 2 mL microfuge tube. After a 3-minute wait, 400 µL of saturated ammonium sulphate and 950 µL of distilled water were added. Both the control and the treatment samples were centrifuged at 10000 rpm for 5 minutes (Eppendorf 5415 D, Hamburg, Germany). Thereafter, the samples stood undisturbed for 10 minutes. The absorbances of the controls and treatments were then measured at 280 nm using a 96 well micro plate and the differences between these were calculated. This value was used to calculate the final tannin

concentration by converting the difference in absorbances into epicatechin equivalents and multiplying by the dilution factor of 40.

4.2.3.3 Colour Density

50 µL of fermenting must was pipetted directly into a 96 well microplate (Thermo Fisher Scientific, Inc., Waltham, MA, USA) and the absorbances were measured at 420 nm, 520 nm and 620 nm using a UV-vis spectrophotometer. The colour density was obtained by calculating the sum of these absorbances (Li, Zhu, Li, *et al.*, 2017).

4.2.3.4 SO_2 Resistant Pigments

The modified Somers Assay adapted by Mercurio, Dambergs, Herderich, and Smith (2007) was used to quantify SO_2 resistant pigments. The buffer solution used was model wine (pH of 3.4 adjusted with 1M NaOH solution) consisting of 0.5% w/v tartaric acid and 12% v/v ethanol. 200 µL of a sample of fermenting must was diluted with 1.8 mL of buffer solution with 0.375% w/v sodium metabisulphite (Mercurio *et al.*, 2007). After vortexing, the samples stood at room temperature for 1 hour. The absorbance was measured at 520 nm and, using Equation 4.1, the concentration of SO_2 resistant pigments in mg/L was obtained.

4.2.4 ATR-MIR Spectroscopy

ATR-MIR spectra were obtained using an Alpha-P ATR FT-MIR spectrometer (Bruker Optics, Ettlingen, Germany) fitted with a 2 mm^2 single bounce diamond crystal sample plate in a closed configuration. When scanning the samples, 128 sample scans were taken with the sample plate set at 30 ^oC and the wavenumber range used was 4000-400 cm^{-1} with a 4 cm^{-1} resolution. A background spectrum, using distilled water, was obtained at the beginning of each scanning session and once every two hours. All instrumental control and set up was done through the OPUS Wine Wizard (OPUS v. 7.0 for Microsoft, Bruker Optics, Ettlingen, Germany).

4.2.5 FT-NIR Spectroscopy

Spectra were collected using a Multi-purpose analyser (MPA) FT-NIR instrument (Bruker Optics, Ettlingen, Germany) in transmission mode. The fibre optic liquid probe attachment of the instrument was lowered into a 20 mL sample of fermenting must and held in place with a stand to prevent movement. A total of 64 sample scans were completed at a 2 cm^{-1} resolution using a wavenumber range of 12,500 – 4000 cm^{-1}. An air background measurement was

obtained when scanning started and once every two hours. The instrument control and set up was performed using OPUS software (OPUS v. 6.5 for Microsoft, Bruker Optics, Ettlingen, Germany). Additional spectra were collected using the Matrix F FT-NIR instrument in diffuse reflectance mode (Bruker Optics, Ettlingen, Germany). For spectral acquisition, two of the four possible tungsten light sources (12 V, 20 W) were used at a measuring distance of 17 cm. A water background spectrum was obtained using a clear glass container set above the reflective spectralon containing 20 mL of distilled water. Sixty-four sample scans were carried out in the wavenumber range 12500 – 4000 cm^{-1} at a resolution of 16 $cm^{-1.}$

4.2.7 Development, Validation and Comparison of PLS Calibrations

Analysis of the data and model performance was done using the QUANT2 method in OPUS (OPUS v. 7.2 for Microsoft, Bruker Optics, Ettlingen, Germany). This software uses PLS regression to correlate the spectral data with reference data for a specific sample set. The optimal rank or number of latent variables was determined by an algorithm which used the predicted residual error sum of squares (Aleixandre-Tudo, Nieuwoudt, Aleixandre, *et al.*, 2018),in this case, however, the software was allowed to explore up to 30 latent variables. As the phenolic parameters account for a small percentage of the samples and may produce a weaker signal, a higher rank was initially allowed. In addition to this, external validation methods were utilised to minimise the chances of overfitting occurring in the model. For each sample preparation method and each instrument, the spectra and the reference data for anthocyanin concentration, tannin concentration, SO_2 resistant pigment concentration, colour density and TPI were imported to OPUS. This sample set was then divided into a calibration set and a test set. To do this, a 66/34 ratio of calibration to validation samples was selected using the Kennard-Stone algorithm. The optimisation of the models was then completed using the “general A” option for ATR-MIR data with no spectral pre-processing. This option is specific to MIR data. The “NIR” option was used for spectra collected in the near infrared band of the IR spectrum, also with no spectral pre-processing. Subdivision of the spectra was not used as part of the strategy as it allowed for an untargeted optimisation strategy, therefore including any abnormal effects that the sample preparation may have had on the spectra. The calibration was built and optimised using a cross validation method where a certain number of samples were excluded and used for internal validation. As only one spectral pre-processing method was used and the entire spectral region was used, only one calibration was built per sample treatment on each instrument. After this, validation of the calibration using the pre-determined test set was performed. During this second optimisation step, outliers were detected using the Mahalanobis distance. This allows for the calculation of a threshold which

determines the reliability of a prediction. Outliers were removed, and the optimisation method was repeated. The average number of outliers for the study was approximately 2.5%.

The following statistics were used to determine whether the prediction models were robust. The percentage of variation explained by the model is estimated for both the calibration and validation set using the coefficient of correlation for calibration (R^2_{cal}) and validation (R^2_{val}) respectively. Although other requirements must also be met, it is necessary for an R^2 value to be as close to 1 as possible for the model to perform. Lower R^2 values indicate either lack of correlation between spectra and reference values or poor reproducibility (Aleixandre-Tudo, Nieuwoudt, Olivieri, *et al.*, 2018). The fit of the predicted values to the model in the calibration and validation set is shown using the root mean square error of calibration (RMSEC) in the case of the calibration and the root mean square error of prediction (RMSEP) in the case of the validation (Fragoso, Aceña, Guasch, *et al.*, 2011). These measure the difference between values predicted by the models and the values given by the reference methods and thus they provide the real, average prediction error. These values are reported in the same units as the reference values.

Another value which is used when assessing the accuracy of a model is the residual predictive deviation (RPD) for both the calibration (RPD_{cal}) and validation (RPD_{val}) (Fragoso *et al.*, 2011). This value aims to standardise the prediction accuracy and to avoid the effects that arise from the range in the calibration and prediction errors. The RPD is the ratio of the standard deviation of the set and the RMSE, as shown in the following equation:

$$RPD = \frac{SD}{RSME} \tag{4.2}$$

As such, higher RPD values are desirable as they show that there is a greater chance of the model accurately predicting the concentrations of compounds in new sample sets. However, as these aforementioned values are based only on the comparison between the error values reported, a precise statistical assessment of the model's performance is not obtained.
The Deming approach, reported by Linnet (1993) was used to further investigate whether there was systematic error between the values reported by the reference methods and those predicted by the models. The test determines whether the differences between the reference values and the predicted values are due to random noise using a joint analysis on the slope and y-intercept. At a 95% confidence interval, if the slope is found to be 1 and the y-intercept is found to be 0, then the null hypothesis is accepted, and any differences are attributed to random noise. In the study this test was conducted on the predicted values from the validation set.

A method of evaluating the reliability of the predictions is to explore the standard error of measurement (SEM). As it is a method of measuring the precision of the individual measurements, this value is useful for providing an absolute measure of reliability (Williams, Dardenne & Flinn, 2017).

Finally, an inter-class correlation (ICC), which is a measure of the consistency of the predicted values, was also investigated to determine the reliability of the predictions (Weir, 2005). At 95% confidence intervals, this value can range from 0 to 1. ICC's closer to one are desirable as an ICC of 1 shows perfect reliability.

To compare the different instruments and sample treatments, certain metrics such as the RPD and R^2 values were obtained during the development of the models and compared. In addition to this, the Deming test was also used in conjunction with ICC and SEM on the predicted data for each model to determine if the differences in predicted values for these instruments could be attributed to random noise.

4.3 Results and Discussion

4.3.1 Reference Data

It is advisable to have a coefficient of variance (CV) higher than 30% to ensure that there is enough variability contained within the sample set (Aleixandre-Tudo, Nieuwoudt, Aleixandre, et al., 2018; Aleixandre-Tudo, Nieuwoudt, Aleixandre, & Du Toit, 2015). Table 4.1 summarises the statistics for the reference data, compiled from 324 samples, used for the study. From Table 4.1 except in the case of MCP Tannins, all the phenolic parameters have an acceptable coefficient of variance (CV). A histogram can be found in Figure 4a in Supplementary Material (S1) with this data.

The ranges for anthocyanins and polymeric pigments are consistent with those reported in literature and therefore can be considered representative of values occurring in South African red wines. However, the maximum value of the colour density and TPI ranges are lower than that reported indicating that the models may not be appropriate for red wines which have higher values of these phenolic related indexes. The range for MCP Tannins was partially consistent with literature as the minimum value is an order of magnitude larger than that reported, and the maximum value is approximately one half of that stated. Therefore, the models developed may encounter difficulties in predicting values for red wines with lower or higher tannin content or samples from early in fermentation.

Table 4.1: Summary Statistics of Phenolic Parameters for Must and Wine

Variable	Units	Range	SD	Mean	CV
Anthocyanins	mg/L	22.58 - 874.51	227.00	450.56	50.38
Colour Density	[-]	0.33 - 33.63	9.97	17.13	58.22
MCP Tannins	mg/L	507.10 – 1400.00	202.45	820.84	24.66
Polymeric Pigments	mg/L	1.36 - 166.75	46.71	63.87	73.14
TPI	[-]	3.94 - 67.42	16.43	38.13	43.06

If more generalised models are to be deployed where a wider variety of samples will be encountered, using a wider range of vintages, cultivars and regions must be added to the sample set. However, for the purposes of this study the ranges of phenolics observed are within normal ranges found in red wines and are, therefore, valid for this study.

4.3.2 Principal Component Analysis

Principal component analysis (PCA) was performed as this allows for the maximum amount of variance in the information to be described whilst minimising the number of latent variables used (Wold, Esbensen & Geladi, 1987). For this data set, the main objective was to visually determine whether groupings were present based on the sample preparation and to determine what regions in the spectra, if any, were most affected by turbidity. The analysis was performed using PCA Toolbox (Ballabio, 2015) for MATLAB software version R2019b (Mathworks Inc., Natik, MA).

A preliminary study of the data was performed in the form of Principal Component Analysis (PCA). This was done to identify possible grouping of data based specifically on sample preparation as well as to detect potential outliers caused by abnormal spectra. PCA was performed on all the raw spectra (wavenumbers of 4000 – 400cm-1 for MIR and 4000 – 14000 cm-1 for NIR) to reduce dimensionality and explain the information contained.

For each instrument, PCA was also performed on the clean samples (i.e., those which centrifugation was applied to remove solids). This was done to determine if prior freezing led to marked differences in the sample. The scores and loadings plots for these can be found in Figure 4.1a through Figure 4.1i in the Supplementary Material (S1). They show no strong groupings, and this may indicate a negligible effect of freezing on sample spectra.

4.3.2.1 Reflection Attenuated Total Reflection Mid-Infrared (ATR-MIR)

For the set of spectra obtained using this infrared technique, five principal components were identified, and these explained 96.9% of variance in the data. The score plots for the other principal components, as well as the relevant loadings plots, can be found Figures 4.3a through 4.3u in Supplementary Material (S1).

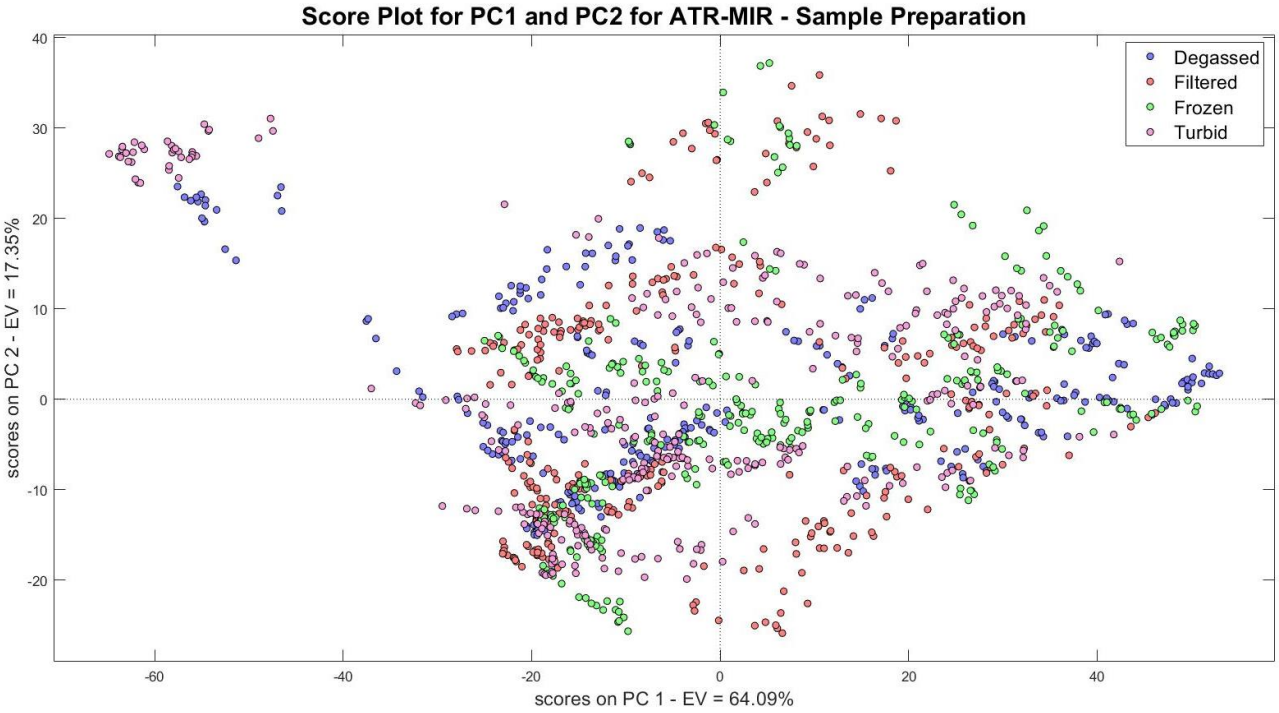

Figure 4.3: PC1 and PC2 for the ATR-MIR with Different Treatments

Different classes have been used to identify potential clustering. These classes are namely day of fermentation, sample treatment, enzyme treatment and cultivar. When considering the plots generated, no clustering is present, and instead the data is distributed throughout the PCA scores space.

The score plots for this instrument show no groupings based on sample treatment (Figure 4.3). This indicates that the sample treatment may have little to no effect on the accuracy of the predictive model developed for ATR-MIR.

4.3.2.2 Diffuse Reflectance Fourier Transform Near-Infrared Spectroscopy (DR-FT-NIR)

In the case of DR-FT-NIR, three principal components were identified. From the score and loadings plots (Figures 4.4a through 4.4k) in Supplementary Material (S1), the points are spread out throughout the space. In the case of cultivar, day of fermentation and enzymatic treatment, no separation or grouping was observed.

When considering the different sample treatments however, the more turbid samples have positive correlation with PC 1 and the frozen and centrifuged samples had a negative correlation with PC 1 as seen in Figure 4.4. The loadings plot associated with PC 1 shown in Figure 4.4a in Supplementary Material (S1) suggests that the suspended solids interact with the IR radiation in the region of 12000 – 7200 cm-1.

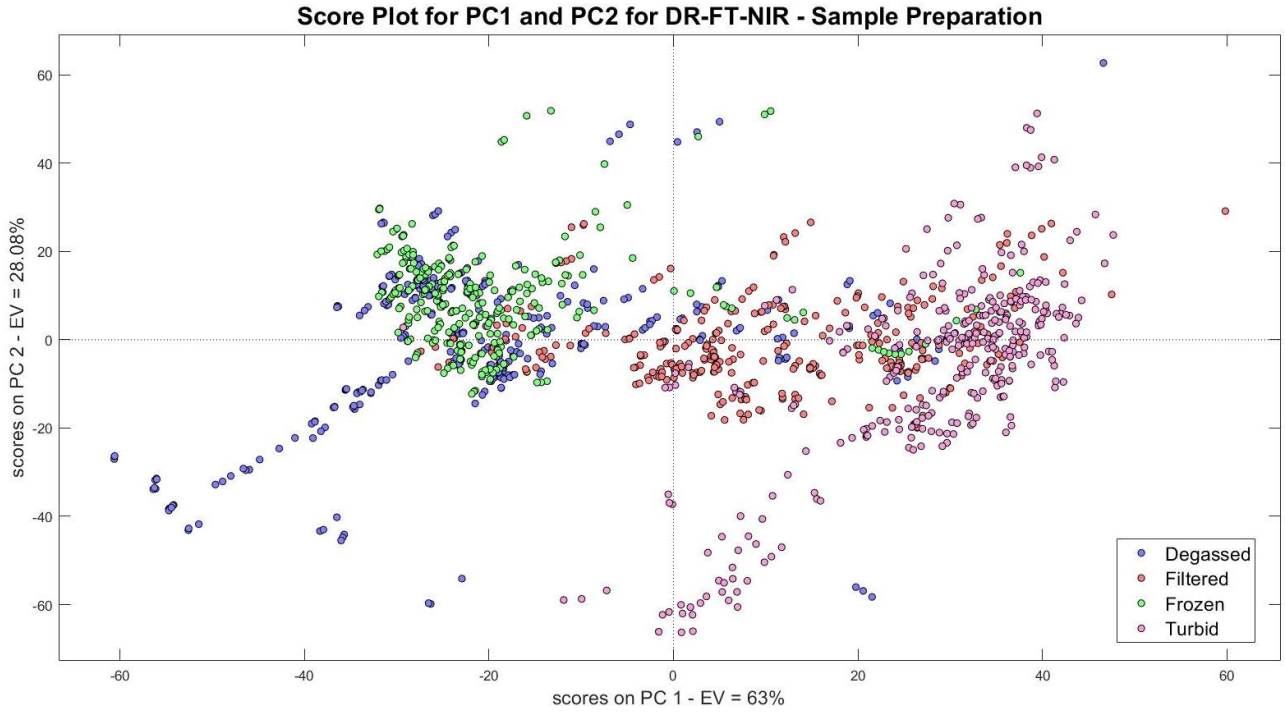

Figure 4.4: PC1 and PC2 for the DR-FT-NIR with Different Treatments

4.3.2.3 Transmission Fourier Transform Near-Infrared Spectroscopy (T-FT-NIR)

Three principal components were identified for the T-FT-NIR instrument. From the score and loadings plots (Figures 4.5a through 4.5k) shown in the Supplementary Material (S1), there appear to be no distinctive groupings based on cultivar, day of fermentation and enzymatic treatment. The samples were found to be distributed throughout the space when considering PC 2 and PC 3.

In the PCA score plot displayed in Figure 4.5, the samples which contain suspended solids have a negative correlation with PC 1 while those which were centrifuged had a positive correlation. However, the filtered samples appeared throughout the plot area. The centrifuged samples appear to cluster more tightly and have a positive correlation with PC 2 while the other sample treatments are more spread out. From the loading's plot for PC 1 in Figure 4.5a in Supplementary Material (S1), this further supports that that the suspended solids interact with the IR radiation in the region of 12000 – 7200 cm^{-1}.

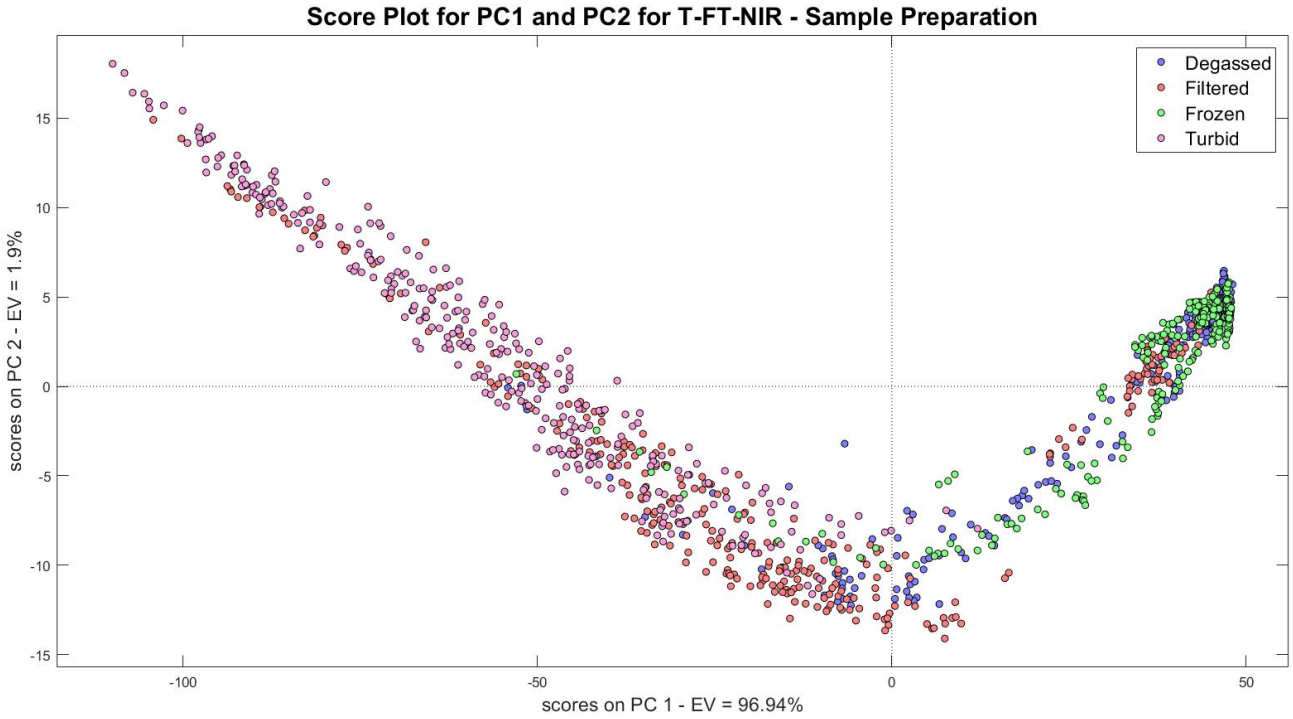

Figure 4.5: PC1 and PC2 for the T-FT-NIR with Different Treatments

4.3.3 PLS Regression Models

The results shown in Table 4.2 were generated using ATR-MIR spectroscopy. In addition to this, graphical representations of selected models can be found in Figure 4.7a – Figure 4.7c in Supplementary Material (S1). Very briefly, this makes use of different refractive indexes at the interface of the sample and the instrument's sample plate. The light is reflected at the internal surface of the crystal and an evanescent wave is allowed to penetrate the sample up to a depth of 2 µm, though usually shallower (Mirabella, 1993) This technique has been reported to allow spectral collection from both turbid opaque samples (Dufour, 2009).

From Table 4.2, there was no one sample treatment that resulted in calibrations that outperformed the others by large margins. The values for R^2, RPD, RMSE and ICC were all in the same magnitude and were similar in value for all the models. For each parameter, the highest RPD and R^2 is not associated with any one particular sample treatment. All the models had values for the performance metrics which indicated that they are suitable for in-line, industrial analysis. This is consistent with information reported in literature, which states that neither turbidity nor opacity should affect this method of analysis. Due to the rapid nature of the analysis, it is also possible that the suspended particulates did not have the time to settle onto the crystal and would therefore not interfere. It seems that the removal of gasses does not significantly affect or improve the models, and, once again, this could be attributed to the nature of the analysis. As the gasses would rise to the top of the sample cell, they would not interact with the light penetrating the sample.

From the SI tests, any differences in prediction of anthocyanins, colour density and polymeric pigments can be attributed to random noise. However, in the case of tannins and total phenolic index, this does not appear to be the case. When considering tannins, a higher level of turbidity might cause errors that cannot be attributed to the random noise of the instrument. Interestingly enough, the predictions for total phenolic index appear to be more reliable when the sample has been filtered due to the values obtained for the SEM.

Table 4.2: Summary Statistics for the ATR-MIR Models for Phenolic Parameters

Component	*Sample Treatment*	*Rank*	*N*	R^2_{Cal}	R^2_{Val}	RPD_{Cal}	RPD_{Val}	*RMSEC*	*RMSEP*	*SI*	*ICC*
Anthocyanins - DG	Degassed	17	324	95.83	92.24	4.9	3.6	47.7	64	Ho Accepted	0.961
Anthocyanins - FI	Filtered	16	324	93.9	91.92	4.05	3.53	57.6	65.5	Ho Accepted	0.959
Anthocyanins - FR	Frozen	12	322	88.85	90.03	2.99	3.17	77.3	71.6	Ho Accepted	0.95
Anthocyanins - T	Turbid	12	318	91.38	89.13	3.41	3.03	68	73.4	Ho Accepted	0.946
TPI - DG	Degassed	5	324	88.46	91.43	2.94	3.42	5.4	4.99	Ho Rejected	0.955
TPI - FI	Filtered	12	324	92.06	93.58	3.55	3.99	4.54	4.39	Ho Accepted	0.967
TPI - FR	Frozen	12	322	93.33	92.14	3.87	3.58	4.17	4.92	Ho Rejected	0.959
TPI - T	Turbid	9	318	89.33	93.32	3.06	3.88	5.23	4.45	Ho Rejected	0.946
Tannins - DG	Degassed	4	324	80.52	80.15	2.27	2.25	90.5	87.4	Ho Accepted	0.894
Tannins - FI	Filtered	2	324	73.71	77.89	1.95	2.14	105	91.5	Ho Rejected	0.88
Tannins - FR	Frozen	3	322	79.29	76.91	2.2	2.1	92.5	97	Ho Accepted	0.877
Tannins - T	Turbid	2	317	73.07	76.83	1.93	2.09	104	93.5	Ho Rejected	0.871
Polymeric Pigments - DG	Degassed	9	324	91.11	92.33	3.35	3.64	14.3	12.2	Ho Accepted	0.961
Polymeric Pigments - FI	Filtered	9	324	91.82	92.36	3.5	3.63	13.7	12.2	Ho Accepted	0.962
Polymeric Pigments - FR	Frozen	10	322	91.99	92.3	3.53	3.61	13.7	12.3	Ho Rejected	0.959
Polymeric Pigments - T	Turbid	14	317	93.48	90.61	3.92	3.29	12.3	13.9	Ho Accepted	0.952
CD - DG	Degassed	10	324	93.94	87.38	4.06	2.82	2.6	3.19	Ho Accepted	0.936
CD - FI	Filtered	12	324	93.52	88.72	3.93	2.98	2.71	3.03	Ho Accepted	0.942
CD - FR	Frozen	12	322	93.57	85.97	3.94	2.67	2.69	3.37	Ho Accepted	0.927
CD - T	Turbid	12	318	94.48	89.27	4.26	3.05	2.5	2.9	Ho Accepted	0.947

For the DF-FT-NIR method, the radiation is directed towards a sample and the variations in intensity and direction of the radiation after reflecting from the surface is measured (Hapke, 2010).The sample is usually required to be in powdered form for this method of analysis (Hapke, 2010). However, this method was used for liquid samples to determine if a new application could be found.

In Table 4.3, the performance values show that the best performing models for colour density, tannins, polymeric pigments and TPI all had some form of turbidity and suspended solids present. Only in the case of anthocyanins, was the best performing model built from those samples that were centrifuged before analysis. The lack of turbidity in the sample leading to models with lower performance metrics can be attributed to the radiation completely penetrating a clear sample fully rather than interacting with the molecules in the sample. In only two of the models, namely for MCP Tannins, did the degassed samples or turbid samples perform notably worse than the other sample pre-treatments and this was not a trend observed throughout. This could suggest that the removal of entrained gasses may also reduce the scattering and reflection of the radiation, allowing the light to penetrate the fluid more easily. This being said, the performance metrics indicate suitability of this instrument for application to an in-line system where turbidity is present.

The SI tests indicate that the variation in predicted values generated using models built for colour density, tannins and polymeric pigments can be attributed to random noise. This could indicate that the sample preparation has very little effect on the accuracy and reliability of the models for these phenolic parameters. For this instrument, dissolved gasses may affect the prediction of anthocyanins. This instrument does not appear to be reliable when predicting total phenolic index regardless of sample treatment before scanning as the SI test indicates that large differences between the predicted values and the reference values exist.

Table 4.3: Summary Statistics for the DR-FT-NIR Models for Phenolic Parameters

Component	*Sample Treatment*	*Rank*	*N*	R^2_{Cal}	R^2_{Val}	RPD_{Cal}	RPD_{Val}	*RMSEC*	*RMSEP*	*SI*	*ICC*
Anthocyanins - DG	Degassed	10	324	85.95	88.89	2.67	3	86	77.1	Ho Rejected	0.941
Anthocyanins - FI	Filtered	13	324	89.47	88.97	3.08	3.03	75	76.3	Ho Accepted	0.944
Anthocyanins - FR	Frozen	12	321	89.38	90.54	3.07	3.26	75.1	71.1	Ho Accepted	0.951
Anthocyanins - T	Turbid	10	321	87.41	89.06	2.82	3.02	80.9	75.8	Ho Accepted	0.944
TPI - DG	Degassed	12	324	90.6	89.68	3.26	3.13	4.96	5.6	Ho Rejected	0.944
TPI - FI	Filtered	12	324	89.14	89.05	3.03	3.03	5.33	5.78	Ho Rejected	0.941
TPI - FR	Frozen	11	321	88.74	89.02	2.98	3.04	5.32	5.93	Ho Rejected	0.938
TPI - T	Turbid	8	321	89.52	92.82	3.09	3.74	5.18	4.51	Ho Rejected	0.962
Tannins - DG	Degassed	7	324	78.27	72.79	2.15	1.95	96.2	105	Ho Accepted	0.853
Tannins - FI	Filtered	7	324	81.52	78.01	2.33	2.15	88.5	94.6	Ho Accepted	0.886
Tannins - FR	Frozen	6	321	78.2	75.25	2.14	2.01	96	96.3	Ho Accepted	0.871
Tannins - T	Turbid	6	321	80.25	73.9	2.25	1.98	91.8	102	Ho Accepted	0.864
Polymeric Pigments - DG	Degassed	10	324	88.7	85.33	2.97	2.72	16.1	17.1	Ho Accepted	0.925
Polymeric Pigments - FI	Filtered	13	324	92.29	92.71	3.7	3.6	11.8	13.4	Ho Accepted	0.963
Polymeric Pigments - FR	Frozen	11	321	91.49	88.44	3.43	2.97	14.1	15.4	Ho Accepted	0.939
Polymeric Pigments - T	Turbid	11	321	92.06	92.11	3.55	3.6	13.6	12.4	Ho Accepted	0.959
CD - DG	Degassed	8	324	87.25	81.21	2.8	2.31	3.76	3.9	Ho Accepted	0.901
CD - FI	Filtered	15	324	94.38	86.05	2.54	2.69	2.54	3.36	Ho Accepted	0.927
CD - FR	Frozen	11	321	92.02	84.37	3.54	2.54	2.99	3.6	Ho Accepted	0.920
CD - T	Turbid	10	321	90.29	84.03	3.21	2.51	3.29	3.57	Ho Accepted	0.917

T-FT-NIR spectroscopy involves the transmission of infrared radiation through a sample aliquot (Ye & Spencer, 2017).

These models all show much poorer performance than the other two instruments with six of the models not being suitable for the defined analytical purposes due to lower values for RPD, R^2 and ICC as well as higher RSMEP and rejected null hypotheses in the cases of SI testing. This is shown in Table 4.4, where the performance metrics were lower for the models built using samples which were more turbid or where dissolved gasses were present. This could be due to increased interference from suspended solids and dissolved gasses as the radiation passes through the sample. The increased interference from the solid particulates and the dissolved gasses would contribute towards the generation of abnormal spectra due to interference in the transmission of light to the receiver. In addition to this, abnormal operations can be also be caused by suspended solids collecting on the apparatus even with thorough cleaning. There appears to be significant interference in the spectra themselves as seen in Figure 4.6 in Supplementary Material (S2) comparing a turbid sample (blue) with a centrifuged sample (red). However, with this being said, the highest performing models did not necessarily always correlate with samples that were spun down and degassed. The main region associated with phenolic compounds is 6500 – 5700 cm-1 (Aleixandre-Tudo, Nieuwoudt, Aleixandre, *et al.*, 2018) as opposed to the region where solids may interact (12000 – 7200 cm^{-1}).

Table 4.4: Summary Statistics for the T-FT-NIR Models for Phenolic Parameters

Component	*Sample Treatment*	*Rank*	*N*	R^2_{Cal}	R^2_{Val}	RPD_{Cal}	RPD_{Val}	*RMSEC*	*RMSEP*	*SI*	*ICC*
Anthocyanins - DG	Degassed	6	324	64.01	72.26	1.67	1.9	136	122	Ho Rejected	0.828
Anthocyanins - FI	Filtered	2	321	56.94	64.1	1.52	1.69	148	139	Ho Rejected	0.777
Anthocyanins - FR	Frozen	5	324	39.23	50.37	1.28	1.44	177	162	Ho Accepted	0.638
Anthocyanins - T	Turbid	3	314	49.25	51.52	1.4	1.44	161	161	Ho Rejected	0.663
TPI - DG	Degassed	5	324	78.33	78.71	2.15	2.18	7.41	8.1	Ho Rejected	0.871
TPI - FI	Filtered	4	321	79.41	82.86	2.2	2.45	7.32	7.24	Ho Rejected	0.906
TPI - FR	Frozen	6	324	73.1	79.53	1.93	2.21	8.21	7.98	Ho Rejected	0.870
TPI - T	Turbid	5	314	82.42	83.96	2.39	2.53	6.65	6.64	Ho Rejected	0.908
Tannins - DG	Degassed	5	324	80.99	78.95	2.29	2.2	89.5	92.5	Ho Rejected	0.887
Tannins - FI	Filtered	3	321	66.94	73.36	1.74	1.94	118	101	Ho Accepted	0.858
Tannins - FR	Frozen	5	324	74.73	75.01	1.99	2	103	97.5	Ho Rejected	0.860
Tannins - T	Turbid	5	314	81.24	69.79	2.31	1.82	88.6	107	Ho Rejected	0.877
Polymeric Pigments - DG	Degassed	5	324	86.43	82.33	2.71	2.46	17.5	18.9	Ho Accepted	0.909
Polymeric Pigments - FI	Filtered	4	321	81.82	85.97	2.35	2.7	20.3	16.5	Ho Accepted	0.926
Polymeric Pigments - FR	Frozen	6	324	84.32	83.13	2.53	2.48	18.8	18.4	Ho Accepted	0.913
Polymeric Pigments - T	Turbid	5	314	86.37	79.83	2.74	2.23	17.6	19.7	Ho Accepted	0.892
CD - DG	Degassed	4	324	79.02	74.94	2.18	2.01	4.77	4.53	Ho Accepted	0.870
CD - FI	Filtered	4	321	83.39	75.55	2.45	2.03	4.27	4.3	Ho Accepted	0.872
CD - FR	Frozen	8	324	97.33	74.46	2.81	1.98	3.74	4.54	Ho Accepted	0.866
CD - T	Turbid	5	314	86.68	79.54	2.74	2.22	3.81	3.96	Ho Accepted	0.892

4.3.4 Instrument and Sample Treatment Comparison

The table summarising the statistics of the instrument comparisons can be found in Table 4.1a of Supplementary Material (S3).

From the slope and intercept (SI) testing summarised in this table it can be seen that the differences between the predictions made by the ATR-MIR and the DR-FT-NIR are due to random noise, except in the cases of polymeric pigments in degassed samples and total phenolic index for frozen samples. Additionally, higher ICC values (>0.9) and SEM values also indicate that there are no significant differences between the predictions made by these two spectroscopic methods. This can be attributed to these spectroscopic methods being able to handle presence of solids in a sample. When comparing T-FT-NIR to the other instruments, however, the majority of cases showed the null hypothesis being rejected indicating that there are significant differences between the predictions. This can be attributed to the cleanliness of the sample having an impact on the functionality of the T-FT-NIR resulting in less reliable models with larger errors in prediction.

The outcomes of slope and intercept test, the ICC and the SEM for comparison of sample treatment for the ATR-MIR method can be found in Table 4.2a in the Supplementary Material (S3). From this table, the majority of these tests showed no significant differences between the predictions in the case of ATR-MIR indicating the suitability of the instrument for application where very little sample pre-treatment (if any) takes place.

A statistical summary for the DR-FT-NIR method is presented in Table 4.3a in the Supplementary Material (S3). For each sample pre-treatment comparison, the null hypothesis was accepted in all cases. In conjunction with high ICC values and SEM values within reported values, this indicates that the sample treatment causes no significant difference in the predicted values. The differences which occur in the predictions are due to random instrument noise rather than any influence from the sample pre-treatments performed before analysis. For this study liquid samples were used, and this is also indicative that this method can be used in a wider range of applications.

A summary of the statistics for the T-FT-NIR method can be found in Table 4.4a in Supplementary Material (S3). When considering the SI tests, the majority of the null hypotheses were accepted indicating the prevalence of random noise rather than influence from the pre-treatment. However, it should be noted that a much large number of comparisons showed rejected null hypotheses than for the other two methods. However, when considering the predictions for anthocyanins, all the comparisons, except for degassed vs. filtered and frozen vs. turbid, the null hypothesis was rejected. This can indicate that the sample pre-treatment appears to have a much larger effect for the other components than for the prediction of anthocyanins.

4.4 Concluding Remarks

Currently, techniques allowing for rapid and in-line monitoring of fermentations would benefit the wine industry immensely (Ricci, Parpinello, Laghi, *et al.*, 2014). It would reduce the time and cost of sampling due to limited need for manual and off-site analysis and, further, it would allow for continuous monitoring. Even though, IR spectroscopy has been proven to be suitable for phenolic analysis(Canal & Ozen, 2017; Cavaglia *et al.*, 2020; Ferreiro-González, Ruiz-Rodríguez, Barbero, *et al.*, 2019; Parpinello, Ricci, Arapitsas, *et al.*, 2019), there are certain challenges to overcome and adaptations which must be made. One such challenge that must be considered when implementing an in-line system is turbidity. In the case of red wine fermentations, this turbidity would be as a result of yeast as well as the solid parts of the grape berries. As automatic and non-destructive sampling directly from a tank will likely not result in a sample completely free of turbidity, the effect of this on the accuracy and reliability of the models has to be considered.

To the best of our knowledge, this study represents the first attempt to explore the effect of different sample pre-treatments on the accuracy and reliability of PLS calibration models developed for the prediction of phenolic compounds in red wine fermentations. The study demonstrates that the effect of turbidity and dissolve gasses is largely dependent on the instrument and the type of spectroscopy used. Four different sample pre-treatments were studied across three different instruments to determine the suitability of both the pre-treatment as well as that of the instrument. The results showed that the ATR-MIR and DR-FT-NIR instrumentation were very suitable for in-line application where turbidity is present. In the case of ATR-MIR spectroscopy, the sample pre-treatment does not influence the models due to the manner in which the instrument operates. By contrast, a certain level of turbidity is beneficial to the contactless method utilising DF-FT-NIR spectroscopy as this relies on the scattering and reflection caused by solids. The one method of spectroscopy which underperforms due to turbidity uses transmission FT-NIR spectroscopy as there appears to be too much interference from the solid particles. Multiple instruments being suitable for a particular application allows industries more flexibility when purchasing and installing a system.

It should be noted at this point, that the models were developed using no spectral pre-processing techniques and no wavenumber selection to determine only the effect of the sample treatment and the instrument. This being the case, the models can be further improved with the use of these techniques to reduce the root mean square errors of prediction. This is an area where large improvements in accuracy and reliability can potentially be seen due to the effects of noise reduction in the spectra (Dong *et al,* 2019) as well as the ability of pre-processing and wavenumber selection to aid in reducing the effect of interference. For these models to be effectively deployed into industry, it is advisable to incorporate a larger selection of cultivars and vintages to increase the range of values used to build the calibration models.

4.5 Literature Cited

Aleixandre-Tudo, J.., Nieuwoudt, H. & du Toit, W. 2019. Towards on-line monitoring of phenolic content in red wine grapes: A feasibility study. *Food Chemistry*. 270(March 2018):322–331.

Aleixandre-Tudo, J.L., Nieuwoudt, H., Olivieri, A., Aleixandre, J.L. & du Toit, W. 2018. Phenolic profiling of grapes, fermenting samples and wines using UV-Visible spectroscopy with chemometrics. *Food Control*. 85:11–22.

Aleixandre-Tudo, J.L., Nieuwoudt, H., Aleixandre, J.L. & du Toit, W. 2018. Chemometric compositional analysis of phenolic compounds in fermenting samples and wines using different infrared spectroscopy techniques. *Talanta*. 176(August 2017):526–536.

Ballabio, D. 2015. A MATLAB Toolbox for Principle Component Analysis and Unsupervised Exploration of Data Structure. *Chemometrics and Intelligent Laboratory Systems*. 149:1–9.

Basalekou, M., Pappas, C., Kotseridis, Y., Tarantilis, P.A., Kontaxakis, E. & Kallithraka, S. 2017. Red wine age estimation by the alteration of its color parameters: Fourier transform infrared spectroscopy as a tool to monitor wine maturation time. *Journal of Analytical Methods in Chemistry*. 2017.

Basalekou, M., Kallithraka, S., Tarantilis, P.A., Kotseridis, Y. & Pappas, C. 2019. Ellagitannins in wines: Future prospects in methods of analysis using FT-IR spectroscopy. *Lwt*. 101(June 2018):48–53.

Bindon, K.A., Kassara, S., Cynkar, W.U., Robinson, E.M.C., Scrimgeour, N. & Smith, P.A. 2014. Comparison of extraction protocols to determine differences in wine-extractable tannin and anthocyanin in vitis vinifera L. Cv. shiraz and cabernet sauvignon grapes. *Journal of Agricultural and Food Chemistry*. 62(20):4558–4570.

Boulton, R. 1980. The Prediction of Fermentation Behaviour by a Kinetic Model. 31(1).

Canal, C. & Ozen, B. 2017. Monitoring of Wine Process and Prediction of Its Parameters with Mid-Infrared Spectroscopy. *Journal of Food Process Engineering*. 40(1).

Cavaglia, J., Schorn-García, D., Giussani, B., Ferré, J., Busto, O., Aceña, L., Mestres, M. & Boqué, R. 2020. ATR-MIR spectroscopy and multivariate analysis in alcoholic fermentation monitoring and lactic acid bacteria spoilage detection. *Food Control*. 109:1–7.

Cozzolino, D. & Curtin, C. 2012. The use of attenuated total reflectance as tool to monitor the time course of fermentation in wild ferments. *Food Control*. 26(2):241–246.

Cozzolino, D., Kwiatkowski, M.J., Parker, M., Cynkar, W.U., Dambergs, R.G., Gishen, M. & Herderich, M.J. 2004. Prediction of phenolic compounds in red wine fermentations by visible and near infrared spectroscopy. *Analytica Chimica Acta*. 513(1):73–80.

Cusmano, L., Morrison, A. & Rabellotti, R. 2010. Catching up trajectories in the wine sector: A comparative study of Chile, Italy, and South Africa. *World Development*. 38(11):1588–1602.

Dong, D., Jiao, L., Li, C., & Zhao, C. (2019). Rapid and real-time analysis of volatile compounds released from food using infrared and laser spectroscopy. TrAC - Trends in Analytical Chemistry, 110, 410–416.

Dufour, E. 2009. Fundamentals and Principles of Infrared Spectroscopy. in *Fundamentals and Principles of Infrared Spectroscopy*. 3–27.

Ferreiro-González, M., Ruiz-Rodríguez, A., Barbero, G.F., Ayuso, J., Álvarez, J.A., Palma, M. & Barroso, C.G. 2019. FT-IR, Vis spectroscopy, color and multivariate analysis for the control of ageing processes in distinctive Spanish wines. *Food Chemistry*. 277(July 2018):6–11.

Fragoso, S., Aceña, L., Guasch, J., Busto, O. & Mestres, M. 2011. Application of FT-MIR spectroscopy for fast control of red grape phenolic ripening. *Journal of Agricultural and Food Chemistry*. 59(6):2175–2183.

Gishen, M., Dambergs, R.. & Cozzolino, D. 2008. Grape and wine analysis - enhancing the power of spectroscopy with chemometrics.. *Australian Journal of Grape and Wine Research*. 11(3):296–305.

Hapke, B. 2010. Reflectance Methods and Applications. in *Encyclopedia of Spectroscopy and Spectrometry*. 931–935.

Iland, P. 2000. *Techniques for chemical analyses and quality monitoring during winemaking*. P. Iland (ed.). Campbelltown, Australia: Patrick Iland Wine Promotions.

Li, S.Y., Zhu, B.Q., Li, L.J. & Duan, C.Q. 2017. Extensive and objective wine color classification with chromatic database and mathematical models. *International Journal of Food Properties*. 20(53):S2647–S2659.

Linnet, K. 1993. Evaluation of Regression Procedures for Methods Comparison Studies. 39(3):424–432.

Mercurio, M.D., Dambergs, R.G., Herderich, M.J. & Smith, P.A. 2007. High throughput analysis of red wine and grape phenolics - Adaptation and validation of methyl cellulose precipitable tannin assay and modified somers color assay to a rapid 96 well plate format. *Journal of Agricultural and Food Chemistry*. 55(12):4651–4657.

Mirabella, F.M. 1993. *Practical Spectroscopy Series; Internal reflection spectroscopy: Theory and applications*.

Parpinello, G.P., Ricci, A., Arapitsas, P., Curioni, A., Moio, L., Segade, S.R., Ugliano, M. & Versari, A. 2019. Multivariate characterisation of Italian monovarietal red wines using MIR spectroscopy. *Oeno One*. 53(4):741–751.

Patz, C.D., Blieke, A., Ristow, R. & Dietrich, H. 2004. Application of FT-MIR spectrometry in wine analysis. *Analytica Chimica Acta*. 513(1):81–89.

Ricci, A., Parpinello, G.P., Laghi, L., Lambri, M. & Versari, A. 2014. Application of infrared spectroscopy to grape and wine analysis. in *Infrared Spectroscopy: Theory, Developments and Applications*.

dos Santos Costa, D., Oliveros Mesa, N.F., Santos Freire, M., Pereira Ramos, R. & Teruel Mederos, B.J. 2019. Development of predictive models for quality and maturation stage attributes of wine grapes using vis-nir reflectance spectroscopy. *Postharvest Biology and Technology*. 150(May 2018):166–178.

Sen, I., Ozturk, B., Tokatli, F. & Ozen, B. 2016. Combination of visible and mid-infrared spectra for the prediction of chemical parameters of wines. *Talanta*. 161:130–137.

Setford, P.C., Jeffery, D.W., Grbin, P.R. & Muhlack, R.A. 2017. Factors affecting extraction and evolution of phenolic compounds during red wine maceration and the role of process modelling. *Trends in Food Science and Technology*. 69:106–117.

Shah, N., Cynkar, W., Smith, P. & Cozzolino, D. 2010. Use of attenuated total reflectance midinfrared for rapid and real-time analysis of compositional parameters in commercial white grape juice. *Journal of Agricultural and Food Chemistry*. 58(6):3279–3283.

Urtubia, A., Pérez-correa, J.R., Pizarro, F. & Agosin, E. 2008. Exploring the applicability of MIR spectroscopy to detect early indications of wine fermentation problems. *Food Control*. 19(4):382–388.

Wang, Q., Li, Z., Ma, Z. & Liang, L. 2014. Real time monitoring of multiple components in wine fermentation using an on-line auto-calibration Raman spectroscopy. *Sensors and Actuators, B: Chemical*. 202:426–432.

Weir, J.P. 2005. Quantifying Test-Retest Reliability Using the Intraclass Correlation Coefficient and the SEM. *Journal of Strenght and Conditioning Reasearch*. 19(1):231–240.

Williams, P., Dardenne, P. & Flinn, P. 2017. Tutorial: Items to be included in a report on a near infrared spectroscopy project. *Journal of Near Infrared Spectroscopy*. 25(2):85–90.

Wold, S., Esbensen, K. & Geladi, P. 1987. Principal Component Analysis. *Chemometrics and Intelligent Laboratory Systemsntelligent laboratory systems*. 2(1–3):37–52.

Ye, Q. & Spencer, P. 2017. *Analyses of material-tissue interfaces by Fourier transform infrared, Raman spectroscopy, and chemometrics*.

Chapter 5

Moving Towards Automated, In-Line Monitoring of Phenolic Extraction During Red Wine Fermentations. Part 2: Optimisation of PLS Calibrations for Turbid Samples

Chapter 5 - Moving Towards Automated, In-Line Monitoring of Phenolic Extraction During Red Wine Fermentations. Part 2 - Optimisation of PLS Calibrations for Turbid Samples

Kiera Lambrecht, Wessel du Toit, Hélène Nieuwoudt, José Luis Aleixandre-Tudo

Department Viticulture and Oenology, SAGWRI, University of Stellenbosch, Private Bag X1, Matieland (Stellenbosch), 7602, South Africa

*Corresponding E-mail: joaltu@sun.ac.za

Abstract

Infrared spectroscopy provides an efficient, robust, and multivariate means to measure phenolic levels during the fermentation of wine. Previously, robust calibrations have provided a way to quantify these compounds, however, their use was limited to off-line sampling. With the aim of assessing the possibility of using minimally pre-treated or untreated samples and implement the resulting calibrations in an in-line monitoring set-up, in Part 1 of this study, PLS calibrations were built to explore the effect of sample pre-treatment on the reliability and accuracy of the calibrations. The purpose of the second part of this study was to apply different spectral pre-processing techniques when building similar models to improve precision and robustness as well as to evaluate if the models would be used to assess lower levels of phenolics from the start of fermentation. Evaluation of the models' performance was conducted using a variety of metrics, including slope and intercept tests, interclass correlations and, limits of detection and quantification. The models were shown to be useful for quantification of phenolic compounds and phenolic parameters with minimal or no sample pre-treatment during red wine fermentation. Upon evaluation of performance, the calibrations built for ATR-MIR and DF-FT-NIR were shown to be the most suitable for eventual application in an automated and in-line system with values for Limits of Detection and Quantification being suitable for the duration of fermentation as well as the application of a lower rank.

Key words: Spectral Pre-processing, PLS regression, Infrared Spectroscopy, Phenolic Compounds

5.1 Introduction

Winemaking has been a part of civilisation since as early as 6000 BC, with signs of winemaking practices being documented in Mesopotamia and Caucasus (Robinson, 2014). In modern times, winemaking is a worldwide industry, with many countries being frontrunners in this industry (Cusmano, Morrison & Rabellotti, 2010). As such, this leads to a highly competitive global market, where consistency and quality are required by consumers (Lochner, 2006).

With new technologies becoming available and rapid improvement in software and computing, more methods to monitor parameters of oenological importance have become available and more widely used. In particular, the use of near infrared (NIR) and mid infrared (MIR) spectroscopy in conjunction with chemometrics has become an area of interest in both industrial and research communities for this purpose (Bureau, Cozzolino & Clark, 2019; Daniel, 2015; Debebe, Redi-Abshiro & Chandravanshi, 2017; Gishen, Dambergs & Cozzolino, 2008; Lourenço, Lopes, Almeida, *et al.*, 2012; Oliveira-Folador, Bicudo, de Andrade, *et al.*, 2018). As with most industrial processes, control of the winemaking process is essential to avoid problems that may arise leading to low-quality wines and, therefore, loss of a competitive edge (Cavaglia, Schorn-García, Giussani, *et al.*, 2020). Previously, time consuming and, often, destructive methods were used to quantify certain phenolic and oenological parameters during fermentation (Debebe *et al.*, 2017).

Phenolic components present in wine contribute towards the sensory qualities such as mouthfeel, colour, and taste (Cozzolino, D; Dambergs, 2009; Setford, Jeffery, Grbin, *et al.*, 2017). As such, measuring and monitoring the extraction of these compounds during fermentation is an important aspect of ensuring quality parameters are achieved and process control is maintained (Aleixandre-Tudo, Nieuwoudt, Aleixandre, *et al.*, 2018; Lourenço *et al.*, 2012). Robust and multivariate models utilising both NIR and MIR instrumentation have been developed to quantify oenological parameters, however, these rely on discrete samples which have received treatments to remove particles in suspension and therefore negate turbidity (Aleixandre-Tudo, Nieuwoudt, Aleixandre, *et al.*, 2018; Cavaglia *et al.*, 2020; Patz, Blieke, Ristow, *et al.*, 2004). To our knowledge, there have been no attempts to build or optimise PLS calibrations for phenolic parameters and concentration of phenolic compounds in turbid red wine samples using infrared (IR) spectroscopy.

Previously, a study was conducted to explore the effect of different sample treatments on spectral data and PLS calibrations built for a variety of different instruments and spectroscopic techniques. In this case, the PLS calibrations built using samples which received various levels of clarification showed promise with quantifying phenolic parameters during wine fermentation. The purpose of this study is to further move towards automated and in-line methods of analysis by optimising calibrations with spectral pre-processing techniques and wavenumber selection. This was done

in order to improve the robustness and accuracy of the models and to evaluate whether the models are applicable from the start of a fermentation when lower phenolic levels are present as the limit of detection and quantification was not explored before optimisation. Again, this was explored across a variety of different instruments using three different infrared spectroscopic techniques. PLS regression models were only optimised for samples containing turbidity as these would more accurately represent samples taken directly from a fermentation vessel.

5.2 Materials and Methods

5.2.1 Small Scale Vinifications and Sample Treatment

Small-scale fermentations of 20 kg were conducted for this investigation and the same fermentations were used as in Part 1. One hundred and twenty kilograms each of Shiraz and Cabernet Franc were collected from a collaborating cellar in the Stellenbosch region of South Africa. Before crushing and destemming took place, the grapes were stored at 4 ^{o}C for a total of two days. To ensure that no cross contamination occurred during this step of the process, the cultivars were processed separately with the machinery receiving pressure washing between batches.

To ensure homogeneity between the 20 kg fermentations, the juice and skins of each cultivar were mixed thoroughly in a bin after crushing and destemming before subdivision. Once subdivided and the SO_2 concentration had been adjusted to 30ppm using a 2% SO_2 solution, each fermentation was moved into a fermentation room held at 25 ^{o}C. The strain of *Saccharomyces cerevisiae* used for alcoholic fermentation (AF) was ICV D21® (Lalvin) and this was prepared according to manufacturer's instructions.

Half of the fermentations received enzymatic treatments at the same time as inoculation with *S. cerevisiae*. The enzyme used was Lafase® HE Grand CRU Vin Rouge and rehydration and dosing was performed according to manufacturer's instructions. During the course of the AF, three punch downs were done at 08:00, 12:00 and 16:00 each day until dry fermentation was achieved. Samples were collected immediately after the 08:00 punch down. Briefly, the sample was subdivided into equal volumes and each volume received different pre-treatments. The two pre-treatments of interest for this study were filtration through a 400µm mesh (Xylem Floject Process Pump Filter, RS Components) and no pre-treatment, resulting in a turbid sample. 2mL samples were used for ATR-MIR spectroscopy whilst 20mL samples were used for FT-NIR spectroscopy.

5.2.2 ATR-MIR Spectroscopy

An Alpha-P Attenuated Total Reflectance Mid Infrared (ATR-MIR) spectrometer (Bruker Optics, Ettligen, Germany) with a 2 mm^2 single bounce diamond sample plate was used to obtain the spectra in a closed environment. A resolution of 4 cm^{-1} was used over a range of 4000-400 cm^{-1} for 128 sample scans at a temperature of 30 ^{o}C. Prior to sample scanning, a background spectrum was obtained using distilled water and this background was repeated every 2 hours. All control and selections were performed using OPUS Wine Wizard (OPUS v. 7.0for Microsoft, Bruker Optics, Ettlingen, Germany).

5.2.3 Transmission FT-NIR Spectroscopy

Transmission Fourier transform near infrared (FT-NIR) was performed using the liquid probe attachment of the Multi-purpose analyser (MPA) FT-NIR instrument (Bruker Optics, Ettlingen, Germany). A resolution of 2 cm^{-1} was used over a range of 12500 – 4000 cm^{-1} for 64 sample scans at ambient temperature. An air background spectrum was taken prior to scanning and then every two hours. All control and selections were made using OPUS for Microsoft, Bruker Optics, Ettlingen, Germany).

5.2.4 Diffuse Reflectance FT-NIR Spectroscopy

Spectra were also collected using a contactless Matrix F FT-NIR spectrometer in diffuse reflectance mode (DR-FT-NIR) (Bruker Optics, Ettlingen, Germany). For sample scanning, two of the four existing tungsten bulbs (12V, 20W) were used with a 17 cm measuring distance. A background spectrum was obtained prior to scanning using a 20 mL volume of distilled water in a clear glass container. 64 sample scans were performed over a wavenumber range of 12500 – 4000 cm^{-1} at a resolution of 16 $cm^{-1.}$

5.2.5 Reference Methods

5.2.5.1 Iland Analysis for Total Anthocyanin and Total Phenolic Content

For the quantification of total anthocyanin content as well as the total phenolic index of the samples, the method reported by Iland et al. (2000) was used (Aleixandre-Tudo, Nieuwoudt, Olivieri, *et al.*, 2018; Iland, 2000). Briefly, this involves the dilution of a 100µL sample of fermenting must in 5 mL of 1M HCl after centrifugation of the sample. This is then left in the dark for one hour (Bindon, Kassara, Cynkar, *et al.*, 2014). A Multiskan GO Microplate Spectrophotometer (Thermo Fisher Scientific, Inc., Waltham, MA, USA) was then used to measure the absorbances of 200 µL of the samples at 520 nm and 280 nm for each component, respectively. To obtain the total phenolics index (TPI), the absorbance measured at 280 nm was multiplied by the dilution factor. The anthocyanin content was quantified in terms of malvidin-3-glucoside equivalents, with the use of the following equation (Aleixandre-Tudo, Nieuwoudt, Olivieri, *et al.*, 2018):

$$Anthocyanins\ \left(\frac{mg}{L}\right) = \frac{A_{520nm} \cdot MW \cdot DF}{\varepsilon \times L} \tag{5.1}$$

Where A_{520nm} refers to the measured absorbance at 520nm, MW and ε refer to the molecular weight of malvidin-3-glucoside (529 $\frac{g}{mol}$) and the extinction coefficient (28.000 $\frac{L}{cm \cdot mol}$) of this compound respectively, DF represents the dilution factor and L refers to the 1cm pathlength used.

5.2.5.2 Methylcellulose Tannin Precipitation Assay

The concentration of tannins in the samples was quantified using a high throughput method adapted by Mercurio, Dambergs, Herderich, and Smith (2007). The reagents required for this include a 0.04% w/v methylcellulose solution as well as a saturated ammonium sulphate solution (Mercurio, Dambergs, Herderich, *et al.*, 2007). The method requires both a control receiving no methylcellulose and a treated sample receiving the solution. To prepare the control, a 50µL measure of a sample was added to a 2mL microfuge tube, followed by 400µL of the saturated ammonium sulphate solution and, finally, topped up with 1550µL of distilled water. Preparation of the sample receiving treatment involved adding 600µL of the methylcellulose solution to a 50µL measure of the sample. After an elapsed time of three minutes, 400µL of saturated ammonium sulphate was added and 950µL of distilled water was used to bring the volume to 2mL. Both control and treatment were centrifuged at 10000rpm or 11180g for 5 minutes using an Eppendorf 5415 D (Hamburg, Germany) centrifuge after allowing precipitation of the tannins to occur, approximately 10 minutes. The absorbances at 280nm was measured for both the control and treatment. The difference between these values was used to determine the concentration of tannins with the use of a calibration curve using epicatechin equivalents and multiplication by the dilution factor.

5.2.5.3 Colour Density

A 50µ measure of each sample was pipetted into a 96 well microplate (Thermo Fisher Scientific, Inc., Waltham, MA, USA) and the total absorbance measured at 420nm, 520nm and 620nm with distilled water as a blank. The sum of these absorbances yielded the colour density (Li, Zhu, Li, *et al.*, 2017).

5.2.5.4 SO_2 Resistant Pigments

To quantify the concentration of SO_2 resistant pigments in a sample, the modified Somers Assay, adapted by Mercurio, Dambergs, Herderich, and Smith (2007), was used. A buffer solution consisting of model wine (0.5% w/v tartaric acid and 12% v/v ethanol adjusted to a pH of 3.4 using 1M NaOH solution) was used. A 200 µL measure of a sample was diluted with 1.8 mL of the aforementioned buffer solution with 0.375% w/v sodium metabisulphite (Mercurio *et al.*, 2007). After addition of reagents and vortexing, the samples stood for an hour at room temperature. Finally, the absorbance of a 200 µL at 520nm was measured and using Equation 5.1, the final levels of SO_2 resistant pigments was obtained.

5.2.6 Development and Validation of PLS Calibrations

All modelling and evaluation of the models was performed using PLS Toolbox 8.8 for MATLAB R2019b (Mathworks Inc., Natik, MA). The data set was split into a calibration and test set with a ratio of 66/34, respectively. For the calibration, the optimal number of latent variables was calculated using a cross validation procedure. For this, the venetian blinds approach was used using 10 data splits. To determine the best pre-processing method and wavenumber selection for a particular variable, all pre-processing options (including no pre-processing) were considered using both forward and reverser iPLS interval selection. The pre-processing option and interval selection which corresponded with the lowest root mean square error (RMSECV) was selected for further model optimisation.

Certain statistics were used to determine the accuracy and reliability of the models. The coefficient of correlation for calibration (R^2_{cal}) and validation (R^2_{val}) was used to explain the percentage of variation. Although this is not the only requirement for a model to be considered useful for screening or analysis, it is necessary for the respective R^2 value to be as close to 1 as possible. This is the case because low values are indicative of either poor correlation between spectra and the reference values or poor reproducibility in the reference methods themselves (Aleixandre-Tudo, Nieuwoudt, Olivieri, *et al.*, 2018). Another value used in evaluation is the root mean square error (RMSE), which is a measure of the difference between predicted values and the true values determined by the reference methods (Williams, Dardenne & Flinn, 2017). This value, therefore, is able to provide the average prediction error and is reported in the same units as the reference values. Values are reported for both the calibration (RMSECV) and the prediction (RMSEP) (Fragoso, Aceña, Guasch, *et al.*, 2011).

Residual predictive deviation (RPD) is the ratio of standard deviation of the data set to the RMSE and is calculated as follows:

$$RPD = \frac{SD}{RSME} \tag{5.2}$$

This was calculated for both the calibration (RPD_{cal}) and validation (RPD_{val}) (Fragoso *et al.*, 2011). Higher RPD values are more desirable as they indicate a wide range of values in the data set and a small average error between predicted and true values.

Further, slope and intercept tests, reported by (Linnet, 1993) were used in each case to determine if systematic error exists between the predicted values and reference values or if the differences are a product of random noise. As this method of analysis makes no assumptions regarding which set of values is the reference, it is suitable for this analysis. For this test, the null hypothesis is accepted if the slope is found to be 1 and the y-intercept is found to be 0 at 95% confidence intervals. In the study, this test is used on both the predicted values and the reference values for

a particular model as well as the predicted values for sample treatments and different instruments. The inter-class correlation (ICC) is a value which is used to determine the consistency values predicted by the models, and this value also formed part of the statistical analysis used in the validations of the models and in the comparisons between sample treatments and instruments (Weir, 2005). This is a value which can range from 0 to 1. where a value of 1 indicates perfect reliability, and, therefore, values as close to 1 as possible are desirable. Finally, the standard error of measurement (SEM) was also used to validate the models. This method can determine the precision of each individual measurement, and can, therefore, provide an absolute value of the reliability of a model (Williams *et al.*, 2017).

The limit of detection (LOD) and limit of quantification (LOQ) were calculated in MATLAB R2019b (Mathworks Inc., Natik, MA) and used to determine at which point in the fermentation the model could be accurately applied. The regression coefficients of the calculated PLS regression model are used in conjunction with the standard deviations of the reference and spectroscopic methods to calculate the LOD and LOQ. This is possible as the LOD is an indication of the lowest concentration of an analyte which can be detected and therefore accurately predicted. The LOQ is calculated at three times the LOD (Allegrini & Olivieri, 2014).

5.3 Results and Discussion

5.3.1 Reference Data

Table 5.1 shows a summary of the statistics for the reference data used in the refined models. Shown are the standard deviation, mean and coefficient of variation for each component. The variability can be explained using the coefficient of variation, and in each case (except for the MCP tannins) the variability was deemed high enough (i.e. above 30%) to provide sufficient variability for building PLS calibrations (Aleixandre-Tudo, Nieuwoudt, Aleixandre, *et al.*, 2015).

Table 5.1: Summary Statistics of Phenolic Parameters for Must and Wine, (Lambrecht, 2020)

Variable	*Units*	*Range*	*SD*	*Mean*	*CV*
Anthocyanins	mg/L	22.58 - 874.51	227.00	450.56	50.38
Colour Density	[-]	0.33 - 33.63	9.97	17.13	58.22
MCP Tannins	mg/L	507.10 – 1400.00	202.45	820.84	24.66
Polymeric Pigments	mg/L	1.36 - 166.75	46.71	63.87	73.14
TPI	[-]	3.94 - 67.42	16.43	38.13	43.06

5.3.2 ATR-MIR Prediction Models

The mid infrared region of the electromagnetic spectrum has a wavenumber range of 4000 – 400 cm-1 and is the region which provides fundamental vibrational frequencies for certain functional groups in molecules (Larkin, 2011; Ricci, Parpinello, Laghi, *et al.*, 2014). There are certain bands within this region which correspond with different components in wine. Water, ethanol and carbon dioxide are associated with bands at 3305 and 1640 cm-1, 2985 and 1050 cm-1 , and 2341 cm-1 respectively (Aleixandre-Tudo, Nieuwoudt, Aleixandre, *et al.*, 2018). The region associated with phenolic compounds, the fingerprint region, has been reported to be between 1500-1100 cm-1 (Jensen, Egebo & Meyer, 2008).

When considering the R^2 values for a prediction model, a value above 0.8 is considered to be a high degree of correlation (Aleixandre-Tudo, Nieuwoudt & du Toit, 2019) and is thus desirable for the following models. For the ATR-MIR technique, all ten models showed a high degree of correlation as seen in Table 5.2 along with other relevant statistics. RPD values ranging from 1.5-2.5 might be considered suitable for industrial purposes (Aleixandre-Tudo, Nieuwoudt, Olivieri, *et al.*, 2018) although only for screening purposed, while those above 2.5 are considered of sufficient accuracy for prediction of compounds (Santos & Colnago, 2018). The RPD statistic is somehow controversial as varying ranges of accuracy have been reported in literature. The values presented here are used in the context of this application and they should therefore not be extrapolated to different applications. Again, eight of the 10 models showed RPD_{val} that were all adequate for predictions. In the case of MCP tannins, however, these values were instead 2.21

for filtered samples and 2.33 for turbid samples showing less suitability. However, taking into account this particular application, these models can be considered suitable for quantification purposes. The null hypothesis for the models was in most cases accepted. This indicates that differences between the true and predicted values for the models where the null hypothesis was accepted can be considered negligible. To further analyse the reliability and accuracy of the models, the ICC and SEM were investigated. It was found that 80% of the models had an ICC of over 0.9 while the SEM was the same magnitude and lower as the RMSEP in all cases. The models used to predict the MCP tannins had ICC values of 0.88 and 0.89 for turbid and filtered samples, respectively, but had SEM values lower than the RMSE, which can be suggest model reliability (Aleixandre-Tudo, Nieuwoudt, Olivieri, *et al.*, 2018).

When exploring the LOD and LOQ, it was found that all the models except for the one developed for anthocyanins in a filtered sample had LODs lower than the lowest predicted value. In addition to this, the low values of the LOD indicates that they can be used for prediction during the full course of a fermentation.

Different spectral pre-processes were selected based on which resulted in the best performance for each compound, and these can be seen in Table 5.2a in the Supplementary Information S4. The wavenumber regions selected using the iPLS interval selections included the fingerprint region for phenolic compounds. In five of the cases, other regions between 2500 – 4000 cm^{-1} were also selected, which is consistent with the absorption of IR radiation for phenolic compounds such as tannins (Basalekou, Kallithraka, Tarantilis, *et al.*, 2019).

Table 5.2: Summary Statistics for ATR-MIR Models

Component	*Sample Treatment*	*Rank*	*N*	R^2_{Cal}	R^2_{Val}	RPD_{Cal}	RPD_{Val}	*RMSEC*	*RMSEP*	*SEM*	*Bias*	*SI*	*ICC*	*LOD*	*LOQ*
Anthocyanins	Filtered	7	214	0.926	0.8877	3.77	2.97	60.85	77.24	54.431	-9.82	Ho Accepted	0.94	7.22-15.13	21.65-45.39
Anthocyanins	Turbid	8	209	0.836	0.853	2.47	2.61	90.11	85.72	60.858	-3.73	Ho Accepted	0.924	5.06-13.98	15.17-41.93
Colour Density	Filtered	6	214	0.924	0.901	3.65	3.21	2.69	3.19	2.27	0.13	Ho Accepted	0.949	0.35-1.05	1.04-3.16
Colour Density	Turbid	4	209	0.914	0.889	3.43	3	2.87	3.33	2.369	-0.03	Ho Accepted	0.944	0.26-0.40	0.77-1.19
Polymeric Pigments	Filtered	8	214	0.894	0.882	3.09	2.92	15.37	15.53	11.019	-0.83	Ho Accepted	0.938	0.74-2.37	2.21-7.12
Polymeric Pigments	Turbid	7	209	0.906	0.874	3.06	2.82	14.53	15.92	11.288	1.18	Ho Accepted	0.934	0.74-2.80	2.23-8.41
Tannins	Filtered	5	214	0.79	0.804	2.19	2.21	91.33	92.11	65.431	-1.72	Ho Rejected	0.884	38.70-56.06	116.11-168.19
Tannins	Turbid	3	209	0.768	0.816	2.08	2.33	95.89	85.23	60.459	5.17	Ho Rejected	0.895	38.09-45.73	117.27-137.20
TPI	Filtered	9	214	0.894	0.9	3.09	3.18	5.24	5.22	4.766	0.04	Ho Accepted	0.921	0.48-1.28	1.36-3.83
TPI	Turbid	8	209	0.924	0.922	3.67	3.58	4.47	4.53	3.141	0.26	Ho Accepted	0.963	0.96-1.32	2.06-3.95

5.3.3 Transmission Fourier Transform Near Infrared (T-FT-NIR) Prediction Models

Vibrational information given when using the NIR region of the electromagnetic spectrum is in the form of combination bands and overtones. Single compounds form characteristic bands within the spectrum, making this a highly suitable technique for analytical quantification (Ricci *et al.*, 2014). Water and ethanol can be seen at wavenumbers of 6900 cm-1 and 5100 cm-1 respectively. The region surrounding 5600 cm-1 is associated with the main sugars in juice as well as phenolic compounds present in red wine (Cozzolino, Kwiatkowski, Parker, *et al.*, 2004).

The R^2 values reported for the models in this case, were lower than those reported for the ATR-MIR models. However, as seen in Table 5.3, only four of the models showed values below 0.8 and these were for both anthocyanin models, TPI and MCP Tannins for a turbid environment. The RPD_{val} values were lower than those for the MIR models, and only two of those built had an RPD_{val} higher than 2.5. Regarding the slope and intercept testing, the null hypothesis was rejected for all but three models. This indicates that there were significant differences between the true and predicted values for these compounds. This can be attributed to the interference of the solids present in the samples. Even with the rejection of the null hypothesis in most of the cases, the ICC was still greater than 0.9 for six cases and the SEM was lower than the RMSEP in all cases. The ICC values can indicate that the differences are due to the variance in the true vs predicted values, and the SEM values which can be indicative of a certain level of accuracy.

LOD and LOQ values for these models were also investigated. In only six of the cases was the LOD lower than the lowest predicted value indicating that the model may be inaccurate at lower concentrations of the analyte in question. This can also show that the models may suffer inaccuracies in the first few days of a fermentation and that they should rather be used from the middle to later stages of fermentation.

As with the previous spectroscopic technique, different pre-processing techniques were used when building the models. The method which was used most frequently was the baseline correction with automatic weighted least squares with median centering being the second most frequently used technique. Wavenumber regions were identified by the iPLS interval selection and these were 5800 – 6000 cm^{-1}, 7000 – 8000 cm^{-1}, 8500 – 9500 cm^{-1} and 10000-11500 cm^{-1}. The pre-processing methods and interval selections can be found in Table 5.3a in the Supplementary Material (S4). The regions identified by the iPLS do include the region near 5600 cm^{-1} which is known to correlate to phenolic compounds.

Table 5.3: Summary Statistics for T-FT-NIR Models

Component	*Sample Treatment*	*Rank*	*N*	R^2_{Cal}	R^2_{Val}	RPD_{Cal}	RPD_{Val}	*RMSEC*	*RMSEP*	*SEM*	*Bias*	*SI*	*ICC*	*LOD*	*LOQ*
Anthocyanins	Filtered	4	236	0.709	0.729	1.85	1.89	121.03	128.86	89.16	-30.32	Ho Rejected	0.839	89.54-92.01	268.62-276.03
Anthocyanins	Turbid	4	208	0.576	0.652	1.54	1.62	145.4	143.25	97.87	-39.33	Ho Rejected	0.759	62.26-68.53	186.77-205.60
Colour Density	Filtered	5	236	0.838	0.882	2.49	2.85	3.96	3.74	2.615	-0.72	Ho Rejected	0.931		
Colour Density	Turbid	5	208	0.835	0.822	2.48	2.38	3.97	4.26	3.03	-0.15	Ho Rejected	0.903	8.35-8.65	25.05-25.94
Polymeric Pigments	Filtered	3	236	0.8	0.827	2.24	2.4	21.29	18.63	13.19	1.98	Ho Accepted	0.908	3.04-3.28	9.12-9.84
Polymeric Pigments	Turbid	4	208	0.813	0.811	2.32	2.26	20.523	19.83	13.98	2.51	Ho Accepted	0.9	7.02-7.46	21.06-22.39
Tannins	Filtered	2	236	0.785	0.836	2.16	2.46	95.03	82.11	57.90	11.33	Ho Rejected	0.908	37.07-40.45	111.22-121.34
Tannins	Turbid	7	208	0.815	0.748	2.33	1.99	87.12	100.37	70.73	12.89	Ho Rejected	0.855	54.19-78.21	162.57-234.62
TPI	Filtered	4	236	0.863	0.858	2.71	2.62	6.01	6.7	4.77	-0.36	Ho Accepted	0.921	21.94-22.39	65.81-67.18
TPI	Turbid	3	208	0.71	0.757	1.86	2.11	8.58	8.47	6.01	-0.48	Ho Rejected	0.844	27.74-31.46	83.21-94.38

5.3.4 Diffuse Reflectance Fourier Transform Near Infrared (DR-FT-NIR) Prediction Models

The vibrational information provided by this instrument is the same as that for the T-FT-NIR technique discussed in Section 5.3.3.

As shown in Table 5.4, for all the models built for the DR-FT-NIR instrument, R^2 values higher than 0.8 were observed indicating that a high degree of correlation was obtained using this technique. In addition to this, seven of the ten models showed an RPDval above 2.5. However, the models built for prediction of tannins in both turbid and filtered samples and total phenolic index of turbid samples have lower RPDval values (2.29 and 2.33 respectively). Only 50% of the models had a positive result for the slope and intercept test which does indicate that errors between the models and the reference values are not negligible. However, this cannot quantify the magnitude of this error. To investigate the reliability of the models, the ICC was used in conjunction with the SEM. For this IR technique, 70% of the models showed an ICC above 0.9, with the remainder still being above 0.85. The ICC values show that the error observed is more likely due to the variance of the true vs predicted values. Lastly the SEM was in the same order of magnitude at the RMSE and it was lower in every case. In this case, it is indicative of increased accuracy in the models.

The LOD in all cases was lower than the lowest predicted concentration. The LOQ in all cases was also lower than the lower predicted concentration. It is important to note that the first sample of the reference data set used to build the model was collected immediately after crushing. As can be seen from the range presented in Table 5.4, this indicates that the models may start to be used from the first day of fermentation. This indicates that the models are not only accurate and reliable but are useful throughout the entire fermentation which allows for better control over the process.

The different pre-processing methods and wave number regions used can be seen in Table 5.3a of the Supplementary Material (S4). Several different pre-processing methods were applied for the different models, the most common being the Multiway Scaling method. The wavenumber selections in all cases included the region 4100-12000 cm^{-1}, which included the majority of the spectrum taken.

Table 5.4: Summary Statistics for DR-FT-NIR Models

Component	*Sample Treatment*	*Rank*	*N*	R^2_{Cal}	R^2_{Val}	RPD_{Cal}	RPD_{Val}	*RMSEC*	*RMSEP*	*SEM*	*Bias*	*SI*	*ICC*	*LOD*	*LOQ*
Anthocyanins	Filtered	9	212	0.89	0.901	3.03	3.11	74.19	73.77	52.419	-0.34	Ho Accepted	0.95	5.01-18.25	15.03-54.74
Anthocyanins	Turbid	8	213	0.849	0.883	2.58	2.9	86.06	78.56	55.233	-0.22	Ho Rejected	0.937	5.05-11.23	15.16-33.68
Colour Density	Filtered	7	212	0.901	0.889	3.18	3.01	3.07	3.39	2.406	0.19	Ho Accepted	0.942	0.83-1.16	2.50-3.48
Colour Density	Turbid	7	213	0.864	0.887	2.72	3	3.59	3.4	2.419	0.17	Ho Accepted	0.942	0.26-0.58	0.79-1.74
Polymeric Pigments	Filtered	7	212	0.887	0.868	2.99	2.74	15.84	16.71	11.802	-1.84	Ho Accepted	0.931	0.75-3.61	2.24-10.83
Polymeric Pigments	Turbid	3	213	0.962	0.957	5.1	4.78	9.24	9.64	6.811	2	Ho Rejected	0.977	0.75-1.56	2.24-4.67
Tannins	Filtered	6	212	0.791	0.81	2.19	2.29	91.34	90.32	63.889	1.08	Ho Rejected	0.892	38.88-57.02	116.64-171.05
Tannins	Turbid	6	213	0.763	0.823	2.05	2.33	97.348	89.69	63.73	-1.26	Ho Rejected	0.889	38.82-51.53	116.45-154.60
TPI	Filtered	8	212	0.879	0.91	2.88	3.33	5.64	5.04	3.567	-0.5	Ho Accepted	0.954	0.49-1.51	1.38-4.53
TPI	Turbid	7	213	0.795	0.809	2.21	2.3	7.26	7.25	5.152	0.05	Ho Rejected	0.895	0.48-1.86	1.45-5.57

5.3.5 Instrument and Sample Treatment Comparison

For instrument comparison, slope and intercept tests were performed and the ICC and SEM were explored and the summary of these can be seen in Table 5.5. Of the pairwise comparisons for both sample treatments, the null hypothesis was confirmed for 66% of the cases. In the cases where the null hypothesis was accepted, this shows that the differences between the values predicted by different instruments is due to random noise rather than and existing systematic error. In all the cases where the null hypothesis was rejected, the T-FT-NIR technique was found to be in common. This can be due to the fact that this technique is one where the turbidity of the sample does interfere with the infrared scanning in a negative way.

Table 5.5: Summary Statistics for Instrument Comparison

Treatment	*Component*	*Comparison*	*SI*	*ICC*	*SEM*
Filtered	Anthocyanins	Alpha/MPA	Ho Accepted	0.811	90.09
		Alpha/MF	Ho Accepted	0.833	92.25
		MPA/MF	Ho Accepted	0.834	90.16
	Colour Density	Alpha/MPA	Ho Rejected	0.861	3.303
		Alpha/MF	Ho Accepted	0.935	2.468
		MPA/MF	Ho Accepted	0.897	3.003
	Polymeric Pigments	Alpha/MPA	Ho Rejected	0.875	9.52
		Alpha/MF	Ho Accepted	0.938	10.819
		MPA/MF	Ho Rejected	0.851	10.249
	Tannins	Alpha/MPA	Ho Rejected	0.737	66.333
		Alpha/MF	Ho Accepted	0.93	47.064
		MPA/MF	Ho Rejected	0.745	68.207
	TPI	Alpha/MPA	Ho Accepted	0.879	4.581
		Alpha/MF	Ho Accepted	0.958	3.303
		MPA/MF	Ho Accepted	0.869	4.796
Turbid	Anthocyanins	Alpha/MPA	Ho Rejected	0.821	81.508
		Alpha/MF	Ho Accepted	0.887	72.118
		MPA/MF	Ho Rejected	0.767	92.018
	Colour Density	Alpha/MPA	Ho Rejected	0.939	2.36
		Alpha/MF	Ho Accepted	0.953	2.129
		MPA/MF	Ho Accepted	0.912	2.818
	Polymeric Pigments	Alpha/MPA	Ho Accepted	0.929	11.462
		Alpha/MF	Ho Accepted	0.893	14.18
		MPA/MF	Ho Accepted	0.852	16.792
	Tannins	Alpha/MPA	Ho Accepted	0.902	53.353
		Alpha/MF	Ho Accepted	0.916	49.972
		MPA/MF	Ho Accepted	0.875	60.205
	TPI	Alpha/MPA	Ho Rejected	0.88	5.059
		Alpha/MF	Ho Accepted	0.908	4.709
		MPA/MF	Ho Rejected	0.814	6.074

A summary of the statistics comparing the sample treatments for each instrument can be found in Table 5.6. For the ATR-MIR instrument, in all cases the differences in predicted values for the sample treatments can be seen to be a product of random noise. This is confirmed by the accepted null hypothesis for each component as well as ICC values which are consistently higher than 0.9 and SEM values which are within the RMSEP values reported. This may be in part due to the way in which ATR-MIR spectroscopy functions, as well as the spectral pre-processing reducing the interference which may have been caused by solids present in the sample.

For the T-FT-NIR, the null hypothesis was rejected for anthocyanins and total phenolic index. As the null hypothesis is accepted in the other cases and the values for ICC and SEM also suggest that the differences are simply a product of random noise. This suggests that the level of turbidity does not have an effect when predicting certain of the components, whereas, for anthocyanins and total phenolic index, the interreference plays a significant role. As the solid components present in the samples are primarily grape skin and yeast cells, this could be caused by the solids containing reabsorbed anthocyanin molecules.

The statistics given for the DF-FT-NIR also suggest that the turbidity does play a significant role with the predicted values. As this spectroscopic technique is reliant on the presence of solids to function correctly, it was expected that a certain degree of turbidity would improve the model performance.

Table 5.6: Summary Statistics for Sample Treatment Comparison

ATR-MIR				
Component	**Comparison**	**SI**	**ICC**	**SEM**
Anthocyanins	Filtered/Turbid	Ho Accepted	0.939	55.661
Colour Density	Filtered/Turbid	Ho Accepted	0.984	1.225
Polymeric Pigments	Filtered/Turbid	Ho Accepted	0.979	5.873
Tannins	Filtered/Turbid	Ho Accepted	0.949	35.882
TPI	Filtered/Turbid	Ho Accepted	0.978	2.35
T-FT-NIR				
Component	***Comparison***	***SI***	***ICC***	***SEM***
Anthocyanins	Filtered/Turbid	Ho Rejected	0.929	59.321
Colour Density	Filtered/Turbid	Ho Accepted	0.967	1.763
Polymeric Pigments	Filtered/Turbid	Ho Accepted	0.893	13.786
Tannins	Filtered/Turbid	Ho Accepted	0.929	46.16
TPI	Filtered/Turbid	Ho Rejected	0.888	5.2
DR-FT-NIR				
Component	***Comparison***	***SI***	***ICC***	***SEM***
Anthocyanins	Filtered/Turbid	Ho Rejected	0.82	86.131
Colour Density	Filtered/Turbid	Ho Accepted	0.929	2.608
Polymeric Pigments	Filtered/Turbid	Ho Rejected	0.975	7.059
Tannins	Filtered/Turbid	Ho Accepted	0.91	55.64
TPI	Filtered/Turbid	Ho Rejected	0.917	4.492

5.4 Concluding Remarks

NIR and MIR spectroscopy is already beneficial in that it is rapid, non-destructive and requires very little sample preparation (Canal & Ozen, 2017; Cavaglia *et al.*, 2020; Parpinello, Ricci, Arapitsas, *et al.*, 2019). The incorporation of samples which are more representative of those which would be taken directly from a tank is another step in moving towards better process control in the wine industry. PLS regression models developed often make use of spectral pre-processing techniques to improve the accuracy and reliability of the models (Aleixandre-Tudo, Nieuwoudt, Aleixandre, *et al.*, 2018; Debebe *et al.*, 2017; Lourenço *et al.*, 2012; Preys, Roger & Boulet, 2008). In addition to this, wavenumber selection is common when developing calibrations once fingerprint regions have been identified. Further, the applicability of a model is also dependent on the limit of detection as this will determine at what point in the fermentation it can be applied. This metric has been reported in studies conducted on wine fermentations (Aleixandre-Tudo, Nieuwoudt, Olivieri, *et al.*, 2018; Debebe *et al.*, 2017)

To our knowledge, this is the first study of its kind, seeking to use IR technology and chemometric techniques in conjunction with different spectral pre-processing techniques and wavenumber selection to improve PLS regression models for phenolic compounds in wine/must incorporating turbidity. A study by Shrake et al., 2014 demonstrated that non-destructive, in-line monitoring of colour and total phenolic content of red wine is a possibility with very positive results. In this study, samples were filtered in line using a 2 µm filter and analysed using light emitting diode sensors. However, in this study, yeast and pulp were removed with the use of peristaltic pumps before scanning took place (Shrake, Amirtharajah, Brenneman, *et al.*, 2014). The remaining particles, therefore, did not exceed 2 µm in size when scanning took place. In contrast, this study incorporates samples where the size of the solid particulates is not controlled by means of a filter as well as samples where the size of the particles would not exceed 400um in size. This study therefore, allows for more simplistic in-line monitoring, as expensive filters would not need to be incorporated into the system for sampling purposes. However, one aspect addressed in Shrake et al, 2014, which would be beneficial to this study is the development of an in-line flow cell which would replace the physical instrument.

New PLS calibrations for three different spectroscopic methods, namely ATR-MIR, DF-FT-NIR, and T-FT-NIR, were built using different pre-processing techniques and wavenumber selection. The final models for ATR-MIR were shown to be suitable for use in industry, as they had sufficiently high RPD values while also having an LOD and LOQ suitable for lower levels of phenolic compounds. This was the case for ATR-MIR for samples which were filtered and those which received no treatment. This is consistent with how this particular spectroscopic method functions. As the IR radiation is only allowed to penetrate the sample by 2 µm (Mirabella, 1993), entrained gasses and solid particles are expected to not have a substantial influence when the

spectra are obtained. In the case of ATR-MIR, it appears that filtration is more desirable than completely turbid samples. Coupled with spectral pre-processing and wavenumber selection, models with good performance metrics, specifically with regard to RPD and LOD, can be expected from instrumentation such as this in a setting where samples will be taken directly from a fermentation vessel. Of the three spectroscopic acquisition methods, the ATR-MIR had the best performances in terms of RPD and LOD, allowing for accuracy as well as versatility with monitoring a fermentation.

DF-FT-NIR spectroscopy relies on variations in direction and intensity in the IR radiation after it has reflected from a sample's surface (Hapke, 2010). When considering the PLS calibrations built, the most suitable models were those built with filtered samples as these models showed good performance in all the metrics. For samples with higher levels of turbidity, the scattering may be too intense and cause lower performance in these cases. The spectral pre-processing allows for better LOD and LOQ whilst still ensuring that RPD values remain high enough for practicality and reliability. As with the ATR-MIR, these models show promise with regards to industrial application.

In the case of T-FT-NIR, the performance was substantially lower than that of the other two techniques. The spectral pre-processing and wavenumber selection appeared to have little effect with model improvement when turbidity is present, and the models built using these techniques showed higher LODs and LOQs in conjunction with lower RPD values. However, it should still be noted that in certain cases, namely for polymeric pigments and TPI, the models were still appropriate for industrial application. In these cases, it might be pertinent to include better filtration techniques or combine two or more spectral pre-processing techniques to improve the accuracy and reliability of the other PLS calibrations relying on this method.

With the ease of using the instrument and a further reduction in necessary sample treatment, these calibrations can be applied to in-line sampling systems. When deploying models into an industrial setting, it would be beneficial to incorporate a more complete sample set during the modelling stage consisting of a range of different cultivars and fermenting samples with a wider range of values for each phenolic component. These models used in conjunction with process control software can lead to the incorporation of alarms and suggests, therefore, providing an easier way for winemakers to control their fermentations. As most of the models showed good performance and suitability, it would be beneficial to consider other aspects such as cost and ease of installation when selecting a final system to be deployed.

5.5 Literature Cited

Aleixandre-Tudo, J.., Nieuwoudt, H., Aleixandre, J.. & Du Toit, W.. 2015. Robust Ultraviolet-Visible (UV-Vis) Partial Least-Squares (PLS) Models for Tannin Quantification in Red Wine. *Journal of Agricultural and Food Chemistry*. 63(4):1088–1098.

Aleixandre-Tudo, J.., Nieuwoudt, H. & du Toit, W. 2019. Towards on-line monitoring of phenolic content in red wine grapes: A feasibility study. *Food Chemistry*. 270(March 2018):322–331.

Aleixandre-Tudo, J.L., Nieuwoudt, H., Aleixandre, J.L. & du Toit, W. 2018. Chemometric compositional analysis of phenolic compounds in fermenting samples and wines using different infrared spectroscopy techniques. *Talanta*. 176(August 2017):526–536.

Aleixandre-Tudo, J.L., Nieuwoudt, H., Olivieri, A., Aleixandre, J.L. & du Toit, W. 2018. Phenolic profiling of grapes, fermenting samples and wines using UV-Visible spectroscopy with chemometrics. *Food Control*. 85:11–22.

Allegrini, F. & Olivieri, A.C. 2014. IUPAC-consistent approach to the limit of detection in partial least-squares calibration. Analytical Chemistry. 86(15):7858–7866.

Basalekou, M., Kallithraka, S., Tarantilis, P. A., Kotseridis, Y., & Pappas, C. (2019). Ellagitannins in wines: Future prospects in methods of analysis using FT-IR spectroscopy. Lwt, 101(June 2018), 48–53

Bindon, K.A., Kassara, S., Cynkar, W.U., Robinson, E.M.C., Scrimgeour, N. & Smith, P.A. 2014. Comparison of extraction protocols to determine differences in wine-extractable tannin and anthocyanin in vitis vinifera L. Cv. shiraz and cabernet sauvignon grapes. *Journal of Agricultural and Food Chemistry*. 62(20):4558–4570.

Bureau, S., Cozzolino, D. & Clark, C.J. 2019.

Canal, C. & Ozen, B. 2017. Monitoring of Wine Process and Prediction of Its Parameters with Mid-Infrared Spectroscopy. *Journal of Food Process Engineering*. 40(1).

Cavaglia, J., Schorn-García, D., Giussani, B., Ferré, J., Busto, O., Aceña, L., Mestres, M. & Boqué, R. 2020. ATR-MIR spectroscopy and multivariate analysis in alcoholic fermentation monitoring and lactic acid bacteria spoilage detection. *Food Control*. 109:1–7.

Cozzolino, D; Dambergs, R.G. 2009. Wine and Beer. in *Infrared Spectroscopy for Food Quality Analysis and Control*. 127–168.

Cozzolino, D., Kwiatkowski, M.J., Parker, M., Cynkar, W.U., Dambergs, R.G., Gishen, M. & Herderich, M.J. 2004. Prediction of phenolic compounds in red wine fermentations by visible and near infrared spectroscopy. *Analytica Chimica Acta*. 513(1):73–80.

Cusmano, L., Morrison, A. & Rabellotti, R. 2010. Catching up trajectories in the wine sector: A comparative study of Chile, Italy, and South Africa. *World Development*. 38(11):1588–1602.

Daniel, C. 2015. The role of visible and infrared spectroscopy combined with chemometrics to measure phenolic compounds in grape and wine samples. *Molecules*. 20(1):726–737.

Debebe, A., Redi-Abshiro, M. & Chandravanshi, B.S. 2017. Non-destructive determination of ethanol levels in fermented alcoholic beverages using Fourier transform mid-infrared

spectroscopy. *Chemistry Central Journal*. 11(1):1–8.

Fragoso, S., Aceña, L., Guasch, J., Busto, O. & Mestres, M. 2011. Application of FT-MIR spectroscopy for fast control of red grape phenolic ripening. *Journal of Agricultural and Food Chemistry*. 59(6):2175–2183.

Gishen, M., Dambergs, R.. & Cozzolino, D. 2008. Grape and wine analysis - enhancing the power of spectroscopy with chemometrics.. *Australian Journal of Grape and Wine Research*. 11(3):296–305.

Hapke, B. 2010. Reflectance Methods and Applications. in *Encyclopedia of Spectroscopy and Spectrometry*. 931–935.

Iland, P. 2000. *Techniques for chemical analyses and quality monitoring during winemaking*. P. Iland (ed.). Campbelltown, Australia: Patrick Iland Wine Promotions.

Jensen, J.S., Egebo, M. & Meyer, A.S. 2008. Identification of spectral regions for the quantification of red wine tannins with fourier transform mid-infrared spectroscopy. *Journal of Agricultural and Food Chemistry*. 56(10):3493–3499.

Lambrecht, K.N. 2020. In-Line Monitoring of Red Wine Fermentation. Stellenbosch University.

Larkin, P. 2011. *Infrared and Raman Spectroscopy; Principles and Spectral Interpretation*.

Li, S.Y., Zhu, B.Q., Li, L.J. & Duan, C.Q. 2017. Extensive and objective wine color classification with chromatic database and mathematical models. *International Journal of Food Properties*. 20(53):S2647–S2659.

Linnet, K. 1993. Evaluation of Regression Procedures for Methods Comparison Studies. 39(3):424–432.

Lochner, E. 2006. The evaluation of Fourier transform infrared spectroscopy (FT-IR) for the determination of total phenolics and total anthocyanins concentrations of grapes by.

Lourenço, N.D., Lopes, J.A., Almeida, C.F., Sarraguça, M.C. & Pinheiro, H.M. 2012. Bioreactor monitoring with spectroscopy and chemometrics: A review. *Analytical and Bioanalytical Chemistry*. 404(4):1211–1237.

Mercurio, M.D., Dambergs, R.G., Herderich, M.J. & Smith, P.A. 2007. High throughput analysis of red wine and grape phenolics - Adaptation and validation of methyl cellulose precipitable tannin assay and modified somers color assay to a rapid 96 well plate format. *Journal of Agricultural and Food Chemistry*. 55(12):4651–4657.

Mirabella, F.M. 1993. *Practical Spectroscopy Series; Internal reflection spectroscopy: Theory and applications*.

Oliveira-Folador, G., Bicudo, M. de O., de Andrade, E.F., Renard, C.M.G.C., Bureau, S. & de Castilhos, F. 2018. Quality traits prediction of the passion fruit pulp using NIR and MIR spectroscopy. *Lwt*. 95(October 2017):172–178.

Parpinello, G.P., Ricci, A., Arapitsas, P., Curioni, A., Moio, L., Segade, S.R., Ugliano, M. & Versari, A. 2019. Multivariate characterisation of Italian monovarietal red wines using MIR spectroscopy. *Oeno One*. 53(4):741–751.

Patz, C.D., Blieke, A., Ristow, R. & Dietrich, H. 2004. Application of FT-MIR spectrometry in wine analysis. *Analytica Chimica Acta*. 513(1):81–89.

Preys, S., Roger, J.M. & Boulet, J.C. 2008. Robust calibration using orthogonal projection and experimental design. Application to the correction of the light scattering effect on turbid NIR spectra. *Chemometrics and Intelligent Laboratory Systems*. 91(1):28–33.

Ricci, A., Parpinello, G.P., Laghi, L., Lambri, M. & Versari, A. 2014. Application of infrared spectroscopy to grape and wine analysis. in *Infrared Spectroscopy: Theory, Developments and Applications*.

Robinson, J. 2014. *The Oxford Companion to Wine*.

Santos, P.M. & Colnago, L.A. 2018. Comparison Among MIR, NIR, and LF-NMR Techniques for Quality Control of Jam Using Chemometrics. *Food Analytical Methods*. 11(7):2029–2034.

Setford, P.C., Jeffery, D.W., Grbin, P.R. & Muhlack, R.A. 2017. Factors affecting extraction and evolution of phenolic compounds during red wine maceration and the role of process modelling. *Trends in Food Science and Technology*. 69:106–117.

Shrake, N.L., Amirtharajah, R., Brenneman, C., Boulton, R. & Knoesen, A. 2014. In-line measurement of color and total phenolics during red wine fermentations using a light-emitting diode sensor. *American Journal of Enology and Viticulture*. 65(4):463–470.

Weir, J.P. 2005. Quantifying Test-Retest Reliability Using the Intraclass Correlation Coefficient and the SEM. *Journal of Strenght and Conditioning Reasearch*. 19(1):231–240.

Williams, P., Dardenne, P. & Flinn, P. 2017. Tutorial: Items to be included in a report on a near infrared spectroscopy project. *Journal of Near Infrared Spectroscopy*. 25(2):85–90.

Chapter 6

Monitoring Phenolic Extraction During Fermentation with Infrared Technology and PLS Calibrations

Chapter 6 – Monitoring Phenolic Extraction During Fermentation with Infrared Technology and PLS Calibrations

6.1 Introduction

The process of red wine making involves extraction of phenolic compounds from the solid constituents of the grape berry. During periods of time where the skin and seeds are in contact with the must or wine, these substances will diffuse into the liquid. As this is a bioprocess with many different layers of complexity, certain factors will contribute towards varying levels of wine quality (Cavaglia, Schorn-García, Giussani, *et al.*, 2020). These factors can include grape quality, choice of yeast and cellar practices applied during fermentation. Specifically, with regard to the latter, different wine making techniques have been known to influence both the rate of this diffusion as well as the final concentrations of these compounds in a wine after alcoholic fermentation (AF) (Sacchi, Bisson & Adams, 2005).

There are many different process variables which can be changed during wine making to influence the phenolic composition of the must/juice. One variable which can be used to manipulate the fermentation is temperature. Certain wine making techniques such as thermovinification, cold soaking, must freezing, or simply fermenting at higher temperatures have been applied in the wine industry (Apolinar-Valiente, Romero-Cascales, Williams, *et al.*, 2014; Boulton, 1980; Favre, Peña-Neira, Baldi, *et al.*, 2014; Federico Casassa, Bolcato, Sari, *et al.*, 2016; González-Neves, Gil, Barreiro, *et al.*, 2010; Medina-Plaza, Beaver, Miller, *et al.*, 2020; Miller, Oberholster & Block, 2019; Ortega-Heras, Pérez-Magariño & González-Sanjosé, 2012). Another practice which is easily performed with winemaking is the addition of certain compounds to the must. The compounds can include enzymes which cause degradation of the cell wall, industrial tannins, or even addition of oxygen through sparging (Geldenhuys, 2009; Kelebek, Canbas & Selli, 2008; McRae, Day, Bindon, *et al.*, 2015; Moenne, Saa, Laurie, *et al.*, 2014; Smith, Mcrae & Bindon, 2015).Whilst manipulation of these variables and, subsequently, the concentration of certain phenolic compounds is possible, it is important to incorporate tools to monitor and measure the composition of the wine. This is mainly due to the need to ensure a product that meets the necessary quality parameters.

The use of infrared spectroscopy in the food and beverage industry has become very widespread due to its versatility, robustness and simplicity (Ayvaz, Sierra-Cadavid, Aykas, *et al.*, 2016; Cavaglia *et al.*, 2020; Cen, Bao, He, *et al.*, 2007; Daghbouche, Garrigues, Teresa Vidal, *et al.*, 1997; Huang, Yu, Xu, *et al.*, 2008; Karoui, Mouazen, Dufour, *et al.*, 2006). It allows for the

implementation of real-time process monitoring and control with minimal sample preparation. This is also the case for red wine fermentations, where the technology, in conjunction with chemometrics, has been shown to be appropriate (Aleixandre-Tudo, Nieuwoudt, Aleixandre, *et al.*, 2018; Basalekou, Kallithraka, Tarantilis, *et al.*, 2019; Cozzolino, Kwiatkowski, Parker, *et al.*, 2004; Patz, Blieke, Ristow, *et al.*, 2004; Wang, Li, Ma, *et al.*, 2014). With the suitability of these technologies being established, it is expected that they can be used to differentiate between fermentations which have received different wine making treatments.

This chapter details the suitability of attenuated total reflectance mid-infrared (ATR-MIR) instrumentation combined with chemometric models developed for in-line sampling to monitor trends in phenolic extraction. Different wine making practices were applied to influence the phenolic composition during fermentation and the ability of the system, as a whole, to be used to differentiate between this was evaluated.

6.2 Methodology

6.2.1 Vinifications

Twelve small scale vinifications were conducted for the purpose of this study. Nine hundred and sixty kg of Shiraz grapes were collected from the Cape Winelands region of South Africa and stored at 4 ºC. On the day of crushing and destemming, the must was placed in a large bin for homogenisation before being subdivided into the relevant tanks. The SO_2 concentration was adjusted to 30 mg/L using a 2% SO_2 solution. Pump overs were conducted three times daily and all fermentations took place at 25 ºC. Different treatments were applied to certain tanks, namely those used illustrated in Figure 3.1 in Chapter 3, to induce varying extraction of certain compounds present in red wine, whilst two tanks were kept untreated. These treatments were namely enzymatic treatment, tannin addition, combined enzyme and tannins addition, and oxygen sparging. Where necessary, enzymes (Lafase® HE Grand CRU Vin Rouge at 5g/100kg of grapes) and oenological tannins (30g/dL) were added before inoculation according to manufacturer's instructions. Once this had been completed, the tanks were inoculated with *Saccharomyces cerevisiae* (Lalvin ICV D21®). On the third day of alcoholic fermentation (AF), a second dose (30g/dL) of industrial tannins was added to the tanks which received this treatment. Also, on the third day of AF, oxygen sparging began where the tanks were sparged three times daily with oxygen for 5 minutes at 2 bar resulting in a dosage of 5 mg/l per sparging. Table 6.1 summarises the treatments which each tank received where D represents duplicate number. AF lasted for a total of 12 days.

Table 6.1: Summary of Treatments for Each Tank

Tank Number	***Treatment***
1	No treatment – D1
2	No treatment – D2
3	Enzymatic Treatment – D1
4	Enzymatic Treatment – D2
5	Tannin Addition – D1
6	Tannin Addition – D2
7	Oxygen Addition – D1
8	Oxygen Addition – D2
9	Enzyme + Tannin Addition – D1
10	Enzyme + Tannin Addition – D2
11	Tannin Addition – D3
12	Enzyme + Tannin Addition – D3

6.2.2. Sampling and Infrared (IR) Scanning

Samples (2 mL in volume) were taken using automatic dosing pumps three times daily at 08:00, 13:00 and 18:00 from crushing until dry fermentation had been reached. Each outlet was also fitted with a 400 µm in-line filter mesh. These samples were immediately scanned, with no further pre-treatment, to obtain the infrared spectra.

Attenuated total reflectance mid infrared (ATR-MIR) spectra were obtained using an Alpha-P ATR FT-MIR spectrometer (Bruker Optics, Ettlingen, Germany). This instrument was outfitted with a 2 mm^2 single bounce diamond crystal sample plate. Further, the samples were scanned using the instrument in a closed configuration using a stainless-steel cap. For the scanning, 128 sample scans were taken at a temperature of 30^{o}C. The wavenumber region selected for these scans was between 4000-400 cm^{-1} with a 4 cm^{-1} resolution. The background spectrum was taken for each sampling, using distilled water. All instrumental control and set up was done using the OPUS Wine Wizard (OPUS v. 7.0 for Microsoft, Bruker Optics, Ettlingen, Germany).

6.2.3 Quantification of Compounds and Trend Monitoring

PLS regression models constructed for filtered samples in Chapter 5 were used to predict oenological parameters of the fermenting must samples and the finished wine. These models were applied to the generated spectra using the QUANT 2 analysis method, where the PLS regression models were loaded, followed by the spectra and analysis results were obtained.

If a negative result was returned by the modes, this time point was removed before the results were plotted for each graph and fitted with a polynomial trend line to determine whether different trends were observed for different treatments.

6.3. Results and Discussion

It should be noted at this point that the purpose of this study is to provide a preliminary evaluation of the capabilities of the system, rather than to provide an in depth statistical analysis of the values predicted by the system. As such, the overall trends and differences were reported between the control and the different treatments. As the main aim was to assess whether the system could distinguish between the control and treatments, only this was compared statistically The predicted values for each phenolic parameter and a summary of the statistics can be found in Tables 6.2 through 6.6a in Supplementary Material (S5).

From Figure 6.1, the fermentations which received only tannins showed an initial higher concentration of anthocyanins than that receiving no treatment 72 hours into fermentation. The trend line, however, was still showing an increase as opposed to the fermentation receiving no treatments. This is expected as commercial tannins promote colour stability and might prevent reabsorption of anthocyanins (Keulder, 2006). The treatment receiving both tannins and enzymes did not show consistently higher concentrations of anthocyanins than that observed in the control, however the trend continued to increase throughout fermentation, suggesting that anthocyanins were not being reabsorbed by the solids or lees. The enzyme additions also appeared to have no significant effect on the anthocyanins until the end. This is not unexpected as there are varying results as to the effect of enzymes on the anthocyanin content (Ortega-Heras *et al.*, 2012). The addition of oxygen appeared to have no effects on the concentration of anthocyanins as the trend line overlaps with that of the enzymatic treatment which is contrary to certain findings (Geldenhuys, 2009; Moenne *et al.*, 2014).

The colour density for each treatment can be seen in Figure 6.2. From this graph, the trends show that all treatments had higher values for colour density than those receiving no treatment until approximately 200 hours into AF, where oxygen treatment and tannin addition showed a decrease in the colour density. A combined treatment of enzymes and tannins appeared to show higher values compared to the control when considering the trend lines shown in Figure 6.2. The other treatments showed differences in the trendlines, however the extent of this difference is unclear. This may be due to the treatments, where tannins or enzymes may not contribute to colour significantly (Keulder, 2006; Ortega-Heras *et al.*, 2012) may be due to the system not having sufficient sensitivity for smaller fluctuations. . Previously, a similar study was conducted using a UV-Vis spectrophotometer with samples filtered through a 2 µm filter (Shrake, Amirtharajah, Brenneman, *et al.*, 2014). In this aforementioned case, it was shown that in-line measurements are possible for total phenolics and colour density. The extraction trends observed, however, appear to be similar to those reported by Shrake at al., 2014 which can give a preliminary indication of overall suitability for monitoring of extraction.

From Figure 6.3, the treatments receiving tannins, enzymes, and both tannin additions and enzyme treatment had a higher overall concentration. This is in line with reported observations (Cozzolino, Cynkar, Shah, *et al.*, 2011; Keulder, 2006). The oxygen addition appeared to have had no significant effect on the tannin concentration in comparison to the control, which is possible (Geldenhuys, 2009), however it was expected rather than tannins would decrease (McRae *et al.*, 2015). The observed trends indicate that the system can detect differences in terms of certain phenolic parameters between fermentations undergoing different treatments. However, it may not be appropriate for wines receiving oxygen addition, but this may depend on the dosage of oxygen applied. In such a case, the oxygen treatment might not be causing differences rather than the instrument not being able to pick them up. In addition to this, tannin concentration for the oxygenated fermentations appears to be at the same level of the other treatments at the end of the fermentation. This could be due to some polymeric pigment formation that may provide a form of protection for the tannins and keep their levels similar to those with tannin additions.

For total phenolic index (TPI), the control and the wine receiving enzymatic treatments show similar trends from approximately the third day, while fermentations receiving only tannins showed a slightly higher trend. During the same time, oxygen treatment and combined enzyme and tannin additions were slightly lower than the others. These trends can be seen in Figure 6.4. However, the trendlines are very similar, and as such statistical analysis would have to be performed to determine whether the difference is significance. However, the similar trendlines may suggest that either the treatments had no major effect on the TPI or, more likely, that the equipment and current software used may not be sensitive enough to detect the slight differences between the treatments. As with colour density, the extraction trends for total phenolic index are similar to those reported in Shrake et al., 2014. This could, once again, point to potential for monitoring extraction using IR technology.

In Figure 6.5, the concentration of polymeric pigments, is consistently lower for the fermentations exposed to oxygen. The trend for oxygenated fermentations resulting in lower values for polymeric pigment is unexpected, due to oxygen exposure theoretically favouring the formation of ethyl bridge thus resulting in the formation of these pigments (Setford, Jeffery, Grbin, *et al.*, 2017). Tannin addition alone appears to cause a higher concentration of polymeric pigments throughout fermentation until the final day. Lastly, the enzyme treatment alone showed a similar trend to the control. This has been previously observed with addition of commercial tannins and enzymes (Keulder, 2006). Once again, these results either suggest that the treatments cause insufficient differences in the concentrations or the sensitivity of the system is not sufficient.

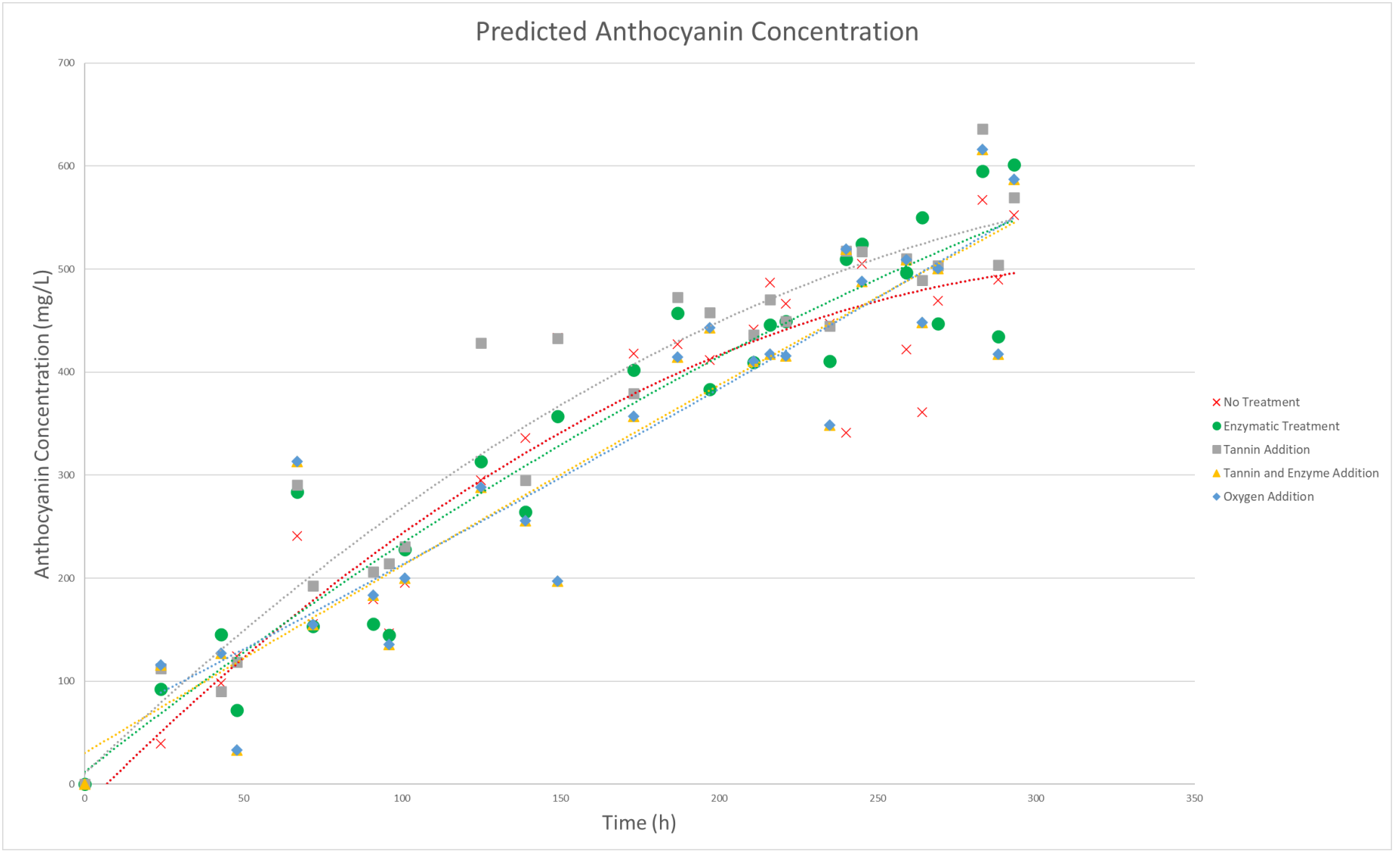

Figure 6.1: Predicted Anthocyanin Concentration

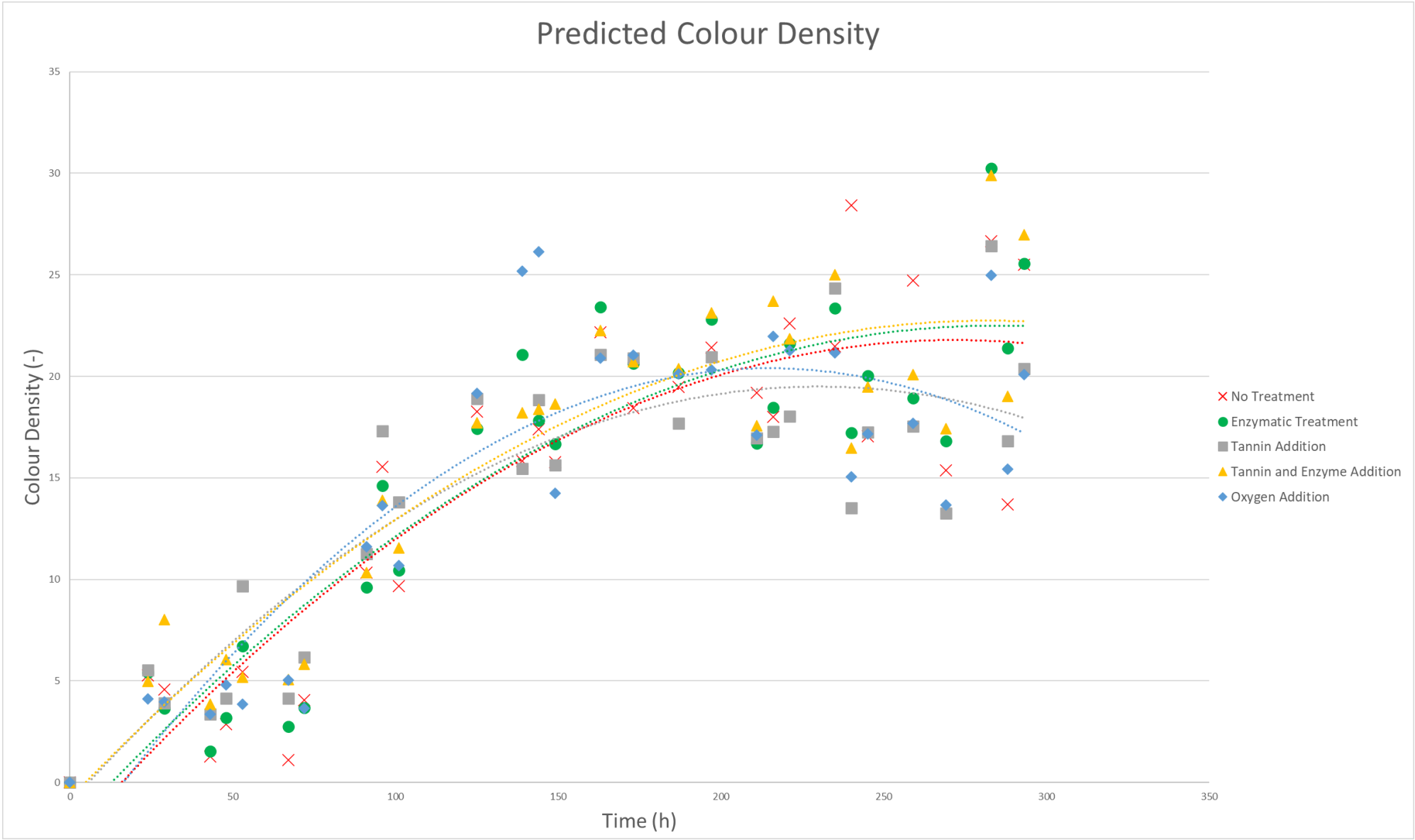

Figure 6.2: Predicted Colour Density

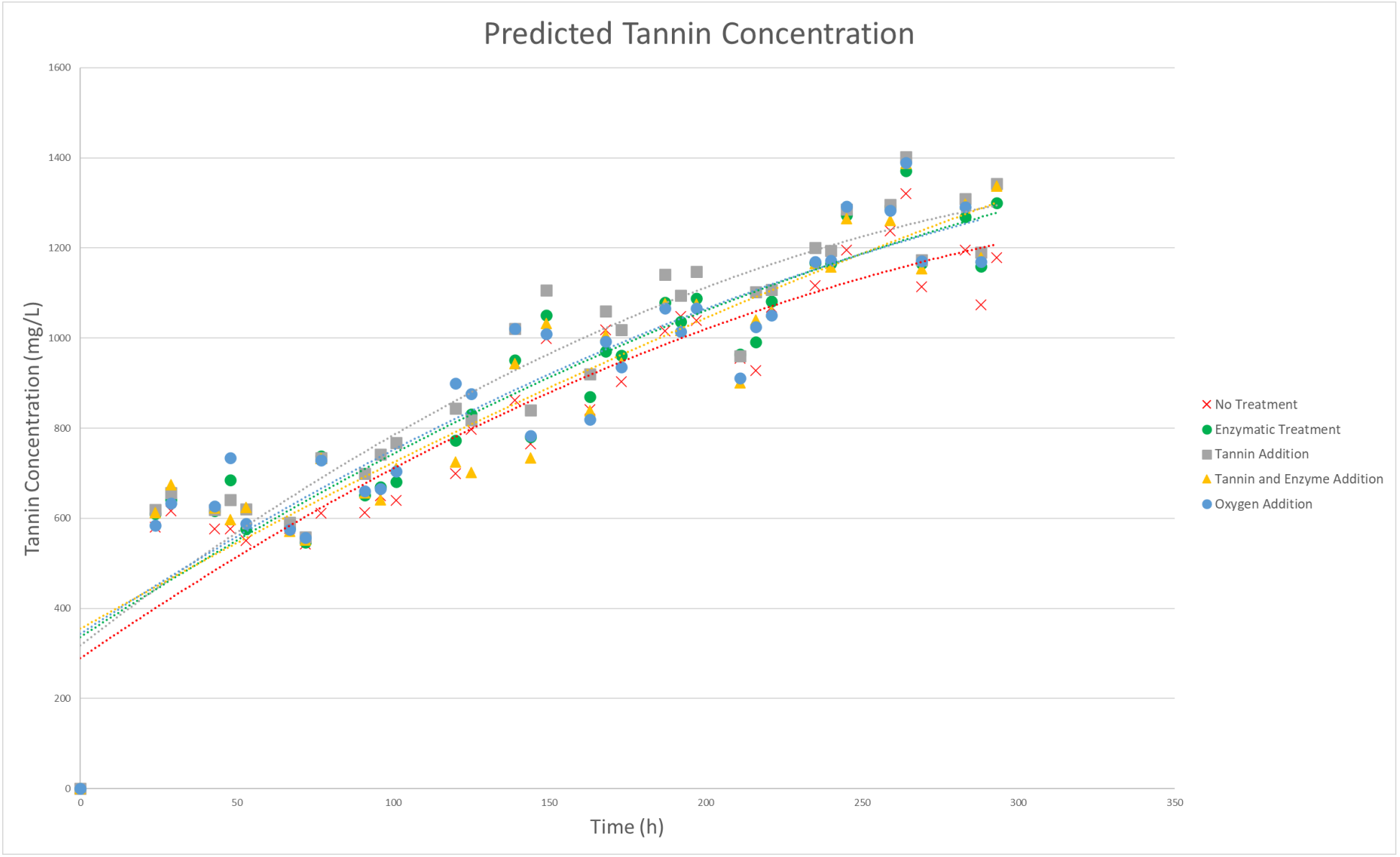

Figure 6.3: Predicted Tannin Concentration

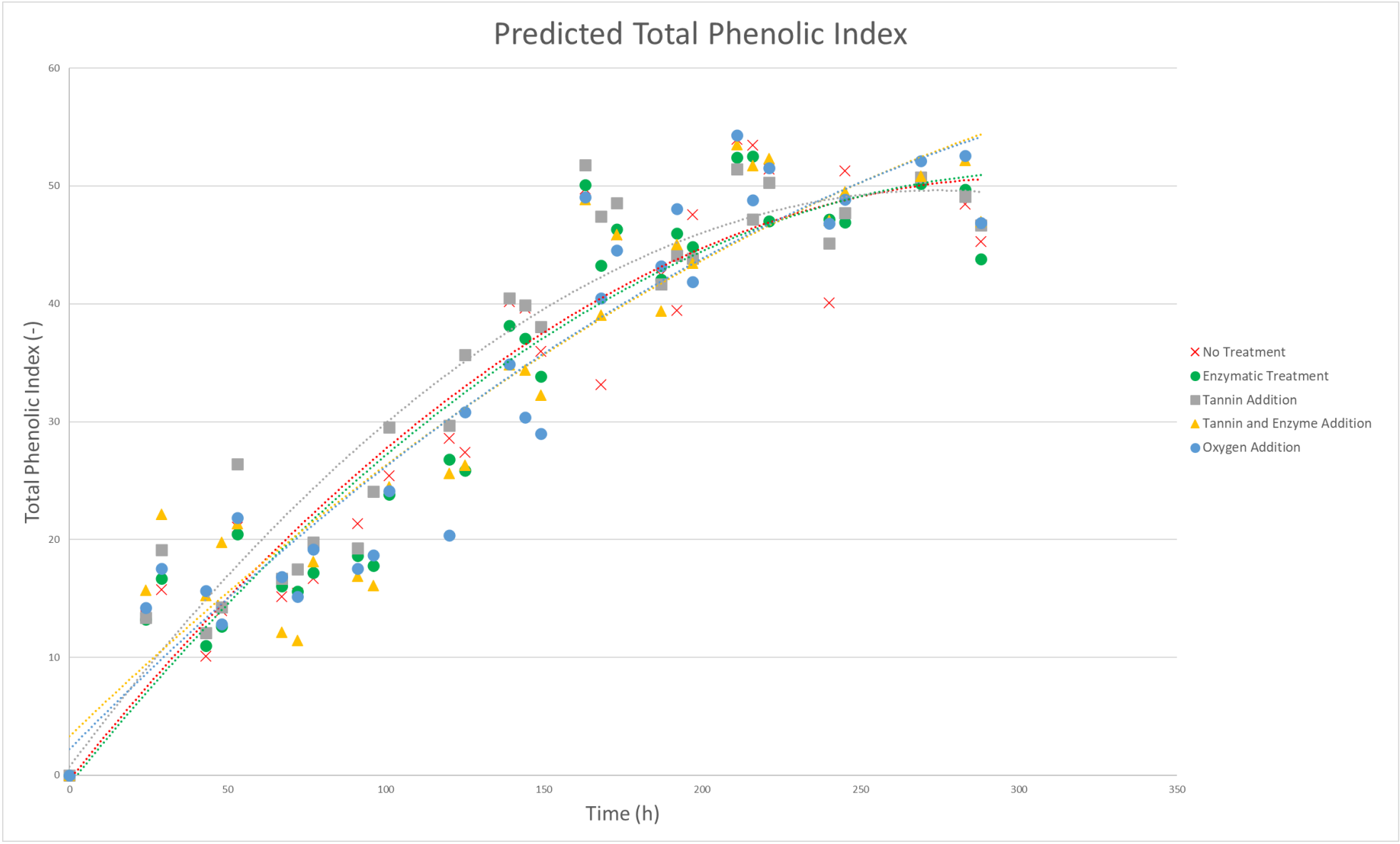

Figure 6.4: Predicted Total Phenolic Index

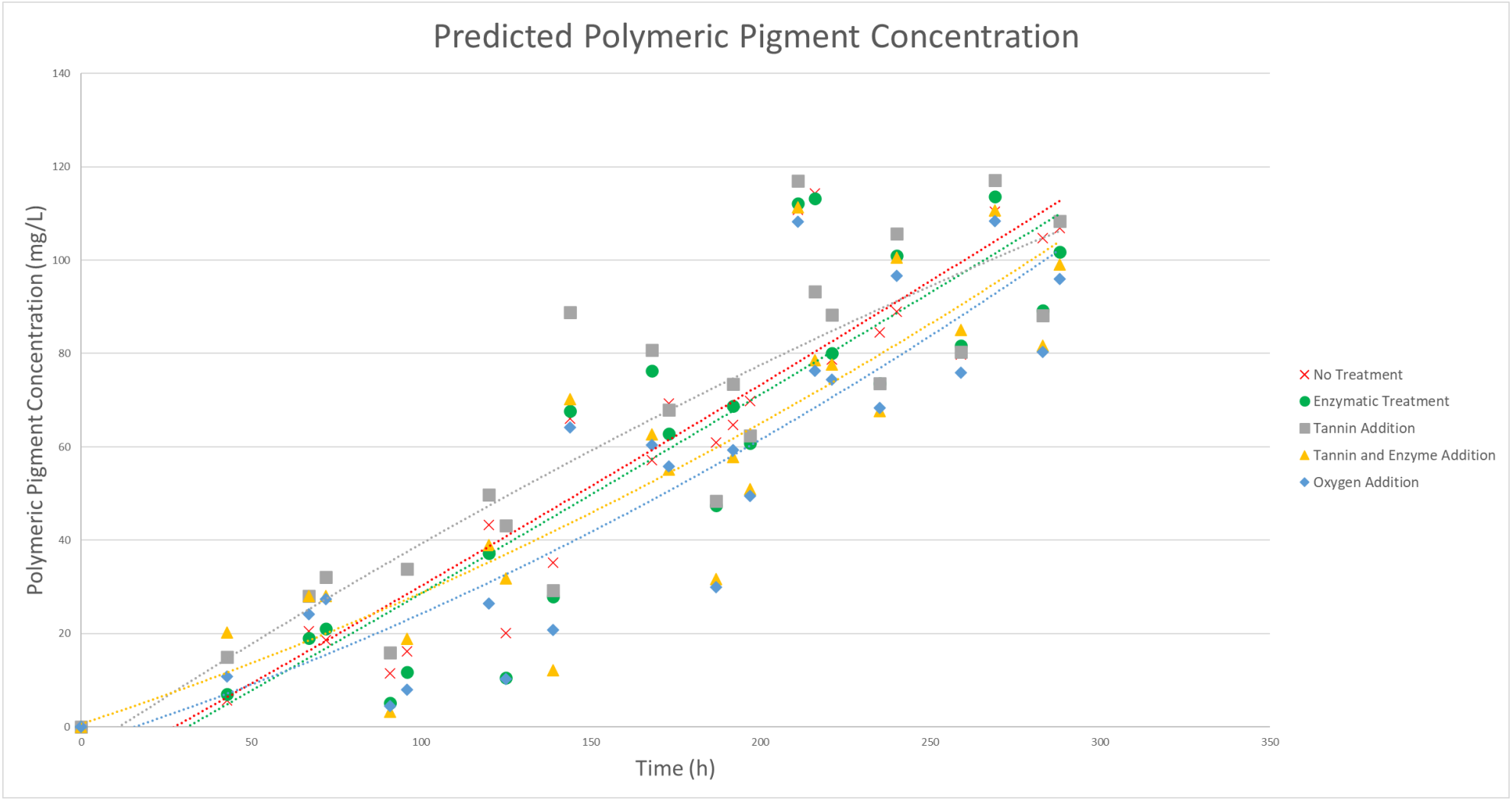

Figure 6.5: Predicted Polymeric Pigment Concentration

6.4 Conclusions

Red wine making is a complex bioprocess involving phenolic extraction from grape solids, where manipulation of certain variables can influence the rate of phenolic extraction and, therefore, the final phenolic composition (Cavaglia *et al.*, 2020). Different wine making techniques have been developed to use this phenomenon to their advantage. Such methods such as oxygen sparging and the addition of different compounds are used in industry and the effects of this have been studied. However, due to the competitive nature of the wine industry, wine makers are in need of ways to constantly monitor quality parameters, thereby ensuing consistency and quality of their products (Aleixandre-Tudo, Nieuwoudt, Olivieri, *et al.*, 2018). This results in an increased need for technologies and software which can monitor the compositions of the wines on a regular basis.

In this case, infrared spectroscopy, coupled with chemometrics, has become widespread in production of pharmaceuticals, and food and beverage Its robustness, rapidity and multivariate nature make it ideal for use in such industries (Ayvaz, Plans, Towers, *et al.*, 2015; Ayvaz *et al.*, 2016; Cavaglia *et al.*, 2020; Helmdach, Feth, Minnich, *et al.*, 2013; Karoui *et al.*, 2006). A comparative approach may also prove to be beneficial to winemakers, so that they can be able to determine the effect of different winemaking techniques. If they can observe trends and effects, it would aid in more informed decision making with changing process variables.

As such, a study was conducted using ATR-MIR spectroscopy and existing PLS Calibrations designed for samples taken directly from a fermentation vessel and in an automated manner, to determine if differences due to winemaking techniques could be detected. The system showed suitability for this application as the expected differences were, to a large extent, noted for these components. In the cases where expected results were not observed, it is unclear whether the lack of statistical distinction was due to marginal effect of the treatments or due to model sensitivity. This can be further explored with an in-depth statistical analysis. In these cases, it would be beneficial to explore the effect on different batches of grapes inclusive of a variety of cultivars and grape characteristics at harvest.

It should be noted, that for industrial application, PLS models and calibrations might not require the same sensitivity as those in use for analytical or research applications. The ability of a system, such as the one used, to monitor the trend and progression of phenolic extraction may be sufficient in most applications. When considering the requirements of industrial applications and the prospects of added measures to increase reliability, this system demonstrated suitability for such an application. The benefits of an approach such as this is the degree to which it can be tailored to a particular scenario. Thus, a more simplistic approach, such as the one used in this study, can be applied with confidence, but it has the capacity for more complexity to be added. For example, updated models or dynamic modelling techniques could be added along with set

points for certain parameters to ensure that these phenolic parameters do not fall outside of desired boundaries.

6.5 Literature Cited

Aleixandre-Tudo, J.L., Nieuwoudt, H., Aleixandre, J.L. & du Toit, W. 2018. Chemometric compositional analysis of phenolic compounds in fermenting samples and wines using different infrared spectroscopy techniques. *Talanta*. 176(August 2017):526–536.

Aleixandre-Tudo, J.L., Nieuwoudt, H., Olivieri, A., Aleixandre, J.L. & du Toit, W. 2018. Phenolic profiling of grapes, fermenting samples and wines using UV-Visible spectroscopy with chemometrics. *Food Control*. 85:11–22.

Apolinar-Valiente, R., Romero-Cascales, I., Williams, P., Gómez-Plaza, E., López-Roca, J.M., Ros-García, J.M. & Doco, T. 2014. Effect of winemaking techniques on polysaccharide composition of Cabernet Sauvignon, Syrah and Monastrell red wines. *Australian Journal of Grape and Wine Research*. 20(1):62–71.

Ayvaz, H., Plans, M., Towers, B.N., Auer, A. & Rodriguez-Saona, L.E. 2015. The use of infrared spectrometers to predict quality parameters of cornmeal (corn grits) and differentiate between organic and conventional practices. *Journal of Cereal Science*. 62:22–30.

Ayvaz, H., Sierra-Cadavid, A., Aykas, D.P., Mulqueeney, B., Sullivan, S. & Rodriguez-Saona, L.E. 2016. Monitoring multicomponent quality traits in tomato juice using portable mid-infrared (MIR) spectroscopy and multivariate analysis. *Food Control*. 66:79–86.

Basalekou, M., Kallithraka, S., Tarantilis, P.A., Kotseridis, Y. & Pappas, C. 2019. Ellagitannins in wines: Future prospects in methods of analysis using FT-IR spectroscopy. *Lwt*. 101(June 2018):48–53.

Boulton, R. 1980. The Prediction of Fermentation Behaviour by a Kinetic Model. 31(1).

Cavaglia, J., Schorn-García, D., Giussani, B., Ferré, J., Busto, O., Aceña, L., Mestres, M. & Boqué, R. 2020. ATR-MIR spectroscopy and multivariate analysis in alcoholic fermentation monitoring and lactic acid bacteria spoilage detection. *Food Control*. 109:1–7.

Cen, H., Bao, Y., He, Y. & Sun, D.W. 2007. Visible and near infrared spectroscopy for rapid detection of citric and tartaric acids in orange juice. *Journal of Food Engineering*. 82(2):253–260.

Cozzolino, D., Kwiatkowski, M.J., Parker, M., Cynkar, W.U., Dambergs, R.G., Gishen, M. & Herderich, M.J. 2004. Prediction of phenolic compounds in red wine fermentations by visible and near infrared spectroscopy. *Analytica Chimica Acta*. 513(1):73–80.

Cozzolino, D., Cynkar, W., Shah, N. & Smith, P. 2011. Feasibility study on the use of attenuated total reflectance mid-infrared for analysis of compositional parameters in wine. *Food Research International*. 44(1):181–186.

Daghbouche, Y., Garrigues, S., Teresa Vidal, M. & De la Guardia, M. 1997. Flow Injection Fourier Transform Infrared Determination of Caffeine in Soft Drinks. *Analytical Chemistry*. 69(6):1086–1091.

Favre, G., Peña-Neira, Á., Baldi, C., Hernández, N., Traverso, S., Gil, G. & González-Neves, G. 2014. Low molecular-weight phenols in Tannat wines made by alternative winemaking procedures. *Food Chemistry*. 158:504–512.

Federico Casassa, L., Bolcato, E.A., Sari, S.E., Fanzone, M.L. & Jofré, V.P. 2016. Combined effect of prefermentative cold soak and SO2 additions in Barbera D'Asti and Malbec wines: Anthocyanin composition, chromatic and sensory properties. *LWT - Food Science and Technology*. 66:134–142.

Geldenhuys, L. 2009. Influence of oxygen addition on the phenolic composition of red wine.

González-Neves, G., Gil, G., Barreiro, L. & Favre, G. 2010. Pigment profile of red wines cv. Tannat made with alternative winemaking techniques. *Journal of Food Composition and Analysis*. 23(5):447–454.

Helmdach, L., Feth, M.P., Minnich, C. & Ulrich, J. 2013. Application of ATR-MIR spectroscopy in the pilot plant—Scope and limitations using the example of Paracetamol crystallizations. *Chemical Engineering & Processing: Process Intensification*. 70:184–197.

Huang, H., Yu, H., Xu, H. & Ying, Y. 2008. Near infrared spectroscopy for on/in-line monitoring of quality in foods and beverages: A review. *Journal of Food Engineering*. 87(3):303–313.

Karoui, R., Mouazen, A.M., Dufour, É., Pillonel, L., Schaller, E., Picque, D., De Baerdemaeker, J. & Bosset, J.O. 2006. A comparison and joint use of NIR and MIR spectroscopic methods for the determination of some parameters in European Emmental cheese. *European Food Research and Technology*. 223(1):44–50.

Kelebek, H., Canbas, A. & Selli, S. 2008. Pectolytic Enzyme Addition on the Anthocyanin. *Journal of Food Processing and Preservation*. 33(2009):296–311.

Keulder, D.B. 2006. The influence of commercial tannin additions on wine composition and quality. *Master thessis*. (February):101.

McRae, J.M., Day, M.P., Bindon, K.A., Kassara, S., Schmidt, S.A., Schulkin, A., Kolouchova, R. & Smith, P.A. 2015. Effect of early oxygen exposure on red wine colour and tannins. *Tetrahedron*. 71(20):3131–3137.

Medina-Plaza, C., Beaver, J.W., Miller, K. V., Lerno, L., Dokoozlian, N., Ponangi, R., Blair, T., Block, D.E., et al. 2020. Cell Wall–Anthocyanin Interactions during Red Wine Fermentation-Like Conditions. *American Journal of Enology and Viticulture*. 71(2):149–156.

Miller, K. V., Oberholster, A. & Block, D.E. 2019. Predicting the impact of red winemaking practices using a reactor engineering model. *American Journal of Enology and Viticulture*. 70(2):162–168.

Moenne, M.I., Saa, P., Laurie, V.F., Pérez-Correa, J.R. & Agosin, E. 2014. Oxygen Incorporation and Dissolution During Industrial-Scale Red Wine Fermentations. *Food and Bioprocess Technology*. 7(9):2627–2636.

Ortega-Heras, M., Pérez-Magariño, S. & González-Sanjosé, M.L. 2012. Comparative study of the use of maceration enzymes and cold pre-fermentative maceration on phenolic and anthocyanic composition and colour of a Mencía red wine. *LWT - Food Science and Technology*. 48(1):1–8.

Patz, C.D., Blieke, A., Ristow, R. & Dietrich, H. 2004. Application of FT-MIR spectrometry in wine analysis. *Analytica Chimica Acta*. 513(1):81–89.

Sacchi, K.L., Bisson, L.F. & Adams, D.O. 2005. Effect of Winemaking Techniques on Phenolic Extraction. *American Journal of Enology and Viticulture*. 56(3):197–206. [Online], Available: https://www.ajevonline.org/content/ajev/56/3/197.full.pdf%0Ahttps://pdfs.semanticscholar.org/e40f/0c5a805a79380ae5645f0f78dca4893e02ee.pdf.

Setford, P.C., Jeffery, D.W., Grbin, P.R. & Muhlack, R.A. 2017. Factors affecting extraction and evolution of phenolic compounds during red wine maceration and the role of process modelling. *Trends in Food Science and Technology*. 69:106–117.

Shrake, N.L., Amirtharajah, R., Brenneman, C., Boulton, R. & Knoesen, A. 2014. In-line measurement of color and total phenolics during red wine fermentations using a light-emitting diode sensor. *American Journal of Enology and Viticulture*. 65(4):463–470.

Smith, P.A., Mcrae, J.M. & Bindon, K.A. 2015. Impact of winemaking practices on the concentration and composition of tannins in red wine. *Australian Journal of Grape and Wine Research*. 21:601–614.

Wang, Q., Li, Z., Ma, Z. & Liang, L. 2014. Real time monitoring of multiple components in wine fermentation using an on-line auto-calibration Raman spectroscopy. *Sensors and Actuators, B: Chemical*. 202:426–432.

Chapter 7

General Discussion and Conclusions

Chapter 7 – General Discussion and Conclusions

7.1 Concluding Remarks

Wine has been a part of human civilisation and many cultures since at 6000BC. In the regions of Mesopotamia and the Caucasus, the earliest signs of wine making can be found. Later on, records were kept which detail the spread and cultivation of the grape vine throughout the Mediterranean regions and Africa. In these records, it is also mentioned how the beverage was held in high regard by the upper echelons of Egyptian society (Robinson, 2014). Wine has since remained a part of culture and high-quality wines are often highly sought after.

The process of winemaking is complex, involving the fermentation of hexose sugars into ethanol and carbon dioxide. Many factors contribute to this complexity, including the utilisation of these sugars in a variety of chemical reactions and in the metabolic pathways of microbial organisms involved in the process (Moreno-Arribas & Polo, 2009). Amongst the compounds of interest in wine, phenolic compounds are important to the sensory qualities of a wine (Aleixandre-Tudo, Buica, Nieuwoudt, *et al.*, 2017). Whist only forming 5% of the chemical composition in wine, they contribute to colour and mouthfeel. In addition to this, many health benefits have been identified such as protection from oxidative damage, anti-cholesterol and anti-diabetic properties and aid in cell function (Beaver, Miller, Medina-Plaza, *et al.*, 2019). These compounds are extracted from the solid constituents of the grapes during maceration and during alcoholic fermentation. This is also a complicated mass transfer process where the molecules move from the solids and into the liquid juice or must (Setford, Jeffery, Grbin, *et al.*, 2017). As with all chemical reactions, the conditions under which they occur can impact their progression and extent significantly. There are many practices in place where certain process variables can be manipulated to influence the concentration of these phenolic compounds, thereby achieving certain styles of wine.

As wine has remained a part of many cultures, the markets have become more demanding and more competitive. The demand is largely with regard to consistency and quality of the wines (Lochner, 2006). Even though desire for a particular wine can be fairly subjective, it is possible to define quantitative parameters which can be used as benchmarks during the industrial winemaking process. Such parameters can include sugar depletion, phenolic extraction and the concentration of certain compounds (Aleixandre-Tudo, Nieuwoudt, Aleixandre, *et al.*, 2018). When rapid and multiparametric methods, such as infrared spectroscopy, are applied to a process, it becomes possible to quantify and monitor these parameters. The use of infrared instrumentation and chemometric software has made this achievable on both small and large scales(Cavaglia, Schorn-García, Giussani, *et al.*, 2020; Cozzolino, McCarthy & Bartowsky, 2012; Cozzolino, Parker, Dambergs, *et al.*, 2006; Patz, Blieke, Ristow, *et al.*, 2004; Soriano, Pérez-

Juan, Vicario, *et al.*, 2007). However, to the best of our knowledge, this has yet to be applied automatically and in-line during red wine fermentation to monitor phenolic extraction.

With considerations in mind, such as ease of implementation to existing structures, and cost effectiveness, a design for a prototype sampling and analysis system was started. The design involved the integration and synchronisation of individual process units such as sampling pumps, infrared instrumentation and automation code used to execute certain processes. Initially, a single tank prototype was conducted to test basic design concepts such as system integrity, timing and suitability of the design. This was expanded to incorporate multiple tanks, whilst still only utilising one instrument. It was possible to construct a simplistic automated sampling and analysis system which enable a user to monitor a variety of quality parameters through graphical means. The system also proved to be robust and reliable, experiencing no critical component failures during stress testing or during power failures. This system would be uncomplicated to deploy into industry with minimal set-up times and, coupled with chemometric models, would allow for 24-hour monitoring of a fermentation. As such, the first objective stipulated in Chapter 1 was achieved. However, one aspect of the system still requires improvement and further consideration. As it stands, the system still relies on individual components which work together and require good timing on start up to ensure that they remain in sync. Therefore, it would be ideal if some form of programmable logic controller could be implemented to integrate the individual components to a further degree.

When sampling directly from a tank, obtaining a perfectly clean sample is challenging. Often this will require ultra-filtration or centrifugation. Both unit operations are costly and high risk. A solution to this would be to build PLS calibrations using samples of varying turbidity such as those taken directly from a tank where yeast and grape solids would account for most of the turbidity. In addition to this, the suitability of different infrared instruments for this application could be explored. For this study, fermenting samples were used to build PLS calibrations across three different instruments for turbid samples and samples which had received a level of filtration. The resulting models showed that turbidity could be factored into a calibration to produce a robust and reliable method of quantifying certain phenolic compounds of interest. Interestingly, it also showed that a contactless instrument could be used for this purpose as well. These two findings make industrial application possible as they reduce the need for expensive units and allow for a wider selection of instrumentation which can be used. Further, optimisation was conducted on these calibrations using a variety of spectral pre-processing methods and wavenumber selection. This was done to improve the accuracy and reliability of these calibrations. For this, the limit of detection and quantification were also considered so that it was possible to pin-point timewise exactly when the models could be applied to a fermentation. These calibrations were applicable from the very start of fermentation and they were suitable for the desired application of phenolic

quantification and as such, the second objective outlined in Chapter 1 was achieved. On the other hands, it would be beneficial to incorporate a more complete sample set consisting of a wider range of cultivars, vintages, and a more varied range of phenolic parameters. In addition to this, a multistage filtration technique could be applied to further reduce turbidity in a sample whilst not increasing pressure. Further, it would be beneficial to quantify the turbidity of a sample prior to building the PLS calibrations to be able to quantify the effect of turbidity and to incorporated more varied levels of turbidity.

With the development of a prototype system and models suitable for quantification, fermentation monitoring was performed to determine the ability to monitor the trends in extraction. Here, a series of fermentations were conducted where different treatments were applied to influence the phenolic composition. The results of this showed that monitoring these trends is possible, thus completing the third and final objective. Unfortunately, this was done semi-automatically where the sampling was automatic, but scanning was manual. A fully automated approach would be ideal, where the three different spectroscopic methods could also be incorporated. The system also shows potential for added complexity in the form of process control techniques or updated calibrations. As each winery will have a particular set of requirements regarding implementation of technology, the dynamic nature of the design and the capacity for additional levels of process control could make this system suitable for industrial applications.

The system developed over the course of this study has many avenues for continued improvement and expansion. Using the established system, it would be possible to add a control system which can perform tasks such as temperature manipulation or oxygenation. To further the process control capabilities, it would be desirable to link initial grape composition to the fermentation monitoring. Using these values, future trends could be predicted with the use of mathematical equations and a system of predefined boundaries. As most industries are moving towards a more global approach, another opportunity for improvement would be to introduce an on-line aspect which allows remote access to monitor and effect changes.

7.2 Literature Cited

Aleixandre-Tudo, J.L., Buica, A., Nieuwoudt, H., Aleixandre, J.L. & Du Toit, W. 2017. Spectrophotometric Analysis of Phenolic Compounds in Grapes and Wines. *Journal of Agricultural and Food Chemistry*. 65(20):4009–4026.

Aleixandre-Tudo, J.L., Nieuwoudt, H., Aleixandre, J.L. & du Toit, W. 2018. Chemometric compositional analysis of phenolic compounds in fermenting samples and wines using different infrared spectroscopy techniques. *Talanta*. 176(August 2017):526–536.

Beaver, J.W., Miller, K. V., Medina-Plaza, C., Dokoozlian, N., Ponangi, R., Blair, T., Block, D. & Oberholster, A. 2019. Heat-dependent desorption of proanthocyanidins from grape-derived cellwall material under variable ethanol concentrations in model wine systems. *Molecules*. 24(19):1–13.

Cavaglia, J., Schorn-García, D., Giussani, B., Ferré, J., Busto, O., Aceña, L., Mestres, M. & Boqué, R. 2020. ATR-MIR spectroscopy and multivariate analysis in alcoholic fermentation monitoring and lactic acid bacteria spoilage detection. *Food Control*. 109:1–7.

Cozzolino, D., Parker, M., Dambergs, R.G., Herderich, M. & Gishen, M. 2006. Chemometrics and Visisble-Near Infrared Spectroscopic Monitoring of Red Wine Fermentation in a Pilot Scale. *Biotechnology and Bioengineering*. 95(6):1101–1107.

Cozzolino, D., McCarthy, J. & Bartowsky, E. 2012. Comparison of near infrared and mid infrared spectroscopy to discriminate between wines produced by different Oenococcus Oeni strains after malolactic fermentation: A feasibility study. *Food Control*. 26(1):81–87.

Lochner, E. 2006. The evaluation of Fourier transform infrared spectroscopy (FT-IR) for the determination of total phenolics and total anthocyanins concentrations of grapes by.

Moreno-Arribas, M.V. & Polo, M.C. 2009. *Wine chemistry and biochemistry*. M.C.P.M.V. Moreno-Arribas (ed.). New York.

Patz, C.D., Blieke, A., Ristow, R. & Dietrich, H. 2004. Application of FT-MIR spectrometry in wine analysis. *Analytica Chimica Acta*. 513(1):81–89.

Robinson, J. 2014. *The Oxford Companion to Wine*.

Setford, P.C., Jeffery, D.W., Grbin, P.R. & Muhlack, R.A. 2017. Factors affecting extraction and evolution of phenolic compounds during red wine maceration and the role of process modelling. *Trends in Food Science and Technology*. 69:106–117.

Soriano, A., Pérez-Juan, P.M., Vicario, A., González, J.M. & Pérez-Coello, M.S. 2007. Determination of anthocyanins in red wine using a newly developed method based on Fourier transform infrared spectroscopy. *Food Chemistry*. 104(3):1295–1303.

Chapter 8

Supplementary Material

Supplementary Material (S1)

7.1 Reference Data

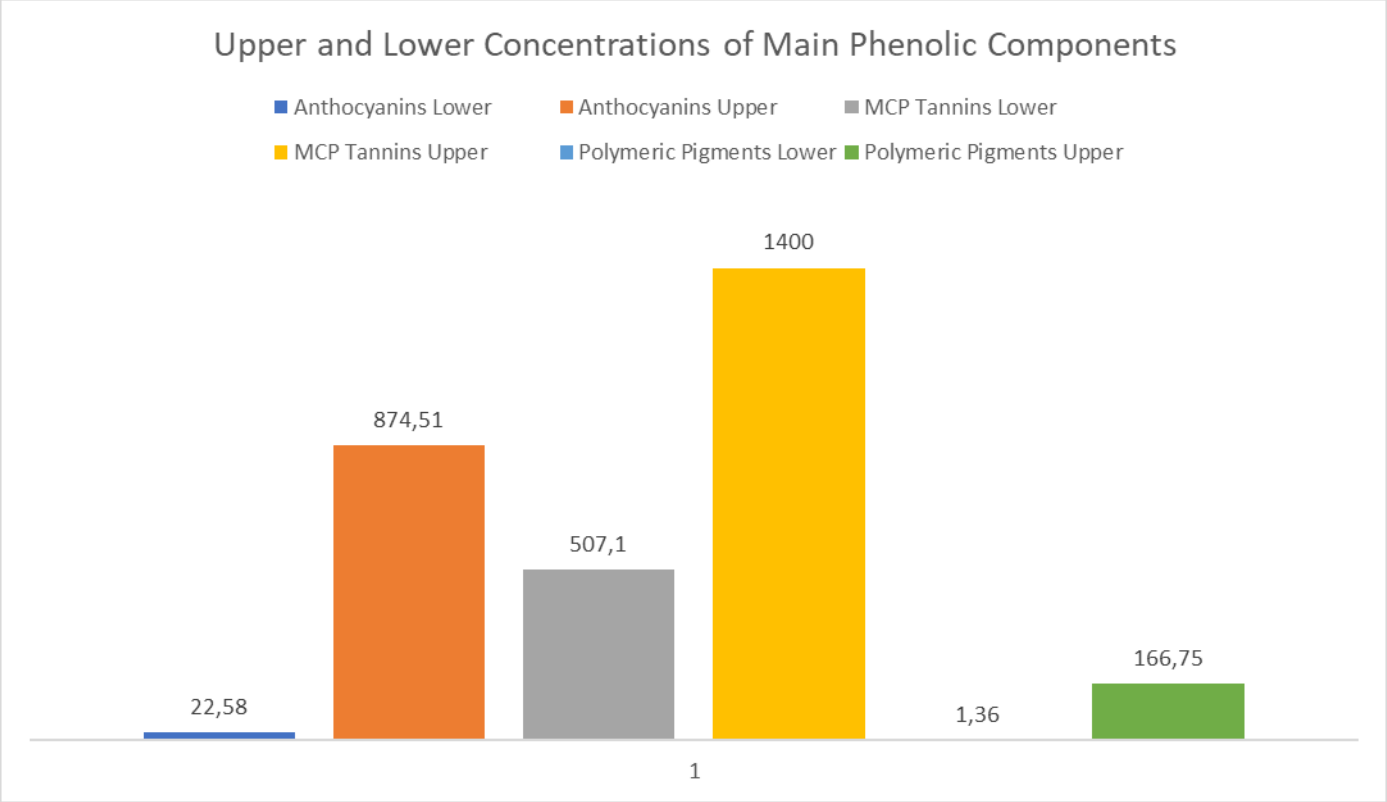

Figure 4a: Histogram showing Concentration Ranges for Main Phenolic Compounds

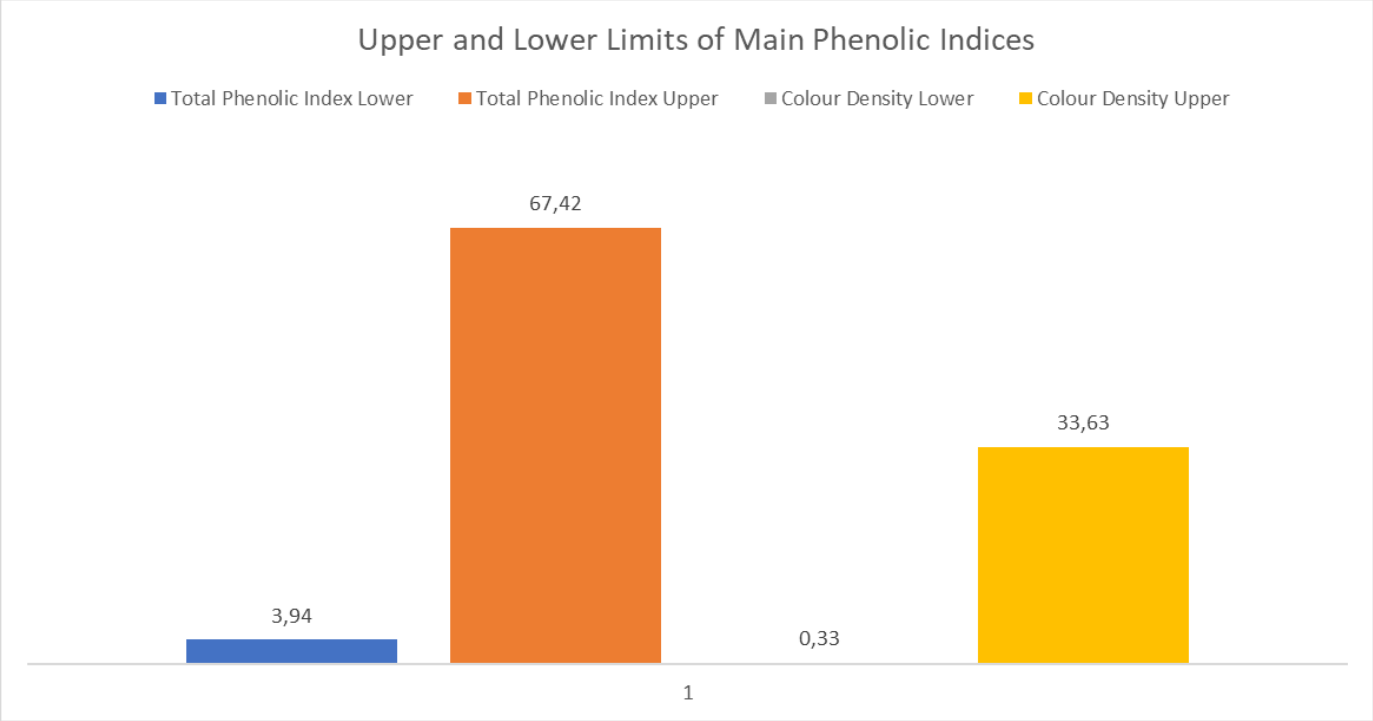

Figure 4b: Histogram showing Ranges for Main Phenolic Indices

7.1 Scores and Loadings Plots for All Instrumentation for Centrifuged Samples

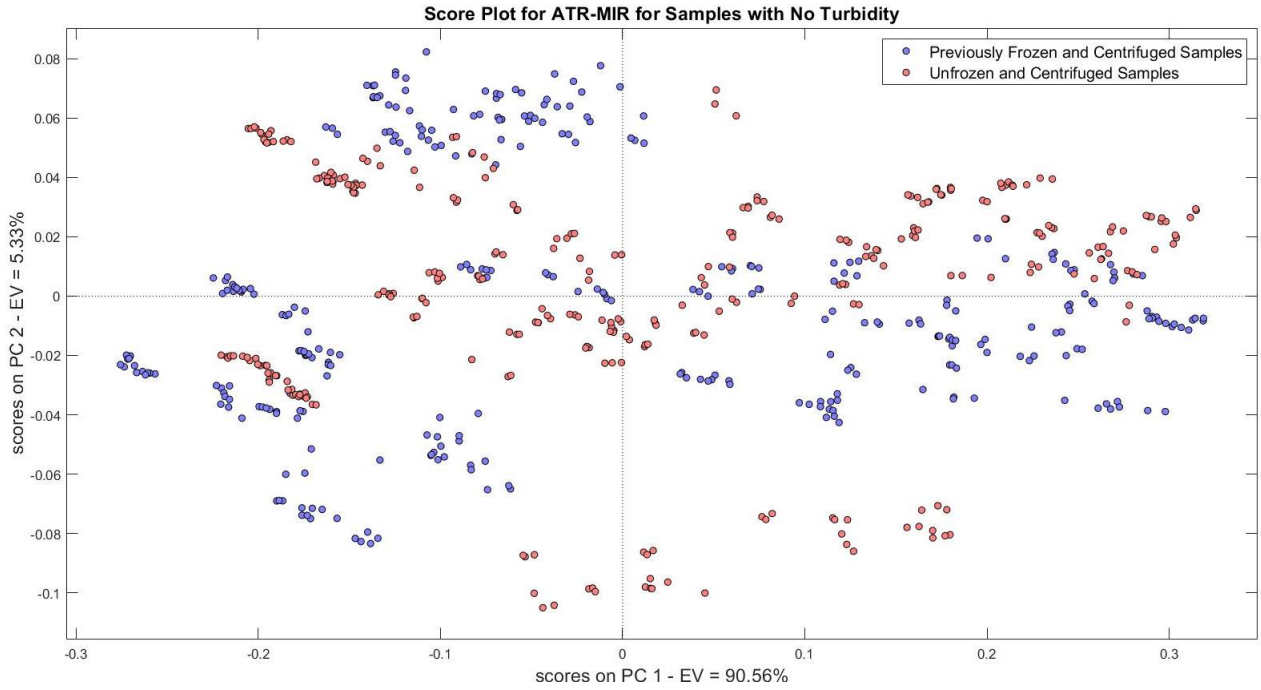

Figure 4.1a: Score plot for ATR-MIR for clean samples

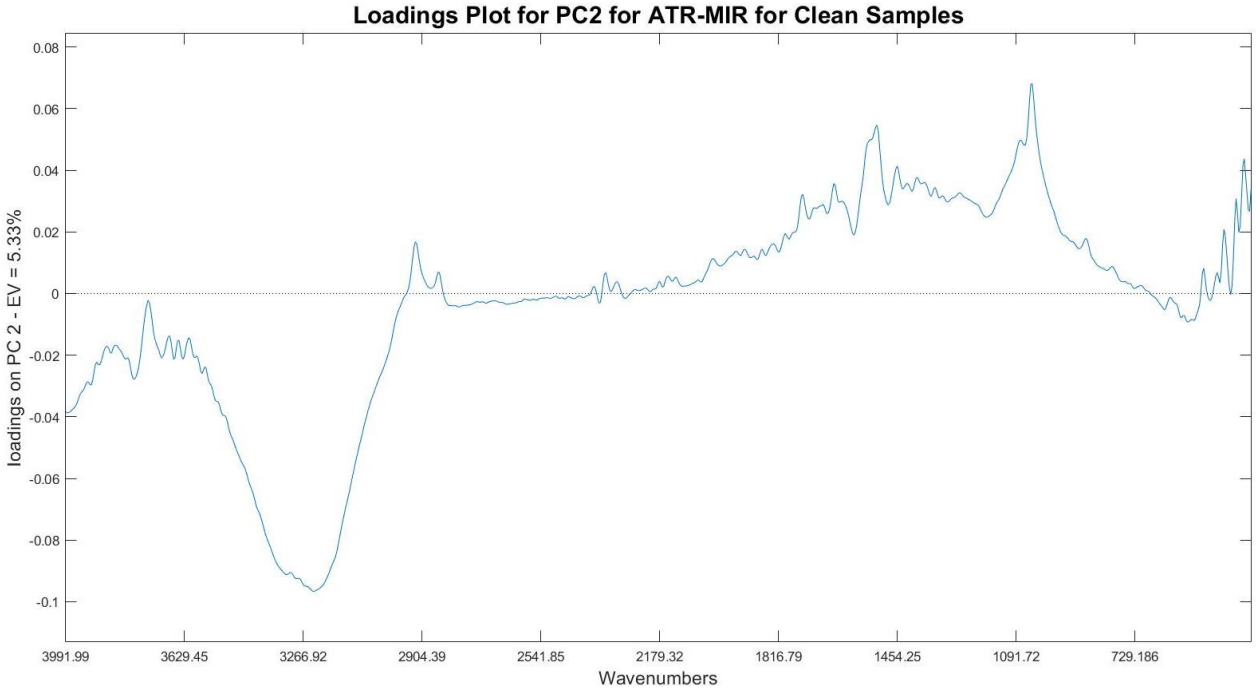

Figure 4.1b: Loadings plot for PC 1 for ATR-MIR for clean samples

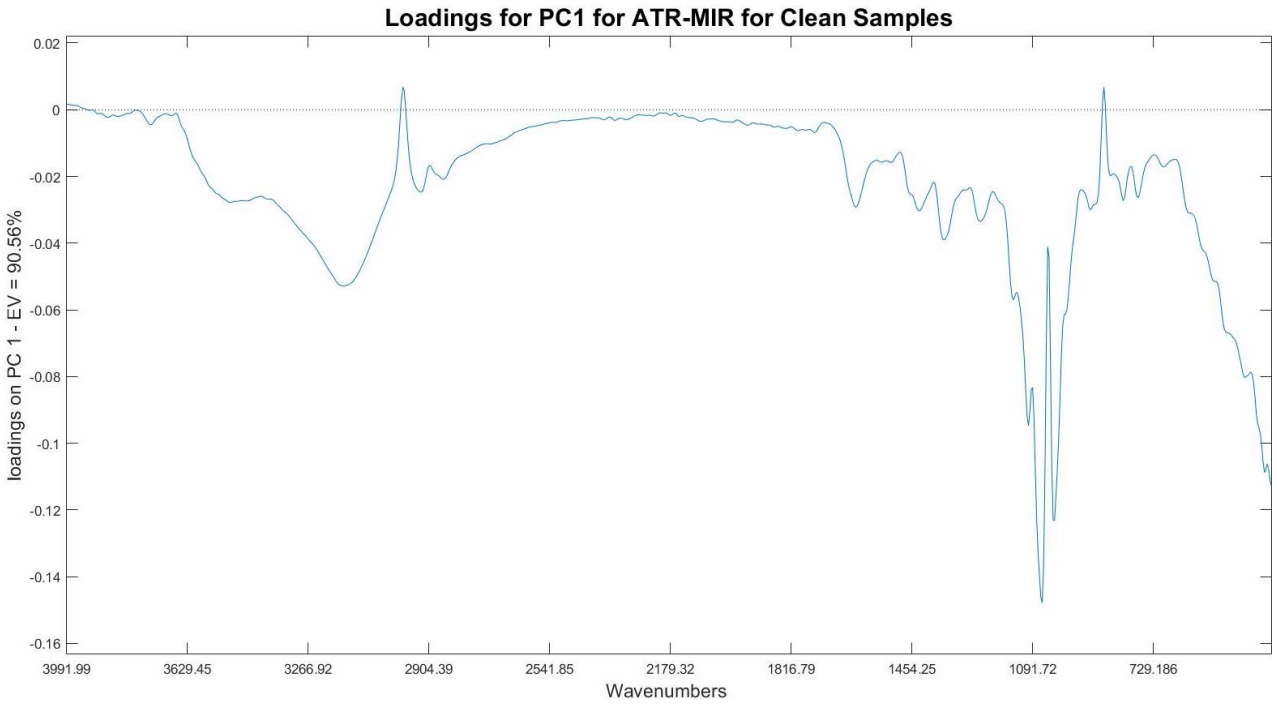

Figure 4.1c: Loadings plot for PC 2 for ATR-MIR for clean samples

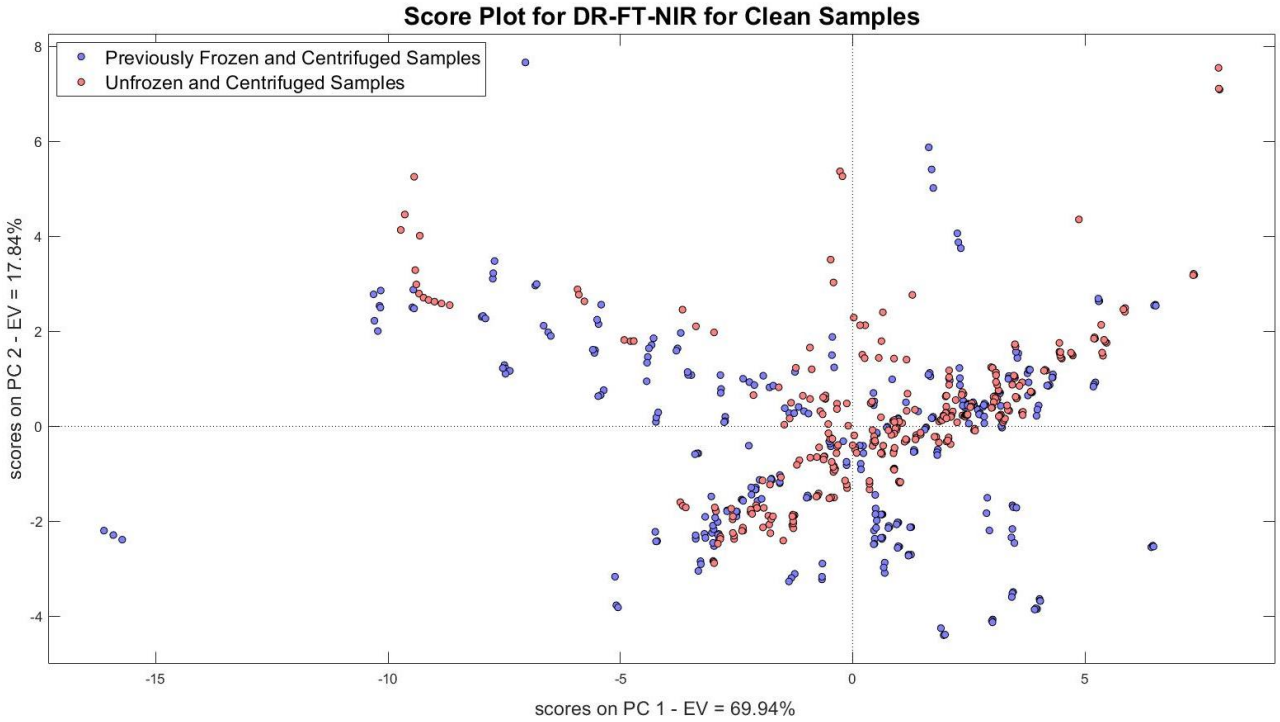

Figure 4.1d: Score plot for DR-FT-NIR for clean samples

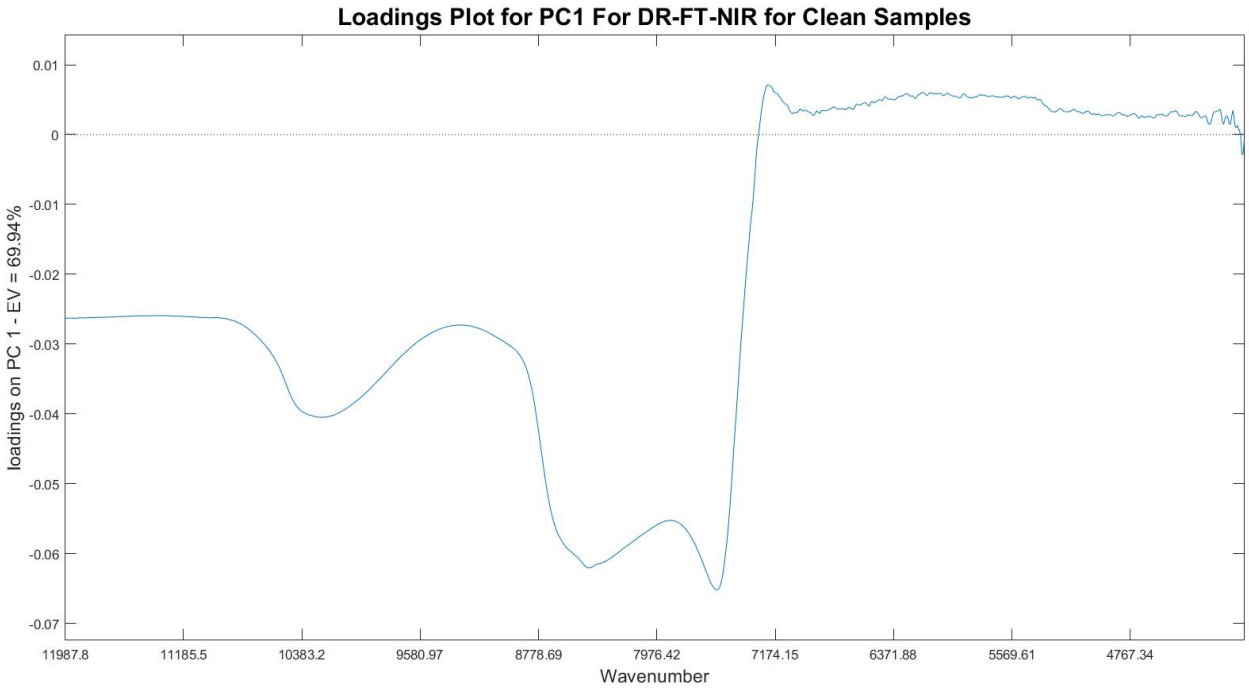

Figure 4.1e: Loadings plot for PC 1 for DR-FT-NIR for clean samples

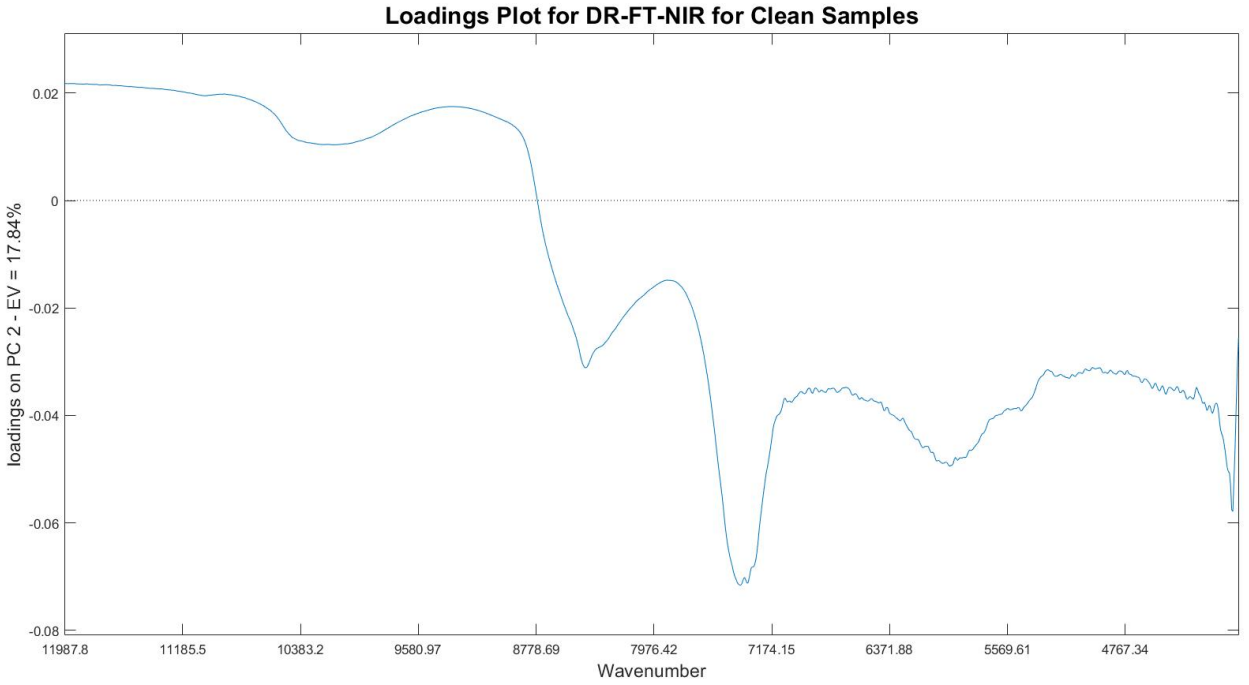

Figure 4.1f: Loadings plot for PC 2 for DR-FT-NIR for clean samples

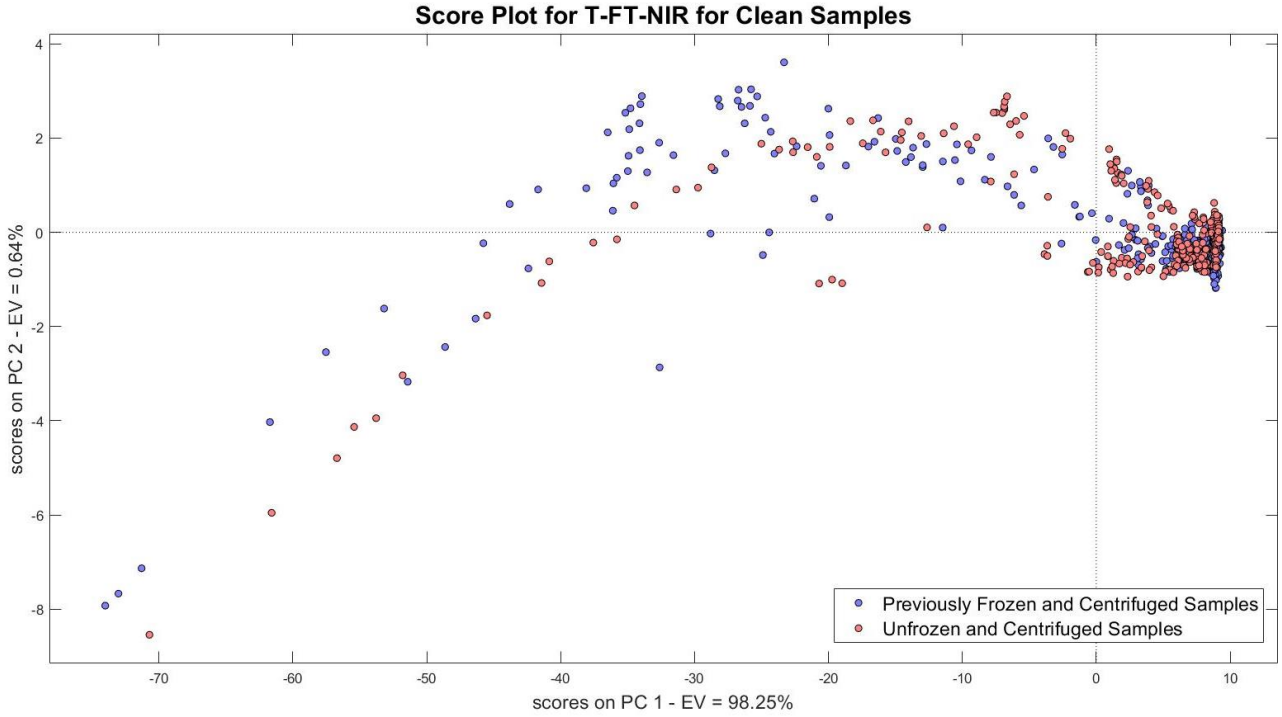

Figure 4.1g: Score plot for T-FT-NIR for clean samples

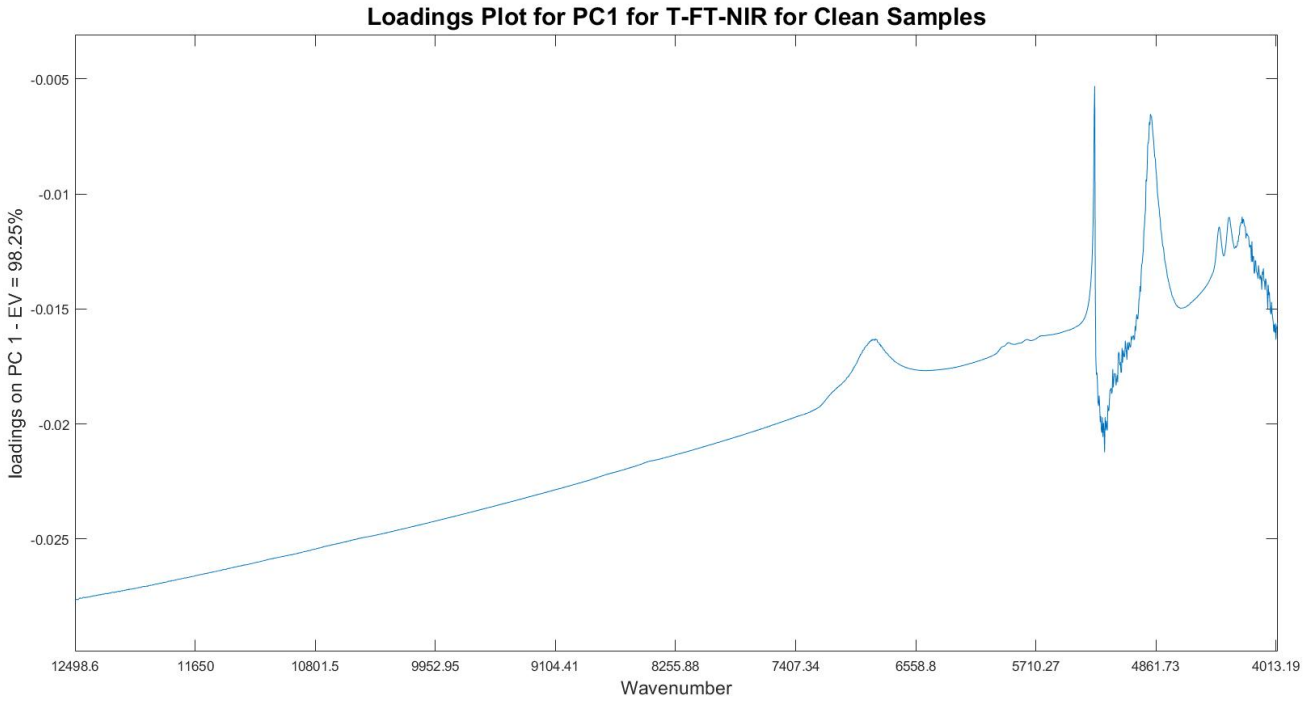

Figure 4.1h: Loadings plot for PC 1 for T-FT-NIR for clean samples

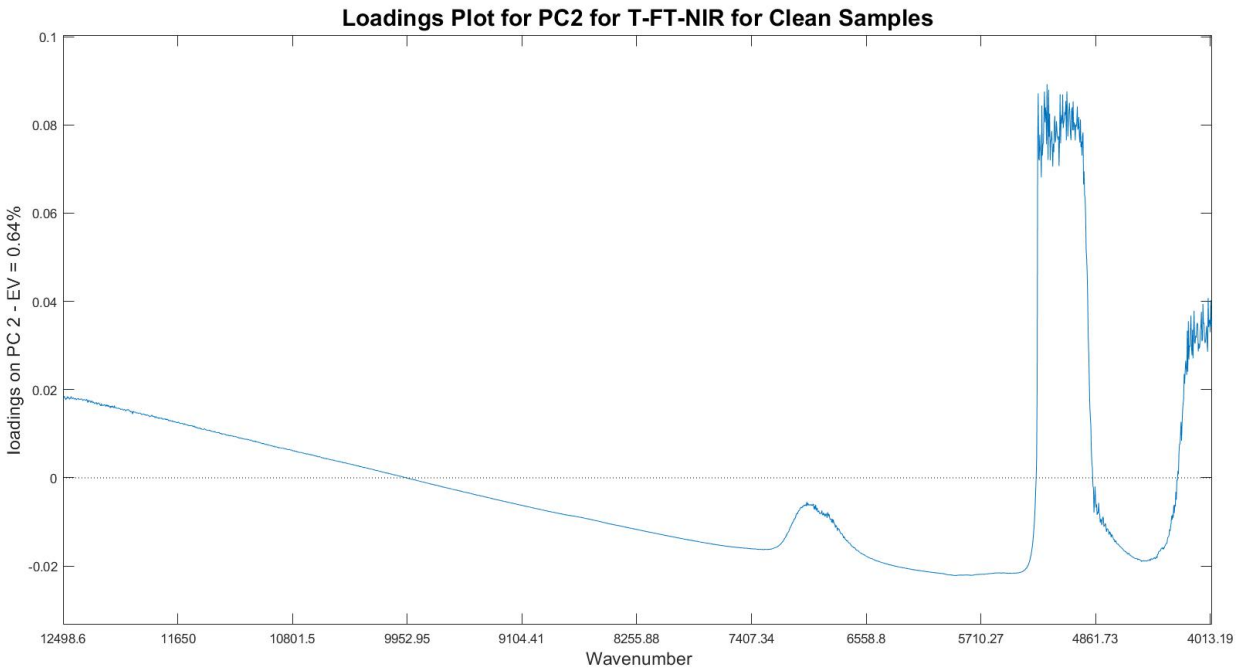

Figure 4.1i: Loadings plot for PC 2 for T-FT-NIR for clean samples

7.2 Loadings and Scores Plots for the ATR-MIR Incorporating All Samples

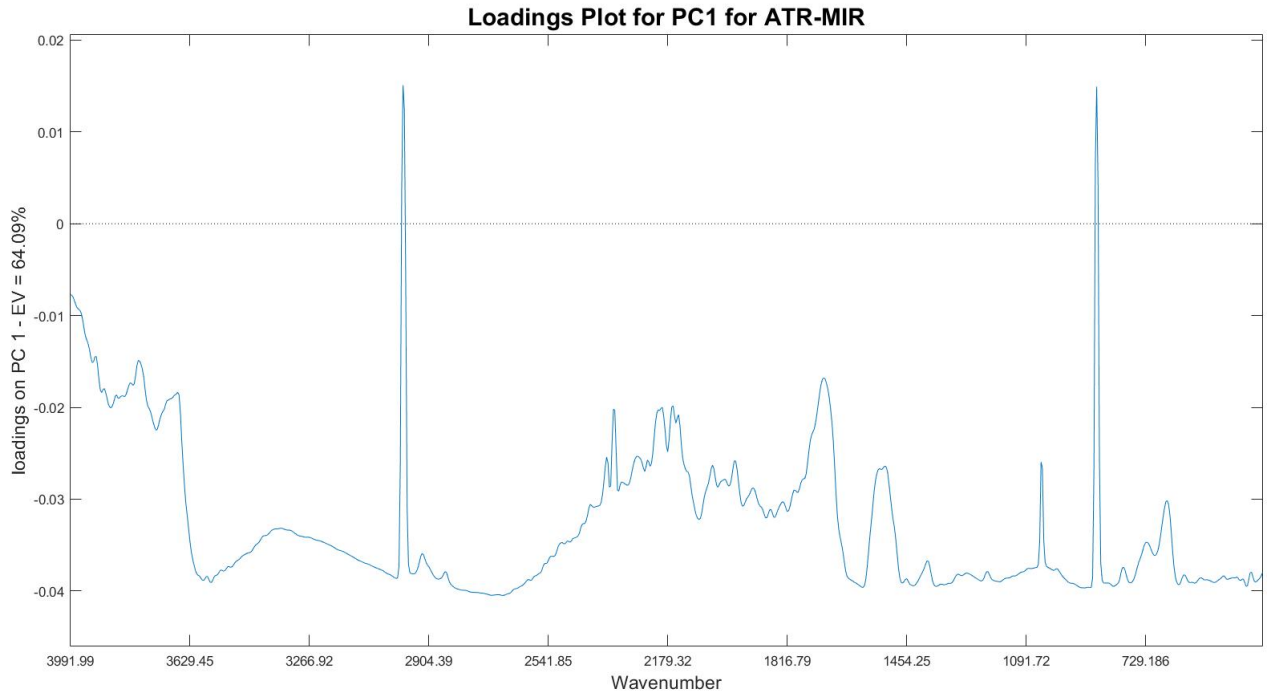

Figure 4.3a: Loadings plot PC 1 for ATR-MIR

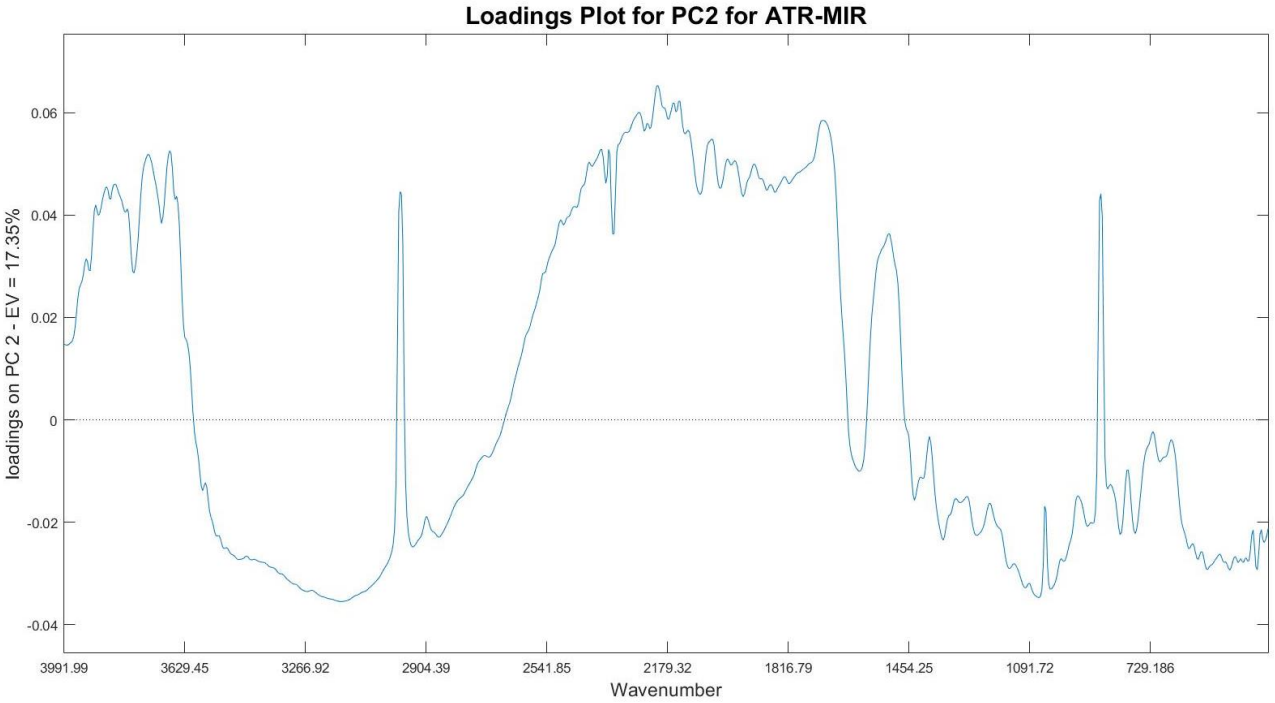

Figure 4.3b: Loadings plot PC 2 for ATR-MIR

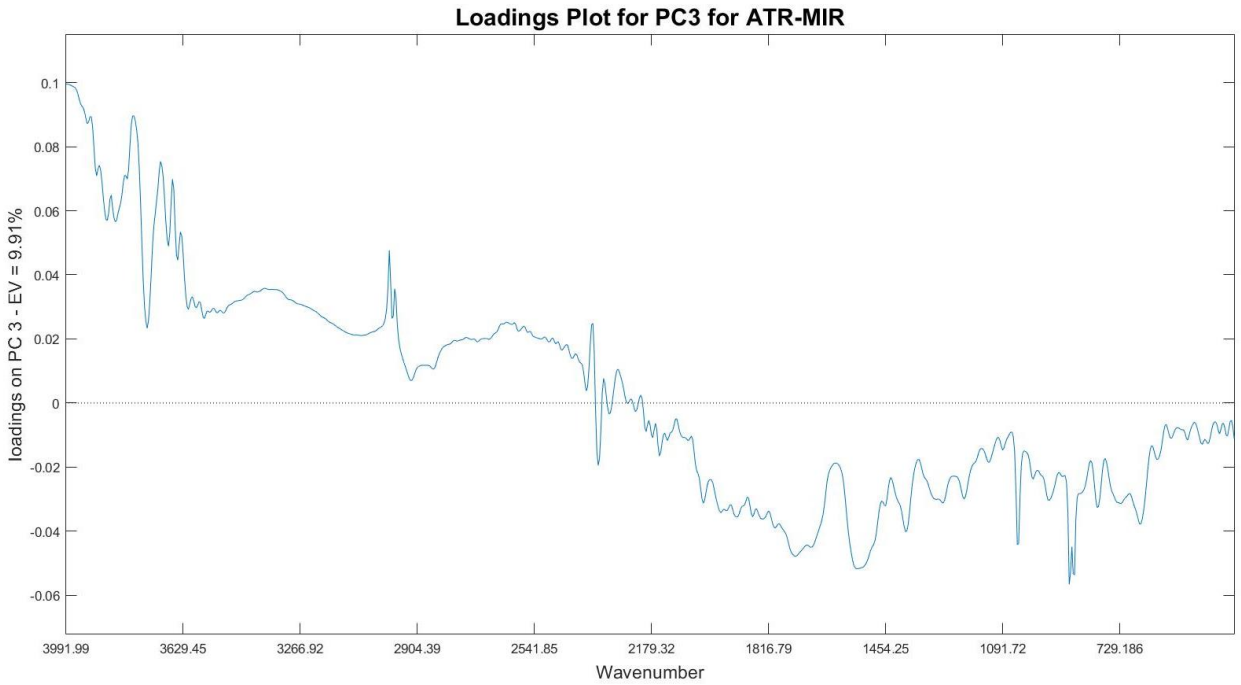

Figure 4.3c: Loadings plot PC 3 for ATR-MIR

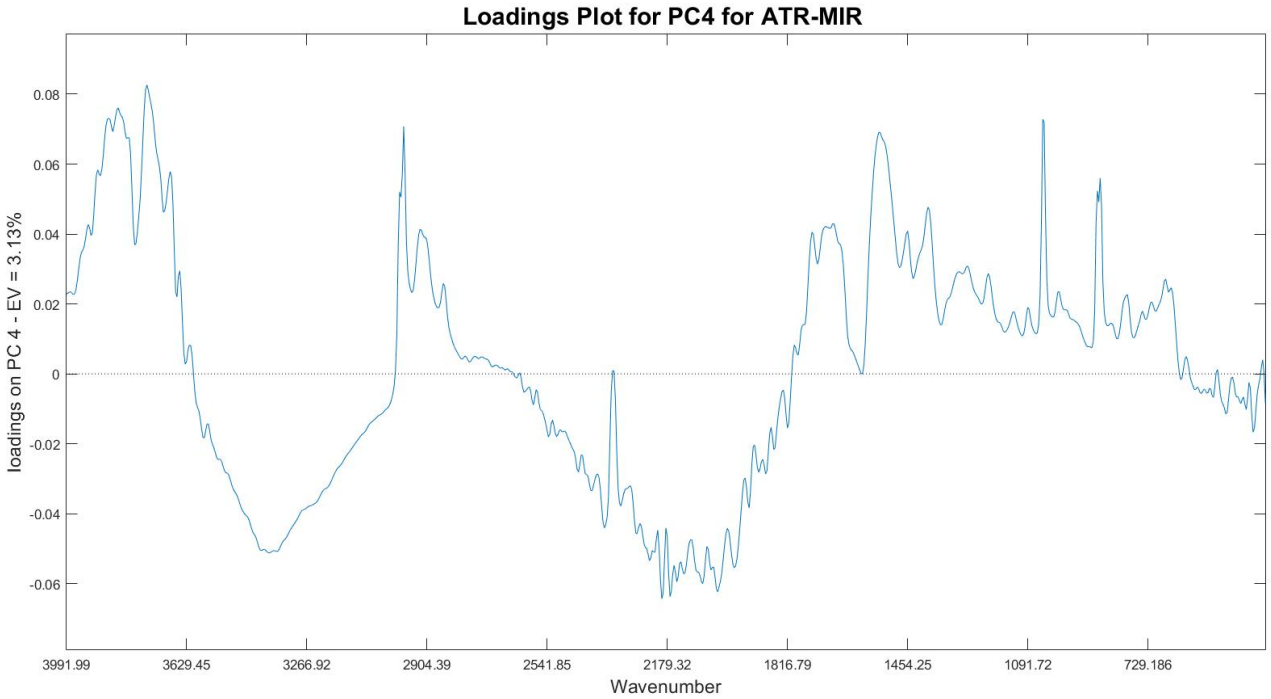

Figure 4.3d: Loadings plot PC 4 for ATR-MIR

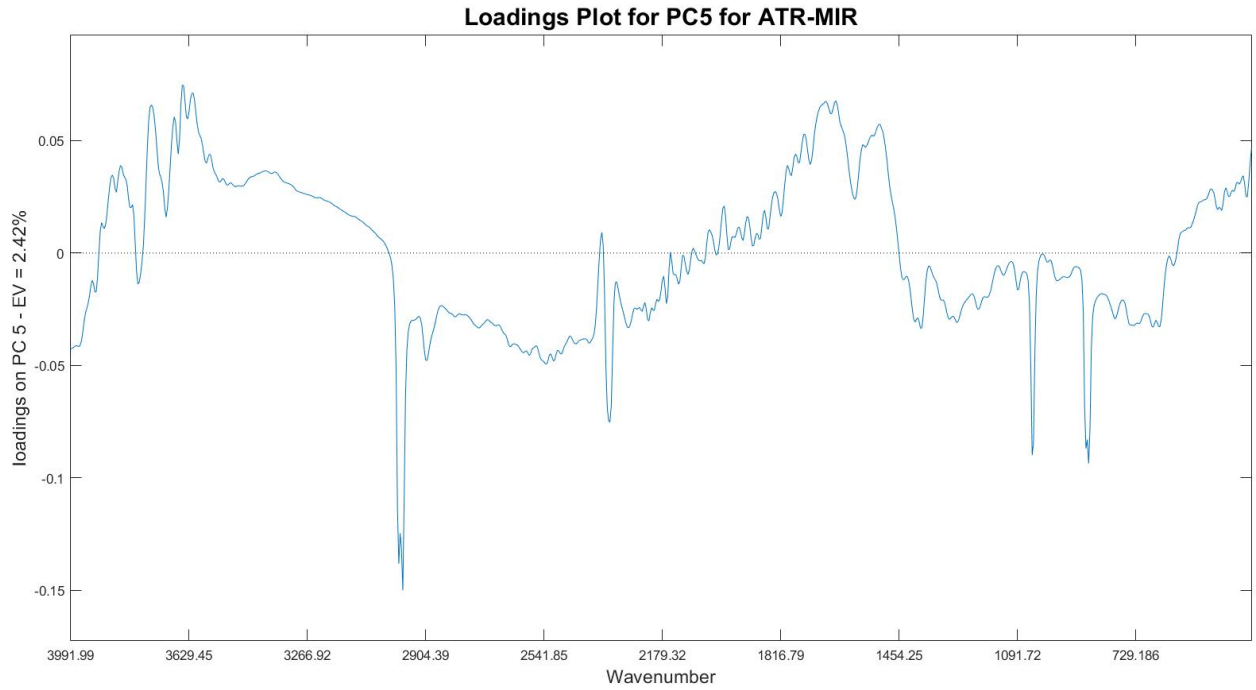

Figure 4.3e: Loadings plot PC 5 for ATR-MIR

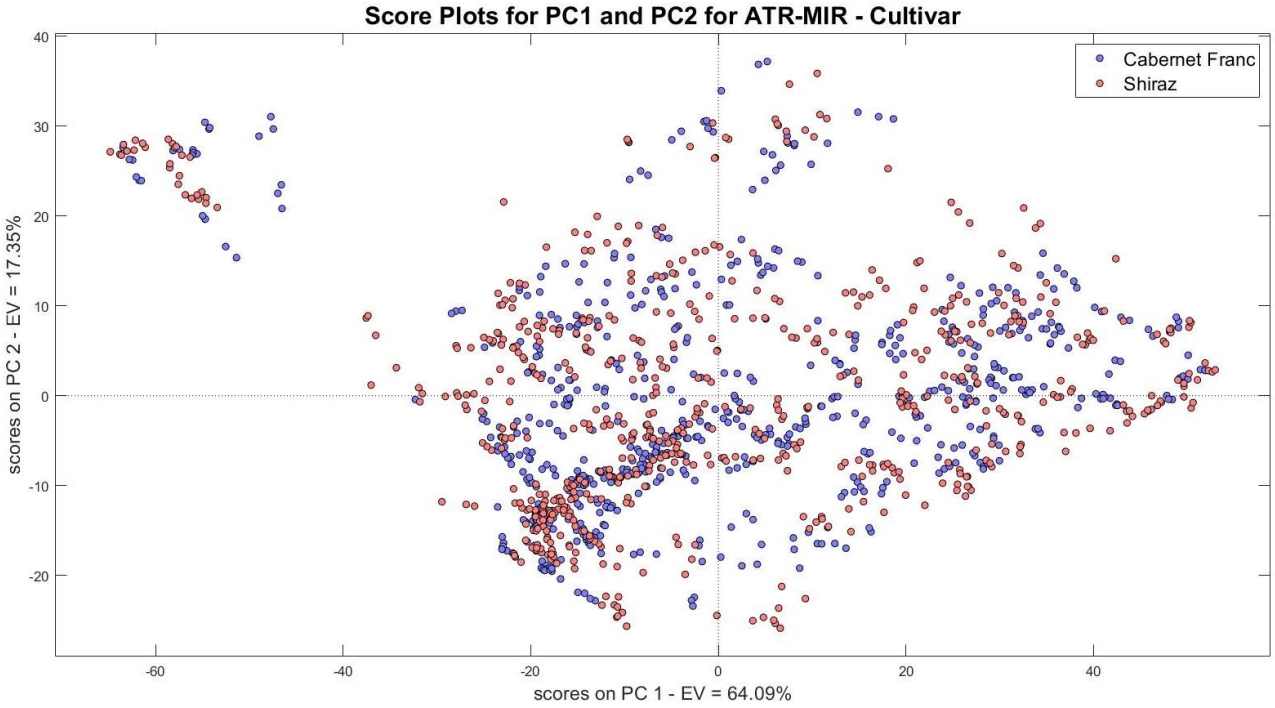

Figure 4.3f: Score plot for ATR-MIR for PC 1 vs PC 2 (Cultivar)

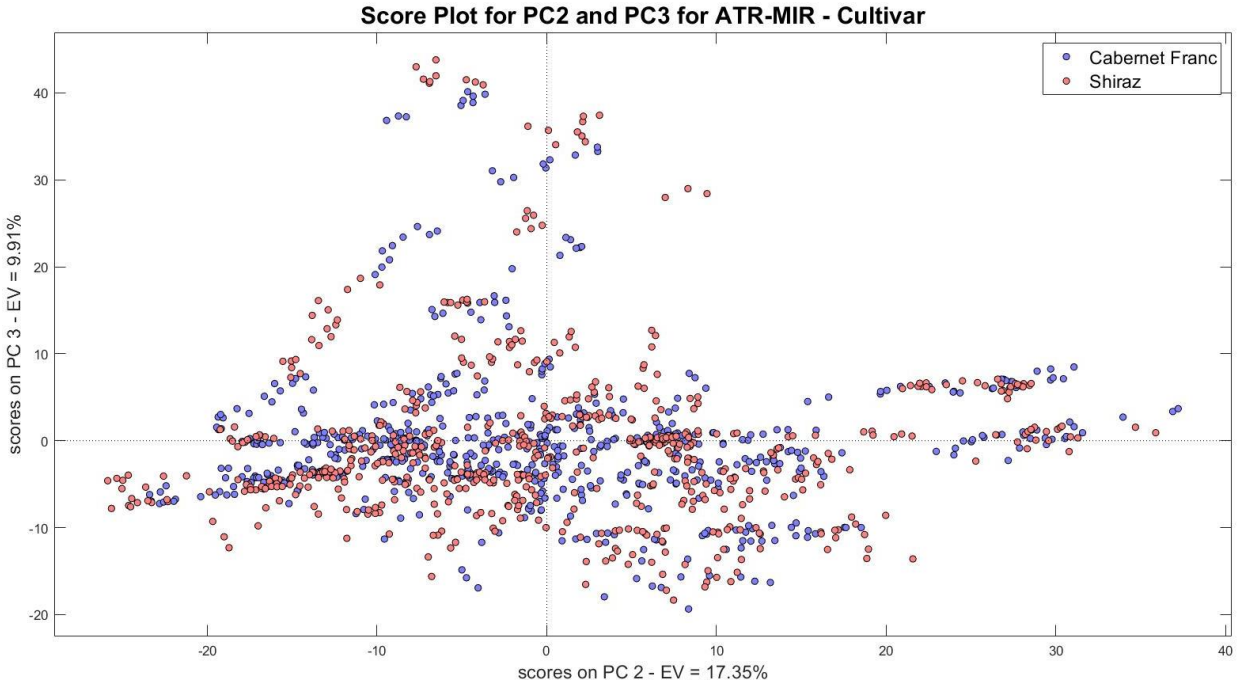

Figure 4.3g: Score plot for ATR-MIR for PC 2 vs PC 3 (Cultivar)

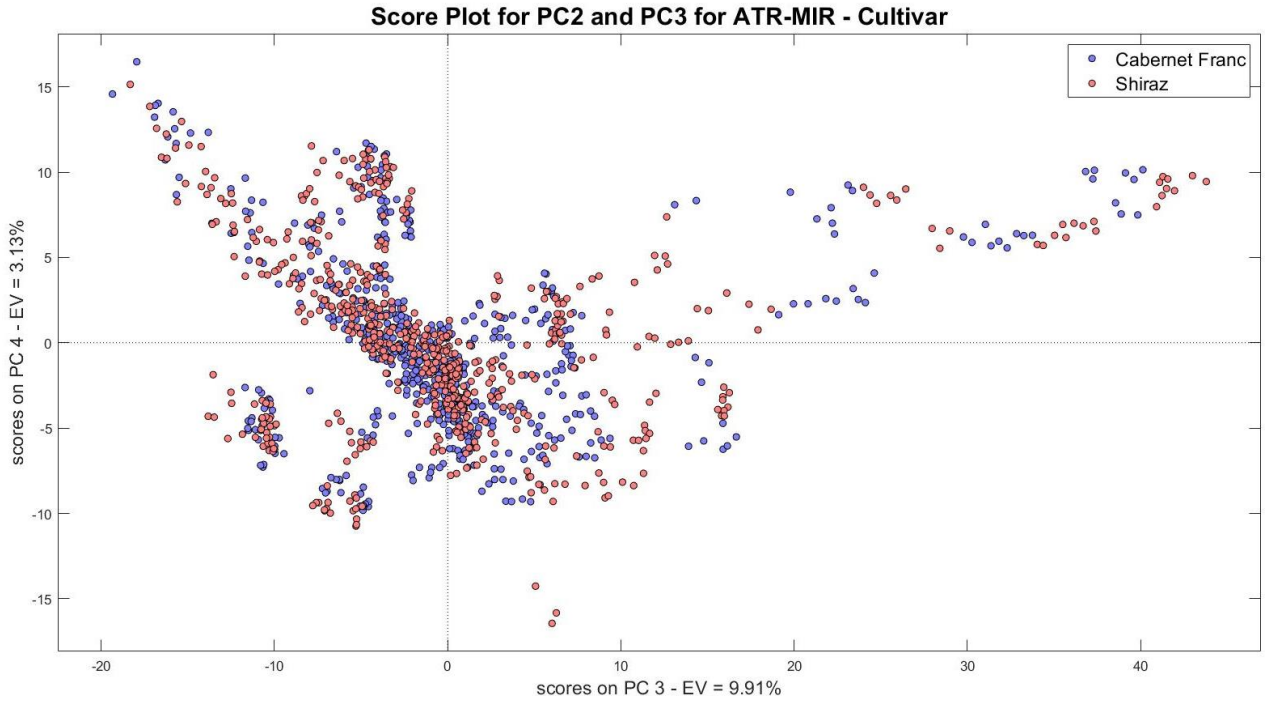

Figure 4.3h: Score plot for ATR-MIR PC 3 vs PC 4 (Cultivar)

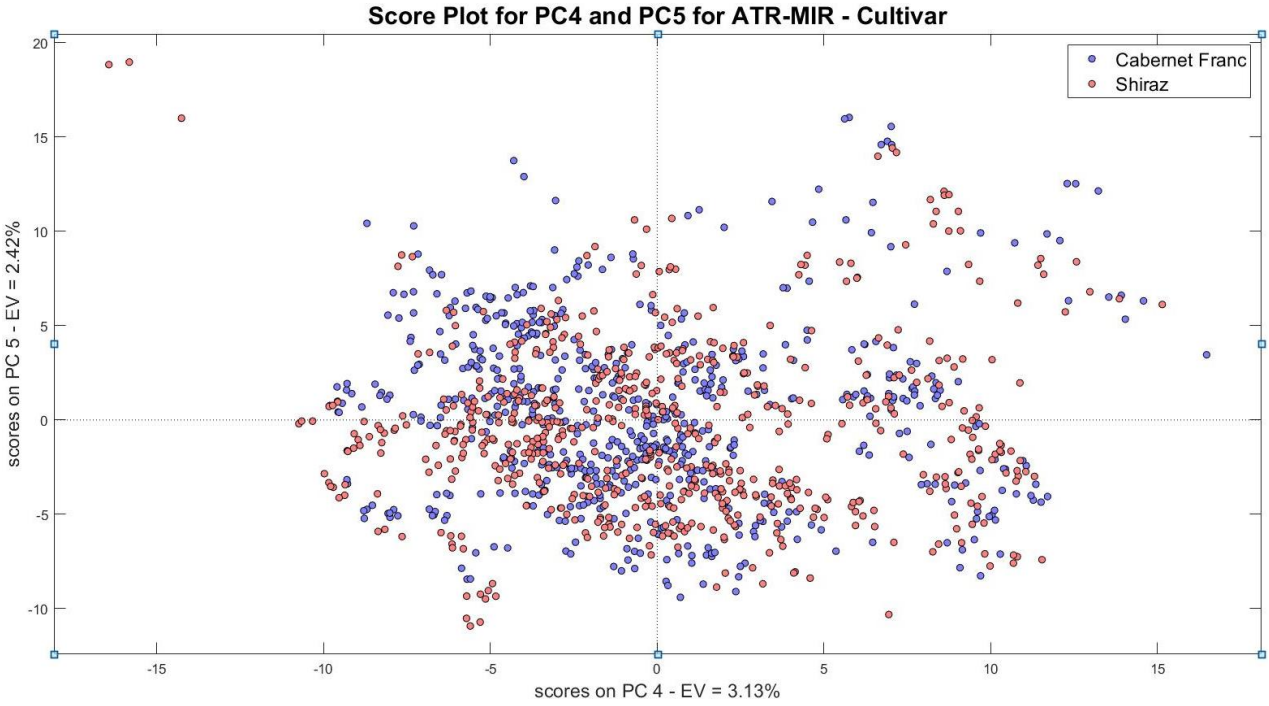

Figure 4.3i: Score plot for ATR-MIR for PC 4 vs PC 5 (Cultivar)

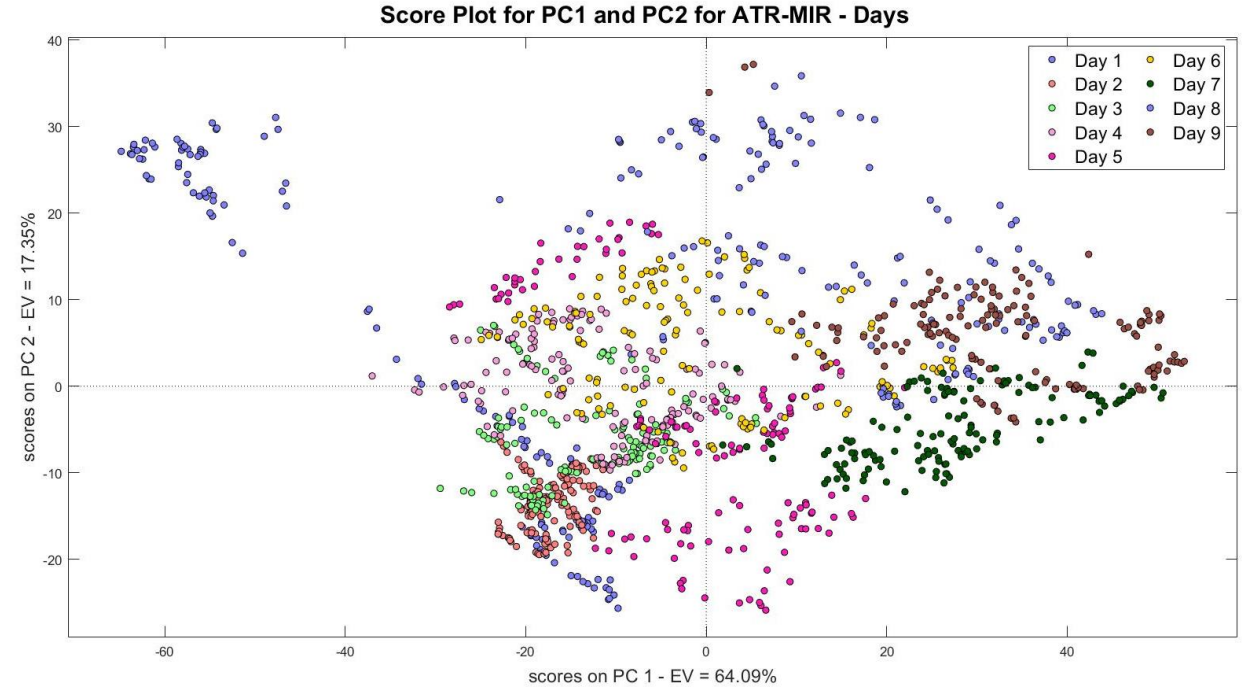

Figure 4.3j: Score plot for ATR-MIR for PC 1 vs PC 2 (Days)

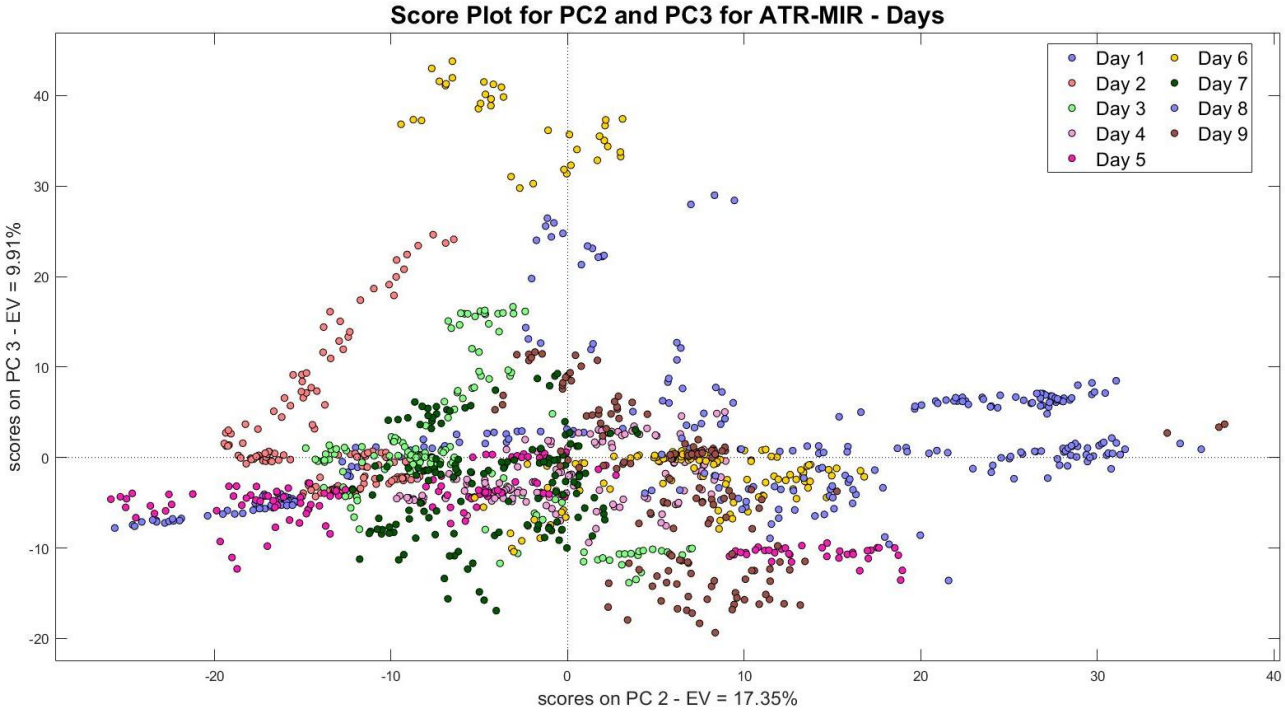

Figure 4.3k: Score plot for ATR-MIR for PC 2 vs PC 3 (Days)

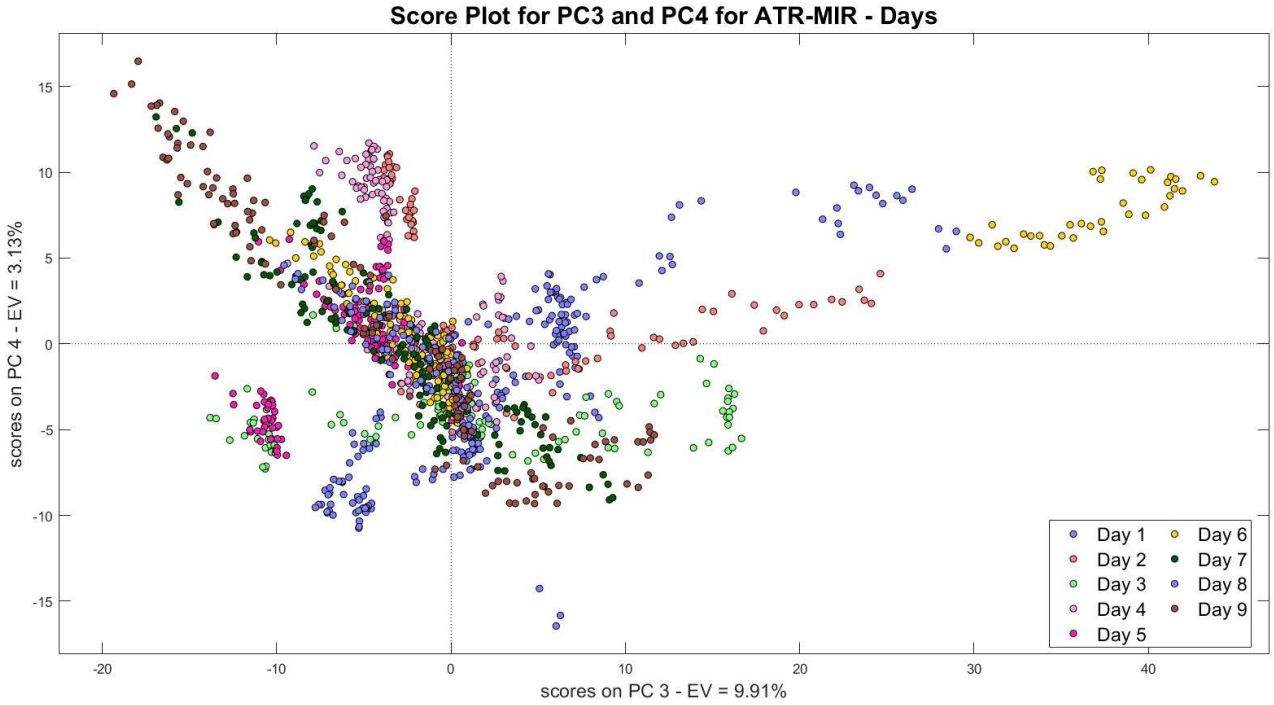

Figure 4.3l: Score plot for ATR-MIR for PC 3 vs PC 4 (Days)

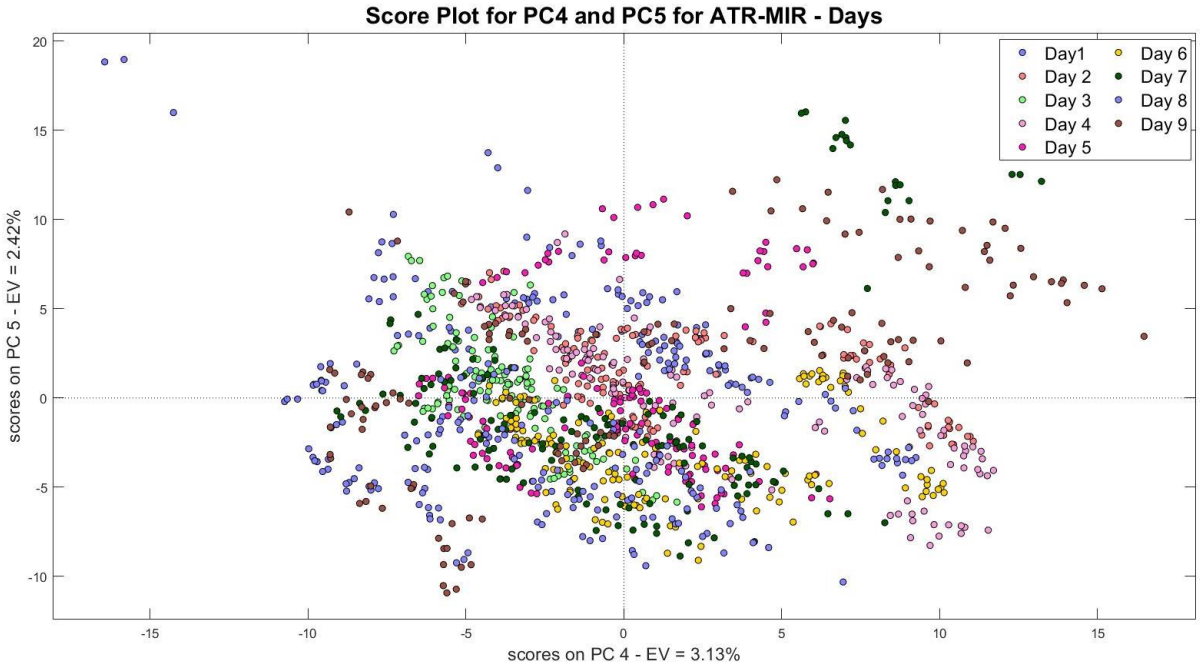

Figure 4.3m: Score plot for ATR-MIR for PC 4 vs PC 5 (Days)

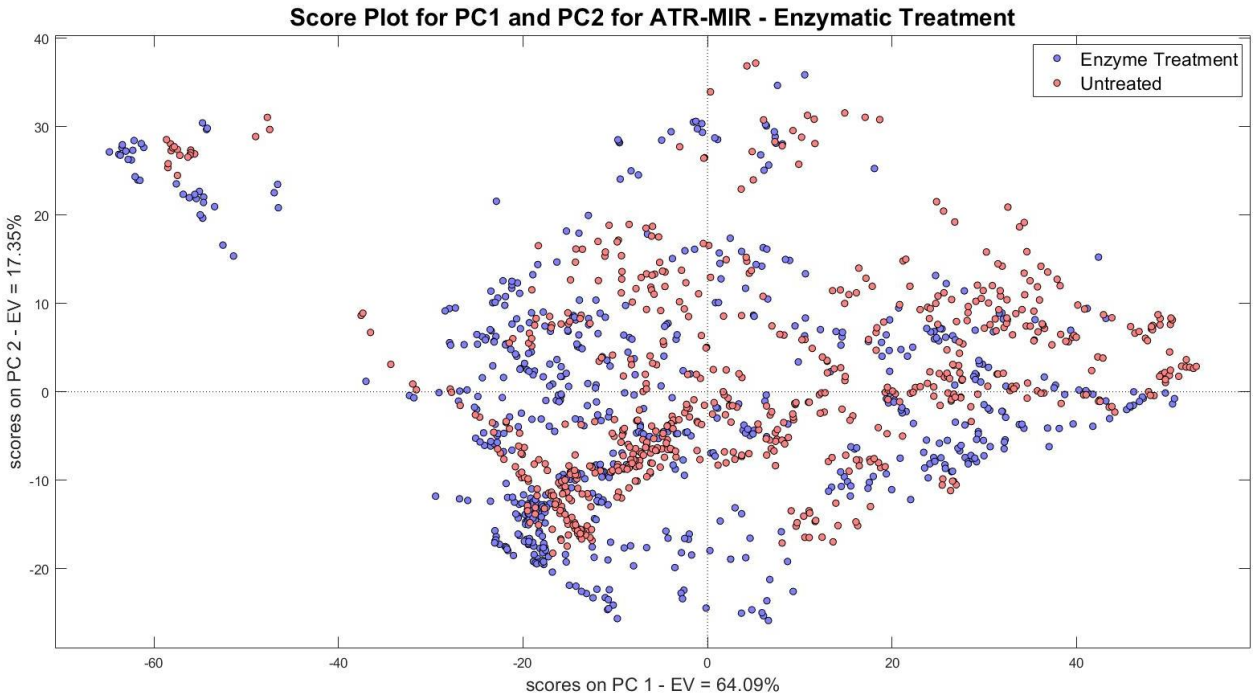

Figure 4.3n: Score plot for ATR-MIR for PC 1 vs PC 2 (Enzymatic Treatment)

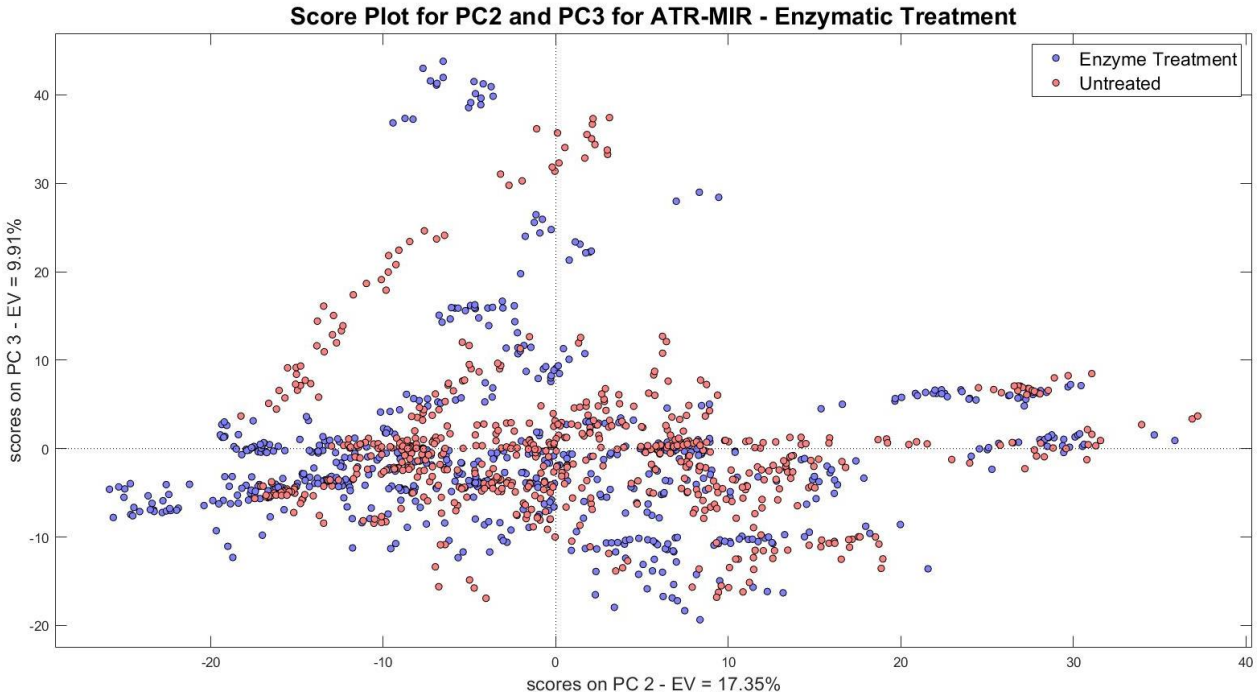

Figure 4.3o: Score plot for ATR-MIR for PC 2 vs PC 3 (Enzymatic Treatment)

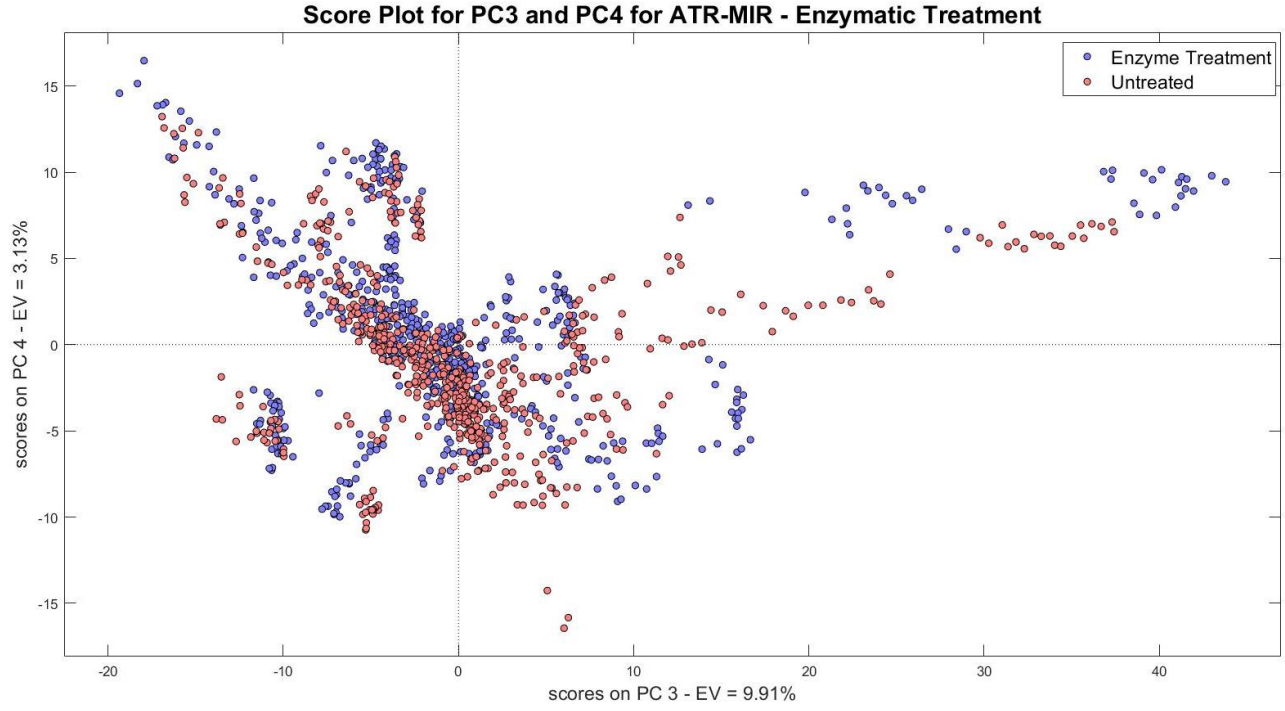

Figure 4.3p: Score plot for ATR-MIR for PC 3 vs PC 4 (Enzymatic Treatment)

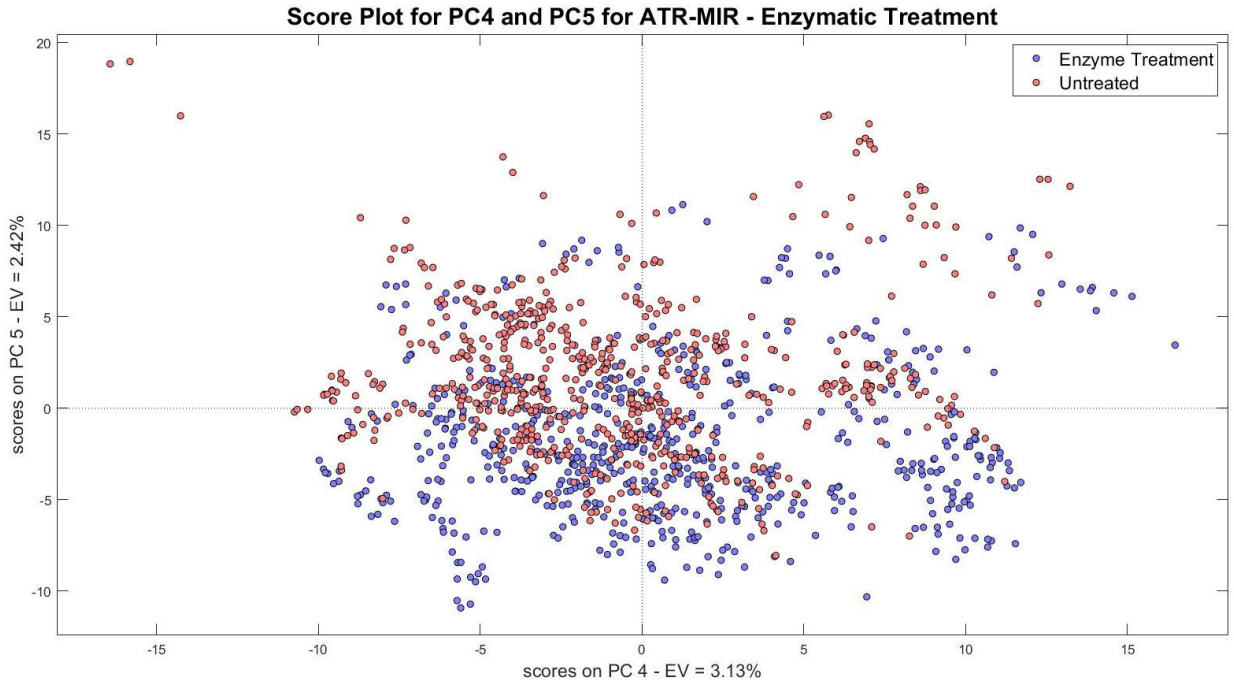

Figure 4.3q: Score plot for ATR-MIR for PC 4 vs PC 5 (Enzymatic Treatment)

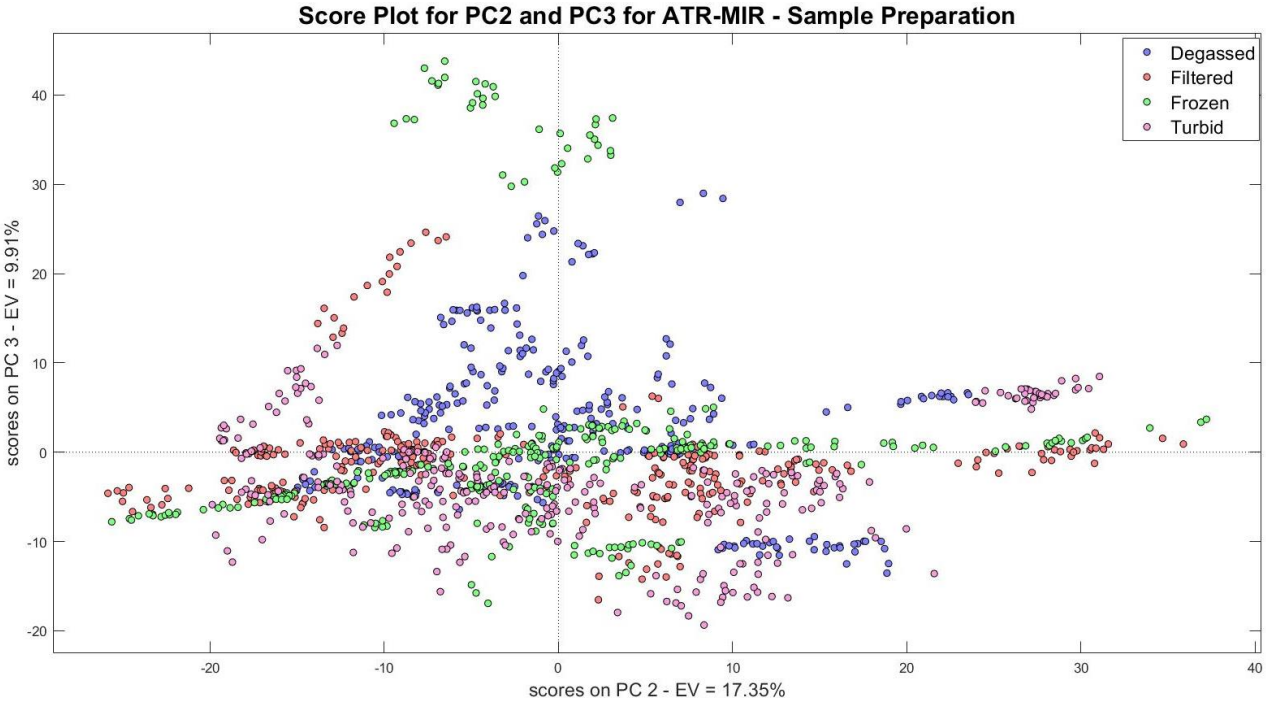

Figure 4.3r: Score plot for ATR-MIR for PC 2 vs PC 3 (Sample Preparation)

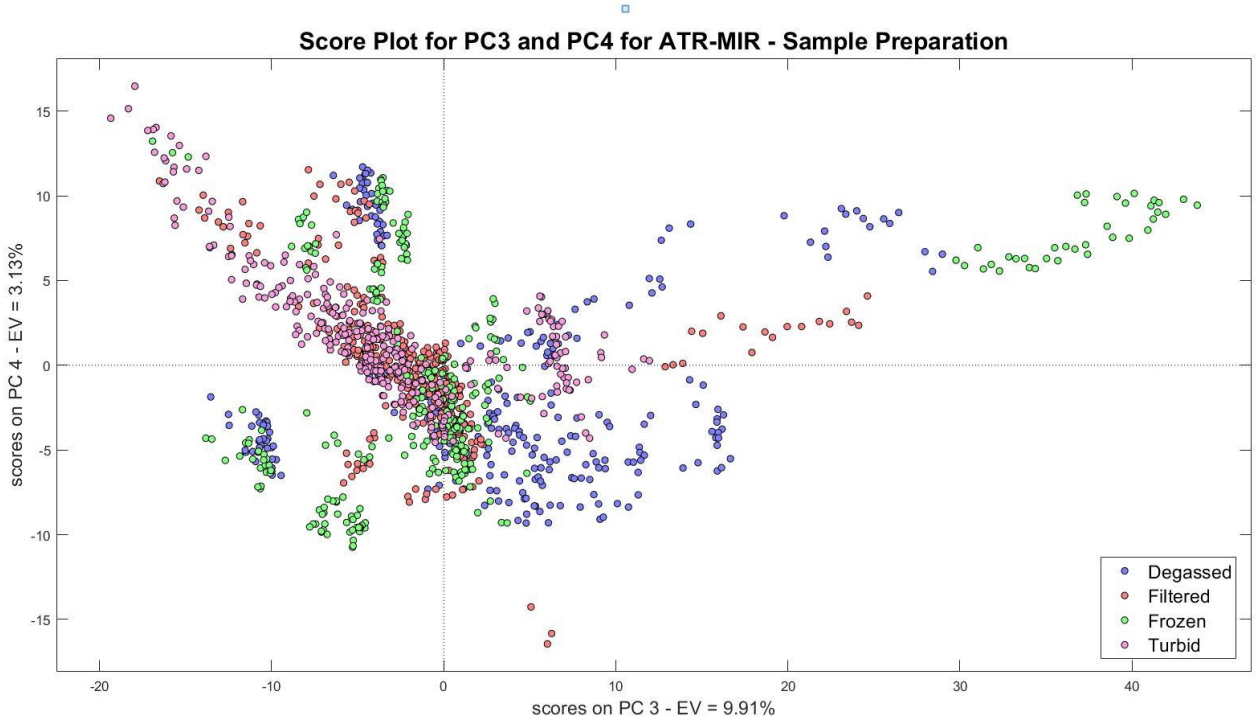

Figure 4.3s: Score plot for ATR-MIR for PC 3 vs PC 4 (Sample Preparation)

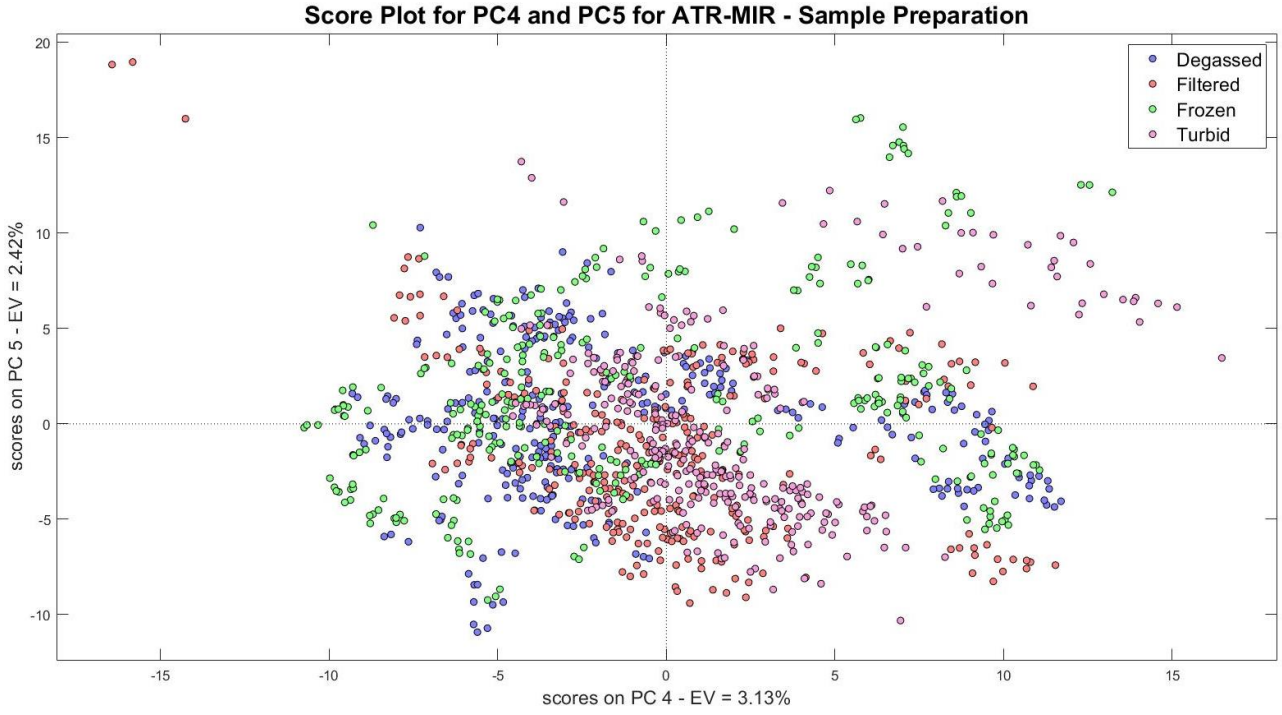

Figure 4.3t: Score plot for ATR-MIR for PC 4 vs PC 5 (Sample Preparation)

7.3 Loadings and Scores Plots for the DR-FT-NIR Incorporating All Samples

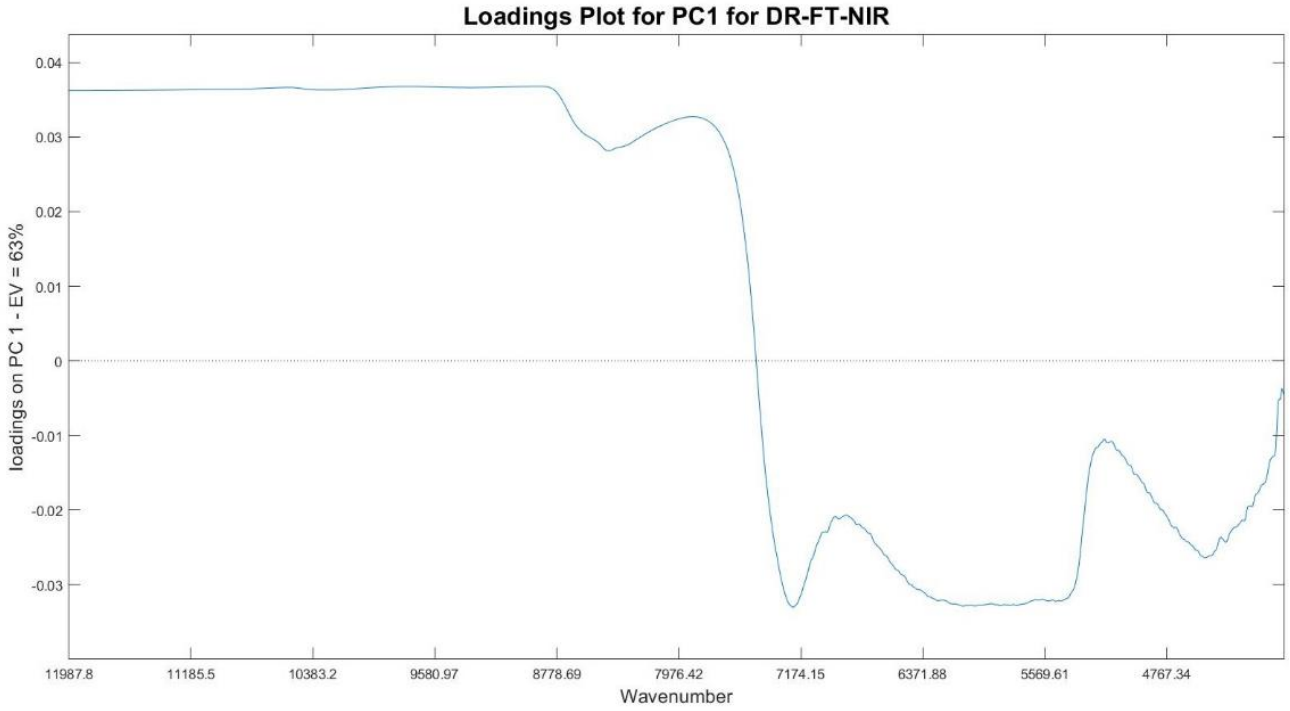

Figure 4.4a: Loadings plot for DR-FT-NIR for PC 1

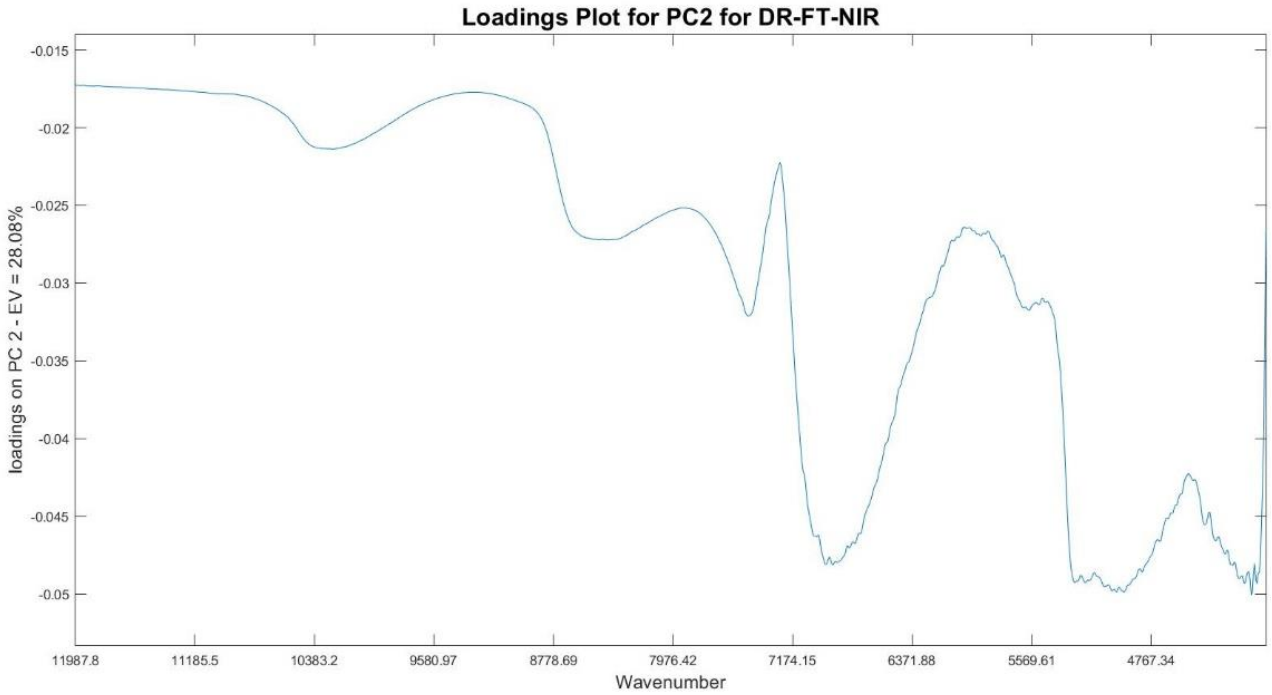

Figure 4.4b: Loadings plot for DR-FT-NIR for PC 2

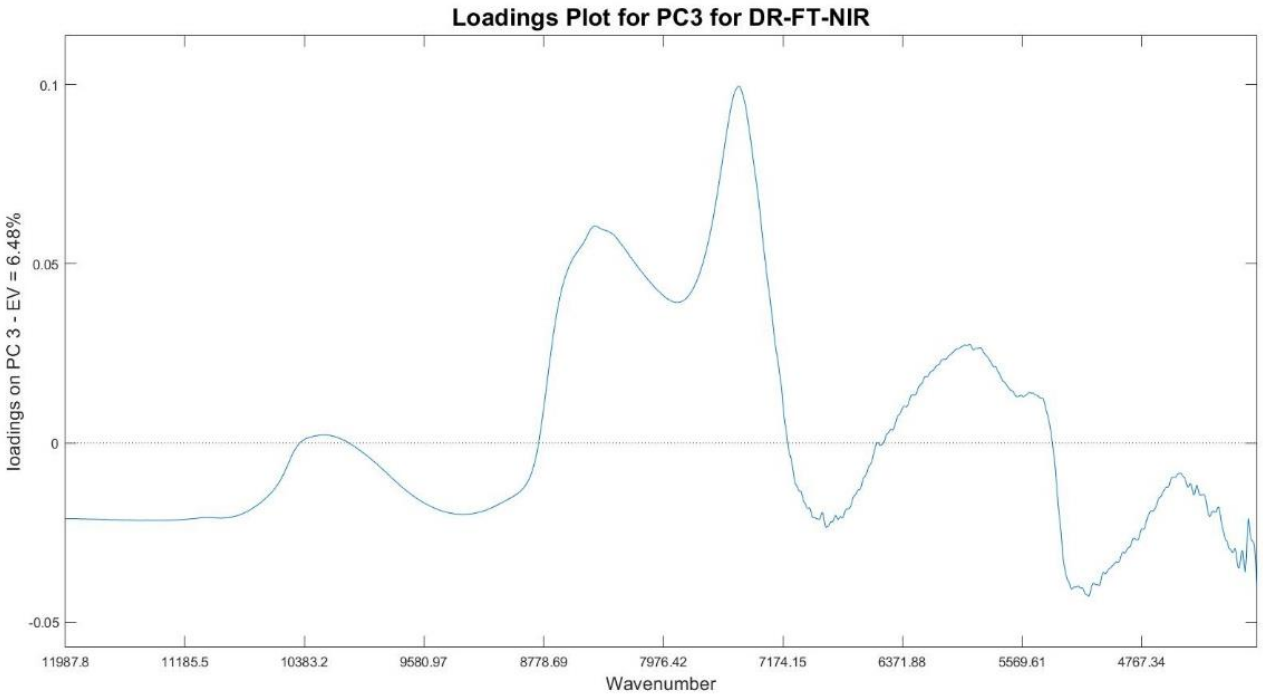

Figure 4.4c: Loadings plot for DR-FT-NIR for PC 3

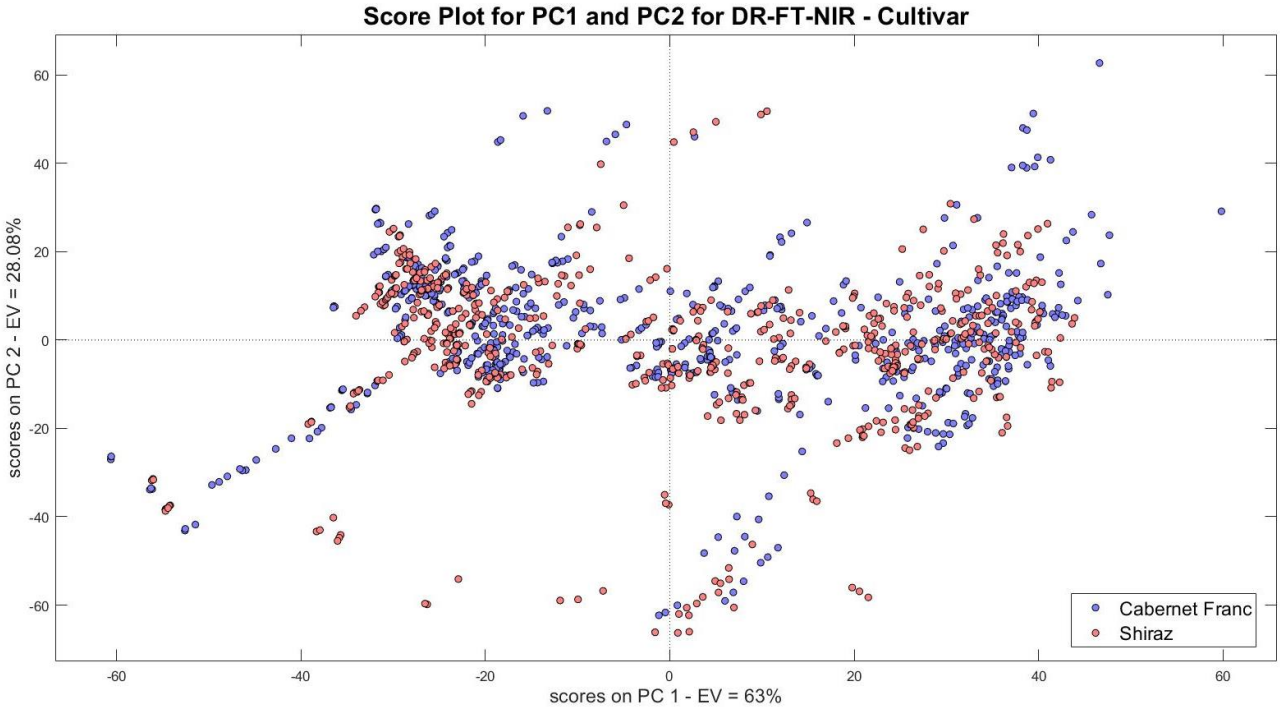

Figure 4.4d: Score Plot for DR-FT-NIR for PC 1 vs PC 2 (Cultivar)

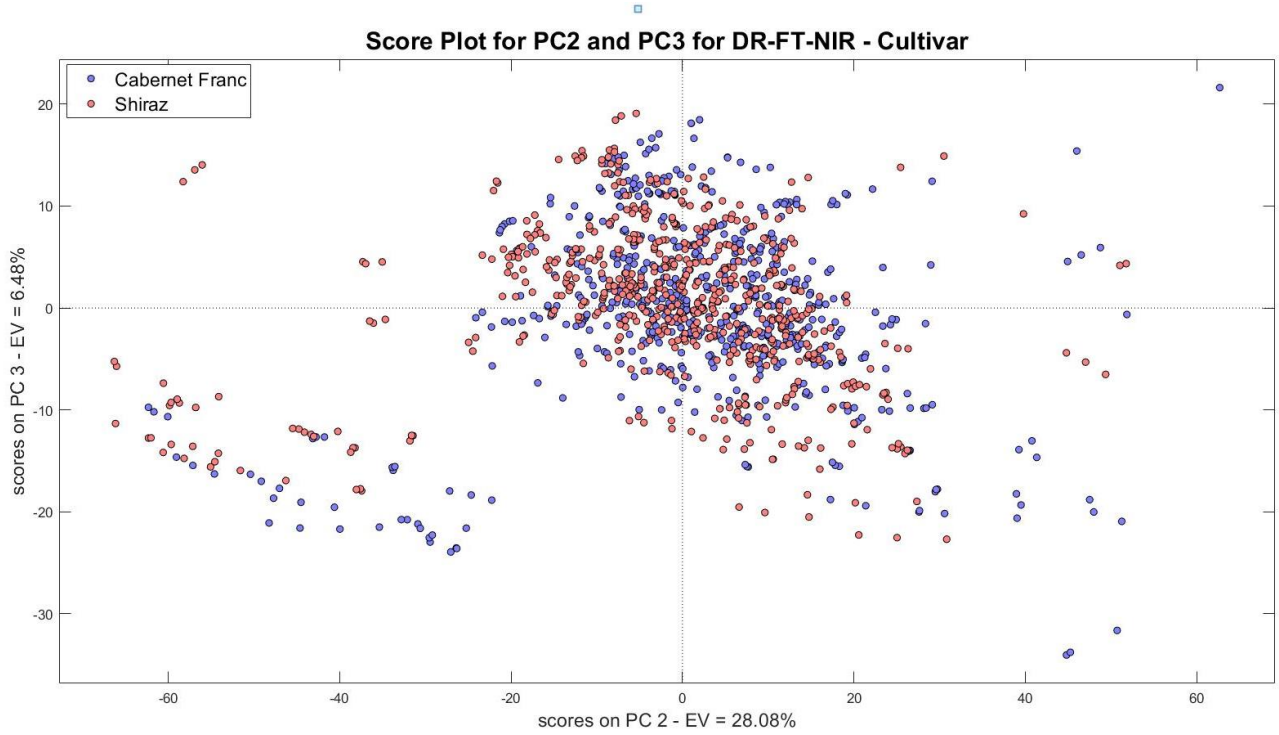

Figure 4.4e: Score plot for DR-FT-NIR for PC 2 vs PC 3 (Cultivar)

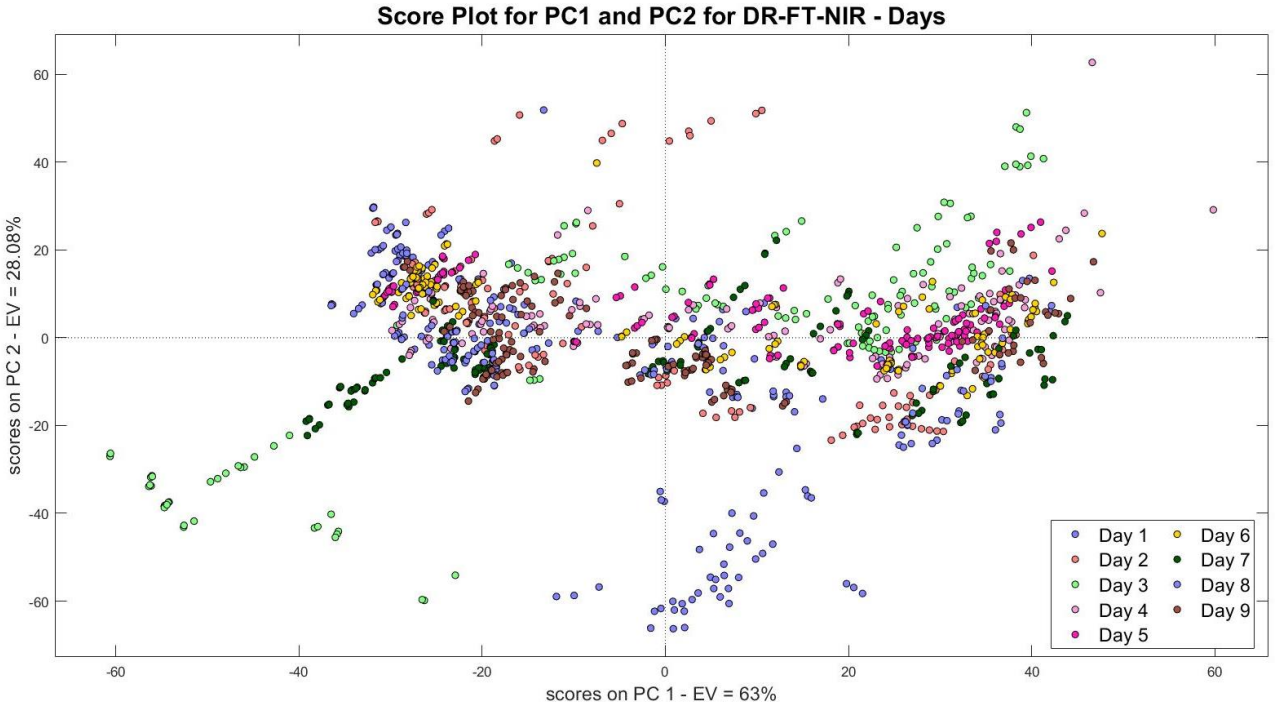

Figure 4.4f: Score plot for DR-FT-NIR for PC 1 vs PC 2 (Days)

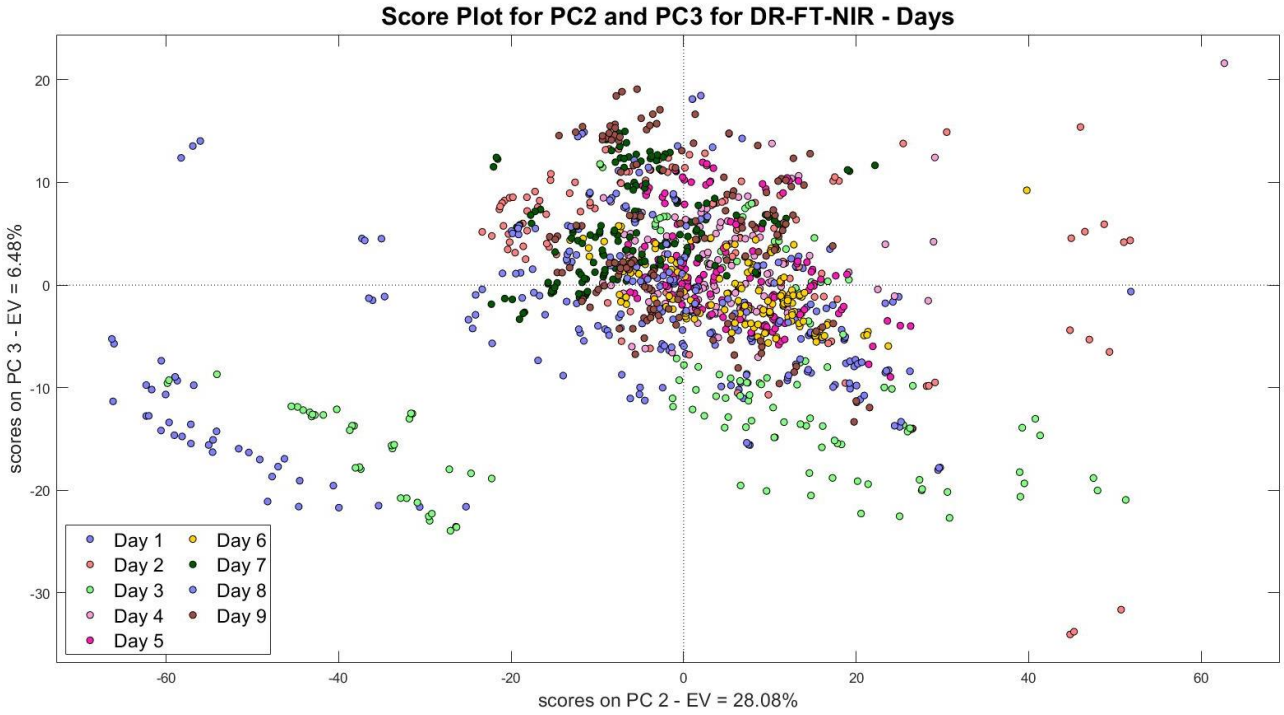

Figure 4.4g: Score plot for DR-FT-NIR for PC 2 vs PC 3 (Days)

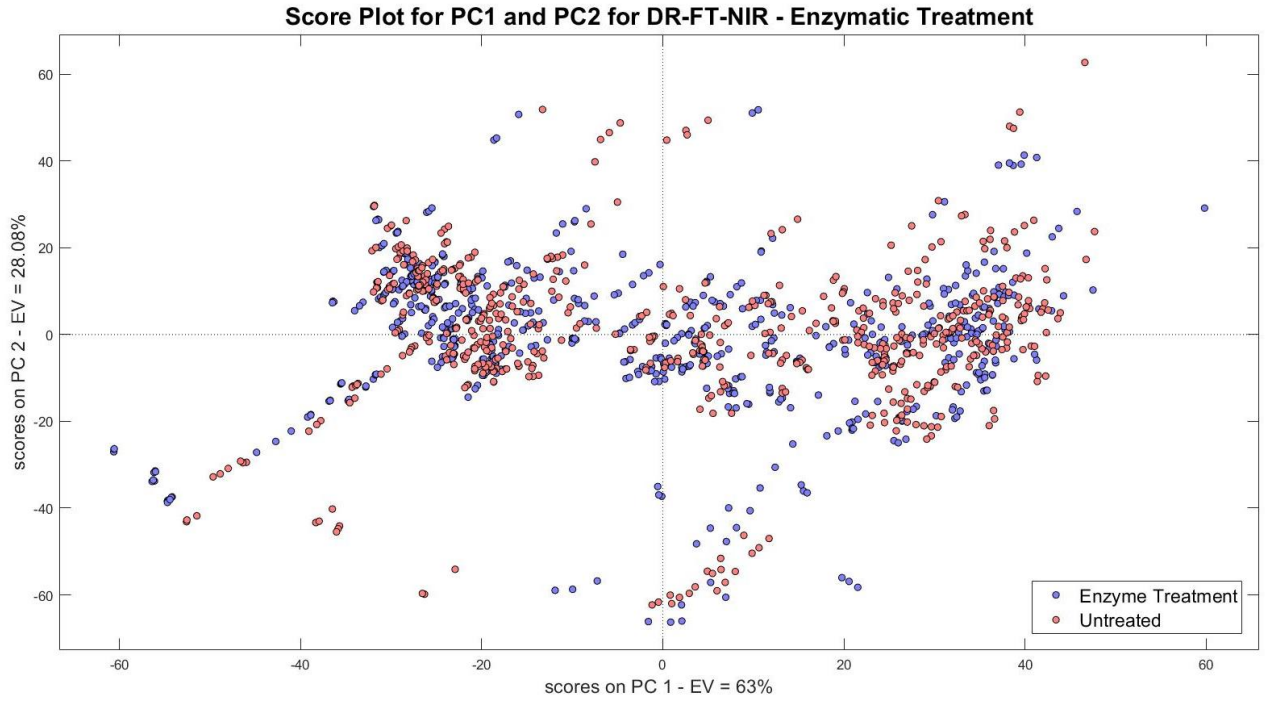

Figure 4.4h: Score plot for DR-FT-NIR for PC 1 vs PC 2 (Enzymatic Treatment)

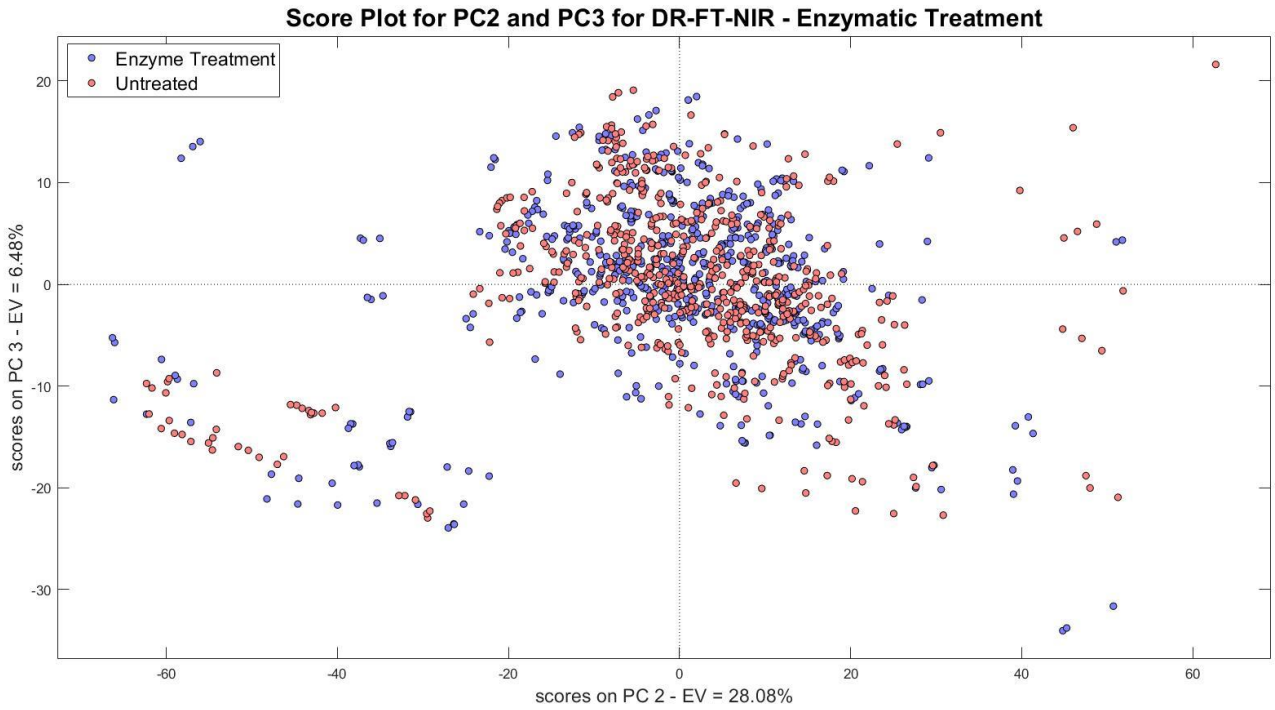

Figure 4.4i: Score plot for DR-FT-NIR for PC 2 vs PC 3 (Enzymatic Treatment)

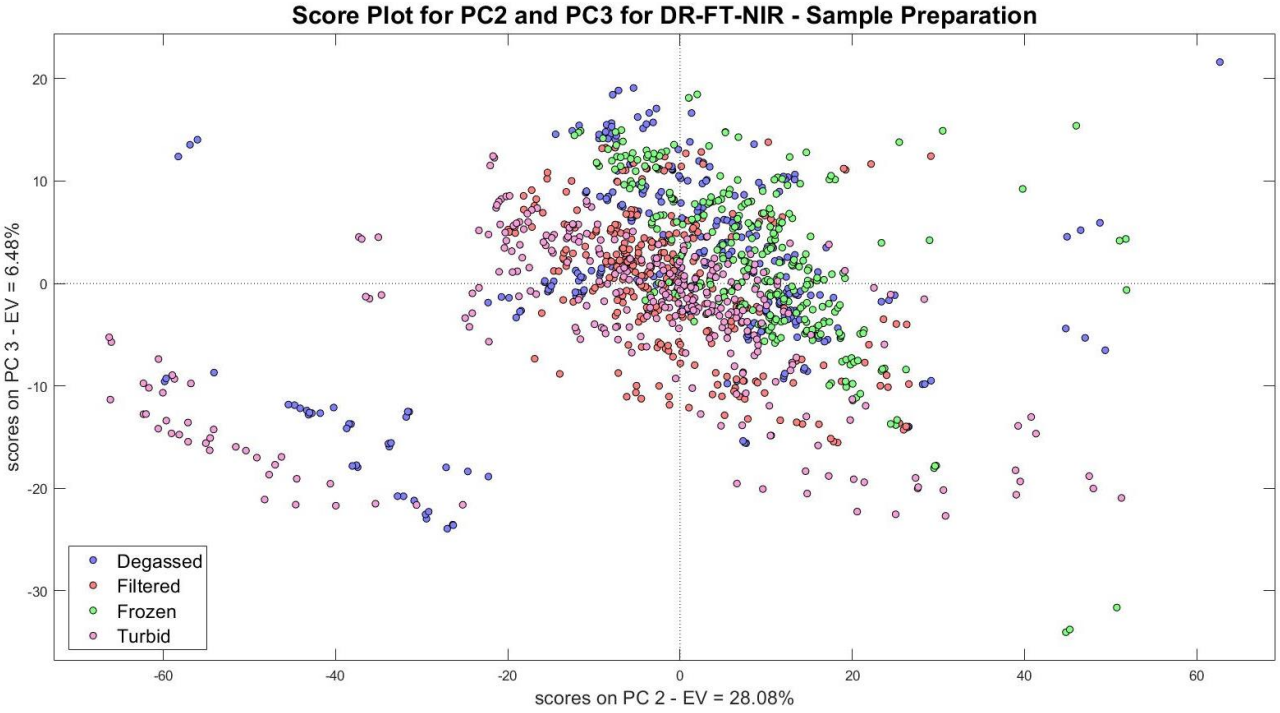

Figure 4.4j: Score plot for DR-FT-NIR for PC 2 vs PC 3 (Sample Preparation)

7.4 Loadings and Scores Plots for the T-FT-NIR Incorporating All Samples

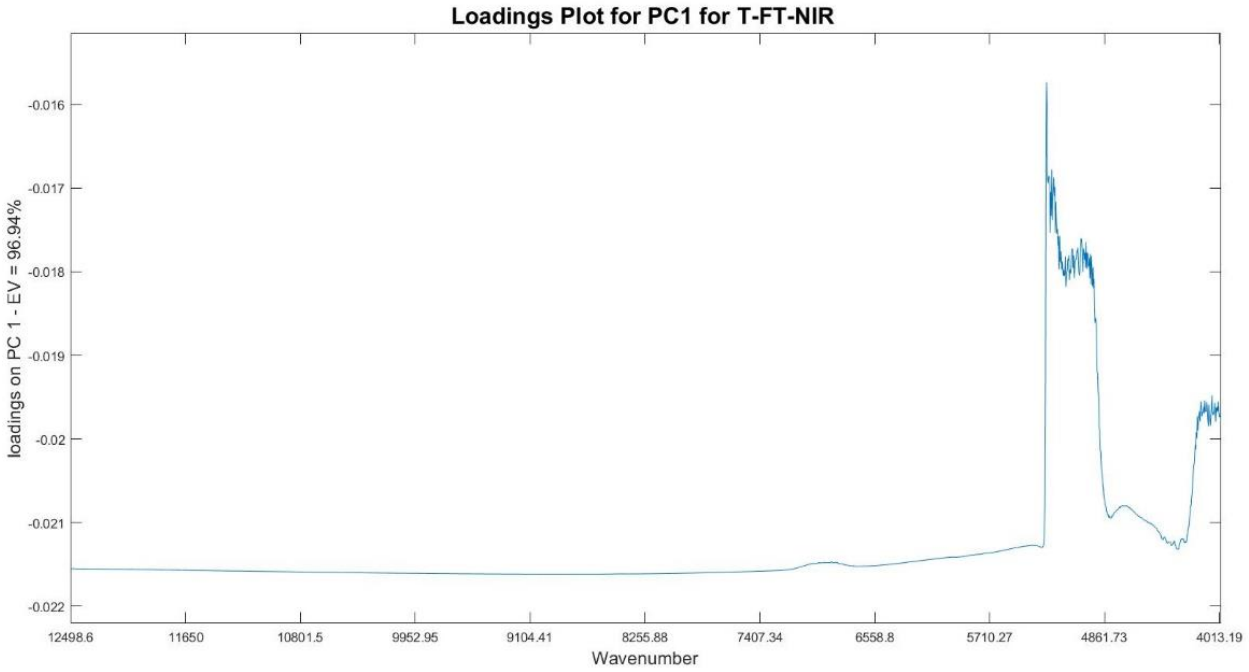

Figure 4.5a: Loadings plot for T-FT-NIR for PC 1

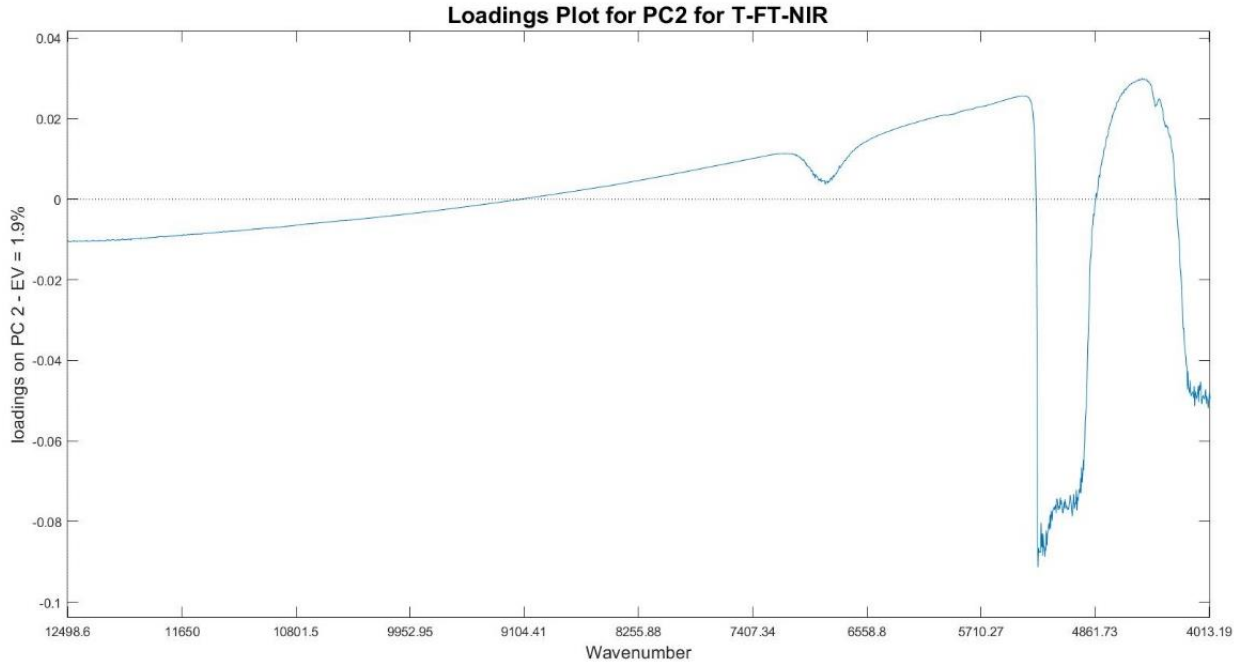

Figure 4.5b: Loadings plot for T-FT-NIR for PC 2

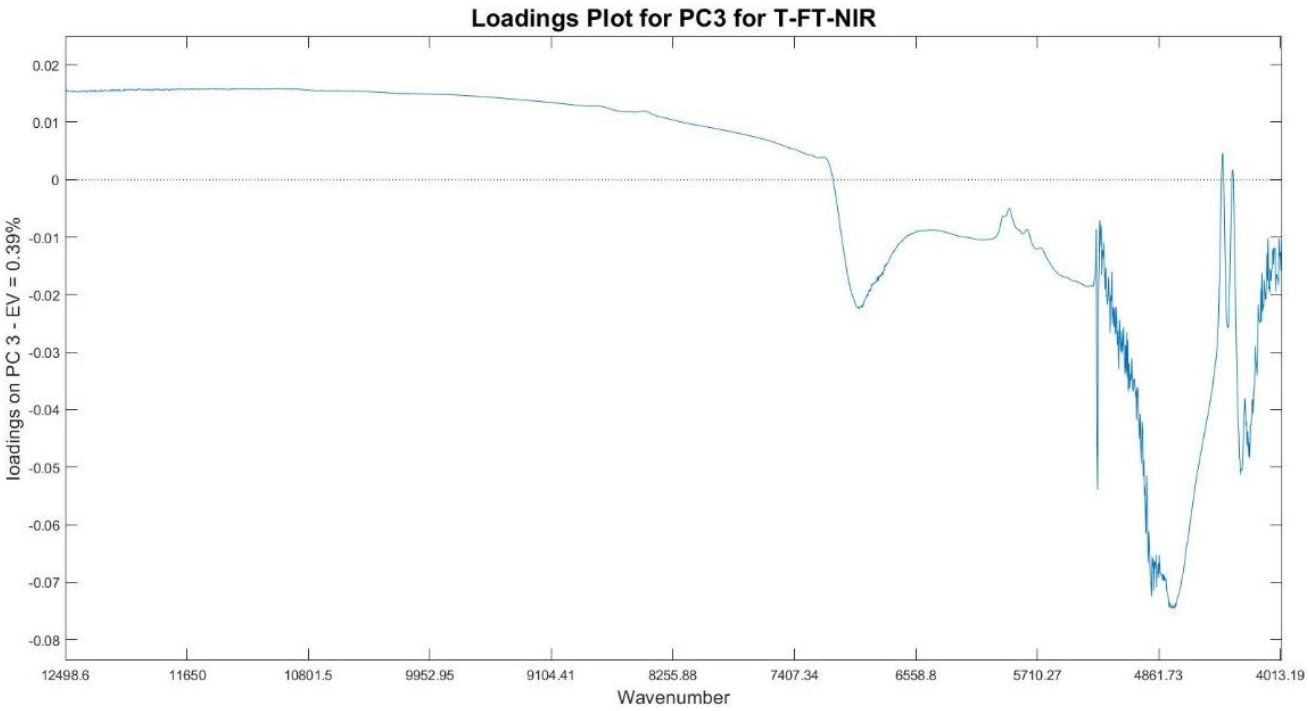

Figure 4.5c: Loadings plot for T-FT-NIR for PC 3

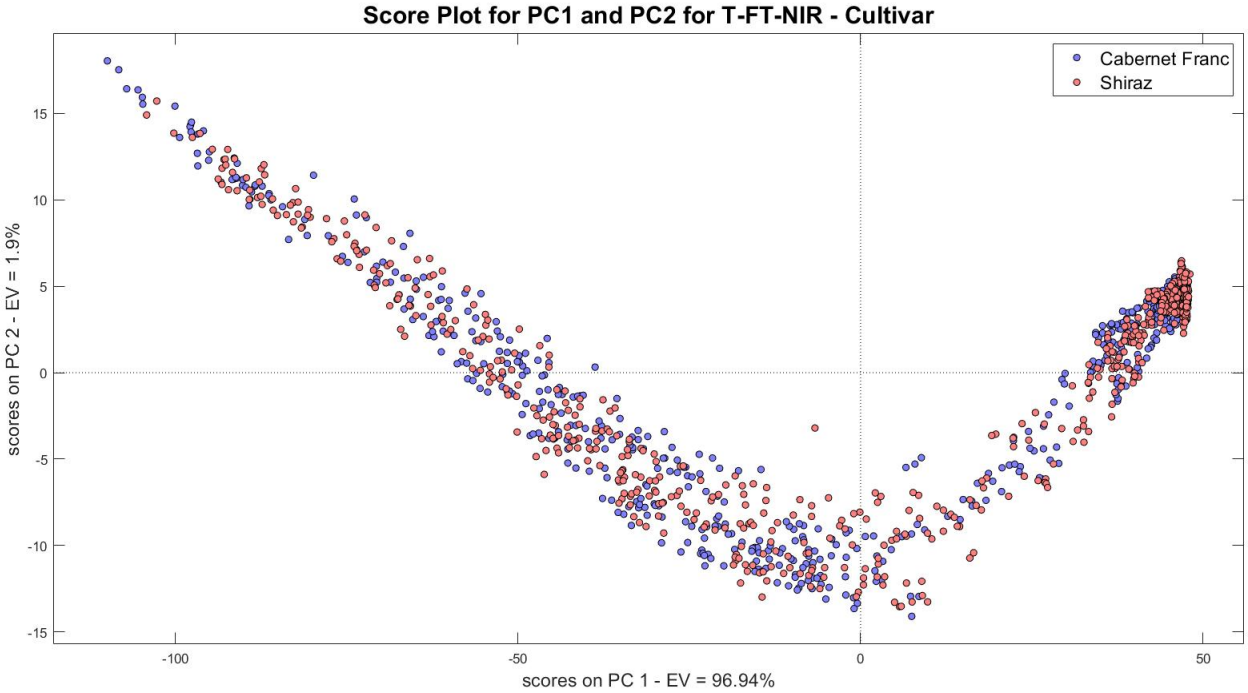

Figure 4.5d: Score plot for T-FT-NIR for PC 1 vs PC 2 (Cultivar)

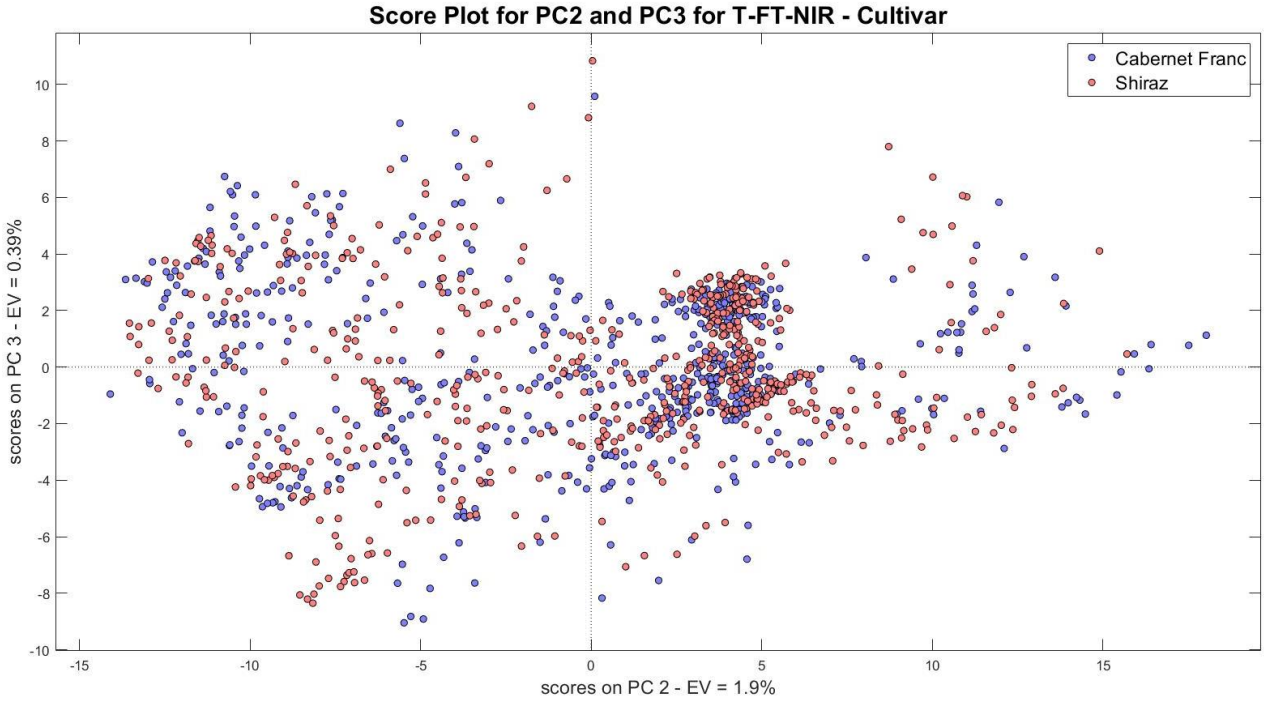

Figure 4.5e: Score plot for T-FT-NIR for PC 2 vs PC 3 (Cultivar)

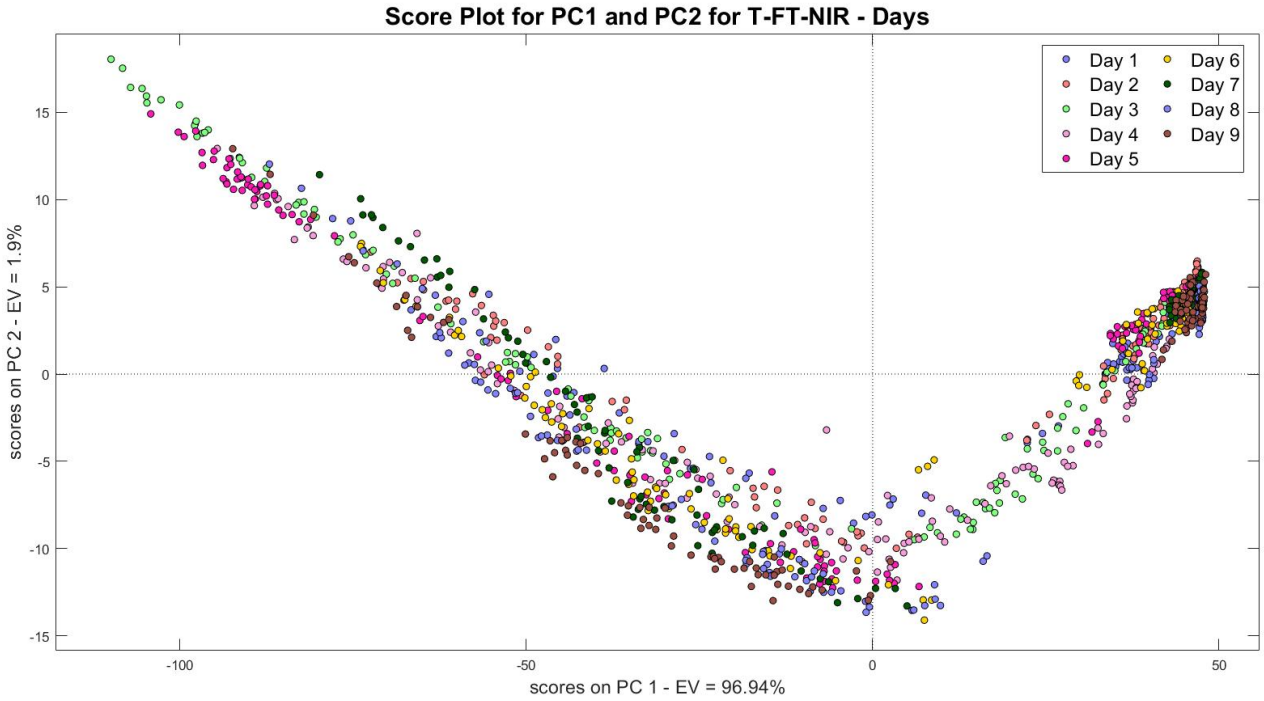

Figure 4.5f: Score plot for T-FT-NIR for PC 1 vs PC 2 (Days)

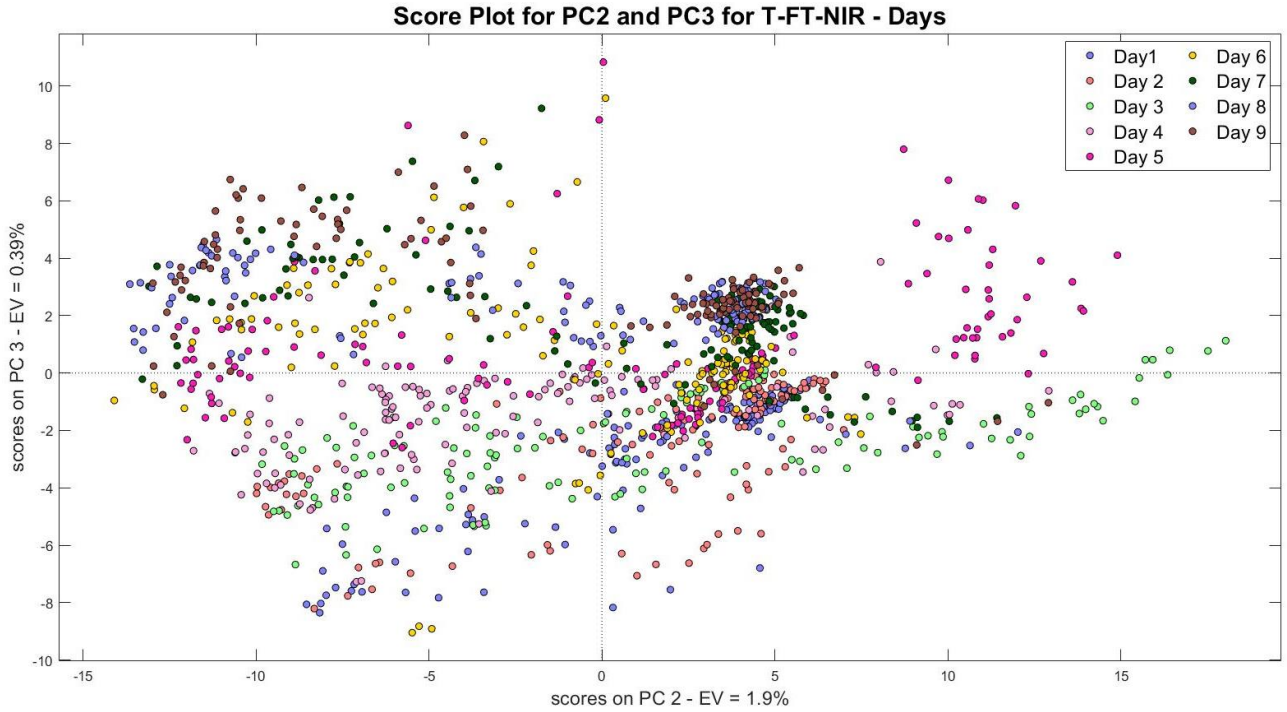

Figure 4.5g: Score plot for T-FT-NIR for PC 2 vs PC 3 (Days)

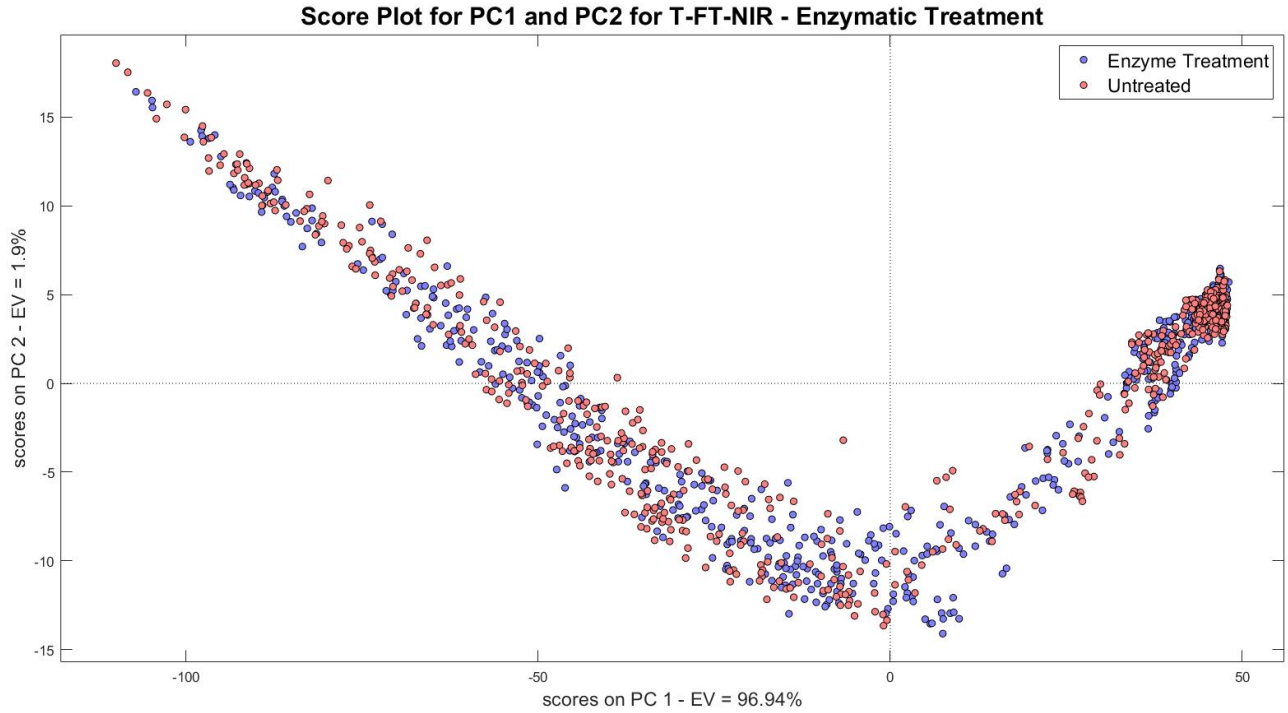

Figure 4.5h: Score plot for T-FT-NIR for PC 1 vs PC 2 (Enzymatic Treatment)

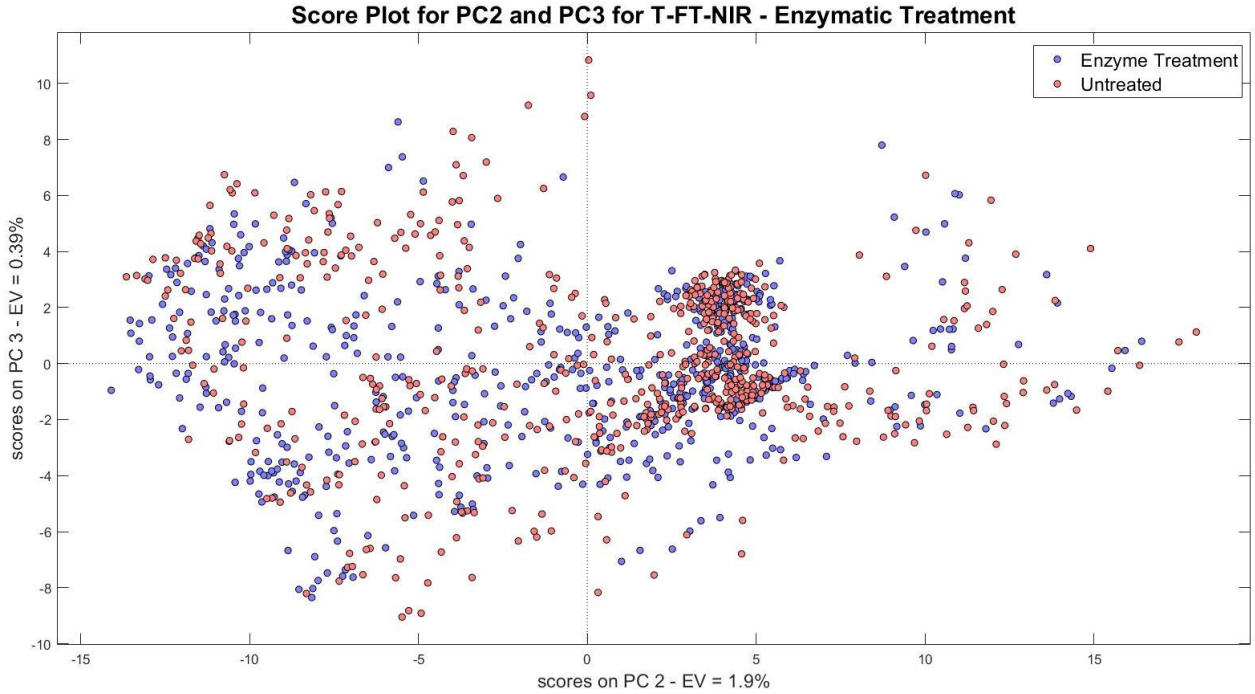

Figure 4.5i: Score plot for T-FT-NIR for PC 2 vs PC 3 (Enzymatic Treatment)

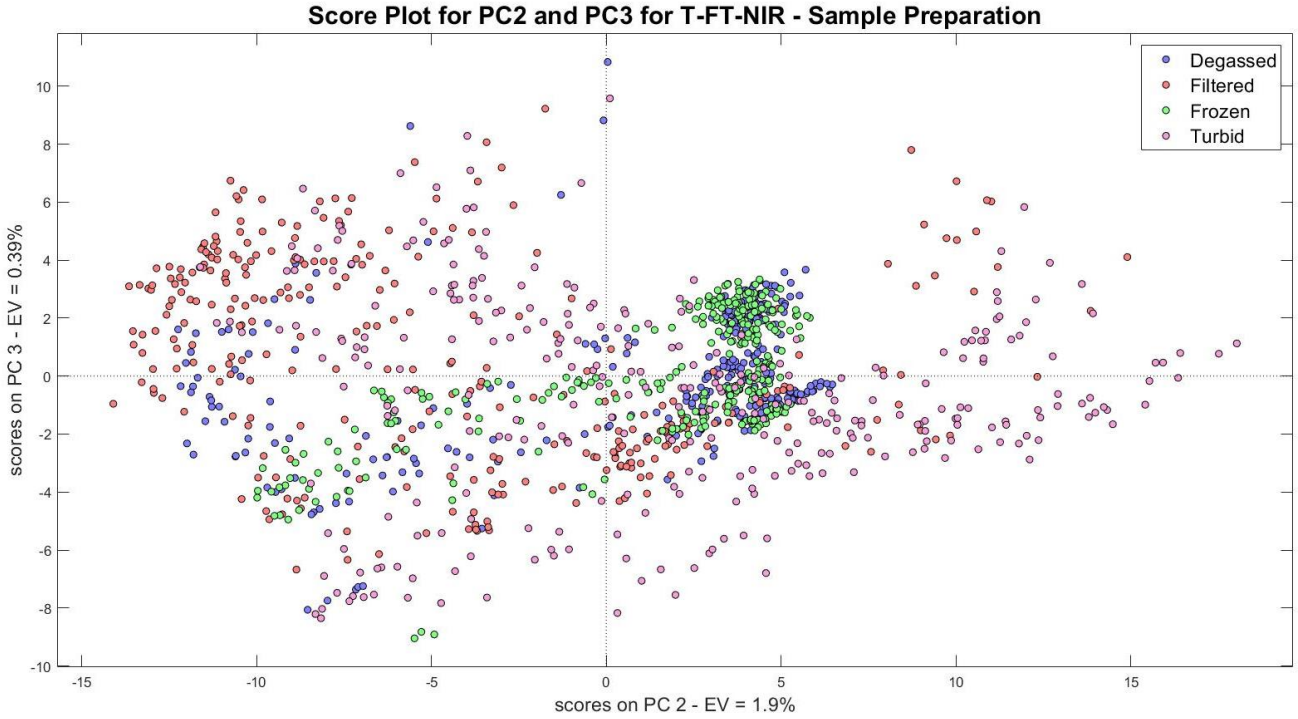

Figure 4.5j: Score plot for T-FT-NIR for PC 2 vs PC 3 (Sample Preparation)

7.4 Selected Partial Least Squares Regression Graphs

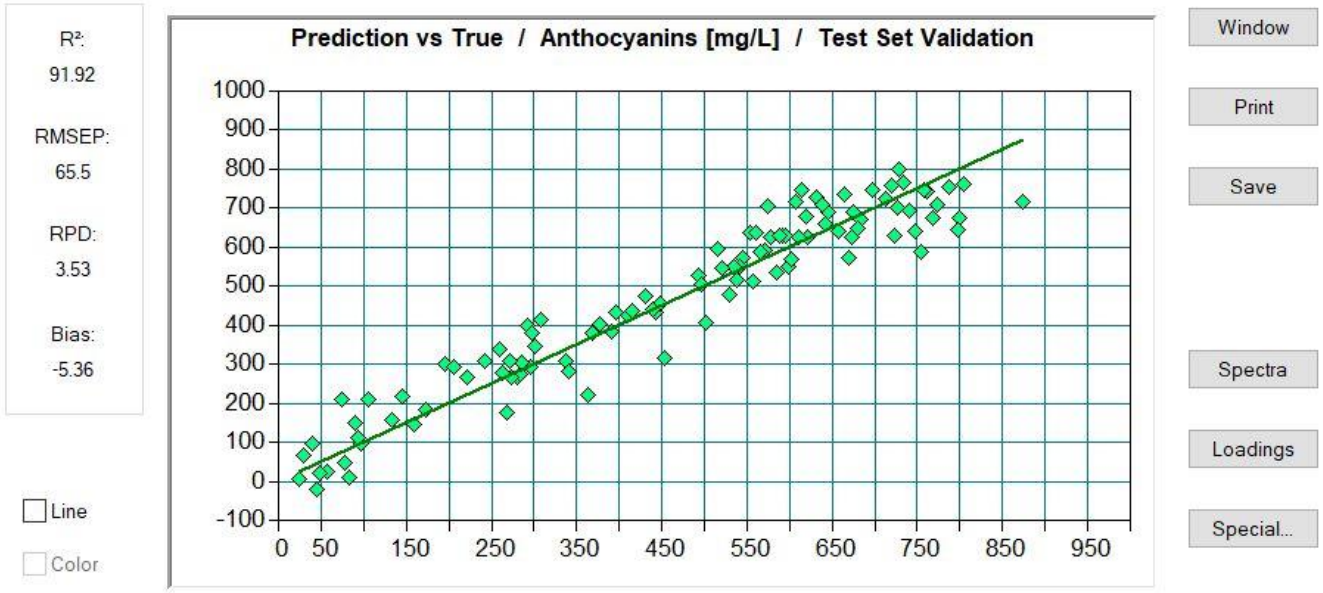

Figure 4.7a: Validation Graph for Anthocyanins for ATR-MIR Spectroscopic Method

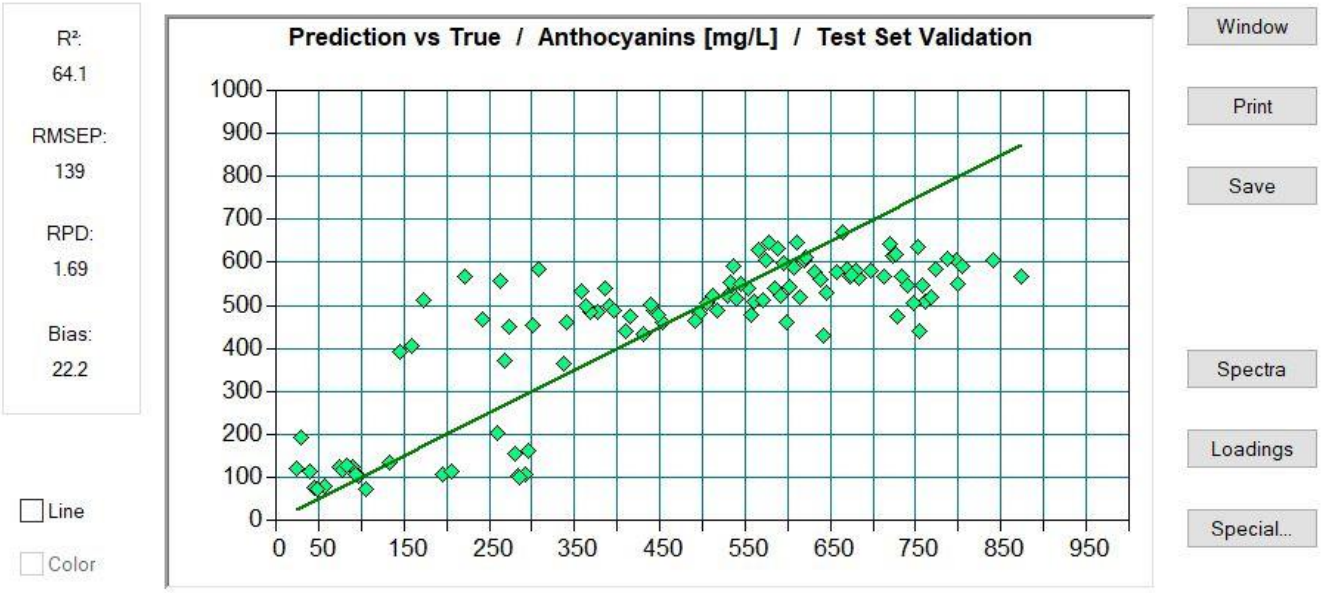

Figure 4.7b: Validation Graph for Anthocyanins for T-FT-NIR Spectroscopic Method

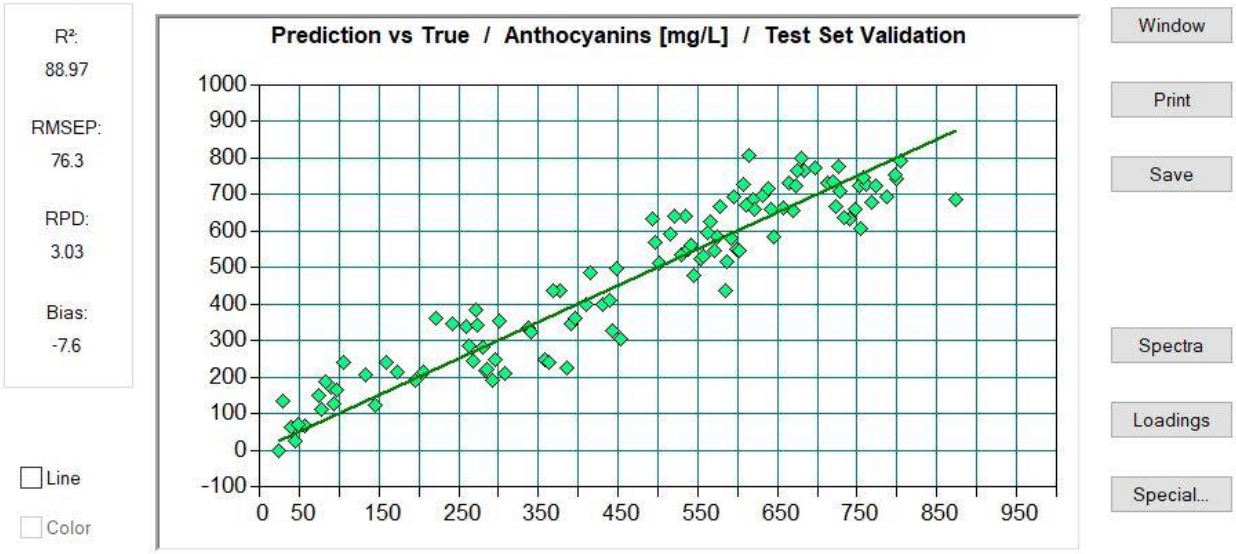

Figure 4.7c: Validation Graph for Anthocyanins for DR-FT-NIR Spectroscopic Method

Supplementary Material (S2)

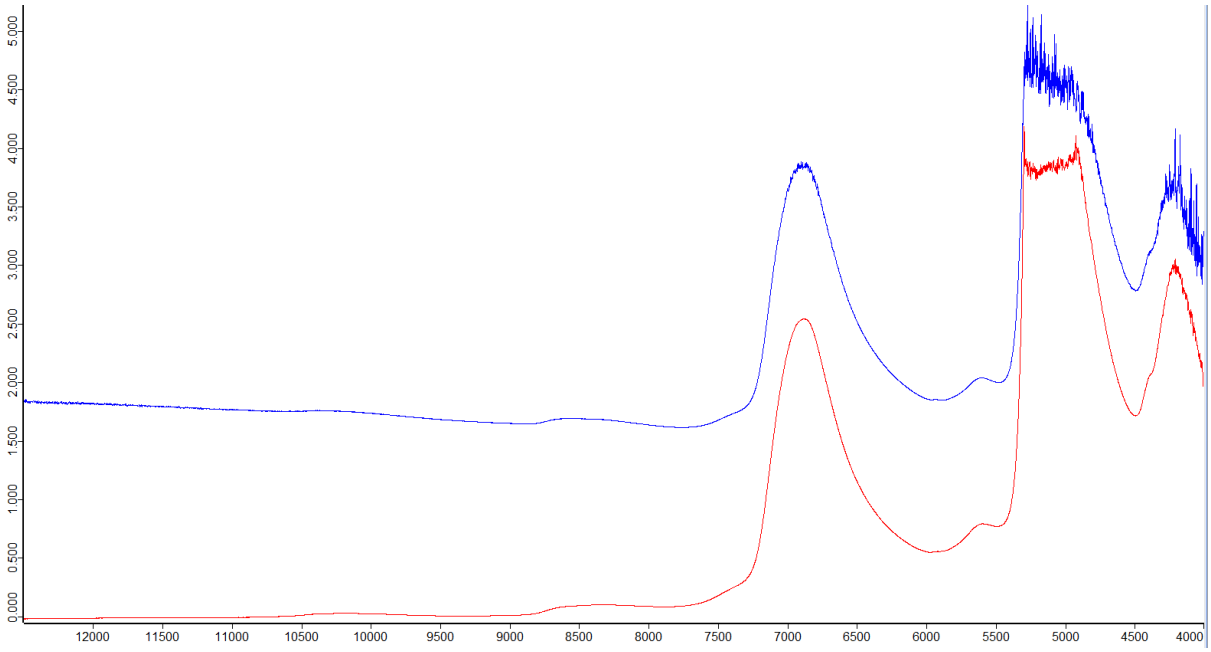

Figure 4.6: NIR spectra comparing a turbid sample with one free of suspended solids

Supplementary Material (S3)

Table 4.1a: Summary Statistics for Instrument Comparison

Treatment	*Component*	*Comparison*	*SI*	*ICC*	*SEM*
Degassed	Anthocyanins	ATR-MIR/T-FT-NIR	Ho Rejected	0.834	83.899
		ATR-MIR/DR-FT-NIR	Ho Accepted	0.95	49.815
		T-FT-NIR/DR-FT-NIR	Ho Rejected	0.826	83.283
	Colour Density	ATR-MIR/T-FT-NIR	Ho Accepted	0.927	2.415
		ATR-MIR/DR-FT-NIR	Ho Accepted	0.95	2.006
		T-FT-NIR/DR-FT-NIR	Ho Accepted	0.958	1.769
	Polymeric Pigments	ATR-MIR/T-FT-NIR	Ho Rejected	0.955	8.53
		ATR-MIR/DR-FT-NIR	Ho Rejected	0.971	7.108
		T-FT-NIR/DR-FT-NIR	Ho Accepted	0.959	8.739
	Tannins	ATR-MIR/T-FT-NIR	Ho Accepted	0.95	40.443
		ATR-MIR/DR-FT-NIR	Ho Accepted	0.94	39.433
		T-FT-NIR/DR-FT-NIR	Ho Accepted	0.932	46.627
	TPI	ATR-MIR/T-FT-NIR	Ho Rejected	0.907	4.789
		ATR-MIR/DR-FT-NIR	Ho Accepted	0.964	3.114
		T-FT-NIR/DR-FT-NIR	Ho Rejected	0.907	4.737
Filtered	Anthocyanins	ATR-MIR/T-FT-NIR	Ho Rejected	0.786	100.865
		ATR-MIR/DR-FT-NIR	Ho Accepted	0.961	47.656
		T-FT-NIR/DR-FT-NIR	Ho Rejected	0.823	90.08
	Colour Density	ATR-MIR/T-FT-NIR	Ho Accepted	0.929	2.25
		ATR-MIR/DR-FT-NIR	Ho Accepted	0.962	1.636
		T-FT-NIR/DR-FT-NIR	Ho Accepted	0.92	2.344
	Polymeric Pigments	ATR-MIR/T-FT-NIR	Ho Accepted	0.928	11.535
		ATR-MIR/DR-FT-NIR	Ho Accepted	0.97	7.749
		T-FT-NIR/DR-FT-NIR	Ho Accepted	0.939	10.582
	Tannins	ATR-MIR/T-FT-NIR	Ho Accepted	0.907	55.345
		ATR-MIR/DR-FT-NIR	Ho Accepted	0.939	45.708
		T-FT-NIR/DR-FT-NIR	Ho Accepted	0.914	55.307
	TPI	ATR-MIR/T-FT-NIR	Ho Accepted	0.936	4.451
		ATR-MIR/DR-FT-NIR	Ho Accepted	0.954	3.807
		T-FT-NIR/DR-FT-NIR	Ho Accepted	0.941	4.171
Frozen	Anthocyanins	ATR-MIR/T-FT-NIR	Ho Rejected	0.711	101.632
		ATR-MIR/DR-FT-NIR	Ho Accepted	0.932	59.278
		T-FT-NIR/DR-FT-NIR	Ho Rejected	0.669	105.497
	Colour Density	ATR-MIR/T-FT-NIR	Ho Accepted	0.901	2.672
		ATR-MIR/DR-FT-NIR	Ho Accepted	0.953	1.851
		T-FT-NIR/DR-FT-NIR	Ho Accepted	0.899	2.755
	Polymeric Pigments	ATR-MIR/T-FT-NIR	Ho Rejected	0.645	15.787
		ATR-MIR/DR-FT-NIR	Ho Accepted	0.903	7.523
		T-FT-NIR/DR-FT-NIR	Ho Rejected	0.592	17.513
	Tannins	ATR-MIR/T-FT-NIR	Ho Rejected	0.929	45.733
		ATR-MIR/DR-FT-NIR	Ho Accepted	0.946	40.593
		T-FT-NIR/DR-FT-NIR	Ho Accepted	0.932	43.501
	TPI	ATR-MIR/T-FT-NIR	Ho Rejected	0.901	5.025
		ATR-MIR/DR-FT-NIR	Ho Rejected	0.967	3.177

		T-FT-NIR/DR-FT-NIR	Ho Rejected	0.945	3.577
Turbid	Anthocyanins	ATR-MIR/T-FT-NIR	Ho Rejected	0.661	107.804
		ATR-MIR/DR-FT-NIR	Ho Accepted	0.935	54.278
		T-FT-NIR/DR-FT-NIR	Ho Rejected	0.688	102.662
	Colour Density	ATR-MIR/T-FT-NIR	Ho Accepted	0.89	2.783
		ATR-MIR/DR-FT-NIR	Ho Accepted	0.947	2.049
		T-FT-NIR/DR-FT-NIR	Ho Accepted	0.878	2.982
	Polymeric Pigments	ATR-MIR/T-FT-NIR	Ho Rejected	0.64	15.73
		ATR-MIR/DR-FT-NIR	Ho Accepted	0.904	7.463
		T-FT-NIR/DR-FT-NIR	Ho Rejected	0.586	17.463
	Tannins	ATR-MIR/T-FT-NIR	Ho Accepted	0.932	43.656
		ATR-MIR/DR-FT-NIR	Ho Accepted	0.906	55.398
		T-FT-NIR/DR-FT-NIR	Ho Rejected	0.886	57.864
	TPI	ATR-MIR/T-FT-NIR	Ho Rejected	0.927	4.08
		ATR-MIR/DR-FT-NIR	Ho Accepted	0.979	2.259
		T-FT-NIR/DR-FT-NIR	Ho Accepted	0.914	4.389

Table 4.2a: Summary Statistics for Pre-Treatment Comparison for ATR-MIR

Component	*Comparison*	*SI*	*ICC*	*SEM*
Anthocyanins	Degassed/Filtered	Ho Accepted	0.957	43.953
	Degassed/Frozen	Ho Accepted	0.959	43.619
	Degassed/Turbid	Ho Accepted	0.969	38.317
	Filtered/Frozen	Ho Accepted	0.947	48.398
	Filtered/Turbid	Ho Accepted	0.955	45.355
	Frozen/Turbid	Ho Accepted	0.966	39.98
Colour Density	Degassed/Filtered	Ho Accepted	0.966	1.478
	Degassed/Frozen	Ho Accepted	0.948	1.842
	Degassed/Turbid	Ho Accepted	0.969	1.433
	Filtered/Frozen	Ho Accepted	0.955	1.685
	Filtered/Turbid	Ho Accepted	0.973	1.314
	Frozen/Turbid	Ho Accepted	0.952	1.758
Polymeric Pigments	Degassed/Filtered	Ho Rejected	0.949	6.46
	Degassed/Frozen	Ho Accepted	0.947	6.108
	Degassed/Turbid	Ho Accepted	0.914	8.121
	Filtered/Frozen	Ho Rejected	0.936	7.079
	Filtered/Turbid	Ho Accepted	0.912	8.591
	Frozen/Turbid	Ho Accepted	0.91	8.128
Tannins	Degassed/Filtered	Ho Accepted	0.95	39.928
	Degassed/Frozen	Ho Accepted	0.945	42.888
	Degassed/Turbid	Ho Accepted	0.965	33.568
	Filtered/Frozen	Ho Accepted	0.944	42.561
	Filtered/Turbid	Ho Accepted	0.971	28.612
	Frozen/Turbid	Ho Accepted	0.951	39.93
TPI	Degassed/Filtered	Ho Accepted	0.983	2.216
	Degassed/Frozen	Ho Accepted	0.969	3.055
	Degassed/Turbid	Ho Accepted	0.989	1.769
	Filtered/Frozen	Ho Accepted	0.964	3.343
	Filtered/Turbid	Ho Rejected	0.98	2.346
	Frozen/Turbid	Ho Accepted	0.976	2.635

Table 4.3a: Summary Statistics for Pre-Treatment Comparison for DR-FT-NIR

Component	*Comparison*	*SI*	*ICC*	*SEM*
Anthocyanins	Degassed/Filtered	Ho Accepted	0.956	45.591
	Degassed/Frozen	Ho Accepted	0.941	52.046
	Degassed/Turbid	Ho Accepted	0.938	53.477
	Filtered/Frozen	Ho Accepted	0.923	60.912
	Filtered/Turbid	Ho Accepted	0.954	46.714
	Frozen/Turbid	Ho Accepted	0.927	58.032
Colour Density	Degassed/Filtered	Ho Accepted	0.942	1.889
	Degassed/Frozen	Ho Accepted	0.932	2.045
	Degassed/Turbid	Ho Accepted	0.939	1.956
	Filtered/Frozen	Ho Accepted	0.93	2.11
	Filtered/Turbid	Ho Accepted	0.953	1.679
	Frozen/Turbid	Ho Accepted	0.937	1.954
Polymeric Pigments	Degassed/Filtered	Ho Accepted	0.963	7.804
	Degassed/Frozen	Ho Accepted	0.952	9.537
	Degassed/Turbid	Ho Accepted	0.969	7.32
	Filtered/Frozen	Ho Accepted	0.968	8.036
	Filtered/Turbid	Ho Accepted	0.975	6.928
	Frozen/Turbid	Ho Accepted	0.961	8.88
Tannins	Degassed/Filtered	Ho Accepted	0.953	39.974
	Degassed/Frozen	Ho Accepted	0.962	35.491
	Degassed/Turbid	Ho Accepted	0.947	42.267
	Filtered/Frozen	Ho Accepted	0.963	35.708
	Filtered/Turbid	Ho Accepted	0.946	43.658
	Frozen/Turbid	Ho Accepted	0.951	40.548
TPI	Degassed/Filtered	Ho Accepted	0.956	3.577
	Degassed/Frozen	Ho Accepted	0.968	3.048
	Degassed/Turbid	Ho Accepted	0.977	2.558
	Filtered/Frozen	Ho Accepted	0.963	3.346
	Filtered/Turbid	Ho Accepted	0.942	3.058
	Frozen/Turbid	Ho Accepted	0.965	3.304

Table 4.4a: Summary Statistics for Pre-Treatment Comparison for the T-FT-NIR

Component	*Comparison*	*SI*	*ICC*	*SEM*
Anthocyanins	Degassed/Filtered	Ho Accepted	0.815	79.833
	Degassed/Frozen	Ho Rejected	0.797	75.968
	Degassed/Turbid	Ho Rejected	0.762	84.912
	Filtered/Frozen	Ho Rejected	0.817	70.442
	Filtered/Turbid	Ho Rejected	0.838	68.235
	Frozen/Turbid	Ho Accepted	0.852	58.015
Colour Density	Degassed/Filtered	Ho Accepted	0.856	3.041
	Degassed/Frozen	Ho Accepted	0.861	3.044
	Degassed/Turbid	Ho Accepted	0.869	2.847
	Filtered/Frozen	Ho Accepted	0.842	3.246
	Filtered/Turbid	Ho Accepted	0.834	3.217
	Frozen/Turbid	Ho Accepted	0.827	3.369
Polymeric Pigments	Degassed/Filtered	Ho Rejected	0.958	8.475
	Degassed/Frozen	Ho Accepted	0.956	8.864
	Degassed/Turbid	Ho Accepted	0.916	11.917
	Filtered/Frozen	Ho Accepted	0.942	9.979
	Filtered/Turbid	Ho Accepted	0.905	12.338
	Frozen/Turbid	Ho Accepted	0.932	10.87
Tannins	Degassed/Filtered	Ho Accepted	0.893	58.881
	Degassed/Frozen	Ho Accepted	0.936	44.507
	Degassed/Turbid	Ho Rejected	0.914	49.096
	Filtered/Frozen	Ho Accepted	0.912	53.673
	Filtered/Turbid	Ho Rejected	0.884	59.634
	Frozen/Turbid	Ho Accepted	0.921	47.461
TPI	Degassed/Filtered	Ho Rejected	0.877	5.344
	Degassed/Frozen	Ho Accepted	0.947	3.215
	Degassed/Turbid	Ho Accepted	0.909	4.477
	Filtered/Frozen	Ho Rejected	0.907	4.612
	Filtered/Turbid	Ho Accepted	0.942	3.799
	Frozen/Turbid	Ho Accepted	0.939	3.604

Supplementary Material (S4)

Table 5.2a: Summary of Pre-processing methods and wavenumber regions selected for ATR-MIR

Component	*Sample Treatment*	*Rank*	*Pre-processing Method*	*Wavenumber Regions*
Anthocyanins	Filtered	7	Log10	(1100-2500) (2700-4000)
Anthocyanins	Turbid	8	Autoscale	4000 - 400
Colour Density	Filtered	6	Baseline (Automatic Whittaker Filter)	4000 - 400
Colour Density	Turbid	4	Glog	4000 - 400
Polymeric Pigments	Filtered	8	Multiway Scaling	(1500 - 1700) (2500 - 3500)
Polymeric Pigments	Turbid	7	Autoscale	(1400 - 1500) (2500 - 2600) (3100 - 3500)
Tannins	Filtered	5	Normalising	4000 - 400
Tannins	Turbid	3	GLog	4000 - 400
TPI	Filtered	9	Autoscale	(1000 - 1500) (2700 - 3000) (3500 - 3700)
TPI	Turbid	8	Baseline (Automatic Weighted Least Squares)	(1400 - 2000) (2700 - 3000)

Table 5.3a: Summary of Pre-processing methods and wavenumber regions selected for T-FT-NIR

Component	*Sample Treatment*	*Rank*	*Pre-processing Method*	*Wavenumber Regions*
Anthocyanins	Filtered	4	Baseline (Automatic Weighted Least Squares)	(5800-6000) (7000 - 7050)
Anthocyanins	Turbid	4	Baseline (Automatic Weighted Least Squares)	5800 -6000
Colour Density	Filtered	5	Baseline (Automatic Whittaker Filter)	(5800-6200) (7000 -8000)
Colour Density	Turbid	5	Median Centering	(5800 - 6200) (8000 - 8400) (10000 - 11400)
Polymeric Pigments	Filtered	3	Min-Max Scaling	(5800 -6200)
Polymeric Pigments	Turbid	4	Median Centering	(5800 - 6200) (8000 - 8400)
Tannins	Filtered	2	Baseline (Automatic Weighted Least Squares)	(6000 -6200) (8500 - 9500) (10000 -10200)
Tannins	Turbid	7	MSC	(5800 -6200)
TPI	Filtered	4	Baseline (Automatic Weighted Least Squares)	(5800 - 6200) (7000 -8000)
TPI	Turbid	3	Baseline (Automatic Weighted Least Squares)	4000 - 11400

Table 5.4a: Summary of Pre-processing methods and wavenumber regions selected for DR-FT-NIR

Component	*Sample Treatment*	*Rank*	*Pre-processing Method*	*Wavenumber Regions*
Anthocyanins	Filtered	9	Multiway Scale	4100 - 12000
Anthocyanins	Turbid	8	Multiway Scale	4000-12000
Colour Density	Filtered	7	Baseline (Automatic Whittaker Filter)	4100 - 12000
Colour Density	Turbid	7	Multiway Scale	4000-12000
Polymeric Pigments	Filtered	7	Autoscale	4000-12000
Polymeric Pigments	Turbid	3	2nd Derivative	4000-12000
Tannins	Filtered	6	Detrend	4000-12000
Tannins	Turbid	6	Detrend	4000-12000
TPI	Filtered	8	Multiway Scale	4100 - 12000
TPI	Turbid	7	Min-Max Scaling	4100 - 12000

Supplementary Material (S5)

Table 3.4a: Summary of Pump Performance and Cost

Pump Name	Approximate Cost	Samplings per Day
Jebao DP-4 Auto Dosing Pumps	R1 500	24
Bubble Magus T11	R4 500	11
Kamoer X4	R5 000	11

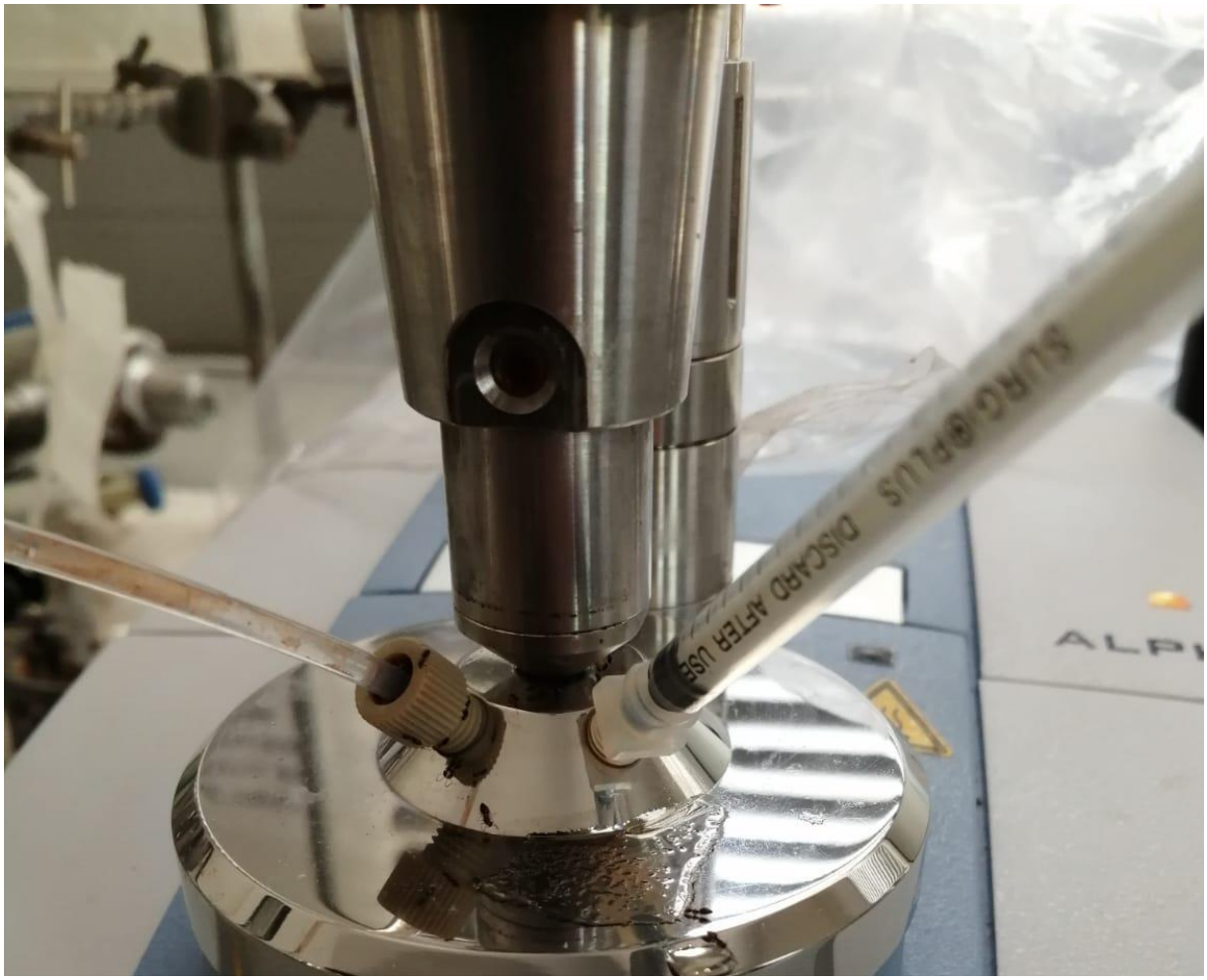

Figure 3.2a: Photograph of Alpha ATR-MIR Attachment and Connections for Sampling